Blank Page

# Determining the role of innate lymphoid cells during bacterial infection

A thesis submitted to The University of Manchester for the degree of Doctor of Philosophy in the Faculty of Biology, Medicine and Health

**2021**

**Joshua WJ Dow**

School of Biological Sciences
Division of Immunology, Immunity to Infection and Respiratory Medicine

## Contents

**Contents** ..... **2**

**List of Figures** ..... **8**

**List of Tables** ..... **10**

**List of Abbreviations** ..... **11**

**Abstract** ..... **15**

**Declaration** ..... **16**

**Copyright statement** ..... **16**

**Acknowledgements** ..... **17**

**Chapter 1 Introduction** ..... **19**

**1.1 Introduction** ..... **20**

**1.2 *Francisella tularensis*** ..... **21**

1.2.1 Taxonomy and genomics ..... 21

1.2.2 Tularaemia ..... 22

1.2.3 *F. tularensis* live vaccine strain (LVS) ..... 24

1.2.4 The life cycle of *F. tularensis* - cellular uptake ..... 25

1.2.5 Escape from the phagosome and cytosolic replication ..... 27

1.2.6 Cell-to-cell transmission ..... 29

1.2.7 Innate immune recognition ..... 29

1.2.7.1 Complement system ..... 29

1.2.7.2 Pattern recognition receptors (PRRs) ..... 30

1.2.7.3 Alveolar epithelial cells in *F. tularensis* infection ..... 31

1.2.8 Innate immune response in *F. tularensis* infection ..... 32

1.2.8.1 Macrophages ..... 32

1.2.8.2 Monocytes ..... 33

1.2.8.3 Dendritic Cells ..... 33

1.2.8.4 Neutrophils ..... 34

1.2.8.5 Natural killer cells ..... 35

1.2.9 Adaptive immune response in *F. tularensis* infection ..... 36

1.2.10 Pro-inflammatory cytokines during *F. tularensis* infection ..... 37

1.2.11 Type 2 cytokines ..... 40

1.2.12 Regulatory cytokines ..... 40

**1.3 Innate lymphoid cells (ILCs) ..... 42**
1.3.1 Group 1 ILCs overview ..... 44
1.3.2 Group 1 ILCs during infection ..... 44
1.3.3 Group 2 ILCs overview ..... 46
1.3.4 Group 2 ILCs during infection ..... 49
1.3.5 Group 3 ILCs overview ..... 53
1.3.6 Group 3 ILCs during infection ..... 54
**1.4 Aims ..... 57**
**Chapter 2 Materials and Methods ..... 58**
**2.1 Bacteria ..... 59**
2.1.1 *Francisella tularensis* live vaccine strain ..... 59
2.1.2 Preparation of master stock ..... 59
2.1.3 Preparation of challenge stock and challenge dose ..... 59
**2.2 Infection models with *F. tularensis* LVS ..... 59**
2.2.1 Animals ..... 59
2.2.2 Intranasal infection with *F. tularensis* LVS ..... 60
2.2.3 Determining organ bacterial burden ..... 61
2.2.4 Administration of anti-NK1.1 antibody ..... 61
2.2.5 Administration of diphtheria toxin ..... 61
2.2.6 Administration of IL-33 ..... 61
2.2.7 Intranasal transfer of ILC2s ..... 62
**2.3 Flow Cytometry ..... 62**
2.3.1 Tissue digestion and processing ..... 62
2.3.2 Anti-*F. tularensis* LVS antibody ..... 62
2.3.3 Cell staining protocol for flow cytometry ..... 63
**2.4 Apoptosis/necrosis assays ..... 65**
**2.5 In vitro ILC2 culture ..... 65**
**2.6 In vitro ILC2-NK co-culture ..... 66**
**2.7 Statistical analysis ..... 66**
**Chapter 3 Determining the role of innate lymphoid cells during pulmonary infection with *Francisella tularensis* LVS ..... 67**
**3.1 Introduction ..... 68**
**3.2 Results ..... 69**

3.2.1 Determining the progression of *F. tularensis* LVS infection 69
3.2.2 Innate lymphoid cells (ILCs) are reduced during infection with *F. tularensis* LVS ..... 70
3.2.3 Dynamic changes are observed in multiple lung immune cell populations during infection with *F. tularensis* LVS ..... 72
3.2.4 Subset-specific changes in ILC1s and ILC2s are observed during infection with *F. tularensis* LVS ..... 74
3.2.5 Phenotypic changes are observed in T-bet$^+$ ILC1s and GATA3$^+$ ILC2s at later stages of infection with *F. tularensis* LVS ..... 76
3.2.6 ILC2s are not infected during LVS infection ..... 79
3.2.7 ILC2s do not show enhanced cell death during infection with *F. tularensis* LVS ..... 81
3.2.8 ILC2 numbers are also reduced in draining lymph nodes during infection with *F. tularensis* LVS ..... 85

**3.3 Discussion ..... 87**
3.3.1 Understanding the changes in the lung ILC compartment during the later stages of infection with *F. tularensis* LVS ..... 87
3.3.2 Investigating the phenotypic changes in ILC2s during the later stages of infection with *F. tularensis* LVS ..... 88
3.3.3 Attempting to uncover how lung ILC2s are reduced during LVS infection ..... 90
3.3.4 Understanding the reduction in cells of the lymphoid lineage during infection with *F. tularensis* LVS ..... 93

**3.4 Conclusion ..... 94**

**Chapter 4 Determining the effects of expanding the ILC compartment during infection with *F. tularensis* LVS ..... 95**

**4.1 Introduction ..... 96**

**4.2 Results ..... 97**
4.2.1 IL-33 treatment results in enhanced mortality and reduced control of infection with *F. tularensis* LVS ..... 97
4.2.2 IL-33 treatment significantly enhances ILC2 numbers during *F. tularensis* LVS infection ..... 98
4.2.3 IL-33-treated LVS-infected mice exhibit an altered myeloid immune response ..... 100

4.2.4 NK cell numbers are unaltered following IL-33 treatment during infection with *F. tularensis* LVS ..... 104
4.2.5 IL-33 significantly alters adaptive immunity during infection with *F. tularensis* LVS ..... 105
4.2.6 Adaptive immunity is dispensable in the control of infection with *F. tularensis* LVS ..... 107
4.2.7 Transfer of ILC2s to mice during *F. tularensis* LVS infection significantly exacerbates bacterial burdens..... 112
4.2.8 ILC2 transfer does not increase type 2 adaptive cell numbers ..... 113
4.2.9 NK-derived IFN-γ is reduced post-ILC2 transfer ..... 114
4.2.10 Intranasal transfer of ILC2s is associated with alterations to the myeloid cell compartment at peak infection..... 116

**4.3 Discussion..... 119**

4.3.1 Determining how IL-33-induced expansion and activation of ILC2s impacts upon infection with *F. tularensis* LVS..... 119
4.3.2 IL-33-activated ILC2 effector functions during infection with *F. tularensis* LVS ..... 120
4.3.3 The relationship between NK cells and ILC2s during LVS infection ..... 122
4.3.4 ILC2-ILC1 plasticity ..... 123
4.3.5 Investigating the effects of IL-33 on T cell responses during infection with *F. tularensis* LVS..... 124
4.3.6 Understanding the relationship between ILC2s and neutrophils during infection with *F. tularensis* LVS..... 125

**4.4 Conclusion ..... 127**

**Chapter 5 Determining the impact of the ablation of innate lymphocytes on the progress of infection with *F. tularensis* LVS .... 128**

**5.1 Introduction..... 129**

**5.2 Results..... 130**

5.2.1 Lack of adaptive immunity does not alter bacterial burdens during infection with *F. tularensis* LVS ..... 130
5.2.2 Common gamma chain (il2rg) deficiency results in enhanced bacterial burdens during infection with *F. tularensis* LVS ..... 130

5.2.3 The proportions of myeloid cells are altered in Rag1$^{-/-}$ and il2rg$^{-/-}$ mice ..... 132
5.2.4 Loss of ILCs and NK cells in Rag1$^{-/-}$il2rg$^{-/-}$ mice is associated with enhanced bacterial burdens during LVS infection ..... 136
5.2.5 ILC1s and NK cells represent innate sources of IFN-γ during infection with *F. tularensis* LVS ..... 138
5.2.6 IFN-γ in the infected lung environment appears important in driving infection-induced reduction in ILC2 numbers ..... 142
5.2.7 Anti-NK1.1-mediated depletion of NK cells does not rescue ILC2 numbers ..... 144
5.2.8 Anti-NK1.1-mediated depletion of NK cells does not rescue ILC2 numbers in Rag1$^{-/-}$ mice ..... 146
5.2.9 Blockade of IFN-γ in NK-ILC2 co-cultures does not reduce ILC2 numbers *in vitro* ..... 148
5.2.10 Treatment with diphtheria toxin results in significantly enhanced bacterial burdens during infection with *F. tularensis* LVS, with this effect attenuated upon depletion of ILC2s ..... 151
5.2.11 The myeloid immune response is significantly altered following DTx treatment ..... 154

**5.3 Discussion ..... 157**

5.3.1 Determining the relative contributions of innate and adaptive lymphocytes during infection with *F. tularensis* LVS ..... 157
5.3.2 Considering the impact of innate lymphocytes on myeloid cells during LVS infection ..... 159
5.3.3 Identifying a soluble mediator to successfully modulate ILC2 numbers during infection with *F. tularensis* LVS ..... 161
5.3.4 Dissecting the importance of ILC2s during infection with *F. tularensis* LVS ..... 162

**5.4 Conclusion ..... 164**

**Chapter 6 General Discussion ..... 165**

**6.1 General Discussion ..... 166**

**6.2 Generating an appropriate immune response against *F. tularensis* ..... 167**

**6.3 Missing the therapeutic window during infection with *F. tularensis* ..... 169**

**6.4 Future directions..... 170**

**6.5 Thesis conclusion..... 173**

**Chapter 7 References..... 175**

**Word count: 37,120**

**List of Figures**

Figure 1.1 - The life cycle of *Francisella tularensis*. ..... 26
Figure 1.2 - Overview of innate lymphoid cell subsets and effector functions ..... 52
Figure 3.1 - Infection kinetics during infection with *F. tularensis* LVS..... 69
Figure 3.2 - Gating strategy for identification of ILCs in the lung of naïve C57BL/6 mice..... 70
Figure 3.3 - *F. tularensis* LVS infection causes a reduction in lung ILCs... 71
Figure 3.4 - Lung immune cell populations exhibit dynamic changes during infection with *F. tularensis* LVS..... 73
Figure 3.5 - Lung ILC subsets are altered during infection with *F. tularensis* LVS ..... 76
Figure 3.6 - Lung T-bet$^{+}$ ILC1s and GATA3$^{+}$ ILC2s are altered during infection with *F. tularensis* LVS..... 78
Figure 3.7 - Lung ILC2s are not infected by *F. tularensis* LVS ..... 80
Figure 3.8 - Gating strategy for identification of cell death in lung immune cell populations during infection with *F. tularensis* LVS..... 82
Figure 3.9 - Levels of apoptotic and necrotic cell death are altered in multiple lung immune cell populations during infection with *F. tularensis* LVS ..... 84
Figure 3.10 - ILCs of the mediastinal lymph node are altered during infection with *F. tularensis* LVS..... 87
Figure 4.1 - IL-33-treated C57BL/6 mice display enhanced bacterial burdens during infection with *F. tularensis* LVS..... 97
Figure 4.2 - IL-33 treatment significantly increases total ILC and ILC2 numbers during infection with *F. tularensis* LVS ..... 100
Figure 4.3 - Effects of IL-33 treatment on the myeloid immune response during infection with *F. tularensis* LVS..... 102
Figure 4.4 - IL-33-treated mice display significantly enhanced levels of infection in multiple immune cells during infection with *F. tularensis* LVS 103
Figure 4.5 - NK Cell numbers are unaffected in IL-33-treated LVS-infected mice ..... 104
Figure 4.6 - IL-33 treatment significantly alters the CD4$^{+}$ T cell compartment during infection with *F. tularensis* LVS..... 106
Figure 4.7 - Infection kinetics in IL-33-treated LVS-infected C57BL/6 and Rag1$^{-/-}$ mice at day 4 p.i..... 107

Figure 4.8 - ILC and ILC2 numbers are significantly elevated in the absence of adaptive immunity during infection with *F. tularensis* LVS ..... 108
Figure 4.9 - Effects of IL-33 treatment on the myeloid immune response in Rag1$^{-/-}$ mice during infection with *F. tularensis* LVS ..... 110
Figure 4.10 - Lack of adaptive immunity alters the relative levels of infection in multiple myeloid immune cells at day 4 p.i. ..... 111
Figure 4.11 - Intranasal transfer of ILC2s results in enhanced bacterial burdens in LVS-infected C57BL/6 mice at day 7 p.i. ..... 112
Figure 4.12 - ILC2 transfer does not alter type 2 CD4$^{+}$ or regulatory T cell numbers during infection with *F. tularensis* LVS ..... 113
Figure 4.13 - NK Cell numbers are significantly reduced following ILC2 transfer during infection with *F. tularensis* LVS ..... 115
Figure 4.14 - Characterisation of the myeloid immune compartment in the lung of LVS-infected C57BL/6 mice following ILC2 transfer ..... 117
Figure 4.15 - Characterisation of infected myeloid cell populations in the LVS-infected lung of C57BL/6 mice following ILC2 transfer ..... 119
Figure 5.1 - il2rg$^{-/-}$ mice display exacerbated bacterial burdens and enhanced mortality, whilst adaptive immunity is dispensable during infection with *F. tularensis* LVS ..... 131
Figure 5.2 - Effects of ablation of adaptive and innate lymphocytes on the myeloid immune response during infection with *F. tularensis* LVS ..... 133
Figure 5.3 - Effects of ablation of adaptive and innate lymphocytes on the infectious niche during infection with *F. tularensis* LVS ..... 135
Figure 5.4 – Rag1$^{-/-}$il2rg$^{-/-}$ mice display enhanced bacterial burdens and altered infectious niche in the lung during infection with *F. tularensis* LVS ..... 137
Figure 5.5 - Rag1$^{-/-}$il2rg$^{-/-}$ mice display enhanced infectious niche in the lung during infection with *F. tularensis* LVS ..... 138
Figure 5.6 - ILC1s display enhanced IFN-γ production during infection with *F. tularensis* LVS ..... 140
Figure 5.7 - ILC2s display enhanced IL-5 production early during infection with *F. tularensis* LVS ..... 141
Figure 5.8 - NK Cells display enhanced IFN-γ production during infection with *F. tularensis* LVS ..... 142
Figure 5.9 - *In vitro* culture of sort-purified lung ILC2s with cell-free lung supernatants ..... 143

Figure 5.10 - Anti-NK1.1-mediated NK cell depletion does not alter ILC2 numbers in C57BL/6 mice during infection with *F. tularensis* LVS ..... 145
Figure 5.11 - T cell-derived IFN-γ compensates for the loss of NK-derived IFN-γ in C57BL/6 mice during infection with *F. tularensis* LVS ..... 146
Figure 5.12 - Anti-NK1.1-mediated depletion of NK cells in Rag1$^{-/-}$ mice does not rescue ILC2 numbers during infection with *F. tularensis* LVS ..... 147
Figure 5.13 - Assessment of ILC2 apoptosis during *in vitro* co-culture of sort-purified lung ILC2s and NK cells..... 151
Figure 5.14 - Diphtheria toxin (DTx)-mediated depletion of ILC2 cells in ICOS-T mice during infection with *F. tularensis* LVS ..... 152
Figure 5.15 - DTx enhances bacterial burdens in WT mice during infection with *F. tularensis* LVS..... 153
Figure 5.16 - Effect of DTx administration on the myeloid compartment during infection with *F. tularensis* LVS..... 155
Figure 5.17 - DTx enhances levels of infection in multiple myeloid cell populations during infection with *F. tularensis* LVS..... 156
Figure 6.1 – ILC2s are detrimental to the host immune response during infection with *F. tularensis* LVS..... 167
Figure 6.2 – Immune cell interactions in the lung during infection with *F. tularensis* LVS ..... 174

**List of Tables**

Table 1.1 - Summary of the phenotypical markers expressed by each innate lymphoid cell subset in mice..... 50
Table 2.1 - Clinical scoring for monitoring of individual mice during infection ..... 60
Table 2.2 - Specifications of fluorophore-conjugated antibodies for cell surface markers ..... 64
Table 2.3 - Specifications of fluorophore-conjugated antibodies for intracellular markers and corresponding isotype controls ..... 65

**List of Abbreviations**

| | |
|---|---|
| AHR | Airway hyperreactivity |
| AM | Alveolar macrophage |
| AREG | Amphiregulin |
| ATII | Type II alveolar epithelial |
| ATP | Adenosine triphosphate |
| BAL | Bronchoalveolar lavage |
| BCGA | Blood cysteine glucose agar |
| BCL11B | B cell leukaemia/lymphoma 11b |
| BM | Bone marrow |
| BMDM | Bone marrow-derived macrophage |
| CCR2 | C-C motif chemokine receptor 2 |
| CCR6 | C-C motif chemokine receptor 6 |
| CD | Cluster of differentiation |
| CD200R | CD200 receptor |
| CDR | Cytosolic DNA receptors |
| CFU | Colony forming units |
| CHILP | Commo helper innate lymphoid precursors |
| CL | Containment level |
| CLP | Common lymphoid progenitor |
| cNK | Conventional natural killer |
| CR | Complement receptor |
| CX3CR1 | CX3C chemokine receptor 1 |
| DC | Dendritic cell |
| DTx | Diphtheria toxin |
| DNA | Deoxyribonucleic acid |
| DSTL | Defence Science and Technology Laboratory |
| EDTA | Ethylenediaminetetraacetic acid |
| EEA1 | Early endosome antigen 1 |
| FACS | Fluorescence-Activated cell sorting |
| FCS | Foetal calf serum |
| FcγR | Fc gamma receptor |
| FCP | *Francisella*-containing phagosome |
| FMO | Fluorescence minus one |

| | |
|---|---|
| FPI | *Francisella* pathogenicity island |
| GATA3 | GATA binding protein 3 |
| GFI-1 | Growth factor independence-1 |
| GFP | Green fluorescent protein |
| GM-CSF | Granulocyte-macrophage colony-stimulating factor |
| ICOS | Inducible T cell co-stimulator |
| ICOS-L | ICOS ligand |
| I.D. | Intradermal |
| Id2 | Inhibitor of DNA binding 2 |
| IFN | Interferon |
| IglE | Intracellular growth locus E |
| IL | Interleukin |
| ILC | Innate lymphoid cell |
| IL2RG | Interleukin 2 receptor gamma chain |
| I.N. | Intranasal |
| iNOS | Inducible nitric oxide synthase |
| I.P. | Intraperitoneal |
| IRF | Interferon regulatory factor |
| KLRG1 | Killer cell lectin-like receptor G1 |
| KO | Knockout |
| LAMP | Lysosomal-associated protein |
| LCMV | Lymphocytic choriomeningitis virus |
| LD | Lethal dose |
| LN | Lymph node |
| Lin | Lineage |
| LP | Lamina propria |
| LPS | Lipopolysaccharide |
| LTi | Lymphoid tissue inducer |
| LVS | Live vaccine strain |
| mAb | Monoclonal antibody |
| MAC | Membrane attack complex |
| MAPK | Mitogen-activated protein kinase |
| MCP | Monocyte chemotactic protein |
| M-CSF | Macrophage colony-stimulating factor |
| MDM | Monocyte-derived macrophages |
| MHC | Major histocompatibility complex |

| | |
|---|---|
| MMP | Matrix metalloprotease |
| NADPH | Nicotinamide adenine dinucleotide phosphate |
| NCR | Natural cytotoxicity receptor |
| NET | Neutrophil extracellular trap |
| NF-κB | Nuclear factor kappa-light-chain-enhancer of activated B cells |
| NFIL | Nuclear factor, interleukin-3 regulated |
| NK | Natural killer |
| NKR | Natural killer receptor |
| NLR | NOD-like receptor |
| PBS | Phosphate-buffered saline |
| PD | Programmed death |
| PD-L1 | PD-ligand-1 |
| $PGE_2$ | Prostaglandin $E_2$ |
| P.I. | Post-infection |
| PI3K | Phosphatidylinositol 3-kinase |
| PMA | Phorbol 12-myristate 13-acetate |
| PRR | Pattern recognition receptor |
| PZLF | Promyelocytic leukaemia zinc finger |
| RAG | Recombinant activating gene |
| RIR | RIG-I-like receptor |
| RNA | Ribonucleic acid |
| ROS | Reactive oxygen species |
| RPMI | Roswell park memorial institute |
| RSV | Respiratory syncytial virus |
| SRA | Scavenger receptor A |
| SCID | Severe combined immunodeficiency |
| STAT | Signal transducer and activator of transcription |
| TCR | T cell receptor |
| TCF | T cell factor |
| TF | Transcription factor |
| TGF | Transforming growth factor |
| Th | T helper |
| TLR | Toll-like receptor |
| TOX | Thymocyte selection-associated high-mobility group box protein |
| TNF | Tumour necrosis factor |

| | |
|---|---|
| TRAF | TNF receptor-associated factor |
| TREM | Triggering receptor expressed on myeloid cells |
| Treg | Regulatory T cell |
| TrN | Triple negative |
| TSLP | Thymic stromal lymphopoietin |
| T6SS | Type 6 secretion system |
| vATPase | Vacuolar proton ATPase |
| WT | Wild type |

## Abstract

Joshua Dow
The University of Manchester
PhD Immunology
2021

**Determining the role of innate lymphoid cells during bacterial infection**

The intracellular bacterium *Francisella tularensis (F. tularensis)* is a highly virulent pathogen. Due to the inherent lethality of infection via the respiratory route, there has been an increasing level of concern that aerosolisation of the bacterium could result in its use as a potential agent for bioterrorism. Until now, research into the early immune response in the lung against *F. tularensis* has focused primarily on the role of myeloid cells. In contrast, the contributions of lymphocyte responses in the control of infection with *F. tularensis* are less understood. Innate lymphoid cells (ILCs) represent an innate lymphocyte population that are frequently found at barrier sites such as the skin, intestine and the lung, and are capable of rapid response to a wide variety of immune insults, including against several respiratory pathogens. Despite this, their role in the context of infection with *F. tularensis* is unknown. With this in mind, ILCs represent a population of particular interest during respiratory infection with this bacterium.

Here, this PhD thesis focuses on addressing the role of ILCs during infection with *F. tularensis*. It demonstrates that infection with *F. tularensis* causes a significant reduction in lung ILC2s. Mechanistically, IFN-γ acts as a soluble mediator capable of driving the reduction in lung ILC2 numbers during infection with *F. tularensis*. Expansion of ILC2 numbers, either by IL-33 treatment or intranasal transfer, results in significantly enhanced bacterial burdens in the lung, liver and spleen of mice. Conversely, selective ablation of ILC2s results in reduced bacterial burdens in the lung.

Overall, this thesis highlights a potential negative role for ILC2s in the control of infection with *F. tularensis*. Thus, manipulation of ILC2 numbers during the early stages of infection with *F. tularensis* could be of potential therapeutic benefit.

**Declaration**

I declare that no portion of the work referred to in the thesis has been submitted in support of an application for another degree or qualification of this or any other university or other institute of learning.

**Copyright statement**

i. The author of this thesis (including any appendices and/or schedules to this thesis) owns certain copyright or related rights in it (the "Copyright") and s/he has given the University of Manchester certain rights to use such Copyright, including for administrative purposes.

ii. Copies of this thesis, either in full or in extracts and whether in hard or electronic copy, may be made **only** in accordance with the Copyright, Designs and Patents Act 1988 (as amended) and regulations issued under it or, where appropriate, in accordance with licensing agreements which the University has from time to time. This page must form part of any such copies made.

iii. The ownership of certain Copyright, patents, designs, trademarks and other intellectual property (the "Intellectual Property") and any reproductions of copyright works in the thesis, for example graphs and tables ("Reproductions"), which may be described in this thesis, may not be owned by the author and may be owned by third parties. Such Intellectual Property and Reproductions cannot and must not be made available for use without the prior written permission of the owner(s) of the relevant Intellectual Property and/or Reproductions.

iv. Further information on the conditions under which disclosure, publication and commercialisation of this thesis, the Copyright and any Intellectual Property and/or Reproductions described in it may take place is available in the University IP Policy (see http://documents.manchester.ac.uk/DocuInfo.aspx?DocID=24420), in any relevant Thesis restriction declarations deposited in the University Library, the University Library's regulations (see http://www.library.manchester.ac.uk/about/regulations/) and in the University's policy on Presentation of Theses.

**Acknowledgements**

First and foremost, I would like to thank my supervisors Mark Travis and Matt Hepworth. Mark for taking a chance on a lowly undergraduate, and Matt for his ILC expertise which helped the project in a great number of ways. I would also like to thank the Dstl for funding my PhD, and providing me with the opportunity to study *Francisella tularensis*. Thanks must go to Riccardo D'Elia specifically, for all of his help and advice throughout the project.

Working in the Travis lab has been a thoroughly rewarding experience. Whilst I have had the pleasure to work alongside many great people, special mention must go to two people in particular. Josh Casulli showed great perseverance to help me get going with the project, and was always on hand to provide both scientific and personal advice. Craig McEntee has been a fierce friend throughout my PhD, helping me through the ups and downs in a way that only an Irishman could.

Whilst studying a PhD in the MCCIR meant collaboration with other labs within the centre, it also meant that several incredible friendships were forged which stretched beyond Immunology - Alexandros, Frankie, and Nikki, thank you for all of your support. Emma C, Dave, and Los Hispanohablantes – whilst my brain thanks you, my liver may not be so kind…

My family's enduring support throughout my studies has been amazing, and is something that helped lift me when I was at rock bottom. Mum and dad - you have always supported me no matter what I do, and I will never be able to thank you enough for the opportunities you have given me, and the sacrifices you've made along the way to get me to where I am today. Jess - thank you for being equal parts annoying and loving, I couldn't ask for a better sister if I tried (or at least that's what you keep telling me). Ollie and Betsy - don't tell mum and dad the real reason I come home every now and again. To my two Grandma's - thank you for everything you have done for me over the years.

Y para acabar tengo que agradecer a mi Abejita. Jamás tendré alguien en mi vida que me apoyara como tú. Me has querido igual durante todo este tiempo - tras mis momentos más bajos y los más altos. ¿Quien supiera hace

5 años que estuviéramos aquí acabando nuestros doctorados juntos? Esto no lo pudiera haber hecho sin tu apoyo y tu amor. Te quiero mucho cómo la trucha al trucho.

# Chapter 1

# Introduction

## 1.1 Introduction

*Francisella tularensis (F. tularensis)* is a gram-negative intracellular bacterium which is the causative agent of tularaemia. With the high level of virulence of this pathogen, and the inherent lethality of pulmonary tularaemia, there has been an increasing level of concern over aerosolisation of the bacterium as a potential agent for bioterrorism (Maurin, 2015). As such, it is essential that all aspects of the early immune response against the bacterium are understood, in order to develop timely therapeutic interventions.

To date, research into the early immune response in the lung against *F. tularensis* has focused primarily on the role of myeloid cells. For example, macrophages and neutrophils serve as sites of extensive replication during respiratory infection, with dysregulation of these mechanisms proving detrimental to the host immune response (Hall *et al.*, 2008; D'Elia *et al.*, 2011; Casulli *et al.*, 2019). In contrast, the contributions of lymphocyte responses in the pathogenesis or control of infection with *F. tularensis* are less understood. Innate lymphoid cells (ILCs) are a relatively newly discovered type of tissue-resident innate lymphocyte, which are capable of a rapid response to a wide variety of immunological challenges, and are frequently found at barrier sites, such as the skin, intestine and the lung (Artis and Spits, 2015). Thus, given that these cells represent an innate effector population, they are of particular interest in the early immune response during respiratory infection with *F. tularensis* LVS. Despite this, the role of ILCs in this context is currently unknown.

Here, this PhD thesis focuses on addressing the role of ILCs during infection with *F. tularensis*. Specifically, it aims to uncover the relative contribution of these cells in the immune response against the bacterium, and whether they can be manipulated to the host's benefit. Herein, the current understanding of the immune response to *F. tularensis* will be reviewed, as well as the phenotypic traits of individual ILC subsets and their roles in the immune response against various infectious diseases. Overall, an enhanced knowledge of the role that ILCs play in the immune response against *F. tularensis* could ultimately help to contribute towards the development of potential novel therapies against this highly infectious bacterium.

## 1.2 *Francisella tularensis*

Like most bacteria, *F. tularensis* can be divided into a number of subspecies, with differences in virulence, geographical distribution and pathology between each. For this particular bacterium, three subspecies exist – *F. tularensis* subspecies (subsp.) *tularensis* (type A), *F. tularensis* subsp. *holarctica* (type B) and *F. tularensis* subsp. *mediasiatica*. Of these subspecies, only *F. tularensis* subsp. *tularensis* and *F. tularensis* subsp. *holarctica* can produce disease in humans. The more virulent strain of *F. tularensis* subspecies is *F. tularensis* subspecies *tularensis* (type A). Type A *F. tularensis* is restricted to North America, with as little as 10 colony-forming units (CFU) required to cause disease (Rotz and Hughes, 2004). The less virulent *F. tularensis* subspecies *holarctica* (type B) is distributed throughout the northern hemisphere, yet it is not as devastating as *F. tularensis* subsp. *tularensis* in that it causes a mild, self-limiting disease. *F. novicida* is another closely related species to *F. tularensis* which some people consider to be a fourth *F. tularensis* subspecies (Keim, Johansson and Wagner, 2007). However, human infection is neither common nor lethal with this species (Cowley and Elkins, 2011).

### 1.2.1 Taxonomy and genomics

Whilst the genomic nucleotide sequences of *F. tularensis* subsp. *tularensis* and *F. tularensis* subsp. *holarctica* are similar to *F. novicida*, the pathogenic strains contain 41 genes that are absent in the non-pathogenic *F. novicida* strain (Rohmer *et al.*, 2007). Moreover, *F. tularensis* subsp. *tularensis* contains 9 more genes that are absent in *F. tularensis* subsp. *holarctica*, highlighting the potential for these genes to contribute to the enhanced virulence observed in *F. tularensis* subspecies *tularensis* (Rohmer *et al.*, 2007). It has also been postulated that the presence of duplicated genes in *F. tularensis* subsp. *tularensis* and *F. tularensis* subsp. *holarctica* that are only present as single genes in *F. novicida* may indicate a gain of function for virulent *Francisella* strains (Rohmer *et al.*, 2007). Indeed, the *Francisella* pathogenicity island (FPI) is a collection of genes that are amongst the duplicates, with the FPI encoding key virulence factors responsible for the pathogenesis of *F. tularensis* (Rohmer *et al.*, 2007). Thus, enhanced expression of these FPI genes could contribute to the virulence of *Francisella*

species in humans. In addition to the differences between pathogenic and non-pathogenic strains, discrepancies exist between *F. tularensis* subsp. *tularensis* and *F. tularensis* subsp. *holarctica*, in that the latter strain possesses a greater number of pseudogenes (defective genes) associated with motility and cellular attachment (Rohmer *et al.*, 2007) – which may help to explain why this strain is less effective in infecting humans and causing disease.

Attempts to further understand the genus of *Francisella* have been significantly impeded over the years. Indeed, isolation and culture of *Francisella* species from the environment is relatively unsuccessful due to overgrowth of other bacterial species on growth media (Öhrman *et al.*, 2021). Moreover, even the most virulent *F. tularensis* subsp. *tularensis* is usually isolated following direct inoculation of environmental samples into animals (Öhrman *et al.*, 2021). Until recently, the intracellular bacterium *Wolbachia persica* was identified as the most closely related bacteria to *Francisella*, before its recent re-classification as a subspecies of *Francisella* (*F. persica*) (Forsman, Sandström and Sjöstedt, 1994; Larson *et al.*, 2016). As of now, it is currently unclear what the most closely related bacteria to *Francisella* is, though *Francisella* species have been identified as members of the gamma subclass of proteobacteria (Forsman, Sandström and Sjöstedt, 1994). This particular subclass encompasses a diverse number of bacterial species, including *Escherichia coli*, as well as *Salmonella, Yersinia,* and *Pseudomonas* species (Williams *et al.*, 2010). It is therefore of interest to further investigate whether *Francisella* shares any common features with these pathogens.

### 1.2.2 Tularaemia

As aforementioned, the more virulent strain of *F. tularensis* is located in North America (Rotz and Hughes, 2004). Despite its high virulence, only 124 cases of human tularaemia were recorded annually between 1990 and 2000 in the USA (Feldman *et al.*, 2003). Moreover, cases of the disease in Europe were also low, with 0.04 cases per 100,000 inhabitants between 2005-2012 (Hestvik *et al.*, 2015). Nevertheless, local outbreaks are possible, exemplified by Finland and Sweden recording 917 and 464 cases in 2000 respectively. Other countries have also experienced outbreaks of human

tularaemia over the years, such as Spain in 2007 (493 cases), Turkey in 2010 (1531 cases), and Norway in 2011 (178 cases) (Hestvik *et al.*, 2015).

Transmission of *F. tularensis* to humans is most commonly attributed to coming into contact with ticks and other arthropods (Boyce, 1975; Morner, 1992; Berdal *et al.*, 1996; Hubalek, Sixl and Halouzka, 1998). However, it is important to note that host species for *F. tularensis* are numerous and diverse, including rabbits, voles and squirrels. The severity of pathology following infection with *F. tularensis* differs according to entry route of the bacterium, with several clinical variants of tularaemia in existence. Ulceroglandular tularaemia is the most common form of the disease, and is contracted subcutaneously, either through vector-borne transmission, or in some cases, direct contact with an infected animal (Sjostedt, 2007). The mortality rate for this form of the disease is less than 3%, and clinical symptoms usually present after an incubation period of 3-6 days. These are generally flu-like symptoms such as fever and headache, with lymphadenopathy also occurring upon dissemination of bacteria through the lymphatics to peripheral organs (Evans *et al.*, 1985; Ohara *et al.*, 1991).

When inhaled however, *F. tularensis* can cause pneumonic tularaemia, which has fatality rates of 30% to 60% if left untreated (Rotz and Hughes, 2004). This form of tularaemia is most often associated with farmers and hunters who come into contact with infected rodents and other small mammals (Stewart, 1996). The symptoms and clinical manifestations of pneumonic tularaemia are highly variable, and often remarkably similar to other illnesses, such as lung cancers, tuberculosis and other pneumonia, which can result in misdiagnosis (Gill and Cunha, 1997; Fachinger *et al.*, 2015; Odegaard, Boersma and Keegan, 2017).

Diagnosis of tularaemia occurs principally through serological tests and staining of tissue sections (Clarridge *et al.*, 1996; Labayru *et al.*, 1999). More specifically, antibodies against *F. tularensis* are detected approximately 2 weeks after the onset of disease by agglutination or enzyme-linked immunosorbent assay (ELISA) (Carlsson *et al.*, 1979; Koskela and Salminen, 1985). Indeed, a capture ELISA using monoclonal antibodies against the lipopolysaccharide (LPS) of *F. tularensis* is capable of recognising all pathogenic strains, with no cross-reactivity across bacterial

species (Grunow *et al.*, 2000). A polymerase chain reaction (PCR)-based assay has also been suggested for use in the diagnosis of tularaemia, with primers against outer membrane protein genes (Grunow *et al.*, 2000). This method is highly sensitive, allowing for detection of as low as $10^2$ CFU/ml in PBS, although optimisation of this method is required due to the presence of compounds in blood which can inhibit a PCR test (Ellis *et al.*, 2002).

For treatment of tularaemia, aminoglycosides (specifically streptomycin and gentamicin), fluoroquinolones (ciprofloxacin and levofloxacin) and the tetracycline doxycycline have all been documented as potential therapeutic strategies, in a situation-dependent manner (Enderlin *et al.*, 1994; Dennis *et al.*, 2001; Johansson *et al.*, 2002). Specifically, streptomycin and gentamicin are the drugs of choice in a contained environment, where patients can be isolated and individually treated (Jacobs and Narain, 1983; Evans *et al.*, 1985; Enderlin *et al.*, 1994; Cross, Schutze and Jacobs, 1995). However, in the event of a larger outbreak or mass infection, a combination therapy of ciprofloxacin and doxycycline is the preferred strategy (Dennis *et al.*, 2001). Despite these existing treatments, attention should still be given to the development of alternative therapeutic strategies, especially considering the rise of anti-microbial resistance, and the potential use of antibiotic-resistant strains in a bioterrorism incident. Thus, an enhanced understanding of the immune response against *F. tularensis* could not only help to achieve this, but also contribute towards the development of an effective vaccine against the bacterium.

### 1.2.3 *F. tularensis* live vaccine strain (LVS)

Despite its inherently infectious nature, and the lethality of type A strains, there is currently no vaccine available at present that is effective on a large scale against *F. tularensis*. There is an attenuated live vaccine strain (LVS) of *F. tularensis*, which is derived from *F. tularensis* subsp. *holarctica* (Elkins, Cowley and Bosio, 2003). However, this strain is not currently licensed for use as a vaccine, due to lack of genetic and molecular explanation for the attenuation (McLendon, Apicella and Allen, 2006). Despite not being used as a vaccine, LVS still presents an attractive alternative to other more virulent Type A *F. tularensis* strains, such as Schu S4, in laboratory research. Indeed, the decreased virulence of LVS means that it can be used at containment

level 2 (CL2), instead of CL3. Combining this comparable ease of use in a laboratory setting, and the lethality of the strain in mice, *F. tularensis* LVS has made significant contributions to furthering our understanding of how *F. tularensis* infection progresses in the host and how an immune response is produced against the bacterium.

In mice, median lethal doses ($LD_{50}$) of LVS differ according to route of infection - reflective of the relative severity of infection with different transmission routes in humans. Indeed, intranasal (i.n.) infection of C57BL/6J mice with LVS potentiates a much lower median lethal dose ($LD_{50}$) than that of an intradermal (i.d.) infection, with $LD_{50}$ values of $1 \times 10^3$ CFU and $1 \times 10^6$ CFU respectively (Cowley and Elkins, 2011). What seems to remain constant however is the dissemination of the bacteria to the liver and spleen (Golovliov *et al.*, 1995; Malik *et al.*, 2006; Roberts *et al.*, 2014). Therefore, when using LVS infection in mice as a model for *F. tularensis* infection in humans, it is important to recognise that differences in the immune response exist according to the route of infection.

### 1.2.4 The life cycle of *F. tularensis* - cellular uptake

*F. tularensis* can infect a wide variety of cells (Hall *et al.*, 2008), and its life cycle is relatively similar across these settings (figure 1.1). As an intracellular bacterium, *F. tularensis* must first enter a host cell to replicate, and this internalisation is dependent upon the opsonisation state of the bacteria. Opsonins are extracellular proteins that facilitate enhanced phagocytosis of pathogens or substances (Taylor *et al.*, 2005). Indeed, opsonised *Francisella* are internalised more easily when compared to non-opsonised bacteria (Ben Nasr *et al.*, 2006; Pierini, 2006; Geier and Celli, 2011).

Several experimental models have proposed different ways in which uptake of the bacterium can occur, and many types of receptor show the potential to facilitate this. For example, the mannose receptor, a C-type lectin receptor, has been shown to play a key role in uptake of non-opsonised bacteria (Schulert and Allen, 2006). Indeed, in support of this, blockade of the mannose receptor with soluble mannan can significantly inhibit the uptake of LVS into monocyte-derived macrophages (MDMs). However, when bacteria are opsonised, uptake is redirected mainly to complement receptors (CRs),

with lesser roles for other receptors such as scavenger receptor A, Fc gamma receptor (FcγR), and surface-exposed nucleolin (Schulert and Allen, 2006). Uptake of opsonised bacteria into individual cell types differs according to CR expression, with CR3 (CD11b/CD18) and CR4 (CD11c/CD18) facilitating uptake of serum-opsonised LVS into macrophages (Schwartz *et al.*, 2012) and dendritic cells (DCs) (Ben Nasr *et al.*, 2006), CR1 (CD35) and CR3 into neutrophils (Schwartz *et al.*, 2012), and CR1/2 (CD35/CD21) into B cells (Plzakova *et al.*, 2015). Taken together, this demonstrates that *F. tularensis* is taken up by an assortment of host cell types, and by numerous mechanisms.

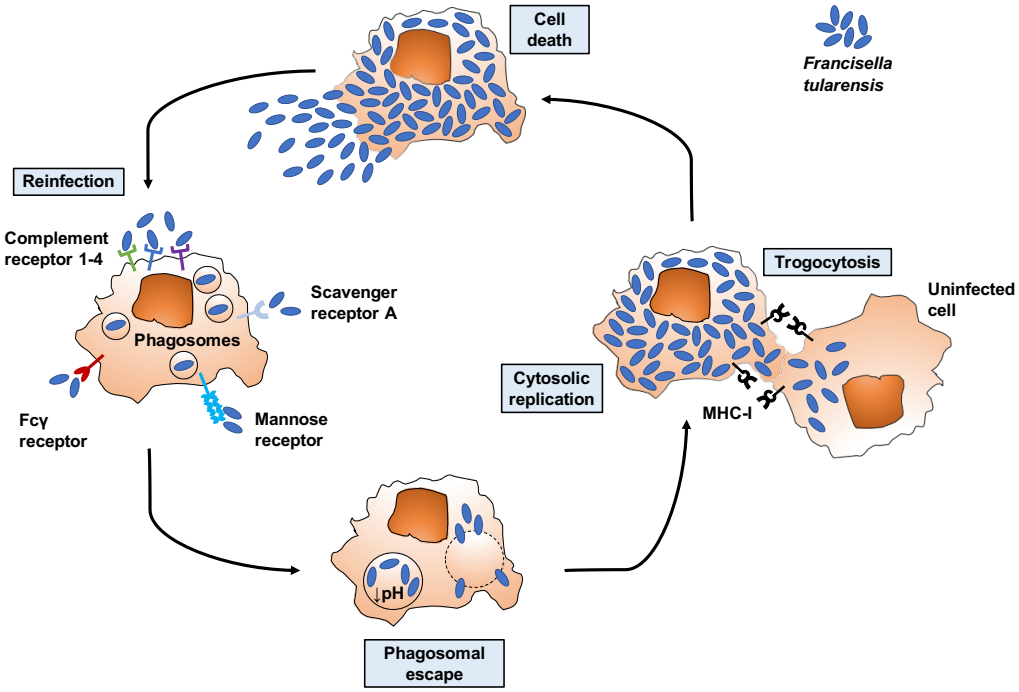


**Figure 1.1 - The life cycle of *Francisella tularensis*.**

The intracellular bacterium *Francisella tularensis* (*F. tularensis*) is initially taken up into the cell through the process of looping phagocytosis into a phagosomal compartment. Uptake is dependent on opsonisation state of bacteria, but can occur through a variety of receptors, such as complement receptors 1-4, scavenger receptor A, Fcγ receptor, and mannose receptor. Once inside the cell, *F. tularensis* utilises a type 6 secretion system (T6SS) to escape the phagosomal compartment within 1-4 hours. Alongside this, *F. tularensis* employs multiple other mechanisms to aid its escape including inhibition of lysosomal fusion, disruption of the phagosomal membrane, and lowering the internal pH of the phagosome. Bacteria then proliferate extensively in the cytosol, culminating in cell death and the release of bacteria to infect other cells. *F. tularensis* can also be transferred between live cells through a process known as trogocytosis. Here, bacteria are transferred, along with fragments of the plasma membrane, to uninfected cells. This process involves acquisition of major histocompatibility complex I (MHC-I). Figure adapted from Chong and Celli (2010).

Despite the numerous receptors that facilitate uptake of *F. tularensis*, and the numerous cell types that display this ability, the principal cell type that is infected during early infection is the macrophage. *F. tularensis* uptake here is mediated by a process known as looping phagocytosis, which involves engulfment of the bacterium by a spacious, asymmetric pseudopod loop which eventually forms a smaller vacuole (Clemens and Horwitz, 2007). Other more general mechanisms of entry have been observed in other cell types, such as macropinocytosis in type II alveolar epithelial cells (Bradburne *et al.*, 2013). Irrespective of the method of cellular uptake, the bacterium is then enclosed in a phagosome, referred to as a *Francisella*-containing phagosome (FCP).

### 1.2.5 Escape from the phagosome and cytosolic replication

Like most phagosomes, the FCP is a vacuolar compartment that is part of a pathway that constitutes progressive maturation into a bactericidal phagolysosome. The FCP acquires both early and late endosomal markers in a sequential manner, such as Rab-5 and early endosome antigen 1 (EEA1) (Chong *et al.*, 2008), lysosomal-associated protein 1 (LAMP-1) and LAMP-2, Rab7 and mannose-6-phosphate, indicative of a normal maturation process (Santic *et al.*, 2005; Santic *et al.*, 2008; Celli and Zahrt, 2013). Yet importantly, the FCP does not mature into a phagolysosome, and therefore avoids degradation, as shown with an absence of lysosomal luminal hydrolases, such as Cathepsin D (Clemens, Lee and Horwitz, 2004). Much debate surrounds the mechanism by which *F. tularensis* escapes from the FCP. Indeed, differences often arise as a result of variations in opsonization state of the bacterium. For example, non-opsonised *Francisella* bacteria escape the phagosome rapidly, within 1 hour post-infection, whereas opsonized *Francisella* seems to exhibit a delayed escape of 2 to 4 hours (Golovliov *et al.*, 2003).

Controversy exists between studies with regards to the overall need for acidification of the FCP for bacterial escape into the cytosol. It has been shown that only 20-30% of phagosomes containing serum-opsonised LVS are acidified, and that this is not necessary for escape, or for replication (Clemens, Lee and Horwitz, 2009). However, for non-opsonised bacteria, this acidification appears essential for rapid escape into the cytosol (30

minutes to 1 hour post infection) (Santic *et al.*, 2008). Indeed, inhibition of the vacuolar proton ATPase (vATPase) pump by bafilomycin A has been shown to delay escape (Santic *et al.*, 2008; Chong *et al.*, 2008). Of note is that experiments demonstrating the need for acidification in rapid phagosomal escape of non-opsonised bacteria used *F. novicida*, and not *F. tularensis* LVS.

Irrespective of a role for acidification in phagosomal escape, the early response of *Francisella* in the phagosome involves upregulation of genes associated with oxidative stress response, possibly through sensing of intraphagosomal ROS (Wehrly *et al.*, 2009). However, in order to facilitate its escape from the phagosome, several other genes known as virulence factors are upregulated by the bacterium. Amongst these is a cluster of genes known as the *Francisella* Pathogenicity Island (FPI) (Mougous *et al.*, 2006; Nano and Schmerk, 2007). The FPI encodes a group of proteins known as the type 6 secretion system (T6SS), which is regarded as a highly conserved means of facilitating intracellular replication. Indeed, it has also been observed in other clinically relevant pathogens, such as *Vibrio cholera* and *Pseudomonas aeruginosa* (Mougous *et al.*, 2006; Bingle, Bailey and Pallen, 2008; Bonemann, Pietrosiuk and Mogk, 2010).

Whilst many proteins in the T6SS appear essential for *F. tularensis* phagosomal escape and intracellular growth, one particular protein in this group is of great interest - intracellular growth locus E (IglE). Out of the 17 FPI proteins of *F. tularensis* LVS, IglE is the most highly secreted during intracellular infection (Broms *et al.*, 2012), and is conserved across all species of *F. tularensis*. In an *in vitro* model, LVS Δ*iglE* mutants fail to escape from phagosomes, and therefore have reduced ability to multiply and cause cytopathogenicity. Moreover, in intradermal infection, an Δ*iglE* mutant showed a reduced ability to activate the inflammasome, and failed to inhibit LPS-stimulated secretion of TNF-α when compared to wild type (WT) LVS bacteria (Bröms, Meyer and Sjöstedt, 2017). Thus, these results demonstrate the importance of IglE in the pathogenesis of *F. tularensis*.

Once in the cytosol, *F. tularensis* can replicate up to 1000-fold, with the amino acid cysteine proving essential for replication in all subspecies. However, *F. tularensis* must exit the cell in order to facilitate its

dissemination. This has been suggested to occur by multiple mechanisms, and in a strain-specific manner. For example, whilst *F. novicida* induces pyroptosis (Mariathasan *et al.*, 2005), both *F. tularensis* LVS and SchuS4 appear to induce either apoptosis or oncosis in macrophages (Lai, Golovliov and Sjostedt, 2001; Lai and Sjostedt, 2003; Wickstrum *et al.*, 2009; Lindgren *et al.*, 2013; Jessop *et al.*, 2018). Thus, this highlights the complexity of host cell death mechanisms during infection with different strains of *F. tularensis*.

### 1.2.6 Cell-to-cell transmission

Whilst induction of cell death is one way in which *F. tularensis* can escape the cytosol to infect new host cells, it can also achieve this through direct cell-cell transfer of bacteria and fragmented plasma membrane between two live cells in a process known as trogocytosis (Steele *et al.*, 2016). Indeed, this process is upregulated in infected cells, and is associated with exchange of major histocompatibility complex 1 (MHC-1) (Steele *et al.*, 2016). Upon transfer, *F. tularensis* is enclosed in a double membrane vesicle, which it is able to escape through use of the T6SS (Steele *et al.*, 2019). Overall, this indicates an alternative and effective way in which *F. tularensis* can disseminate to other cells, resulting in extensive replication.

### 1.2.7 Innate immune recognition

After physical barriers, the innate immune response represents an important line of defence against *F. tularensis* during early infection. In this section, the current understanding of these mechanisms is introduced. Specifically, evidence for both cell surface and intracellular recognition of the bacterium will be explored, and how the host immune response against *F. tularensis* is subverted to dampen a potential pro-inflammatory immune response in these settings.

#### 1.2.7.1 Complement system

As aforementioned, complement is vital for the recognition of *F. tularensis*, with enhanced phagocytosis being a hallmark of recognition through this pathway. Indeed, CR3 and CR4 are crucial for phagocytosis of LVS by macrophages and DCs (Ben Nasr *et al.*, 2006; Ben Nasr and Klimpel, 2008). Importantly however, complement-mediated killing of *F. tularensis* is subverted through recruitment of factor H (fH) to the bacterial cell surface

(Ben Nasr and Klimpel, 2008). This complement regulator inhibits amplification of the complement cascade through conversion of C3b to iC3b, and prevents the formation of the bactericidal membrane attack complex (MAC) on the surface of *F. tularensis* (Ben Nasr and Klimpel, 2008). Thus, the way in which *F. tularensis* is recognised by the complement system provides an example of how the bacterium can facilitate its pathogenesis through perturbing the host immune response.

#### 1.2.7.2 Pattern recognition receptors (PRRs)

Pattern recognition receptors (PRRs) are a fundamental part of innate immune recognition against any pathogen, and are found both on cell surfaces and intracellularly. Indeed, the host immune system can recognise gram-negative bacterial pathogens through the lipid A anchor portions of lipopolysaccharide (LPS) expressed on their outer membranes. Normally, host immune cells recognise this through toll-like receptor (TLR)4, leading to a robust pro-inflammatory immune response (Trent *et al.*, 2006). Despite this, $TLR4^{-/-}$ mice display no significant differences in IFN-γ or interleukin-12p40 (IL-12p40) levels when compared to WT counterparts following either intranasal or intradermal LVS infection (Chen *et al.*, 2004a; Chen *et al.*, 2005b). Furthermore, survival rates did not differ between WT and $TLR4^{-/-}$ mice in intranasal LVS infection, irrespective of dosage (Chen *et al.*, 2004a), suggesting that TLR4 may not be as critical in the immune response against *F. tularensis*.

Interestingly, *F. tularensis* possesses a modified LPS, which may help to explain the dispensability of TLR4 in the response against the bacteria. Specifically, the lipid A portion of *F. tularensis* possesses only three acyl chains instead of six, longer fatty acid chains and no phosphate groups (Phillips *et al.*, 2004). This modified LPS appears to instead divert host cell recognition of *F. tularensis* to TLR2 – a TLR which is commonly associated with recognition of bacterial lipoproteins (Oliveira-Nascimento, Massari and Wetzler, 2012). In the context of infection with *F. tularensis* LVS, TLR2-deficient mice display increased susceptibility following either intranasal or intradermal challenge. Moreover, these mice exhibit impaired macrophage-derived production of TNF-α and IL-6, and a reduced ability to control both the growth of LVS and its dissemination (Abplanalp *et al.*, 2009). Thus, these

data indicate that TLR2 appears to be important in initiation of the immune response against *F. tularensis*.

Several other PRRs are important in recognition of *F. tularensis*, including RIG-I-like receptors (RIRs) and cytosolic DNA receptors (CDRs) (Kumar, Kawai and Akira, 2011; Putzova *et al.*, 2017). Despite this, the downstream effector functions of these receptors can be inhibited through preventing the formation of TRAF3 and TRAF6 complexes (Putzova *et al.*, 2017) - immune complexes that are critical points of control for the transcriptional induction of innate immune mediators and pro-inflammatory cytokines in PRRs (Hacker *et al.*, 2006). Here, this inhibition appears to occur by use of the bacteria's T6SS, and inhibiting the polyubiquitination of TRAF3 and TRAF6, as an LVS mutant defective in the T6SS demonstrates higher polyubiquitination of these immune complexes. Thus, this suggests that multiple PRR pathways can be simultaneously inhibited during infection with *F. tularensis*.

Downstream of multiple TLRs, including TLR2, is the adaptor protein MyD88, which is critical for activation of pro-inflammatory pathways such as NF-κB and MAPK. Mice that are deficient in MyD88 exhibit an altered phenotype to their WT counterparts in the context of both intranasal and intradermal infection. Indeed, like TLR2-deficient mice, MyD88-deficient mice are more susceptible to infection, display increased dissemination of bacteria, a failure to control the growth of LVS in macrophages, as well as a marked reduction in TNF-α and IL-6 in these cells (Abplanalp *et al.*, 2009). Thus, this indicates the importance of this pathway in the control of infection with *F. tularensis*. As aforementioned, MyD88 is also downstream of other TLRs. Despite this, no changes in susceptibility are observed in mice lacking the MyD88-dependent TLRs TLR1, TLR4, TLR6 and TLR9 (Collazo *et al.*, 2006; Abplanalp *et al.*, 2009), indicating the dispensability of these other TLRs in the response against *F. tularensis* and the importance of the TLR2-MyD88 pathway.

#### 1.2.7.3 Alveolar epithelial cells in *F. tularensis* infection

Given their location, alveolar epithelial cells are well-positioned to interact with *Francisella* bacteria during early pulmonary infection, with invasion of

type II alveolar epithelial (ATII) cells demonstrated by multiple groups (Hall *et al.*, 2007; Lindemann *et al.*, 2007; Craven *et al.*, 2008). Following stimulation with *F. tularensis*, primary human ATII cells produce high levels of the neutrophil and monocyte chemoattractants IL-8 and monocyte chemotactic protein (MCP)-1 respectively (Gentry *et al.*, 2007). More recently, murine lung epithelial cells have been shown to inhibit intracellular growth of *F. tularensis* species both *in vitro* and *in vivo* through the induction of iNOS (Maggio *et al.*, 2015). Thus, this indicates that whilst alveolar epithelial cells can serve as an early replicative niche for bacteria, they may also play a key role in the early immune response against *F. tularensis*.

### 1.2.8 Innate immune response in *F. tularensis* infection

#### 1.2.8.1 Macrophages

Several *in vitro* models have demonstrated that *F. tularensis* LVS is able to replicate in a wide variety of murine macrophage populations, including alveolar, peritoneal and bone marrow-derived macrophages (Anthony, Burke and Nano, 1991; Polsinelli, Meltzer and Fortier, 1994), which can lead to the induction of apoptosis (Lai and Sjostedt, 2003). For the first 24 hours post-intranasal infection, alveolar macrophages (AM; which represent over 90% of all leukocytes in the alveolar lumen) are the primary target for intracellular infection (Hall *et al.*, 2008; Snelgrove, Godlee and Hussell, 2011). Several studies have attempted to investigate the importance of AMs as an infectious niche for bacteria during early infection, with contrasting results. Indeed, the infectious outcome following clodronate-induced depletion of AMs appears to be dependent on the infectious dose of bacteria. AM-depleted mice given a lethal dose of *F. tularensis* LVS via the intranasal route display decreased lung burdens up to 3 days post-infection (p.i.) (Bosio and Dow, 2005), whereas administration of a sub-lethal dose results in enhanced susceptibility to infection (Steiner *et al.*, 2017). Thus, this highlights the importance of infectious dose in determining the role of this cell type during infection with *F. tularensis* LVS.

Once inside the cell, *F. tularensis*-infected macrophages begin to display elements of an alternative activation state through upregulation of markers such as Arginase-1, Ym1 and FIZZ1 (Shirey *et al.*, 2008). Moreover, mice

deficient in the IL-4 receptor α chain (which is an integral subunit of both the IL-4 and IL-13 receptor complexes) exhibit classical activation through upregulation of IL-12p70, and these mice display enhanced survival following a typically lethal intraperitoneal (I.P.) dose of *F. tularensis* LVS (Shirey *et al.*, 2008). Thus, this indicates that the immune response of infected macrophages is perturbed from a more beneficial pro-inflammatory cytokine production, and instead appears to benefit the pathogenesis of *F. tularensis*.

#### 1.2.8.2 Monocytes

Monocytes are another immune cell type that are involved in the host immune response against *F. tularensis* (Hall *et al.*, 2008). For example, human monocytes infected with the more virulent *F. tularensis* Schu S4 strain show reduced production of TNF-α and IL-6, and a downregulation of transcripts for TLR2 and its co-receptor CD14 when compared to uninfected cells (Butchar *et al.*, 2008), indicating that elements of a pro-inflammatory host immune response may also be impeded in this cell type. Essential for monocyte migration from the bone marrow to sites of bacterial infection is the chemokine receptor CCR2 (Serbina, Shi and Pamer, 2012). Following intravenous infection, $CCR2^{-/-}$ mice exhibit a reduced expansion of a splenic monocyte population, and increased bacterial burdens in the spleen when compared to WT mice (Pietras *et al.*, 2011), suggesting their importance in control of bacterial burdens in this organ. Another chemokine receptor associated with monocyte trafficking, CX3CR1, has been shown to be involved in infection with *F. tularensis* LVS (Hall *et al.*, 2009). During intranasal infection with *F. tularensis*, $CX3CR1^{-/-}$ mice display no differences in bacterial burdens (Hall *et al.*, 2009). Despite this, they display an enhanced recruitment of monocytes into the lung tissue when compared to WT counterparts (Hall *et al.*, 2009). Nevertheless, it is important to note that both CCR2 and CX3CR1 are not selectively expressed on monocytes. Thus, further studies are required in order to fully understand the importance of monocytes in pathogen clearance.

#### 1.2.8.3 Dendritic Cells

Dendritic cells represent an critical step in priming the adaptive immune response through antigen presentation – with their maturation and migration

to draining lymph nodes proving vital to their function (Hilligan and Ronchese, 2020). With this in mind, they also represent a possible means of bacterial dissemination. During the first few days of infection with *F. tularensis*, the number of infected dendritic cells (DCs) remains relatively constant (~10%) (Hall *et al.*, 2008). *F. tularensis* LVS infection promotes the early maturation of airway DCs within 24 hours of infection, indicated by an upregulation of cell surface markers such as MHC-II and CD86 (Bosio and Dow, 2005). Moreover, intranasal infection results in enhanced production of IL-12 in DCs when compared to those of untreated mice, and facilitates their migration to draining lymph nodes (Slight *et al.*, 2011). Indeed, this has been implicated as a method of bacterial dissemination and progression of infection, and is exemplified elsewhere with use of the sphingosine-1-phosphate receptor agonist FTY720. Here, the number of infected DCs and bacterial burden as a whole in the draining lymph node are significantly reduced in FTY720-treated mice when compared to untreated counterparts (Bar-Haim *et al.*, 2008). Thus, whilst they represent a relatively small proportion of the infected cell population during infection with *F. tularensis*, DCs may serve as a key component in facilitating the pathogenesis of the bacterium during early infection. However, it is important to note that these data did not examine how bacterial burdens were affected in peripheral organs following FTY720 treatment. Thus, it remains to be seen whether this is the only way in which *F. tularensis* can disseminate to other organs – especially considering another study has identified that bacteria are present in the blood of infected animals, and have thus hypothesised that *Francisella* could also disseminate to other organs by this route (Ojeda *et al.*, 2008).

#### 1.2.8.4 Neutrophils

The influx of neutrophils to sites of inflammation is a process associated with a wide variety of infections (Craig *et al.*, 2009). True to this, intranasal infection with *F. tularensis* LVS results in extensive recruitment of neutrophils to the lung early in infection, with neutrophils representing the major infected cell type by day 3 p.i. (Hall *et al.*, 2008). Once at these sites of inflammation, neutrophils can capture and kill pathogens using neutrophil extracellular traps (NETs) and reactive oxygen species (ROS) (Nguyen, Green and Mecsas, 2017; Brinkmann, 2018). Despite this, whilst they can trap the bacteria, NETs exert no bactericidal effects on *F. tularensis* and instead

contribute to lung pathology (Pulavendran *et al.*, 2020). Once internalised, *F. tularensis* is able to escape the phagosome and evade ROS-mediated killing through disruption of NADPH oxidase assembly (McCaffrey and Allen, 2006; McCaffrey *et al.*, 2010). Thus, the inability of neutrophils to carry out their effector function during infection with *F. tularensis* instead allows for extensive cytosolic replication within neutrophils, suggesting that these cells could serve as a replicative niche as infection progresses.

In order to understand the overall role of neutrophils in control of infection with *F. tularensis* LVS, the effects of their depletion have been investigated in this context. Of note, the route of infection greatly affects the infectious outcome in neutrophil-depleted mice. When infected either intravenously or intradermally, neutrophil-depleted mice succumb to an otherwise sub-lethal dose of *F. tularensis* LVS (Sjöstedt, Conlan and North, 1994; Conlan *et al.*, 2002). In an intranasal model of infection, only a minor increase in bacterial burden is observed in peripheral organs, with no effect on lung burdens observed in neutrophil-depleted mice (Conlan *et al.*, 2002). Interestingly however, if depleted at day 3 p.i. instead of the day of infection, mice display enhanced mortality – indicating that the timing of neutrophil depletion plays an important role in infectious outcome (Steiner *et al.*, 2017).

If dysregulated, the immune response against *F. tularensis* can be significantly impeded. In the context of neutrophils, this appears to be at least in part through a receptor involved in immune regulation. CD200 receptor (CD200R) is a negative immune regulator, which is prominently expressed on neutrophils and alveolar macrophages (Wright *et al.*, 2003). Following intranasal infection, $CD200R^{-/-}$ mice display enhanced bacterial burden. Interestingly, this is associated with both enhanced influx and infection of neutrophils, and defective neutrophil-derived ROS production (Casulli *et al.*, 2019). Overall, this suggests that immune regulation via the CD200R pathway may play an important role in control of bacterial infection in neutrophils.

#### 1.2.8.5 Natural killer cells

During infection with *F. tularensis*, natural killer (NK) cells represent one of the primary sources of IFN-γ (Lopez *et al.*, 2004; De Pascalis, Taylor and

Elkins, 2008). Following intranasal infection with LVS, NK cells are among the first cells recruited to the lungs, and can secrete IFN-γ by 72 hours post-infection (Lopez *et al.*, 2004; Baron, Singh and Metzger, 2007). Interestingly, *in vivo* priming of NK cells with bacterial deoxyribonucleic acid (DNA) reduces replication of *F. tularensis* in macrophages, with this effect reversed by antibody-mediated blockade of IFN-γ and TNF-α (Elkins *et al.*, 2009). Thus, these data suggest a critical role for NK cell-derived IFN-γ in limiting early infection with *F. tularensis*.

Like other cell types, antibody-mediated depletion of NK cells has sought to enhance our understanding of these cells during infection with *F. tularensis*. Anti-asialo GM1 antibody-mediated depletion of NK cells results in no difference in lung bacterial burdens following intradermal infection with *F. tularensis* LVS (Bokhari *et al.*, 2008). Yet following intranasal infection, depletion results in a reduction in IFN-γ-secreting cells and enhanced mortality (Lopez *et al.*, 2004). More recently, NK cells have been depleted using an anti-NK1.1 antibody during infection with the more virulent Schu S4 strain of *F. tularensis*. Despite a reduction in total IFN-γ and granzyme B production in the lung, bacterial burdens remain unchanged (Schmitt *et al.*, 2013). Overall, whilst these studies present varying findings, it is important to consider that depletion methods used do not selectively deplete NK cells, and impact upon other immune cell types such as basophils (anti-asialo GM1), and NKT cells and ILC1s (anti-NK1.1) (Nishikado *et al.*, 2011; Hill *et al.*, 2015; Jiao *et al.*, 2016). Thus, more specific methods of depletion are required in order to dissect these discrepancies and create an enhanced understanding of the overall importance of NK cells during infection with *F. tularensis*.

### 1.2.9 Adaptive immune response in *F. tularensis* infection

The role of adaptive immunity in primary pulmonary infection with *F. tularensis* has been studied much less, mainly due to the fact that mice succumb to lethal doses of *F. tularensis* prior to its total development (Roberts, Powell and Frelinger, 2018). However, sub-lethal intranasal infection results in enhanced production of IL-17 from $CD4^+$ T cells and IFN-γ from both $CD4^+$ and $CD8^+$ T cells at day 7 post-infection onwards (Woolard *et al.*, 2008). Moreover, using a model of low dose antibiotic therapy that

maintains a low CFU level during pulmonary infection with *F. tularensis* Schu S4, the importance of αβ T cells in control of infection has been shown. Here, $\alpha\beta TCR^{-/-}$ mice succumb to infection after antibiotic treatment was halted, unlike their WT counterparts (Crane, Scott and Bosio, 2012). Conversely, no differences in the susceptibility of both thymectomised (removal of the thymus, and thus no T cell development) and SCID (deficient in functional T and B cells) mice are observed following intranasal challenge with both type A and type B strains of *F. tularensis* (Chen *et al.*, 2004b). Worthy of note however, is that virulent type A *F. tularensis* depletes lung αβ T cells and induces thymic atrophy (Chen *et al.*, 2005a), indicating that T cell-mediated immunity may be affected during pulmonary infection with *F. tularensis*.

Whilst *F. tularensis* is an intracellular pathogen, part of its life cycle involves an extracellular phase, exposing itself to the antibody response. Despite this, B cell-deficient mice are no more susceptible to primary intranasal or intradermal infection than WT mice (Chen *et al.*, 2004b). It may be that the role of B cells during primary infection with *F. tularensis* is focused more on their ability to internalise the bacteria through the B cell receptor. Indeed, *F. tularensis* can replicate effectively inside B cells, and induce host cell apoptosis in order to continue its life cycle, akin to its behaviour in many other innate immune cell types (Krocova *et al.*, 2008; Plzakova *et al.*, 2015). Overall, this suggests that whilst B cells appear dispensable for control of early infection, they may serve as another site for replication of *F. tularensis*, indicating the highly infectious nature of this pathogen.

### 1.2.10 Pro-inflammatory cytokines during *F. tularensis* infection

Like many intracellular pathogens, a type 1 immune response against *F. tularensis* is important in combatting the infection, involving production of cytokines such as IFN-γ and TNF-α (Celli and Zahrt, 2013). Interestingly, the route of infection impacts significantly on the time required for the production of these cytokines (Stenmark *et al.*, 1999; Lopez *et al.*, 2004). For example, detectable levels of both TNF-α and IFN-γ mRNA can be found in the skin 24 hours after intradermal infection with *F. tularensis* LVS, with levels rising significantly by 48 hours post-infection (Stenmark *et al.*, 1999). However, following intranasal infection with lethal doses of LVS (1000 CFU), an increased level of IFN-γ production can only be seen by 72 hours post-

infection in lung lymphocytes (Lopez *et al.*, 2004; Duckett *et al.*, 2005). Moreover, use of a sub-lethal dose of LVS in intranasal infection has demonstrated that levels of IFN-γ are delayed to as late as day 7 post-infection, and never reach those observed following a sub-lethal dose administered by the intradermal route (Woolard *et al.*, 2008). Thus, this suggests that the immune response is significantly perturbed in pulmonary infection with *F. tularensis*.

Despite the route of infection impacting on the timing of their release, both IFN-γ and TNF-α are critical for host survival during infection with *F. tularensis*. Indeed, both IFN-γ and TNF-α KO mice exhibit enhanced lung bacterial burdens following pulmonary infection when compared to WT mice (Elkins *et al.*, 1996; Chen *et al.*, 2004b; Duckett *et al.*, 2005). The importance of IFN-γ in infection with *F. tularensis* has also been demonstrated through several other experimental models. In an *in vitro* model, alveolar macrophages that are treated with recombinant IFN-γ prior to LVS infection display the ability to eliminate the bacteria by 48 hours post-infection, differing greatly from those that are left untreated, in which bacteria replicate continuously for over 5 days (Polsinelli, Meltzer and Fortier, 1994). Mice given an intravenous dose of recombinant IFN-γ prior to intravenous infection with LVS display enhanced resistance to infection, accompanied by significant reductions in bacterial burden when compared to untreated mice (Anthony and Kongshavn, 1988). In addition to this, neutralisation of IFN-γ and TNF-α with monoclonal antibodies subsequently renders mice susceptible to an otherwise sub-lethal intravenous dose of LVS (Sjostedt, North and Conlan, 1996).

Another important cytokine in the type 1 immune pathway and defence against *F. tularensis* infection is IL-12. IL-12 is a heterodimer, consisting of two subunits, p35 and p40. This cytokine is crucial in upregulation and differentiation of naïve $CD4^+$ T cells to Th1 cells which are known to produce IFN-γ – as well as IFN-γ production by NK cells and ILC1s (Trinchieri, 2003; Spits *et al.*, 2013). The protective role of IL-12 during LVS infection has been well documented, with mice deficient in either IL-12 subunit succumbing to an otherwise sub-lethal intranasal infection (Duckett *et al.*, 2005). Moreover, WT mice treated with exogenous IL-12 prior to infection survive an otherwise lethal intranasal dose of LVS, with IFN-γ proving critical for this protection

(Duckett *et al.*, 2005). Indeed, the protective effects of IL-12 are abrogated in IFN-$\gamma^{-/-}$ mice (Duckett *et al.*, 2005), indicating an interplay between these two cytokines during infection with *F. tularensis*. Additionally, signalling through the IL-12 receptor (IL-12R) is important in the control of infection with *F. tularensis*. Both intranasal and intradermal infection with *F. tularensis* LVS causes lethal infection at significantly lower infectious doses in mice that lack the β2 subunit of the IL-12R (IL-12Rβ2) when compared to WT mice (Melillo, Foreman and Elkins, 2013). Thus, this highlights this cytokine and its signalling pathway as an important component of the pro-inflammatory response against *F. tularensis*.

IL-17 has also been suggested to be important in the immune response against *F. tularensis*. Indeed, intranasal LVS infection results in detectable levels of the cytokine at day 3 post-infection, which contributes to the induction of IL-12p40 and IFN-γ production by DCs and macrophages (Lin *et al.*, 2009). Moreover, at peak infection on day 7, IL-17-deficient mice show enhanced bacterial burdens in the lungs, liver and spleen following inoculation via the intranasal route when compared to WT mice (Cowley *et al.*, 2010). However, during intradermal infection, IL-$17^{-/-}$ mice produced no significant difference in bacterial growth in the lung and liver, and only a marginal increase in the spleen versus their WT counterparts (Cowley *et al.*, 2010). At first, induction of IL-17 during LVS infection was proposed to occur via IL-23-dependent mechanisms (Lin *et al.*, 2009). However, deletion of the IL-23 p19 subunit in mice produced no change in the immune response against LVS (Kurtz *et al.*, 2014), suggesting induction of this pathway occurs independently of IL-23.

Research has also identified IL-6 as a cytokine involved in the immune response against *F. tularensis*. During intradermal infection, IL-6 can be detected in liver homogenates by day 1, with a peak by day 3 post-infection. Moreover, IL-6-deficient mice show significantly decreased survival following intranasal infection when compared to WT mice, with reduced $LD_{50}$ levels and enhanced bacterial burden in the lungs, liver and spleen (Kurtz *et al.*, 2013). Taken together, these data indicate that IL-6 is an important effector molecule in immune response against *F. tularensis*.

### 1.2.11 Type 2 cytokines

Whilst much research has focused on the role of typically type 1-based pro-inflammatory cytokines, type 2 cytokines have also been studied in infection with *F. tularensis*, albeit to a lesser extent. IL-4, IL-5 and IL-13 all appear to be upregulated early during intranasal infection, as shown by analysis of mRNA transcript kinetics in pulmonary lymphocytes (Markel *et al.*, 2010). This early increase then returns to control levels by day 6 post-infection (Markel *et al.*, 2010). Yet, despite these observed increases in type 2 cytokine mRNA transcripts, no detectable differences are observed at the level of protein expression (Markel *et al.*, 2010). Indeed, mice treated with an anti-IL-4 monoclonal antibody prior to intradermal LVS infection show no difference in susceptibility to infection or survival (Leiby *et al.*, 1992).

As aforementioned, macrophages adopt an alternative activation state during infection with *F. tularensis* (Shirey *et al.*, 2008). When infected with *F. tularensis* LVS through the intraperitoneal route, this is prevented in mice deficient for the IL-4 receptor (IL-4Rα$^{-/-}$) – with these mice exhibiting increased survival compared to WT mice (Shirey *et al.*, 2008). However, when subject to intranasal infection, IL-4Rα$^{-/-}$ mice display significantly increased susceptibility to infection in comparison to WT mice. IL-4Rα$^{-/-}$ mice also displayed elevated bacterial burden in lung and spleen at day 3 post-infection, although these differences did not continue up to day 6 (Ketavarapu *et al.*, 2008). Hence, IL-4 appears to play a critical route-dependent role in the immune response against *F. tularensis*, with this proving detrimental to control of early pulmonary infection.

### 1.2.12 Regulatory cytokines

Much controversy remains over the role of regulatory cytokines in the immune response against *F. tularensis*. One such cytokine that has been documented to be involved in this initial suppression of the immune response is IL-10. This cytokine is typically produced by regulatory T cells (Treg) and other CD4$^{+}$ T cells, functioning to suppress self-harmful inflammatory responses, often by modulating pro-inflammatory cytokine production (Ouyang and O'Garra, 2019).

Interestingly, IL-10$^{-/-}$ mice are more susceptible to intranasal infection when compared to WT mice (Metzger, Salmon and Kirimanjeswara, 2013), suggesting that this cytokine may prevent an exacerbated inflammatory response during pulmonary infection with *F. tularensis*. Despite this, IL-10$^{-/-}$ mice show enhanced survival following subcutaneous infection with a lethal dose of LVS - with the same dose killing WT counterparts within 9 days of infection. Indeed, IL-10$^{-/-}$ mice eventually cleared this subcutaneous infection (Metzger, Salmon and Kirimanjeswara, 2013). Moreover, IL-10$^{-/-}$ mice show enhanced levels of IL-17 in their spleens following intradermal infection – a phenomenon that is not observed in WT mice, indicating an IL-10-mediated regulation of the host immune response against *F. tularensis* (McKinstry *et al.*, 2009). Indeed, levels of IL-10 mRNA can be observed at day 1 post-intradermal infection with *F. tularensis* LVS, with subsequent increases in protein levels observed at day 3 (Metzger, Salmon and Kirimanjeswara, 2013). Overall, this indicates that the role of IL-10 in *F. tularensis* infection is route-dependent.

Alongside IL-10, another cytokine that is essential in regulation of the immune response is TGF-β. TGF-β is pleiotropic in nature, with one important role being the regulation of pulmonary homeostasis. In the lung, latent TGF-β is activated by the integrin αvβ6, which is expressed on bronchial and alveolar epithelial cells (Munger *et al.*, 1999). Thus, the importance of the cytokine in maintenance of pulmonary homeostasis has been demonstrated through mice deficient in the β6 subunit of integrin αvβ6. Here, these KO mice develop an age-related emphysema, which can be rescued through transgenic expression of TGF-β (Morris *et al.*, 2003).

Again however, studies have shown conflicting results on the role of this regulatory cytokine in the context of *F. tularensis* infection. Mice infected with LVS through the intratracheal route showed a significant increase in TGF-β secretion (Bosio and Dow, 2005), with results elsewhere displaying similar increases in TGF-β levels 24 hours post-intranasal infection (Periasamy *et al.*, 2011). Despite this, no differences in bacterial burdens are observed between isotype- and anti-TGF-β antibody-treated mice infected with the more virulent SchuS4 strain of *F. tularensis* (Bosio, Bielefeldt-Ohmann and Belisle, 2007). Thus, this suggests that despite an enhanced level of TGF-β

during infection, this cytokine appears to be dispensable for the immune response against *F. tularensis*.

Above all, *F. tularensis* represents a complex intracellular pathogen, capable of rapidly infecting a variety of immune cells, replicating extensively, and disseminating to multiple organs within days of infection. Yet, whilst initially benefiting bacterial pathogenesis, this later results in multi-organ failure, sepsis and death of the host (Mares *et al.*, 2008; Sharma *et al.*, 2011). It is therefore essential to further understand the early immune response against *F. tularensis* in order to improve the outcome for the host following infection. Now, a family of tissue-resident innate immune cells, known as innate lymphoid cells (ILCs) are becoming increasingly important in the early immune response against a wide variety of immunological challenges (Vivier *et al.*, 2018). However, the role of ILCs in the immune response against *F. tularensis* is yet to be considered. Thus, given their function as pre-primed effector cells which are capable of rapid cytokine production, understanding the role that ILCs play during early infection with *F. tularensis* is of paramount importance.

### 1.3 Innate lymphoid cells (ILCs)

ILCs represent an innate lymphocyte population that are analogous to $CD4^+$ T helper cell subsets in their phenotype and effector functions. Group 1 ILCs (ILC1s) have been compared to Th1 cells in their expression of T-bet and ability to produce IFN-γ; group 2 ILCs (ILC2s) are akin to Th2 cells with expression of GATA3 and secretion of type 2 cytokines such as IL-5 and IL-13; and group 3 ILCs (ILC3s) are comparable to Th17 cells with expression of RORγt, and their secretion of IL-17 and IL-22 (Spits and Cupedo, 2012; Spits *et al.*, 2013). ILCs are defined by three characteristics. First, they are of lymphoid origin and arise from a common lymphoid progenitor (CLP). Second, they are defined by a lack of classical immune lineage markers, and expression of IL-7 receptor (IL-7R); and finally, they lack antigen receptors, and thus unlike other lymphoid cells, do not undergo clonal selection or recombination activating gene (RAG)-dependent rearrangement of antigen receptors, and lack antigen specificity (Spits and Cupedo, 2012; Spits *et al.*, 2013). All ILCs require the common cytokine receptor γ-chain for their

development and maintenance, and also require signalling through IL-7R for their survival (Spits *et al.*, 2013).

Once mature, ILCs are widely distributed throughout the body, with tissue-dependent variations in the relative proportions of each subset. For example, ILC1s are the dominant population in the intestinal intraepithelial compartment and the liver (Jiao *et al.*, 2016). ILC2s are the dominant population in the lung, where they are found in collagen-rich interstitial tissues (Mindt, Fritz and Duerr, 2018). ILC2s are also particularly prevalent in the skin, where they help facilitate type 2 immune responses (Roediger and Weninger, 2015), and in the lamina propria (LP) of the large intestine (as well as smaller yet significant numbers in the LP of the small intestine), indicative of their role in inflammatory responses against helminths (Nussbaum *et al.*, 2013; Spencer *et al.*, 2014). Finally, ILC3s have been documented as the dominant cell population in the ileum and colon (Panda and Colonna, 2019), with a notable presence in intestinal cryptopatches, isolated lymphoid follicles and within certain sites of Peyer's patches known as perifollicular areas (Luci *et al.*, 2009; Klose *et al.*, 2013). The relative diversity in the distribution of ILC subsets is therefore indicative of potentially strategic positioning, in order to carry out specific effector functions.

Despite the traditional views of ILCs as tissue-resident cells, it has been shown that these cells are also capable of migration between secondary lymphoid organs and target tissues, in a manner akin to T cells. For example, ILC1s can traffic to lymph nodes in a CD62L and CCR7-dependent manner, where they are capable of rapid production of IFN-γ (Dutton *et al.*, 2019). Moreover, work with $CCR7^{-/-}$ mice has shown that this receptor is required for migration of ILC3s from the intestine to draining lymph nodes (Mackley *et al.*, 2015). Indeed, ILC3s represent a highly migratory ILC subset in response to infection with *Salmonella* Typhimurium, which is associated with enhanced levels of IFN-γ and GM-CSF (Kästele *et al.*, 2021). ILC2s also demonstrate a capacity to migrate from tissue sites to draining lymph nodes, with these cells expressing sphingosine 1-phosphate receptors, CCR7, and CD62L (Kästele *et al.*, 2021). Furthermore, ILC2s have also been shown to migrate from the intestine to the lung in response to helminth infections, where they can also contribute to tissue repair through production of amphiregulin (AREG) (Huang *et al.*, 2018). Overall, this therefore highlights that ILC

subsets can behave as tissue-resident effector cells, but also a migratory population that can elicit a rapid effector function at distal sites.

### 1.3.1 Group 1 ILCs overview

ILC1s express the transcription factor T-bet, and are capable of rapid production of IFN-γ (Spits *et al.*, 2013). Importantly, whilst they have often been compared to NK cells in their effector function and shared expression of T-bet, ILC1s do not express Eomes (Jiao *et al.*, 2016). Indeed, ILC1s have been identified and described as $NKp46^{+}NK1.1^{+}Eomes^{-}T\text{-}bet^{+}$ cells (Klose *et al.*, 2014). Moreover, they have also been identified in mouse lung, and defined as Lineage $(Lin)^{-}CD90^{+}T\text{-}bet^{+}$, expressing IL-12Rβ2 and IL-18Rα (Silver *et al.*, 2016). It is therefore not surprising that ILC1s are responsive to IL-12 and IL-18, and have also been shown to produce TNF-α as an effector cytokine (Bernink *et al.*, 2013; Fuchs *et al.*, 2013; Klose *et al.*, 2014; Silver *et al.*, 2016). They mirror Th1 cells in their effector functions, and play an important role in the immune responses against several intracellular pathogens (figure 1.2) (Fuchs *et al.*, 2013; Klose *et al.*, 2014; Artis and Spits, 2015).

When classifying ILC1s in humans, they can generally be defined based on differential expression of CD56 and expression of CD127 and T-bet (Simoni and Newell, 2018). For example, human $CD56^{-}$ ILC1s have been identified in the intestine, where they respond to IL-12 and produce IFN-γ (Bernink *et al.*, 2013). Moreover, they are present in a much higher proportion in Crohn's disease patients (Bernink *et al.*, 2013), indicating a role for these IFN-γ-producing cells in driving intestinal inflammation. Interestingly, a $CD56^{+}$ ILC1 population that is localised to intraepithelial areas is also enhanced in Crohn's disease patients, illustrating the larger detrimental role of ILC1s in the control of this disease (Fuchs *et al.*, 2013).

### 1.3.2 Group 1 ILCs during infection

Given that a defining characteristic of ILC1s is the production of IFN-γ (Artis and Spits, 2015), much research has focused on their role in protection against intracellular pathogens. During infection with the parasite *Toxoplasma gondii (T. gondii)*, ILC1s are a major source of IFN-γ and TNF-

α (Klose *et al.*, 2014). Indeed, adoptive transfer of ILC1 populations rescues IFN-γ and TNF-α production in $Rag2^{-/-}Il2rg^{-/-}$ mice (which lack adaptive immunity and ILCs) infected with *T. gondii*, which is associated with a significant reduction in *Toxoplasma* burdens. Moreover, using this adoptive transfer model, it was also shown that ILC1s significantly enhance inflammatory monocyte recruitment (Klose *et al.*, 2014). More recently, ILC1-derived IFN-γ has also been shown to be critical for the maintenance of inflammatory $IRF8^{+}$ DCs at the site of *Toxoplasma* infection, propagating parasite expulsion and host survival (López-Yglesias *et al.*, 2021). Together, these results suggest that ILC1s are critical to the host immune response against *Toxoplasma* infection.

ILC1s have also been studied during infection with the intestinal bacterial pathogen *Clostridium difficile (C. difficile)*, where they have been identified as the major IFN-γ-producing subset (Abt *et al.*, 2015). $Rag1^{-/-}$ mice (deficient in T and B cells only) showed an upregulated expression of ILC1-derived IFN-γ and ILC3-derived IL-22 following infection, and no changes in bacterial burden or survival, whereas $Rag2^{-/-}Il2rg^{-/-}$ mice failed to upregulate this expression and displayed enhanced mortality (Abt *et al.*, 2015). Indeed, adoptive transfer of a mixture of all 3 major ILC populations to $Rag2^{-/-}Il2rg^{-/-}$ mice was found to restore this cytokine production, and reduced susceptibility to infection (Abt *et al.*, 2015). Additional support for the role of ILC1s in *C. difficile* infection comes from an ILC1 depletion model ($Rag1^{-/-}Tbx21^{-/-}$), and IFN-γ-deficient mice ($Rag1^{-/-}Ifng^{-/-}$). Indeed, both strains show increased susceptibility to a lethal dose of *C. difficile*, suggesting that ILC1-derived IFN-γ is important in the control of infection (Abt *et al.*, 2015). Notably, adoptive transfer of $T\text{-}bet^{+}CD127^{+}$ LP ILC1s to these ILC1-deficient mice gave partial protection against lethal infection. However, as adoptive transfer did not generate full protection, other sources of IFN-γ were suggested, including conventional NK (cNK) cells and neutrophils (Abt *et al.*, 2015). Moreover, loss of ILC3s also reduced resistance to infection (Abt *et al.*, 2015), indicating the importance of multiple ILC populations in the control of this infection.

In more recent years, ILC1s have been shown to be detrimental to the control of certain infections. For example, IFN-γ derived from an ex-ILC3 $NK1.1^{-}T\text{-}bet^{+}$ ILC population has been identified as a driver of intestinal pathology

during infection with *Campylobacter jejuni* (Muraoka *et al.*, 2021). Indeed, adoptive transfer of sort-purified ILCs ($CD90.2^{+}Lin^{-}NK1.1^{-}$) into $Rag2^{-/-}il2rg^{-/-}$ mice resulted in significantly enhanced bacterial burdens and intestinal inflammation (Muraoka *et al.*, 2021). Elsewhere, recruitment of ILC1s into the brain during mouse cytomegalovirus infection induces an enhanced inflammatory response, which ultimately contributes to enhanced immunopathology and a lack of control of viral infection (Kveštak *et al.*, 2021). Thus, these highlight the potentially pathogenic role of ILC1s in the immune response against certain infections.

ILC1s have been identified to play roles in the defence against certain respiratory pathogens, such as influenza A, *Haemophilus influenzae*, respiratory syncytial virus (RSV) and *Staphylococcus aureus*. Importantly however, controversy remains around whether these represent a bona fide ILC1 population, or simply that they arise from other ILC subsets. For example, during influenza A infection, ILC2s down-regulate their master transcription factor GATA3, ST2, CD25, IL-7Rα and ICOS. Moreover, these cells demonstrate a concurrent increase in expression of T-bet, IL-12Rβ2 and IL-18Rα and an increased production of IFN-γ (Silver *et al.*, 2016). This apparent ILC2-ILC1 conversion was tested further using ST2 green fluorescent protein (GFP) reporter mice in influenza A-infected $Rag2^{-/-}il2rg^{-/-}$ mice. These mice received transferred $GFP^{+}$ ILC2s, which were found to infiltrate the lung at day 7 post-infection, where they downregulated their expression of GATA3, and increased IL-18Rα and IL-12Rβ2 expression (Silver *et al.*, 2016). Thus, this highlights the plastic nature of ILC2s and the potential for their conversion to ILC1-like cells. More recently, a similar phenomenon has been observed in the context of *Mycobacterium tuberculosis (M. tuberculosis)*, although these ILC1-like cells have been proposed to arise from an immature $IL\text{-}18R^{+}$ ILC2 population rather than mature ILC2s (Corral *et al.*, 2021).

### 1.3.3 Group 2 ILCs overview

At first, lineage negative cells that produce IL-5 and IL-13 were reported simultaneously by several groups and termed ‘nuocytes’, ‘natural helper cells’ and ‘innate helper 2 cells’, with these later being grouped together under the term ‘ILC2s’ (Lund, Walford and Doherty, 2013). Akin to Th2 cells,

ILC2s require GATA3 and RORα for their development, functional maturation and maintenance (Spits *et al.*, 2013). Of note, minor roles exist for other transcription factors in the development of ILC2s, including growth factor independence-1 (Gfi-1) and B cell leukaemia/lymphoma 11b (Bcl11b) (Spooner *et al.*, 2013; Yu *et al.*, 2015; Walker *et al.*, 2015). ILC2s are responsive to multiple mediators such as the cytokines IL-25, IL-33 and thymic stromal lymphopoietin (TSLP), as well as neuropeptides (e.g. neuromedin U) and lipids (e.g. prostaglandin D2) (Duerr and Fritz, 2016). These mediators can promote secretion of the effector cytokines IL-4, IL-5, IL-9, IL-13 and amphiregulin (AREG) (Duerr and Fritz, 2016). Specific cell targets for these ILC2-derived cytokines include eosinophils, macrophages, DCs and epithelial cells (Mindt, Fritz and Duerr, 2018), with release of these effector cytokines allowing ILC2s to promote type 2 immune responses, such as protection against helminth infections, induction of allergic inflammation, mediation of tissue repair and maintenance of metabolic homeostasis (figure 1.2) (Artis and Spits, 2015).

Several factors have also been shown to inhibit ILC2s, attenuating their proliferation and cytokine production, including IFN-γ, IL-27, prostaglandin $I_2$, and lipoxin A4 (Molofsky *et al.*, 2015; Zhou *et al.*, 2016; Moro *et al.*, 2016; McHedlidze *et al.*, 2016). For example, prostaglandin $I_2$ impairs ILC2 cytokine production both *in vitro* and during intranasal challenge with the fungal type 2 allergen *Alternaria alternata* (Zhou *et al.*, 2016). Moreover, IFN-γ inhibits the function and proliferation of ILC2s, with IFN-γ over-expressing mice displaying diminished ILC2 responses against *N. brasiliensis* (Molofsky *et al.*, 2015). This IFN-γ-mediated effect is also observed during co-infection with *N. brasiliensis* and *Listeria monocytogenes* – a bacterium that provokes a strong IFN-γ-mediated response (Molofsky *et al.*, 2015). Overall, this demonstrates that ILC2-mediated responses can be modulated in multiple ways.

As previously mentioned, ILC2s are the dominant ILC population in the lung, with murine ILC2s defined as $Lin^-CD90^+CD127^+ICOS^+CD25^+ST2^+$ (Monticelli *et al.*, 2011). Moreover, whilst killer cell lectin-like receptor G1 (KLRG1) can serve as a marker for ILC2s in other tissues (Meininger *et al.*, 2020), it can be used to further subdivide ILC2s into natural ILC2s (nILC2s) and inflammatory ILC2s (iILC2s) in the murine lung. More specifically, nILC2s are

identified as a KLRG1$^{int}$ population that is present under steady-state conditions. In contrast, iILC2s are defined as KLRG1$^{hi}$, which are proposed to appear upon helminth infection, or following IL-25 stimulation (Huang *et al.*, 2015). Interestingly, this iILC2 population has also been shown to express intermediate amounts of the ILC3 master transcription factor RORγt, and are capable of IL-17 production in response to *Candida albicans*. The importance of this effector function is demonstrated in Rag2$^{-/-}$il2rg$^{-/-}$ mice, which display enhanced fungal burden and mortality when compared to WT and Rag2$^{-/-}$ mice. This can be rescued following adoptive transfer of iILC2s to these Rag2$^{-/-}$il2rg$^{-/-}$ mice, which is associated with IL-17 and IL-13 production (Huang *et al.*, 2015).

In humans, ILC2s have been identified in both foetal and adult lung, as well as bronchoalveolar lavage fluid (BLF). These cells are Lin$^{-}$ CD127$^{+}$CD161$^{+}$CRTH2$^{+}$, with populations differentiated by their expression of CD117 (Mjosberg *et al.*, 2011; Monticelli *et al.*, 2011). Furthermore, human lung ILC2s also appear to mirror murine ILC2s in their expression of ICOS, CD25 and ST2 (Monticelli *et al.*, 2011), suggesting a level of cross-species comparability for the identification of ILC2s. These cells are also responsive to the cytokine mediators mentioned previously (Meininger *et al.*, 2020). Akin to their murine counterparts, human ILC2s are involved in allergic airway inflammation. Indeed, significantly higher numbers of IL-5- and IL-13-producing ILC2s have been identified in the blood and sputum of patients (Smith *et al.*, 2016). Moreover, these effector functions appear to induce an eosinophilic airway inflammation akin to that observed in murine airway allergy models, with elevated ILC2 and eosinophil numbers in patients with mild and moderate asthma (Liu *et al.*, 2015). Human ILC2s can also demonstrate plasticity in response to multiple other stimuli such as IL-1β, IL-12, and IL-18 (Ohne *et al.*, 2016; Silver *et al.*, 2016). Indeed, their responsiveness to IL-12 and IL-18 drives their conversion to an ILC1-like population that is enhanced in the blood of patients with chronic obstructive pulmonary disease (COPD), indicating the potentially detrimental role of ILC2 plasticity in this context.

### 1.3.4 Group 2 ILCs during infection

ILC2s represent an important innate effector cell during multiple type 2 immune responses such as allergic airway inflammation, and anti-helminth immunity (Artis and Spits, 2015). A well-studied example of the role ILC2s play in anti-helminth immunity is with the parasite *N. brasiliensis*, which is first carried to the lungs before full maturation, resulting in significant lung inflammation, before travelling to the intestine. The immune response in the lung involves production of TSLP, IL-25 and IL-33 from dying epithelial cells, stimulating the production of IL-5 and IL-13 from ILC2s (Miller and Reinhardt, 2020). In turn, this ILC2-derived IL-5 can promote the recruitment of eosinophils to the lung (Nussbaum *et al.*, 2013). ILC2-derived IL-13 promotes goblet cell hyperplasia and mucus secretion, and this is critical to parasite expulsion, as IL-13-deficient mice display impaired clearance of *N. brasiliensis*, which can be rescued upon transfer of WT IL-13-producing ILC2s (Neill *et al.*, 2010).

Both nILC2 and iILC2s play roles in *N. brasiliensis* infection, with the importance of iILC2s seen in IL-17RB$^{-/-}$ mice, which lack iILC2s – as this inflammatory ILC2 population express IL-25R (IL-17RB) (Huang *et al.*, 2015). Here, IL-17RB $^{-/-}$ mice display enhanced worm burdens when compared to WT mice (Huang *et al.*, 2015). This is also seen in Rag2$^{-/-}$il2rg$^{-/-}$ mice, and adoptive transfer of either iILC2s or nILC2s can rescue these enhanced worm burdens (Huang *et al.*, 2015), indicating the importance of both populations in control of this parasitic infection. Indeed, the overall importance of ILC2s is further highlighted using an ILC2-specific depletion model (ICOS-T), where parasite clearance is noticeably impaired when compared to WT mice (Oliphant *et al.*, 2014).

ILC2s have also been documented to produce IL-9 to facilitate an autocrine feedback loop to enhance their production of IL-5, IL-13 and AREG in the lung (Turner *et al.*, 2013; Mohapatra *et al.*, 2016). The importance of this loop is observed in IL-9R$^{-/-}$ mice, which display impaired clearance of *N. brasiliensis*. In these mice, decreased ILC2 numbers are observed, with concurrent reductions in IL-5, IL-13 and AREG (Turner *et al.*, 2013). Interestingly, Th2 numbers remain constant in this knockout model, suggesting that IL-9 plays a crucial role in the maintenance of the ILC2

population, and that ILC2s appear to be able to coordinate the type 2 immune response.

| Mouse | Group 1 ILCs | Group 2 ILCs | Group 3 ILCs | | |
|---|---|---|---|---|---|
| | | | LTi cells | NCR$^-$ ILC3s | NCR$^+$ ILC3s |
| **Transcription factors** | T-bet | GATA3 | RORγt | RORγt, T-bet | RORγt, T-bet |
| **CD4** | - | - | +/- | - | - |
| **CD25** | - | + | + | + | + |
| **CD49a** | + | - | - | - | - |
| **CD90** | + | + | + | + | + |
| **CD117 (C-kit)** | - | +/- | + | - | + |
| **CD127 (IL-7Rα)** | + | + | + | + | + |
| **Sca-1** | - | + | - | - | - |
| **ICOS** | - | + | - | - | - |
| **NKp46** | + | - | - | - | + |
| **IL-1R** | + | - | + | + | + |
| **IL-12Rβ2** | + | - | - | - | + |
| **IL-17RB (IL-25R)** | - | + | - | - | - |
| **IL-18Rα** | + | +/- | - | - | - |
| **IL-23R** | - | - | + | + | + |
| **ST2 (IL-33R)** | - | + | - | - | - |
| **TSLP-R** | - | + | - | - | - |
| **KLRG1** | - | + | - | - | - |
| **NK1.1** | + | - | - | - | +/- |
| **CCR6** | - | - | + | - | - |

**Table 1.1 - Summary of the phenotypical markers expressed by each innate lymphoid cell subset in mice**

Innate lymphoid cells (ILCs) can be characterised largely by the transcription factors that they require for their development, which are often paralleled with Th cell subsets. ILC1s require T-bet, ILC2s require GATA3, and lymphoid tissue-inducer (LTi) ILC3s require RORγt, whereas NCR$^+$ ILC3s require RORγt and T-bet. Adapted from Spits et al. (2013).

ILC2s also play important roles in the control of other parasitic infections such as *Strongyloides venezuelensis (S. venezuelensis)* and *Heligmosomoides polygyrus (H. polygyrus)*. Here, WT mice display marked increases in IL-33 and IL-25 respectively, resulting in activation of IL-5- and IL-13-producing ILC2s that promote parasite clearance (Yasuda *et al.*, 2012; von Moltke *et al.*, 2016). Moreover, ILC2s have also been shown to be critical for the coordination of adaptive immune responses. Indeed, ILC2-derived IL-13 can promote DC migration to draining lymph nodes, where they prime Th2 cells (Halim *et al.*, 2014). ILC2s can also enhance Th2 cell functions in response to *N. brasiliensis*, through interactions of several cell surface markers such as PD-PD-L1, OX40-OX40L and MHCII (Oliphant *et al.*, 2014; Schwartz *et al.*, 2017; Halim *et al.*, 2018). Specifically, PD-L1-expressing ILC2s stimulate Th2-derived IL-13 production, and conditional deletion of PD-L1 on ILC2s results in impaired Th2 polarisation and impaired worm expulsion (Schwartz *et al.*, 2017). Moreover, ILC2s that express MHCII and OX40L can prime and activate $CD4^+$ T cells, and promote their differentiation to Th2 and Treg cells, with these functions lost in ILC2s deficient in MHCII or OX40L – which leads to impaired parasite expulsion (Oliphant *et al.*, 2014; Halim *et al.*, 2018). Thus, this demonstrates the importance of ILC2s as innate effector cells that can facilitate the mounting of an appropriate adaptive immune response. Of note, ICOS-ICOSL interactions between ILC2s have been shown to be critical in the function and homeostasis of ILC2s, with reduced survival and cytokine production in ICOS-deficient ILC2s (Maazi *et al.*, 2015).

ILC2s have also been observed to play crucial roles in viral infections. Specifically, ILC2s have been documented to maintain the integrity of respiratory epithelium during infection with the influenza A virus subtype $H_1N_1$ (Monticelli *et al.*, 2011). Indeed, $CD90^+CD25^+$ ILCs are recruited to the lungs of both WT and $Rag^{-/-}$ mice post-infection, and a significant reduction in lung function is observed following either $CD90^+$ ILC depletion, or blockade of IL-33 signalling – resulting in a loss of airway epithelial integrity and impaired tissue remodelling. Adoptive transfer of $CD90.1^+$ lung ILCs into anti-CD90.2 mAb-treated $Rag1^{-/-}$ mice restores this epithelial integrity, and is dependent on ILC-derived AREG (Monticelli *et al.*, 2011).

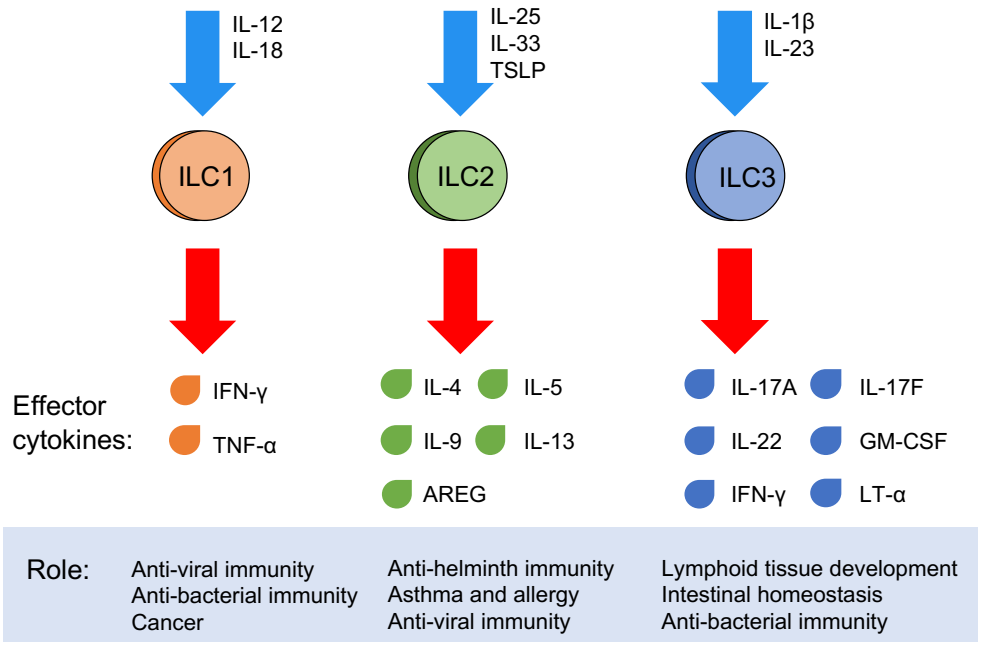


**Figure 1.2 - Overview of innate lymphoid cell subsets and effector functions**

Innate lymphoid cells (ILCs) comprise 3 major subsets in ILC1s, ILC2s and ILC3s. ILC1s secrete IFN-γ and TNF-α in response to IL-12 and IL-18, and are involved in immune responses against viruses and bacteria, as well as the anti-tumour immune response. ILC2s are stimulated by IL-25, IL-33 and thymic stromal lymphopoietin (TSLP) to secrete IL-4, IL-5, IL-9, IL-13 and amphiregulin (AREG). This subset is involved in the immune response against parasites, viruses, and asthma and allergic airway diseases. ILC3s respond to IL-1β and IL-23 to secrete IL-17A, IL-17F, IL-22, granulocyte-macrophage colony-stimulating factor (GM-CSF), IFN-γ and lymphotoxin-α (LT-α) to contribute to lymphoid tissue development, intestinal homeostasis and anti-bacterial immunity. Figure adapted from Artis and Spits (2015).

Conversely, ILC2s have been shown to play a detrimental role in the control of pulmonary infections, contributing to the exacerbation of tissue pathology (Mindt, Fritz and Duerr, 2018). For example, activation of ILC2s drives airway hyper-reactivity in the context of multiple viral infections. More specifically, ILC2-derived IL-13 has been shown to significantly enhance mucus secretion and airway hyper-reactivity (AHR) in respiratory syncytial virus (RSV) infection (Stier *et al.*, 2016). Furthermore, IL-33 derived from alveolar macrophages activates ILC2s, leading to significantly exacerbated AHR in the context of influenza A virus infection (Chang *et al.*, 2011). Conversely, ILC2-derived IL-13 can induce the alternative activation of macrophages, although the maintenance of this effector state appears to require the input of Th2 cells (Bouchery *et al.*, 2015). Overall, this shows that the activation of

lung ILC2s must be carefully modulated, given that these cells appear to play dual roles in the control of intracellular infections in the lung.

### 1.3.5 Group 3 ILCs overview

Group 3 ILCs parallel Th17 cells in their constitutive expression of the transcription factor RORγt and their roles in promotion of antibacterial immunity, chronic inflammation and tissue repair (figure 1.2). Moreover, they respond to the cytokines IL-1β, IL-6 and IL-23, producing IL-17A, IL-17F, IL-22 granulocyte-macrophage colony-stimulating factor (GM-CSF), and lymphotoxin-α (LT-α) in a stimulus-dependent manner (Melo-Gonzalez and Hepworth, 2017).

Group 3 ILCs are the most heterogeneous ILC group in both mice and humans (table 1.1). In mice, they can be subdivided on the basis of expression of NKp46 and chemokine receptor CCR6. Indeed, $CCR6^+$ ILC3s, also termed LTi-like ILC3s, are further divided into $CD4^+$ and $CD4^-$ populations, and contribute towards the development of lymphoid structures and tissue homeostasis. Those ILC3s that are $CCR6^-$ are divided in their expression of NKp46, with $NKp46^+$ and $NKp46^-$ ILC3s, termed natural-cytotoxicity-receptor-positive ($NCR^+$) and $NCR^-$ ILC3s respectively contributing towards immunity against extracellular bacteria and autoimmune inflammation (Melo-Gonzalez and Hepworth, 2017). Interestingly, ILC3s can display plastic behaviours when presented with certain stimuli. For example, RORγt$^+$ ILC3s can downregulate their expression of this master transcription factor during *Salmonella enterica* infection, which is associated with an upregulation in the expression of T-bet and NKp46, and IFN-γ production (Klose *et al.*, 2013). Hence, the loss of RORγt and the subsequent acquisition of T-bet in these ILCs has allowed them to be termed ILC1-like 'ex-ILC3s'. This therefore suggests that ILC3s are adaptable to the tissue signals in their environment, adopting effector functions that are distinct from those under steady-state conditions.

Human ILC3s vary on their expression of NKp44, and constitutively express CCR6 (Killig, Glatzer and Romagnani, 2014; Yudanin *et al.*, 2019). Those that lack NKp44 show enhanced accumulation at sites of intestinal inflammation in Crohn's disease patients, where they produce IL-17 - which

has been proposed to recruit other inflammatory cells (Geremia *et al.*, 2011). Conversely, an NKp44$^{+}$ ILC3 population has been identified in the skin, where they produce IL-22, and their frequency correlates with the severity of disease in psoriasis patients (Teunissen *et al.*, 2014). Thus, these studies highlight how ILC3s can play a detrimental role in multiple inflammatory diseases. Interestingly, ILC3s have also demonstrated the capacity to produce IFN-γ in response to stimulation with IL-12 (Bernink *et al.*, 2013), suggesting that these cells can produce cytokines other than those associated with classic Th17 biology.

### 1.3.6 Group 3 ILCs during infection

ILC3s can play a protective role during infection, via production of the effector cytokines IL-17 and IL-22 (Artis and Spits, 2015). Both effector cytokines act to activate epithelial cells, which produce antimicrobial molecules to aid in defence against extracellular bacteria and fungi (Liang *et al.*, 2006; Aujla *et al.*, 2008).

To study ILC3s in infection, much research has focused on the extracellular bacteria *Citrobacter rodentium (C. rodentium)*, which is an intestinal model of infection. During infection with this pathogen, IL-22-producing cell numbers increase in the intestinal lamina propria (LP) (Sanos *et al.*, 2009; Cella *et al.*, 2009). Interestingly, it has been proposed that NCR$^{+}$ ILC3s are dispensable to the control of early infection in the presence of LTi ILC3s - with T cells also playing a role as infection progresses (Sonnenberg *et al.*, 2011; Rankin *et al.*, 2016). Indeed, whilst a lack of NKp46$^{+}$ ILC3s produced no difference in the control of infection, a lack of total ILC3s resulted in partial impairment of bacterial control (Song *et al.*, 2015), and specific depletion of CD4$^{+}$ LTi ILC3s leads to a reduction in IL-22-induced antimicrobial peptide production, and increased susceptibility to *C. rodentium* infection (Sonnenberg *et al.*, 2011). Overall, this therefore indicates the importance of LTi ILC3s in the control of early intestinal bacterial infection.

Other infectious models lend support to the protective role of ILC3s in the host immune response. For example, ILC3-derived IL-17 is critical for the control of infection with the fungi *Candida albicans*. Indeed, Rag1$^{-/-}$ mice with antibody-mediated depletion of ILCs, and RORc$^{-/-}$ mice, demonstrate

complete failure to control infection (Gladiator *et al.*, 2013). Intriguingly, ILC3s have also been implicated in the control of viral infections. Here, ILC3-derived IL-22 is amplified by the production of IFN-λ from infected epithelial cells, which contributes to the attenuation of rotavirus viral replication (Hernandez *et al.*, 2015).

In the context of infection with *Salmonella enterica* serovar Typhimurium, research into the role of IL-22 has demonstrated a complex control of infection. On the one hand, this ILC3-derived cytokine has been shown to facilitate the colonisation of the bacteria in the inflamed gut, through the production of antimicrobial proteins that sequester metal ions from commensal microbes (Behnsen *et al.*, 2014). Despite this, others have demonstrated that commensal bacteria promote the production of ILC3-derived IL-22, which induces fucosylation of intestinal epithelial cells (Goto *et al.*, 2014). Importantly however, this does not appear to impact upon the colonisation of *Salmonella* in the gut lumen, and is instead important in preventing infection of intestinal epithelial cells (Goto *et al.*, 2014). Thus, this indicates the importance of ILC3-derived IL-22 in control of this bacterial infection.

ILC3s have also been implicated in the control of infection with several respiratory pathogens, and whilst this ILC subset is rare in the steady state lung (Mjosberg and Spits, 2016), enhanced numbers can accumulate in the context of infections. For example, ILC3s accumulate in the lung tissue during infection with the extracellular bacterium *Streptococcus pneumoniae (S. pneumoniae)*, where they produce IL-22 (Van Maele *et al.*, 2014). This response can be augmented through administration of the TLR5 agonist flagellin during infection, which provides enhanced protection against lethal infection (Van Maele *et al.*, 2014). Thus, this suggests that amplification of ILC3-mediated responses may serve as an effective way to combat bacterial infection. This is further highlighted in the context of immunological challenge with an antibiotic-resistant strain of *Klebsiella pneumoniae*. Here, monocytes represent a source of TNF, generating a marked increase in IL-17-producing ILCs, which were shown to enhance pathogen clearance. Indeed, monocyte- or TNF-depleted mice show an impaired IL-17A-dependent clearance of infection (Xiong *et al.*, 2016), suggesting an important link between

monocytes and ILCs that could be crucial in clearing strains of bacteria that are resistant to current frontline treatments.

More recently, ILC3s have also been implicated in the control of infection with *M. tuberculosis* (Ardain *et al.*, 2019). Here, the expansion of ILC3s and their production of IL-17 and IL-22 were shown to be critical to the induction of an early innate immune response, and the formation of protective lymphoid follicles within granulomas. Moreover, ILC3s influenced the accumulation of alveolar macrophages during infection, with an absence of ILC3s resulting in a reduction in this accumulation and enhanced bacterial burdens. Overall, this indicates that ILC3s are also critical in the control of certain intracellular bacterial infections.

Overall, ILCs represent a critical source of early cytokine during a wide variety of immunological challenges. More specifically, these innate effectors play vital roles in the control of a wide variety of infections, with their abundance at mucosal barriers meaning they are often in close proximity to pathogens, and therefore highly adapted to perform their functions. However, the field of ILC biology is still relatively novel, and as such, the roles that these cells play in many infectious diseases is still relatively unknown.

## 1.4 Aims

The lethality of *Francisella tularensis* and overall failure of the host to control infection highlights the importance of understanding the early immune response against the bacteria. Thus, as they have previously been shown to play critical roles in the early immune response against multiple other pathogens (Artis and Spits, 2015), innate lymphoid cells (ILCs) represent a cell population of particular interest when studying the early immune response against *F. tularensis*. The work presented in this thesis therefore began to address the role of ILCs during infection with *F. tularensis*, by utilising a murine model of infection with a live vaccine strain (LVS) of the bacteria. This strain has been instrumental in the study of tularaemia, as it represents a less virulent strain in humans when compared to others such as Schu S4 (Ellis *et al.*, 2002), whilst retaining its lethality in mice when administered via the intranasal route (Fortier *et al.*, 1991). Specific aims of the thesis are outlined below:

**How are ILCs implicated in the immune response against *F. tularensis*?**

This was an overarching aim, and was addressed at multiple points throughout this thesis. Changes to the ILC compartment following intranasal infection, and how these may occur, were investigated in chapter 3. Chapter 5 of this thesis then investigated the cytokine responses by ILCs during infection, and began to determine the impact of infection-induced changes in the lung cytokine milieu on ILC numbers.

**What effect does manipulation of ILC numbers have on the progression of infection?**

Work in chapters 4 and 5 of this thesis addressed this aim. Specifically, ILC numbers were expanded through treatment with IL-33 and intranasal transfers of sort-purified ILCs, and ILCs were depleted using knockout mouse models such as $Rag1^{-/-}il2rg^{-/-}$ and ICOS-T mice. Here, the focus was to determine how changes to the ILC compartment impacted upon the control of infection with *F. tularensis*, and how these changes affected other immune cell populations.

# Chapter 2

# Materials and Methods

## 2.1 Bacteria

### 2.1.1 *Francisella tularensis* live vaccine strain

*Francisella tularensis* live vaccine strain (LVS) was derived from an original NDBR101 *Pasteurella tularensis* live vaccine, experimental lot 4. The vaccine contained $6x10^9$ colony forming units (CFU) of lyophilised *F. tularensis* LVS, which was stored at -20°C at the Defence Science and Technology Laboratory (DSTL).

### 2.1.2 Preparation of master stock

Master stocks were prepared by first diluting the lyophilised vaccine (2.1.1) in 1 ml sterile phosphate-buffered saline (PBS), with 100 µl aliquots of bacterial suspension streaked onto 10 blood cysteine glucose agar (BCGA) plates (Oxoid, Thermo Fisher). Plates were incubated for 48 hours at 37°C, at which point bacterial lawns were scraped into a 15% glycerol solution (diluted in sterile water). Finally, 1 ml aliquots of bacterial suspension were placed into vials, and stored at -80°C.

### 2.1.3 Preparation of challenge stock and challenge dose

For preparation of challenge stocks, a master stock (2.1.2) was thawed, and 100 µl aliquots of bacterial suspension streaked onto 2 BCGA plates. Following the incubation for 48 hours at 37°C, bacterial lawns were again scraped into a 15% glycerol solution, and diluted down to a concentration of $1x10^9$ CFU/ml. Here, 100 µl aliquots of $1x10^6$ CFU/ml bacterial suspension were placed into vials, and stored at -80°C. For intranasal challenge doses, individual vials of challenge stocks were thawed, and diluted in sterile PBS to ~$2x10^4$ CFU/ml for challenge doses (described further in 2.2.2).

## 2.2 Infection models with *F. tularensis* LVS

### 2.2.1 Animals

Eight- to twelve-week-old female mice were kept in specific pathogen-free conditions at the University of Manchester Biological Services Facility, as defined by institutional and UK Home Office guidelines. C57BL/6 (Charles River, United Kingdom), *Rag1*$^{-/-}$ (Mombaerts *et al.*, 1992), *Il2rg*$^{-/-}$ (Cao *et al.*,

1995), *Rag1*$^{-/-}$*Il2rg*$^{-/-}$ (Song *et al.*, 2010) and ICOS-T (Oliphant *et al.*, 2014) mice were given food and water *ad libitum*. All procedures and husbandry were in accordance with the Home Office Animal Scientific Procedures Act (1986), and under the DERFA licence.

### 2.2.2 Intranasal infection with *F. tularensis* LVS

Mice were anaesthetised via inhalation of isoflurane (2.5% v/v for induction and maintenance), and subsequently given an intranasal challenge with 50 µl PBS containing ~1000 CFU *F. tularensis* LVS (obtained from challenge dose, see section 2.1.3). Control mice received 50 µl sterile PBS. Challenge doses were confirmed following serial dilution (1:10) of bacteria and a 5-7 day culture period on BCGA plates at 37$^{o}$C.

| Clinical sign | 0 | 1 | 2 |
|---|---|---|---|
| **Coat** | Normal, smooth | Starring around neck | Pronounced starring all over coat |
| **Dehydration** | Pinched loose skin on back retracts immediately | Pinched skin retracts, but slowly | Pinched skin remains in position (>1 min) |
| **Posture** | Normal | Transient hunching | Permanent, pronounced hunching |
| **Mobility** | Active, moving, socialising | Reluctant to move without provocation, unsteady on feet | Unresponsive to extraneous stimuli and provocation, immobile, not self-righting |
| **Eyes** | Eyes open, clear | Eyes half-closed | Eyes closed and/or congested. |

**Table 2.1 - Clinical scoring for monitoring of individual mice during infection**

Post-challenge, all mice were monitored daily and scored for clinical symptoms. Mice were evaluated based on several factors: coat condition, dehydration, posture, mobility and eye condition (table 2.1). Maximum clinical scores of 6, or individual scores of 2 for mobility, were permitted before euthanasia was deemed necessary. All mice were culled at pre-

determined experimental time points or when pre-determined humane endpoints were met.

### 2.2.3 Determining organ bacterial burden

Bacterial burdens were enumerated from the lung, liver and spleen of mice, with samples processed less than 2 hours post-mortem. All organs were collected in either PBS or 1ml protease inhibitor cocktail where appropriate ((Roche, complete mini, EDTA free) 1 tablet dissolved in 10ml PBS), and weighed. Samples were disrupted through a 40 µm cell sieve, followed by serial dilution of organ homogenates in PBS. Bacteria were incubated for 4-5 days at 37$^{o}$C on BCGA plates, and once grown sufficiently, single colonies were counted and organ weights used to normalise data to CFU per gram of organ.

### 2.2.4 Administration of anti-NK1.1 antibody

InVivo mAb anti-mouse NK1.1 (clone PK136; Bio X Cell) or InVivo mAb mouse IgG2a isotype control (clone C1.18.4; Bio X Cell) were administered to mice via the intraperitoneal (i.p.) route at a dose of 200 µg/mouse administered every 2 days starting 1 day before infection with *F. tularensis* LVS.

### 2.2.5 Administration of diphtheria toxin

Diphtheria toxin (DTx; Merck) was administered daily to mice via the i.p. route at a dose of 1 µg/mouse. DTx treatment started 4 days before infection with *F. tularensis* LVS, and was continued throughout the experiment until mice were culled.

### 2.2.6 Administration of IL-33

Recombinant murine IL-33 (rIL-33; carrier-free, R&D Systems) was administered to mice via the i.p. route at a dose of 0.5 µg/mouse every 2 days starting 5 days before infection with *F. tularensis* LVS. Mice received 3 doses in total, with the final dose 1 day before infection with *F. tularensis* LVS.

### 2.2.7 Intranasal transfer of ILC2s

Naïve C57BL/6 mice were given 4 doses of recombinant IL-33, receiving individual doses every 2 days (i.p.; 0.5 µg/mouse), before being culled 2 days after the final dose. Lung ILC2s (live $CD45^+Lin^-CD127^+KLRG1^+$) were then sort-purified, and $1x10^5$ ILC2s transferred via the intranasal route into LVS-infected mice at day 3 p.i.. All mice in these studies were subsequently culled at day 7 p.i..

## 2.3 Flow Cytometry

### 2.3.1 Tissue digestion and processing

Whole lungs and mediastinal (lung-draining) lymph nodes were collected into separate bijou tubes, each in 2 ml PBS. Lung tissue was cut into small sections, and then left to shake in an incubator at 37ºC with 3 mg/ml Collagenase D (Roche) (diluted in PBS) for 40 minutes. Post-digest, all tissues were disrupted through a 40 µm cell sieve and washed with PBS. Samples were centrifuged at 1500 rpm for 5 minutes, supernatants removed and cell pellets re-suspended in 2 ml Red Blood Cell Lysing Buffer Hybri-Max™ (Merck) for incubation at room temperature for 5 minutes. After this, samples were washed in PBS, centrifuged, and supernatants removed, for acquisition of cell counts following pellet re-suspension in PBS. Cells were centrifuged once more before re-suspension in FACS buffer (2% FCS, 2mM EDTA in 1X PBS) and flow cytometry analysis.

### 2.3.2 Anti-*F. tularensis* LVS antibody

*F. tularensis* LVS was detected by intracellular flow cytometry using an APC-labelled anti-*F. tularensis* lipopolysaccharide (LPS) monoclonal antibody (clone FB11, Abcam). The antibody was labelled in house with an APC conjugation kit (Abcam) to a stock concentration of 1.5 mg/ml. An isotype control (clone RTK2758; BioLegend) was used to determine non-specific intracellular antibody binding.

### 2.3.3 Cell staining protocol for flow cytometry

Samples used for flow cytometry were derived from mice following a digestion and processing protocol (2.3.1), with fluorophore-labelled antibodies used throughout. Antibodies were diluted to desired concentrations in FACS buffer for targeting of cell surface markers (table 2.2), and 1X permeabilisation buffer (concentrate:dH2O, 1:9) (eBioscience) for intracellular markers (table 2.3).

Where appropriate, samples were re-suspended in 200 µl of complete RPMI (cRPMI), and transferred into round-bottom 96-well plates for *ex vivo* stimulations. Samples were incubated at 37°C for 4 hours in cRPMI containing Cell Stimulation Cocktail (plus protein transport inhibitors (1X, eBioscience)). The cocktail consisted of phorbol 12-myristate 13-acetate (PMA) and ionomycin to induce activation of cells to produce cytokines, and brefeldin A and monensin to allow secreted proteins to accumulate in the endoplasmic reticulum and Golgi apparatus. Following incubation, cells were transferred to FACS tubes, and washed in FACS buffer. Samples were then centrifuged, and subsequently stained with antibodies against cell surface markers for 30 minutes at 4$^{o}$C. Where appropriate, cells were washed, centrifuged and stained with a streptavidin conjugate for 15 minutes at 4$^{o}$C. Samples were then washed, centrifuged, and re-suspended in Fixation/Permeabilisation buffer (concentrate:diluent, 1:3) (eBioscience), and left overnight at 4$^{o}$C. For intracellular staining, cells were washed in 1X permeabilisation buffer, before incubation for 45 minutes at 4$^{o}$C with antibodies against intracellular markers. Gating was established using either fluorescence minus one (FMO) or isotype controls. Prior to data acquisition, cells were washed in FACS buffer, and stored at 4$^{o}$C until analysed on a BD LSR Fortessa (BD Biosciences).

| Target | Fluorochrome | Specifications | Concentration |
|---|---|---|---|
| B220 | APC-eFluor 780 | eBioscience; clone RA3-6B2 | 1 µg/ml |
| CD3 | PercP/Cyanine5.5<br>PE-Cy7 | BioLegend; clone 145-2C11 | 1 µg/ml |
| CD4 | PE-eFluor 610<br>BUV395 | eBioscience; clone RM4-5 | 1 µg/ml |
| CD5 | PercP/Cyanine5.5<br>PE-Cy7 | BioLegend; clone 53-7.3 | 1 µg/ml |
| CD11b | APC-eFluor 780 | eBioscience; clone M1/70 | 1 µg/ml |
| CD11c | APC-eFluor 780 | eBioscience; clone N418 | 1 µg/ml |
| CD25 | APC | eBioscience; clone PC61.5 | 1 µg/ml |
| CD45 | BV650 | BioLegend; clone 30-F11 | 1 µg/ml |
| CD64 | PE-Cy7 | BioLegend; clone X54-5/7.1 | 1 µg/ml |
| CD90.2 | AlexaFluor 700 | BioLegend; clone 30-H12 | 2.5 µg/ml |
| CD127 | BV421<br>PE | Biolegend; clone A7R34 | 1 µg/ml |
| ICOS | PE | eBioscience; clone 7E.17G9 | 1 µg/ml |
| KLRG1 | FITC<br>PE-eFluor 610 | eBioscience; clone 2F1 | 1 µg/ml |
| Live/Dead | AmCyan | Invitrogen; Fixable Aqua Dead Cell Stain Kit | 1 µg/ml |
| Ly6G | FITC | BioLegend; clone 1A8 | 2.5 µg/ml |
| NK1.1 | PercP-eFluor 710<br>PE-Cy7<br>BUV395 | BioLegend; clone PK136 | 1 µg/ml |
| Siglec-F | PercP-eFluor 710<br>PE-eFluor 610 | eBioscience; clone 1RNM44N | 1 µg/ml |
| ST2 | Biotin | eBioscience; clone RMST2-33 | 2.5 µg/ml |
| Streptavidin | APC<br>SB600<br>BUV395 | eBioscience; #17-4317-82<br>eBioscience; #63-4317-82<br>BD Biosciences; #564176 | 1 µg/ml |

**Table 2.2 - Specifications of fluorophore-conjugated antibodies for cell surface markers**

| Target | Fluorochrome | Specifications | Concentration |
|---|---|---|---|
| *F. tularensis* LVS LPS | APC | Abcam; clone FB11 | 2.5 µg/ml |
| Rat IgG2a | APC | BioLegend; RTK2758 | 2 µg/ml |
| FOXP3 | eFluor450<br>PE | eBioscience; clone FJK-16s | 2 µg/ml |
| GATA3 | PercP-eFluor 710 | eBioscience; clone TWAJ | 2 µg/ml |
| IFN-γ | eFluor450 | eBioscience; clone XMG1.2 | 2 µg/ml |
| IL-5 | APC | BioLegend; clone TRFK5 | 2 µg/ml |
| IL-13 | FITC | eBioscience; clone eBio13A | 2 µg/ml |
| RORγt | PE | eBioscience; clone B2D | 2 µg/ml |
| T-bet | FITC<br>APC-eFluor 660 | BioLegend; clone 4B10<br>eBioscience; clone 4B10 | 2 µg/ml |

**Table 2.3 - Specifications of fluorophore-conjugated antibodies for intracellular markers and corresponding isotype controls**

## 2.4 Apoptosis/necrosis assays

Lungs of both naïve and LVS-infected mice were processed (2.3.1), and samples stained for cell surface markers as previously described (2.3.3). To monitor the progression of cell death in immune cell populations during infection with *F. tularensis* LVS, samples were subsequently stained with Annexin V Apoptosis Detection Kit PE (eBioscience) at room temperature for 15 minutes. Samples were then washed with PBS and analysed immediately on a BD Fortessa.

## 2.5 In vitro ILC2 culture

Lung ILC2s were sort-purified (2.2.7), and cells transferred to 96-well plates in 200 µl cRPMI at $1x10^5$ ILC2s per well. Cells were then cultured for 7 days with IL-7 (Invitrogen) at 25 ng/ml. Naïve and LVS-infected lung supernatants were generated by 24 hour incubation of homogenised lung samples at 37°C in cRPMI. Cell-free supernatants were collected by centrifugation and filtration through a sterile syringe 0.22 µM microfilter. 100 µl of supernatants

were then added to $1x10^5$ ILC2s (in 100 µl) and cultured for 5 days. All wells were cultured with IL-7 at 25 ng/ml and where indicated, anti-IFN-γ (clone XMG1.2; Bio X Cell) was added to culture media at 10 µg/ml. For live ILC2 cell counts, a hemocytometer counting chamber was used. Cell pellets were resuspended, and 10 µl removed from wells each day where they were mixed with trypan blue solution (0.4% v/v) in a 1:2 dilution. Then, 10 µl of the mixture was applied to a hemocytometer counting chamber and live ILC2 cell counts enumerated.

### 2.6 In vitro ILC2-NK co-culture

ILC2s were isolated from C57BL/6 mice for *in vitro* culture as previously described (2.5). Cells were cultured for 7 days with IL-7 (Invitrogen) at 25 ng/ml. At this point, sort-purified NK cells (live $CD45^+CD3^-CD5^-CD11b^+NK1.1^+$) were isolated from the lung of either naïve or LVS-infected mice at day 5 p.i. and co-cultured with ILC2s in a 1:1 ratio with $2x10^4$ cells total per well. All wells were cultured with IL-7 at 25 ng/ml and where indicated, anti-IFN-γ (clone XMG1.2; Bio X Cell) was added to culture media at 10 µg/ml. Levels of cell death were subsequently quantified at 24, 48 and 72 hours by flow cytometry, using the Annexin V Apoptosis detection kit PE (eBioscience) as previously described (2.4).

### 2.7 Statistical analysis

Data collected by flow cytometry were analysed using Flow Jo software version 10.7.2. Bacterial burdens were converted to CFU/gram of organ for appropriate comparison. Figure legends indicate number of repeats per group. All statistical analyses were performed using GraphPad Prism 9 for Mac. Normality was determined using the Shapiro-Wilk normality test, with appropriate parametric and non-parametric statistical tests performed for each data set. Data were expressed as mean ± standard error of the mean (S.E.M). Statistical significance was considered at $p < 0.05$.

# Chapter 3

## Determining the role of innate lymphoid cells during pulmonary infection with *Francisella tularensis* LVS

## 3.1 Introduction

*Francisella tularensis (F. tularensis)* is an intracellular bacterium that upon exposure via the inhalational route, results in a pneumonic tularemia, which is fatal in 30-60% of cases if left untreated (McLendon, Apicella and Allen, 2006). As there is no vaccine currently licenced for use against *F. tularensis*, there has been increasing concern over use of the bacteria as a potential agent of bioterrorism. *F. tularensis* LVS is an attenuated strain of the bacteria, which is sub-lethal in humans. Importantly, this strain retains its lethality in mice, making it more accessible for use in laboratory research.

During pulmonary infection with *F. tularensis* LVS, the bacteria can replicate extensively and disseminate to peripheral organs within a matter of days (Bosio, 2011). Much of the current understanding of the early immune response against *F. tularensis* LVS has focused on the role of myeloid cells such as macrophages and neutrophils (Celli and Zahrt, 2013). However, the role of innate lymphocytes during the early stages of infection with *F. tularensis* LVS is relatively unknown. Innate lymphoid cells (ILCs) are a relatively newly discovered type of innate lymphocyte, which are capable of a rapid response to a wide variety of immunological challenges. These cells are frequently found at barrier sites, such as the skin, intestine and the lung (Artis and Spits, 2015) – making them a potential cell of interest in the immune response against pulmonary infection with *F. tularensis* LVS.

This chapter begins to address the role of ILCs during pulmonary infection with *F. tularensis* LVS. As ILCs are pre-primed innate effector cells, capable of rapid response to pathogens during the initial stages of infection (Diefenbach, 2013; Artis and Spits, 2015), their role during the early stages of intranasal infection with *F. tularensis* LVS was investigated, and how this changed as infection progressed.

## 3.2 Results

### 3.2.1 Determining the progression of *F. tularensis* LVS infection

A preliminary objective was to establish the infection kinetics of a lethal pulmonary infection with *F. tularensis* LVS in C57BL/6 mice. Thus, mice were infected with a lethal dose of bacteria (1000 CFU) via the intranasal route, with bacterial burdens enumerated and weight loss monitored at multiple time points post-infection (p.i.). Mice were monitored until day 7 p.i., at which point they had reached the endpoint of the licence and required euthanasia.

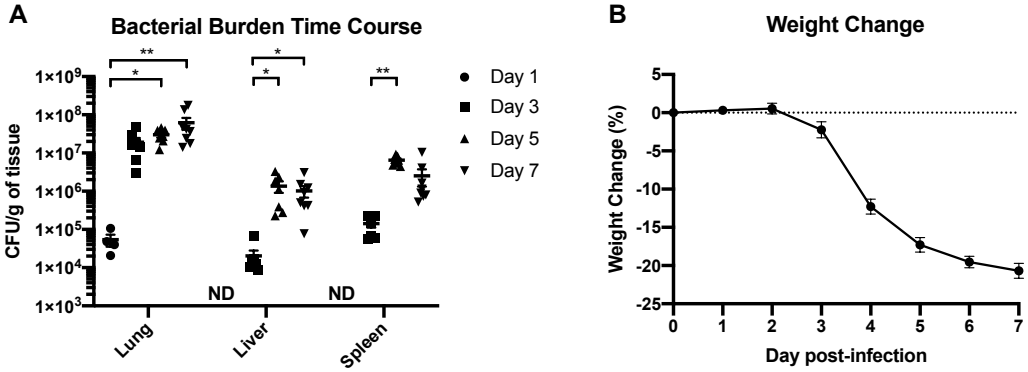


**Figure 3.1 - Infection kinetics during infection with *F. tularensis* LVS**

C57BL/6 mice were infected via the intranasal route with *F. tularensis* LVS (1000 CFU) and monitored at different times p.i. (A) Bacterial burdens (CFU/g of organ) were enumerated in the lung, liver and spleen of mice at days 1, 3, 5 and 7 p.i. (n=4 for day 1; n=7 for days 3 and 5; n=8 for day 7 mice). ND = Not detected. (B) Weight change was monitored daily in all mice, and plotted as a percentage loss of original body weight (0% = body weight at day 0). Statistical analysis was performed using the Kruskal Wallis test for non-parametric data, with Dunn's multiple comparisons tests performed for analysis between groups; * $p<0.05$; ** $p<0.01$.

Bacterial burdens in the lung were significantly elevated at days 5 and 7 p.i. versus day 1 p.i., with an increase of more than 2 logs in colony forming units (CFU) per gram of tissue (CFU/g of tissue) at each time point (figure 3.1A). Dissemination of *F. tularensis* LVS to peripheral organs (namely the liver and spleen) was observed from day 3 p.i. onwards. Here, bacterial burdens rose significantly at day 5 p.i., and remained elevated at day 7 p.i. (figure 3.1A). No changes in weight loss were observed until bacterial dissemination to the peripheral organs (figure 3.1B), when mice began to lose weight rapidly (figure 3.1B). Overall, these data demonstrate that *F. tularensis* LVS is capable of rapid colonisation of multiple organs, establishing a systemic infection that results in significant weight loss.

### 3.2.2 Innate lymphoid cells (ILCs) are reduced during infection with *F. tularensis* LVS

As ILCs are important in the early innate response to infection (Diefenbach, 2013), their potential role was investigated in infection with *F. tularensis* LVS. To this end, flow cytometry was used to identify and characterise ILC populations in the lung of LVS-infected mice (figure 3.2).

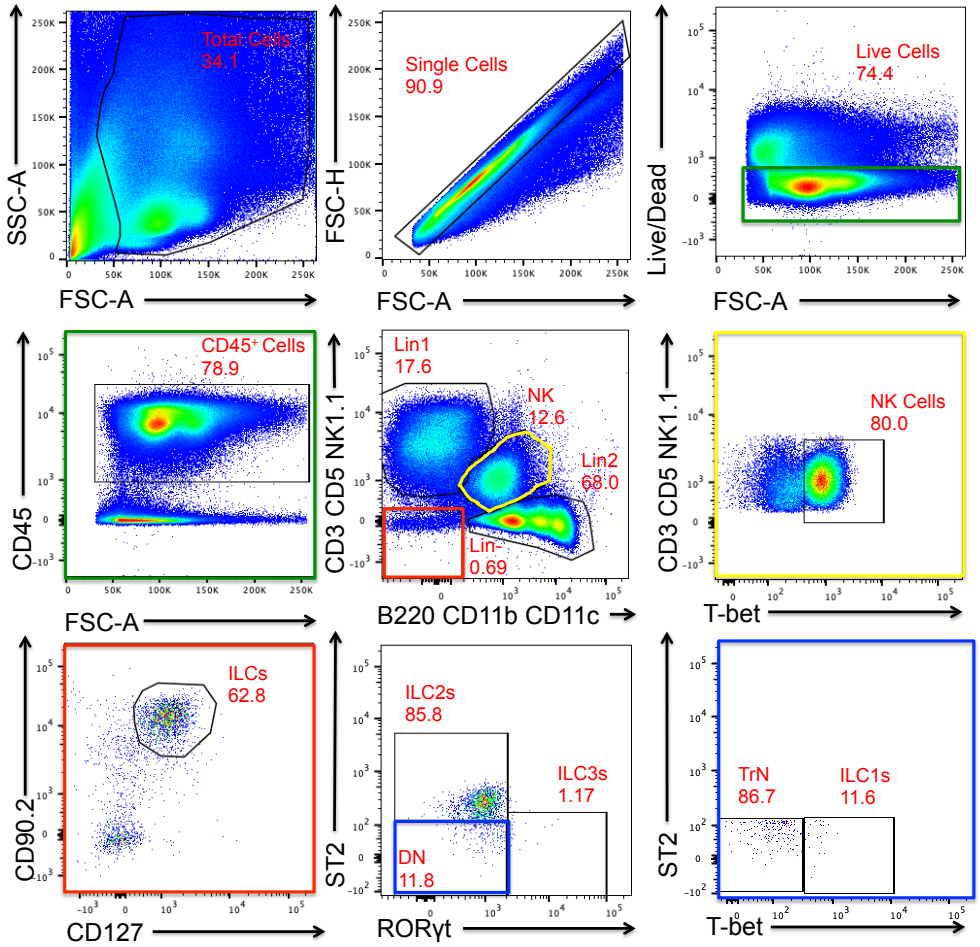


**Figure 3.2 - Gating strategy for identification of ILCs in the lung of naïve C57BL/6 mice**

ILCs were defined as Live $CD45^+Lin^-$ (CD3, CD5 CD11b, CD11c, B220, NK1.1) and $CD90.2^+CD127^+$ cells. Individual subsets were then identified: ILC1s = $ST2^-RORγt^-$ $T\text{-}bet^+$; ILC2s = $ST2^+RORγt^-$; ILC3s = $ST2^-$ $RORγt^+$. Lin1 = CD3, CD5, NK1.1; Lin2 = B220, CD11b, CD11c; NK = Natural Killer; $Lin^-$ = Lineage Negative; DN = Double Negative ($ST2^-RORγt^-$); TrN = Triple Negative ($T\text{-}bet^-ST2^-RORγt^-$). Numbers in FACS plots represent the percentage of the previous gate e.g. $CD45^+$ cells are 78.9% of the live cell gate.

Initially, a gating strategy was developed to successfully identify ILCs in the lungs of naïve mice (figure 3.2). Leukocytes were identified as live $CD45^+$ single cells, and lineage markers (CD3, CD5, NK1.1, B220, CD11b, CD11c)

used to broadly identify a variety of immune cells (figure 3.2). A lineage-negative population was identified, which lacked expression of all these markers. ILCs were identified as a CD90.2$^{+}$CD127$^{+}$ population from this lineage-negative population, and individual ILC subsets characterised based upon the expression of transcription factors and cell surface markers, with ILC1s identified as T-bet$^{+}$ST2$^{-}$RORγt$^{-}$, ILC2s as ST2$^{+}$RORγt$^{-}$, and ILC3s as ST2$^{-}$RORγt$^{+}$ (figure 3.2). A triple negative population was also identified which lacked expression of all 3 markers (figure 3.2).

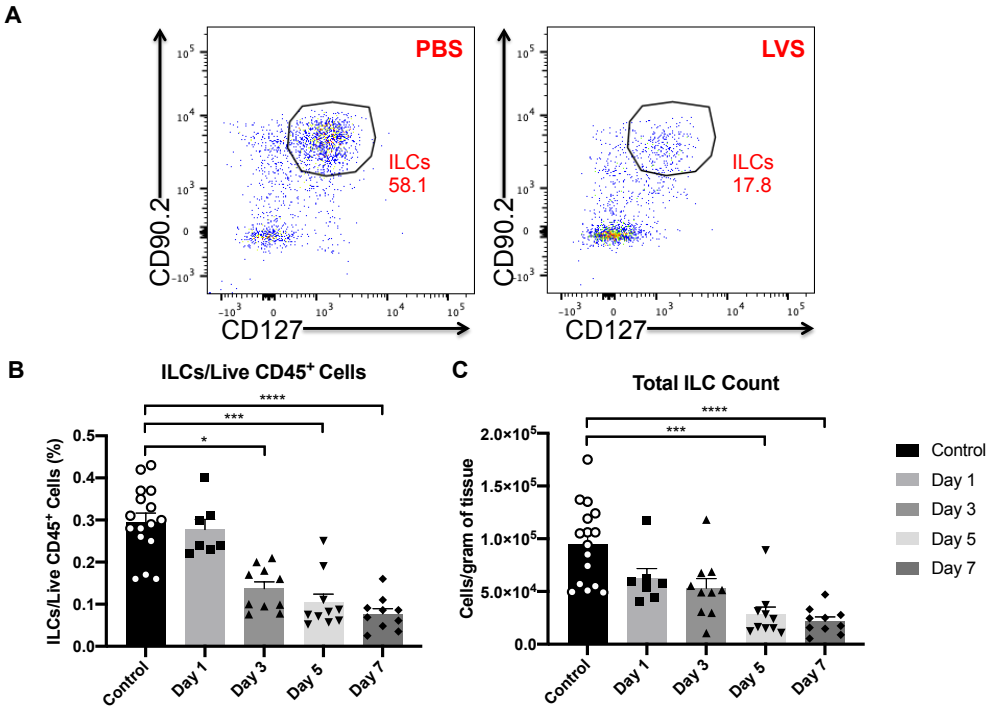


**Figure 3.3 - *F. tularensis* LVS infection causes a reduction in lung ILCs.**

C57BL/6 mice were infected with 1000 CFU *F. tularensis* LVS and total lung ILCs identified by flow cytometry (Lin$^{-}$CD90.2$^{+}$CD127$^{+}$) at different time points p.i. **(A)** Representative plots for ILCs in PBS control and LVS-infected mice (plot from day 5 p.i.). **(B)** Total ILC numbers, expressed as % of live CD45$^{+}$ cells. **(C)** Total ILC counts per gram of tissue. Numbers in FACS plots represent the percentage of ILCs from Lin$^{-}$ cells. Statistical analysis was performed using the Kruskal Wallis test for non-parametric data, with Dunn's multiple comparisons tests performed for analysis between groups; * p<0.05; *** p<0.001; **** p<0.0001.

With the knowledge that this gating strategy was a useful tool to identify ILCs in the lungs of naïve uninfected mice, it was then used to monitor ILCs during infection with *F. tularensis* LVS (figure 3.3). From day 3 p.i. onwards, total ILCs were significantly reduced as a frequency of total live CD45$^{+}$ cells when compared to control (uninfected) mice (figure 3.3A & B). Total ILC numbers were also significantly reduced when compared to control mice, but only from

day 5 p.i. onwards (figure 3.3C). Thus, total ILCs appear to be reduced as infection with *F. tularensis* LVS progresses.

### 3.2.3 Dynamic changes are observed in multiple lung immune cell populations during infection with *F. tularensis* LVS

As the total number of ILCs was reduced during infection with *F. tularensis* LVS, it was important to characterise other lung immune cell populations, in order to investigate how the lung immune environment is affected by the bacteria as infection progresses (figure 3.4). As mentioned, the gating strategy for ILCs utilised a variety of lineage markers (CD3, CD5, NK1.1, B220, CD11b, CD11c), which were spread over two fluorescence channels (figure 3.2). Whilst useful for identification of ILCs, these markers also helped identify other immune cell types. Specifically, total T cells were identified as $CD3^+CD5^+$ (Lin1), with $CD4^+$ T cells identified from this population. A broader $B220^+CD11b^+CD11c^+$ (Lin2) immune cell population served to identify B cells and myeloid cells (figure 3.2 and 3.4A & B). Natural killer (NK) cells were identified from a double positive population from these markers, expressing both NK1.1 and CD11b (figure 3.2). NK cells were further distinguished from other cells which potentially showed expression of markers from both lineage gates through their expression of T-bet, such that NK cells were identified as $NK1.1^+CD11b^+$T-$bet^+$ cells (figure 3.2 and 3.4C & D).

The broader $B220^+CD11b^+CD11c^+$ cell population showed no reduction during infection as a frequency of live $CD45^+$ cells, or of total cell numbers when compared to uninfected mice (figure 3.4 A & B). In fact, from day 3 p.i. onwards, a small but significant increase was observed in the frequency of this population, which remained high at days 5 and 7 p.i. (figure 3.4A). Additionally, an enhanced number of total $B220^+CD11b^+CD11c^+$ cells was observed at day 3 p.i. when compared to day 1 and 5 p.i. (figure 3.4B).

The frequency of NK cells was reduced at days 3 and 7 p.i. (figure 3.4C), with a reduction in total NK cell numbers also observed at this later time point (figure 3.4D). Total T cell ($CD3^+CD5^+$) and $CD4^+$ T cell numbers were markedly decreased from day 3 p.i. onwards (figure 3.4E-H). Overall, these data indicate that the relative proportions of multiple immune cell populations are altered during infection with *F. tularensis* LVS.

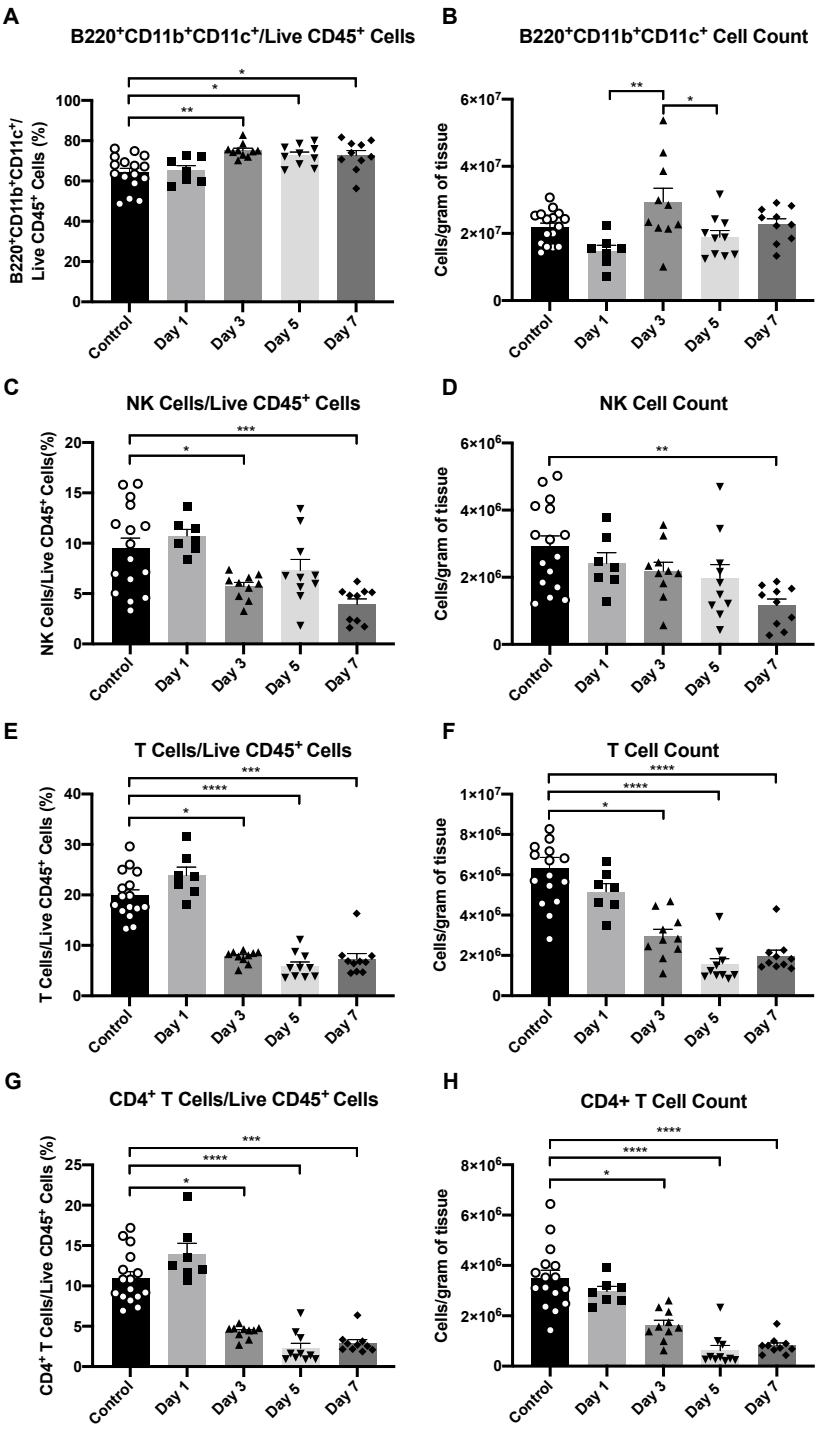


**Figure 3.4 - Lung immune cell populations exhibit dynamic changes during infection with *F. tularensis* LVS**

C57BL/6 mice were infected with 1000 CFU *F. tularensis* LVS and multiple immune cell populations identified in the lung at different time points p.i. **(A-B)** $B220^{+}CD11b^{+}CD11c^{+}$ cells, **(C-D)** NK cells, **(E-F)** total and **(G-H)** $CD4^{+}$ T cells were identified and expressed as a frequency of live $CD45^{+}$ cells, and cell counts per gram of tissue (n=16 for control, n=7 for day 1, n=10 for day 3, 5 and 7 mice). Statistical analysis was performed using either one-way ANOVA for parametric data, or Kruskal Wallis for non-parametric data, with Holm-Sidak's and Dunn's multiple comparisons tests performed for each method of analysis respectively; * $p<0.05$; ** $p<0.01$; *** $p<0.001$; **** $p<0.0001$.

### 3.2.4 Subset-specific changes in ILC1s and ILC2s are observed during infection with *F. tularensis* LVS

Whilst ILC2s are the dominant ILC subset in the lung of naïve mice (Mindt, Fritz and Duerr, 2018), they are predominantly involved in the innate immune response against type 2-based immunological challenges (Artis and Spits, 2015). In contrast, ILC1s are known to play a role in the control of intracellular infections (Artis and Spits, 2015). Thus, it was important to determine whether the lung ILC compartment was altered during early infection with *F. tularensis* LVS – especially given that phenotypic changes have been previously observed here in other intracellular infections (Silver *et al.*, 2016). Thus, individual subsets were identified as ILC1s (T-bet$^{+}$), ILC2s (ST2$^{+}$), ILC3s (RORγt), and a triple negative (TrN) population (figure 3.5A & B). Fluorescent minus one (FMO) markers were used for appropriate identification of individual subsets (figure 3.5B). As observed by others (Dutton *et al.*, 2017), a TrN population was identified which lacked expression of all three phenotypic markers .

ILC1s represented a small proportion (~2%) of the overall ILC compartment in uninfected mice (figure 3.5C). However, from day 5 pi. onwards, a significant increase in their frequency was observed, with total cell numbers also elevated by day 7 p.i. (figure 3.5C & D). ILC2s are the dominant lung ILC subset in the naïve lung (Mindt, Fritz and Duerr, 2018), which was confirmed here, with ILC2s comprising approximately 90% of the total lung ILC compartment in uninfected mice (figure 3.5E). From day 5 p.i. however, a reduction in ILC2s was observed, both as a frequency of the total ILC compartment and total cell numbers (figure 3.5E & F). ILC3 numbers were unchanged during infection (figure 3.5G & H). Overall, these results show that the lung ILC compartment undergoes dynamic changes during infection with *F. tularensis* LVS.

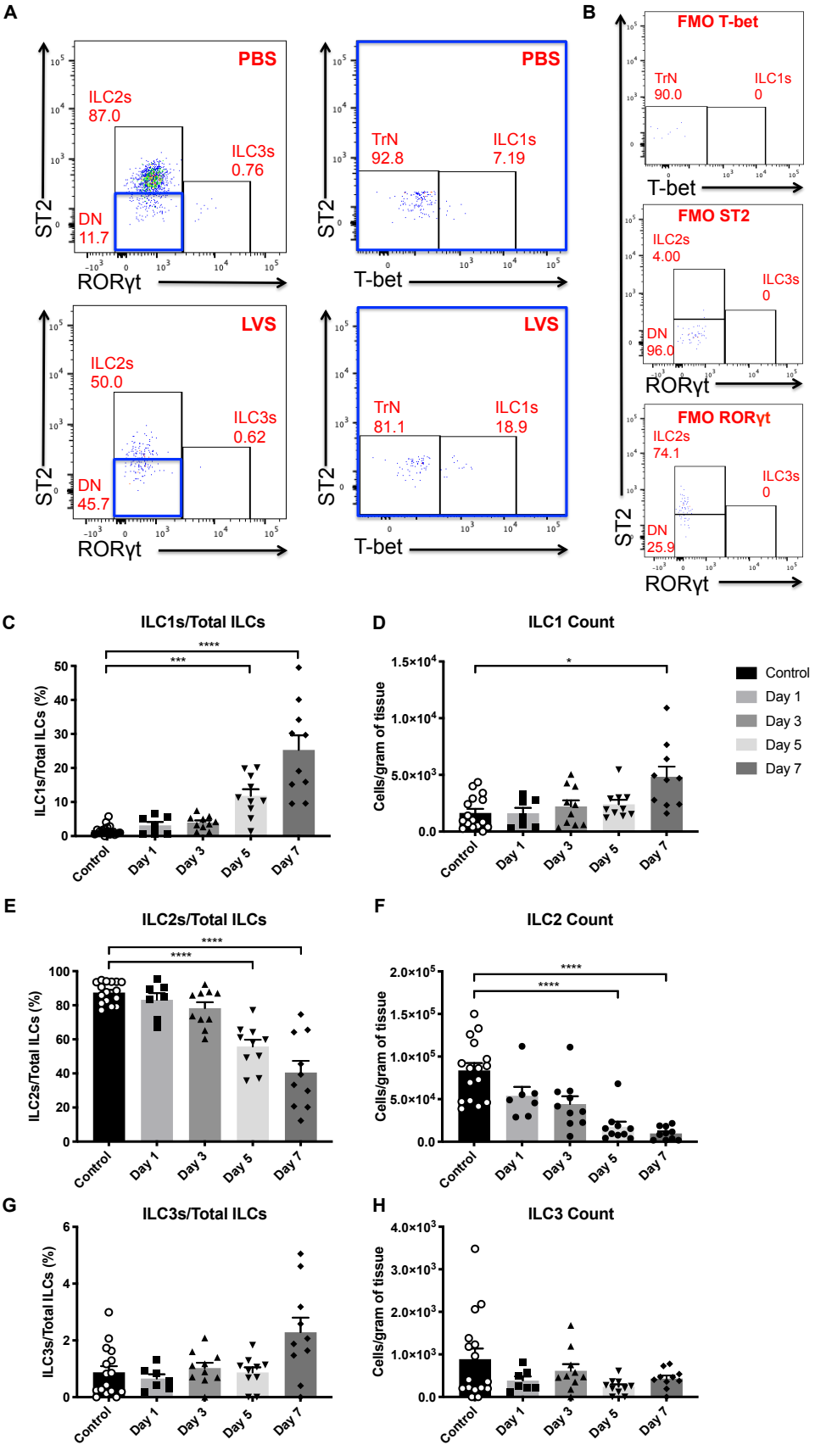
A
PBS
ILC2s
87.0
ILC3s
0.76
DN
11.7
ST2
RORγt
PBS
TrN
92.8
ILC1s
7.19
T-bet
LVS
ILC2s
50.0
ILC3s
0.62
DN
45.7
LVS
TrN
81.1
ILC1s
18.9
B
FMO T-bet
TrN
90.0
ILC1s
0
T-bet
FMO ST2
ILC2s
4.00
ILC3s
0
DN
96.0
FMO RORγt
ILC2s
74.1
ILC3s
0
DN
25.9
C
ILC1s/Total ILCs
ILC1s/Total ILCs (%)
D
ILC1 Count
Cells/gram of tissue
Control
Day 1
Day 3
Day 5
Day 7
E
ILC2s/Total ILCs
ILC2s/Total ILCs (%)
F
ILC2 Count
G
ILC3s/Total ILCs
ILC3s/Total ILCs (%)
H
ILC3 Count

### 3.2.5 Phenotypic changes are observed in T-bet$^+$ ILC1s and GATA3$^+$ ILC2s at later stages of infection with *F. tularensis* LVS

Whilst lung ILC2s express ST2 under steady-state conditions (Mindt, Fritz and Duerr, 2018), they can down-regulate this expression and transition into a more inflammatory ILC2 phenotype under certain conditions (Huang *et al.*, 2015). Thus, it was critical to establish whether the apparent reduction in ST2$^+$ ILC2s observed during infection with *F. tularensis* LVS reflected a reduction in ILC2 numbers, or was due to a specific down-regulation of ST2 expression, and a transition into a more inflammatory phenotype. Thus, ILC2s were identified by their master transcription factor, as GATA3$^+$ ILCs, and the lung ILC compartment characterised (figure 3.6A & C-D). Here, a significant reduction in GATA3$^+$ ILC2s was seen from day 5 p.i. onwards when compared to control uninfected mice (figure 3.6B & C). This reduction in GATA3$^+$ ILC2s was accompanied by a concurrent increase in T-bet$^+$ ILC1s (figure 3.6B & C), confirming ILC1s and ILC2s as the ILC subsets that are altered during infection with *F. tularensis* LVS (figure 3.5C & D).

Next, it was important to further investigate the relationship between ILC1s and ILC2s during infection with *F. tularensis* LVS, given that ILC2s have previously been shown to adopt an ILC1-like phenotype during other intracellular infections (Silver *et al.*, 2016). Specifically, it was important to determine how the phenotype of ILC2s is altered during the course of infection, and whether ILC2s display any capacity to convert to an ILC1-like phenotype. To this end, the expression of the ILC2-specific cell surface markers CD25, ICOS, KLRG1 and ST2 were measured on both ILC1s (T-bet$^+$) and ILC2s (GATA3$^+$) during infection with *F. tularensis* LVS (figure 3.6).

**Figure 3.5 - Lung ILC subsets are altered during infection with *F. tularensis* LVS**

C57BL/6 mice were infected with 1000 CFU *F. tularensis* LVS and individual lung ILC subsets identified by flow cytometry at different time points p.i. **(A)** Representative plots for ILC subsets in PBS (control) and LVS-infected mice (plots from day 5 p.i.). **(B)** FMO controls were used to establish gating. Subsets were defined based upon expression of transcription factors and specific cell surface markers. **(C-D)** ILC1s (T-bet$^+$), **(E-F)** ILC2s (ST2$^+$) and **(G-H)** ILC3s (RORγt$^+$) were quantified and expressed as a frequency of total ILCs, and cell counts per gram of tissue (n=16 for control, n=7 for day 1, n=10 for days 3, 5 and 7 mice). Numbers in FACS plots represent the percentage of the previous gate (ILC2s, ILC3s and DN as a % of total ILCs, and TrN and ILC1s as a % of the DN population). Statistical analysis was performed using either one-way ANOVA for parametric data, or Kruskal Wallis for non-parametric data, with Holm-Sidak's and Dunn's multiple comparisons tests performed for each method of analysis respectively; *p<0.05; *** p<0.001; **** p<0.0001.

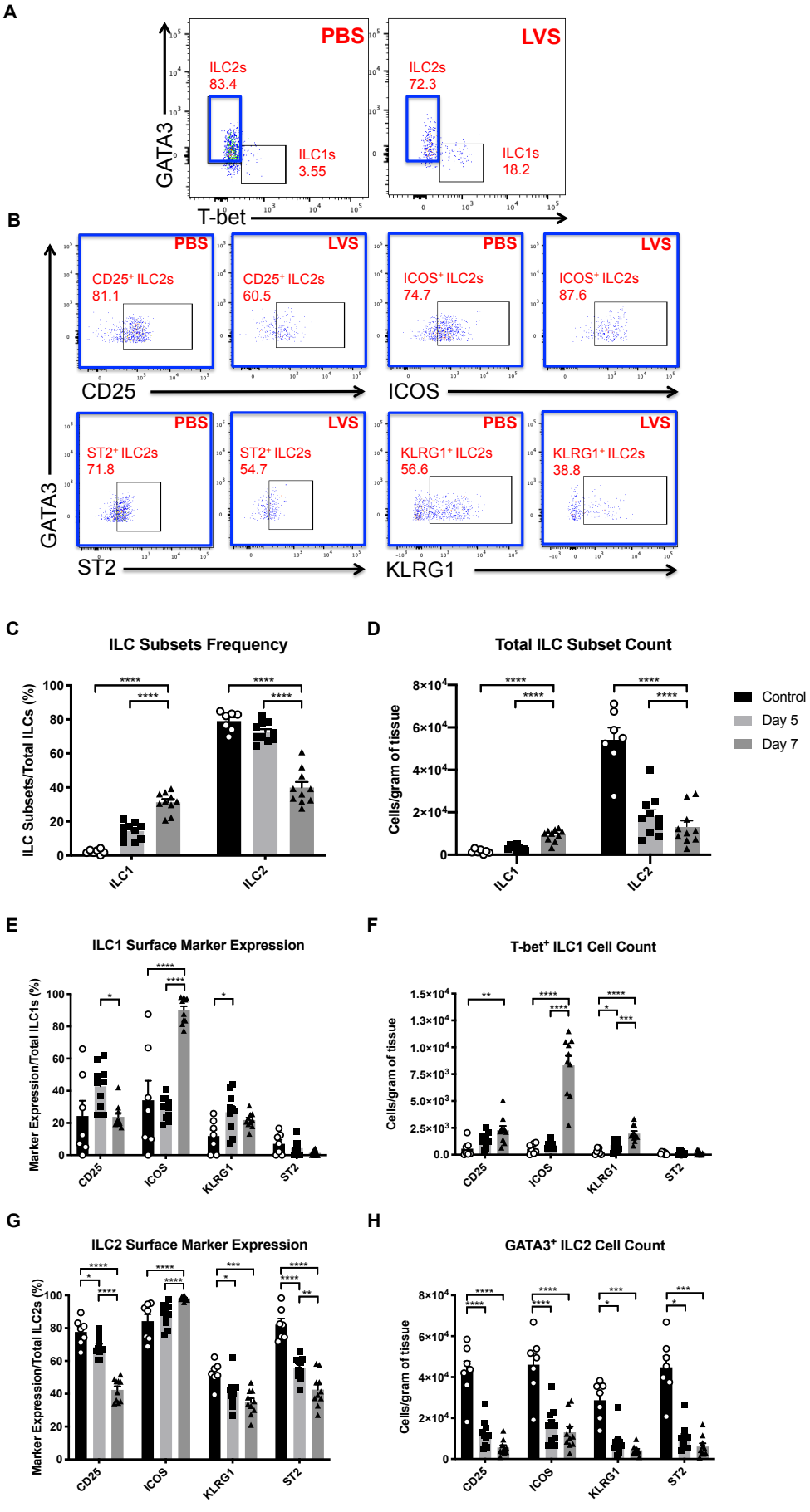
A
PBS
LVS
ILC2s
83.4
ILC1s
3.55
ILC2s
72.3
ILC1s
18.2
GATA3
T-bet
B
CD25⁺ ILC2s
81.1
CD25⁺ ILC2s
60.5
ICOS⁺ ILC2s
74.7
ICOS⁺ ILC2s
87.6
ST2⁺ ILC2s
71.8
ST2⁺ ILC2s
54.7
KLRG1⁺ ILC2s
56.6
KLRG1⁺ ILC2s
38.8
CD25
ICOS
ST2
KLRG1
C
ILC Subsets Frequency
ILC Subsets/Total ILCs (%)
ILC1
ILC2
D
Total ILC Subset Count
Cells/gram of tissue
Control
Day 5
Day 7
E
ILC1 Surface Marker Expression
Marker Expression/Total ILC1s (%)
CD25
ICOS
KLRG1
ST2
F
T-bet⁺ ILC1 Cell Count
Cells/gram of tissue
G
ILC2 Surface Marker Expression
Marker Expression/Total ILC2s (%)
H
GATA3⁺ ILC2 Cell Count
Cells/gram of tissue

Here, ILC1s displayed significantly enhanced expression of KLRG1 at day 5 p.i., and ICOS at day 7 p.i. when compared to control mice (figure 3.6E). Total KLRG1$^+$ ILC1s were enhanced at day 5 p.i., with increased numbers of CD25$^+$ ILC1s and ICOS$^+$ ILC1s also observed at day 7 p.i. (figure 3.6F). Thus, this suggests that ILC1s can adopt expression of ILC2 cell surface markers during infection with *F. tularensis* LVS. When compared to control mice, ILC2s (GATA3$^+$) showed a reduction in the expression of CD25, KLRG1, and ST2 during infection with *F. tularensis* LVS (figure 3.6G). In contrast, ICOS expression was elevated in ILC2s (figure 3.6G). Despite this, a reduction in the total number of GATA3$^+$ ILCs expressing CD25$^+$, ICOS$^+$, KLRG1$^+$ and ST2$^+$ was observed at both day 5 and 7 p.i. (figure 3.6H). Thus, this shows that infection with *F. tularensis* LVS alters the cell surface marker expression of ILC2s, indicating a potential change in ILC2 phenotype as infection progresses. Moreover, with the enhanced expression of some of these ILC2 cell surface markers on ILC1s, this may suggest a potential conversion of ILC2s to ILC1s, and thus begin to uncover how ILC2s are reduced during the later stages of infection with *F. tularensis* LVS.

**Figure 3.6 - Lung T-bet$^+$ ILC1s and GATA3$^+$ ILC2s are altered during infection with *F. tularensis* LVS**

Lung ILC subsets were identified in C57BL/6 mice at days 5 and 7 p.i. with *F. tularensis* LVS (1000 CFU). **(A)** Representative plots for identification of ILC1s (T-bet$^+$) and ILC2s (GATA3$^+$) and **(B)** expression of CD25, ICOS, KLRG1 and ST2 on GATA3$^+$ ILC2s in PBS control and LVS-infected mice (plots from day 5 p.i.). ILC subsets were quantified and expressed as **(C)** a frequency of total ILCs and **(D)** cell counts per gram of tissue. Expression of individual markers was quantified on **(E-F)** T-bet$^+$ ILC1s and **(G-H)** GATA3$^+$ ILC2s and expressed as a frequency of respective subsets and cell counts per gram of tissue (n=7 for control, n=10 for day 5 and day 7 mice). Numbers in FACS plots represent the percentage of ILC2s expressing the identified markers. Statistical analysis was performed using either one-way ANOVA for parametric data, or Kruskal Wallis for non-parametric data, with Holm-Sidak's and Dunn's multiple comparisons tests performed for each method of analysis respectively; * $p<0.05$; *** $p<0.001$; **** $p<0.0001$.

### 3.2.6 ILC2s are not infected during LVS infection

Whilst ILC2s may possess some ability to convert to an ILC1-like phenotype, the observed increase in ILC1 numbers seen during the later stages of infection with *F. tularensis* LVS does not fully compensate for the total reduction in ILC2s. Thus, other possible reasons for this reduced number of ILC2s were considered, with lung samples analysed before and after their reduction, at days 3 and 5 p.i.

Throughout the course of infection, *F. tularensis* LVS is known to infect multiple cell types (Hall *et al.*, 2008). Thus, it was hypothesised that ILC2s may be amongst these cells, which resulted in enhanced cell death that contributed to a reduction in total ILC2 numbers. Using an antibody specific to *F. tularensis* LVS LPS and its isotype control, intracellular infection of immune cells was monitored during infection (figure 3.7A). Both $ST2^+$ ILCs (ILC2s) and $ST2^-$ ILCs (ILC1s and ILC3s) were uninfected at days 3 and 5 p.i. (figure 3.7B). Infection in neutrophils and macrophages, immune cell types known to be infected by *F. tularensis* LVS (Hall *et al.*, 2008), was apparent at day 3 p.i., with the number of these infected cells rising significantly at day 5 p.i. (figure 3.7B). Thus, these data indicate that ILC2s are not infected by *F. tularensis* LVS, and therefore their numbers are not reduced by direct infection with the bacteria.

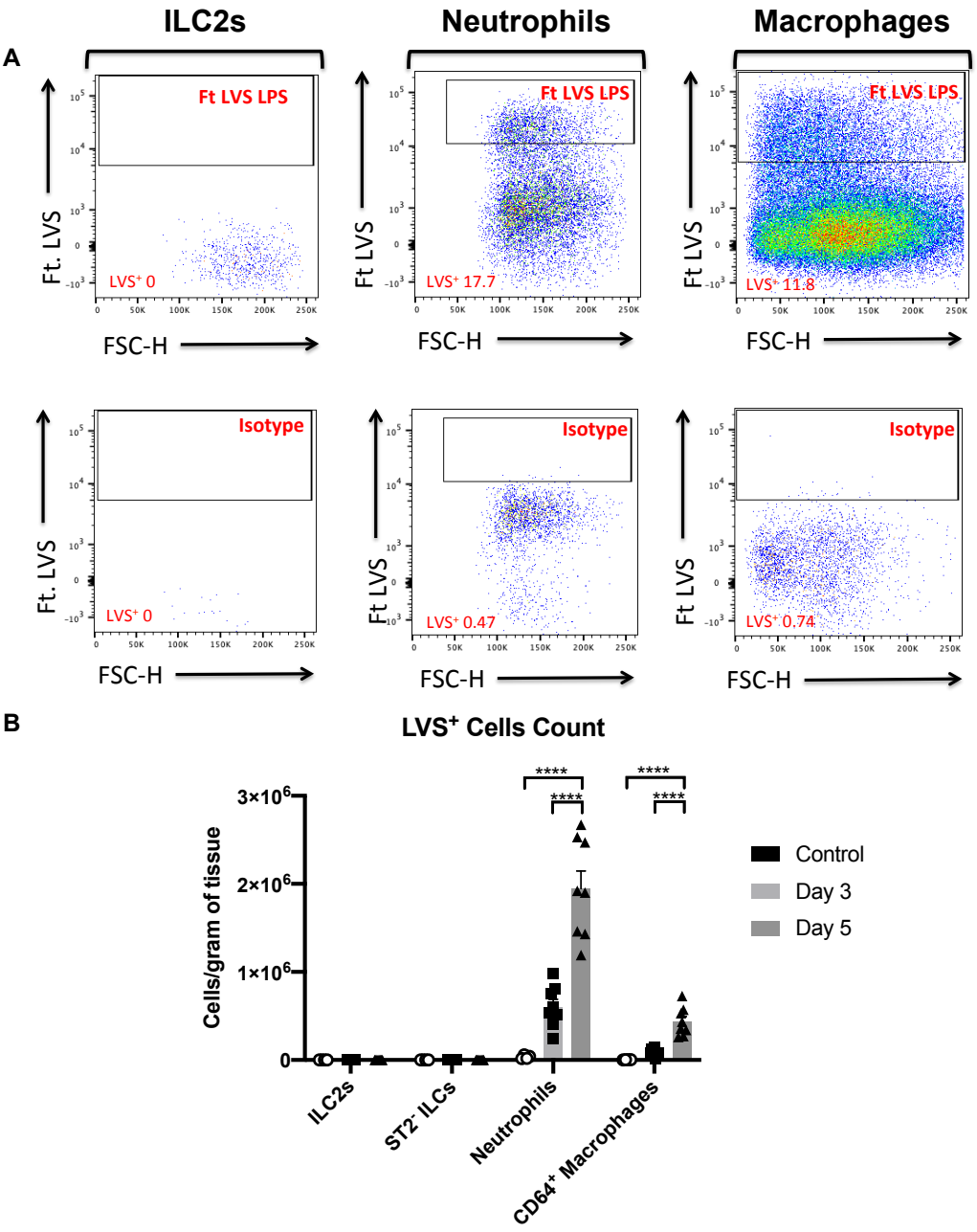


**Figure 3.7 - Lung ILC2s are not infected by *F. tularensis* LVS**

Infected immune cell populations were analysed in the lung of C57BL/6 mice at day 3 and day 5 p.i. with 1000 CFU *F. tularensis* LVS. **(A)** Representative plots for identification of LVS-infected cells using an antibody against the LVS-LPS, and an isotype control. **(B)** $LVS^+$ $ST2^+$ ILC2s (Live $CD45^+Lin^-CD90.2^+CD127^+$), $ST2^-$ ILCs, neutrophils (Live $CD45^+CD11b^+Ly6G^+$) and $CD64^+$ macrophages (Live $CD45^+CD11b^+Ly6G^-Siglec\text{-}F^-CD64^+$) were quantified, and expressed as cell counts per gram of tissue (n=4 for control; n=8 for day 3 and 5 p.i.). Numbers in FACS plots represent the percentage of infected cells in each immune cell population. Statistical analysis was performed with either one-way ANOVA for parametric data, or Kruskal Wallis for non-parametric data, with Holm-Sidak's and Dunn's multiple comparisons tests performed for each method of analysis respectively; **** $p<0.0001$.

### 3.2.7 ILC2s do not show enhanced cell death during infection with *F. tularensis* LVS

Whilst ILC2s are not directly infected by *F. tularensis* LVS, it remained of interest to determine whether the reduced number of ILC2s during the later stages of infection was due to enhanced ILC2 cell death. Annexin V is a cellular protein that binds to phosphatidylserine, which is a marker of apoptotic cells. Hence, viability of ILC2s was identified by flow cytometry via staining for Annexin V in combination with a Live/Dead (LD) viability dye (figure 3.8). In combination, these viability stains allowed for identification of live ($LD^-Annexin\ V^-$), apoptotic (apop.; $LD^-Annexin\ V^+$), necrotic (necro.; $LD^+Annexin\ V^+$), and dead ($LD^+Annexin\ V^-$) cells. A pooled lung cell suspension from both PBS-control and LVS-infected mice was heat-treated at 95$^o$C for 2 minutes as a positive control for cell death (figure 3.8).

Total apoptotic ILC2s were reduced at both day 3 and 5 p.i. when compared to control mice (figure 3.9A & B). Moreover, the number of necrotic ILC2s was also reduced at day 5 p.i. (figure 3.9C & D). Thus, this suggests that an enhanced level of cell death in ILC2s is not likely to be responsible for the reduction in total ILC2 numbers during infection with *F. tularensis* LVS.

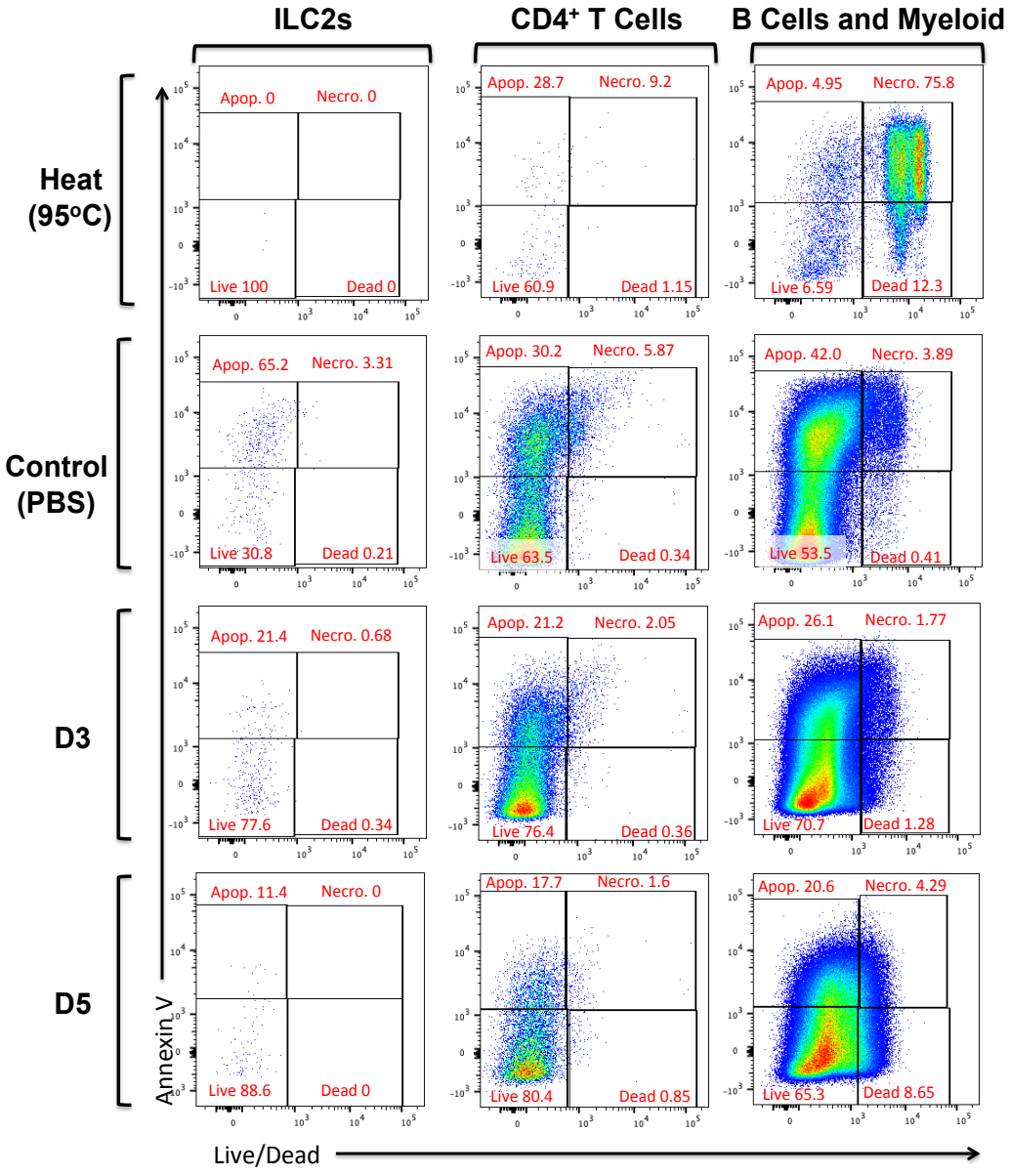


**Figure 3.8 - Gating strategy for identification of cell death in lung immune cell populations during infection with *F. tularensis* LVS**

Apoptotic (apop.; $LD^-Annexin\ V^+$) and necrotic (necro.; $LD^+Annexin\ V^+$) immune cell populations in the lung of C57BL/6 mice at day 3 (D3) and day 5 (D5) p.i. with 1000 CFU *F. tularensis* LVS. Control mice were given PBS. A pooled lung cell suspension of control and LVS-infected mice was heat-treated at 95°C for 2 minutes as a positive control for cell death. ILC2s were identified as $CD45^+Lin^-CD90.2^+CD127^+ST2^+$, $CD4^+$ T cells as $CD45^+CD3^+CD5^+CD4^+$, and B cells and myeloid immune populations (BCM) as $CD45^+B220^+CD11b^+CD11c^+$ cells. Numbers in FACS plots represent the percentage of live, apop., necro., and dead cells for individual immune cell populations.

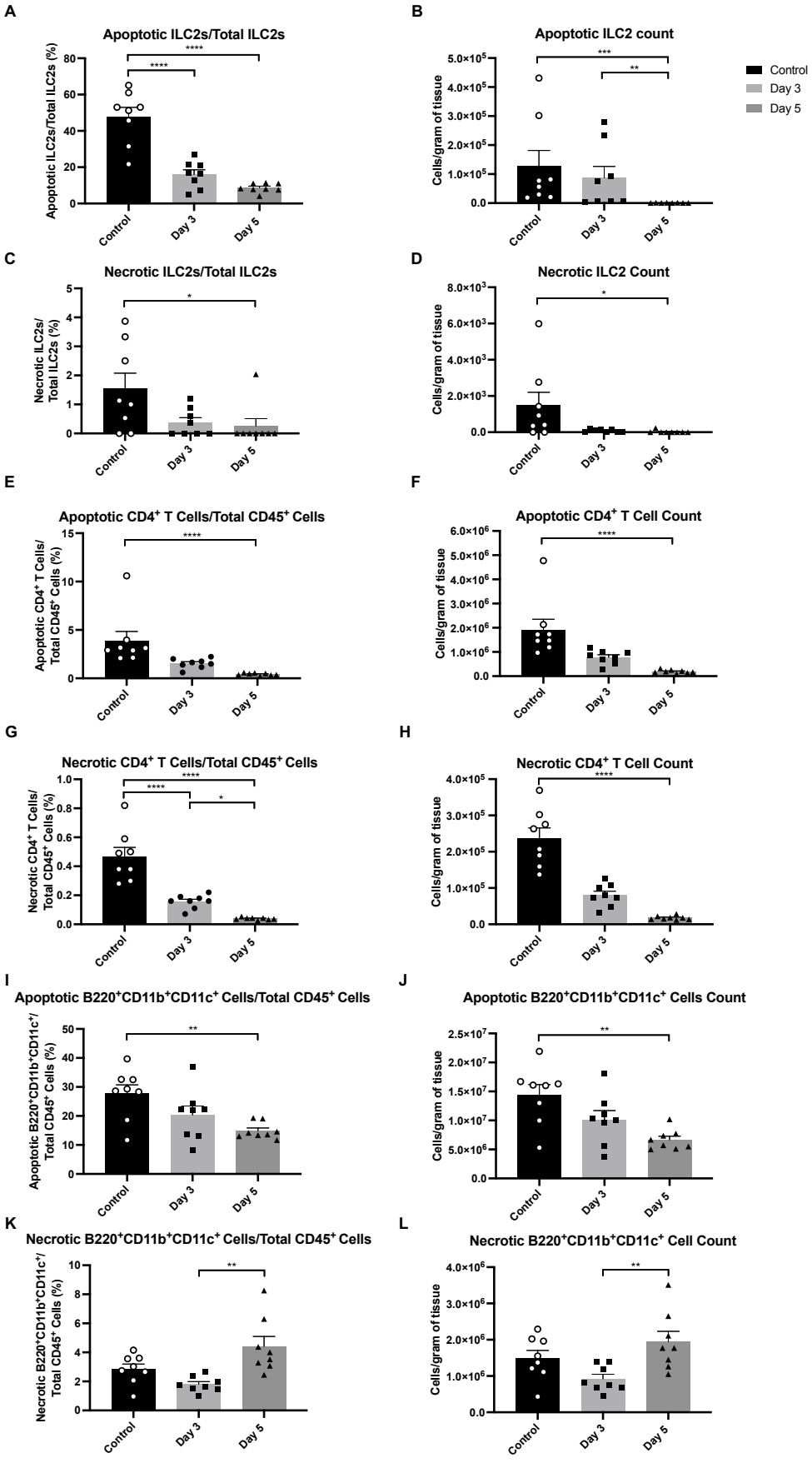
A
Apoptotic ILC2s/Total ILC2s
Apoptotic ILC2s/Total ILC2s (%)
B
Apoptotic ILC2 count
Cells/gram of tissue
Control
Day 3
Day 5
C
Necrotic ILC2s/Total ILC2s
Necrotic ILC2s/ Total ILC2s (%)
D
Necrotic ILC2 Count
Cells/gram of tissue
E
Apoptotic CD4+ T Cells/Total CD45+ Cells
Apoptotic CD4+ T Cells/ Total CD45+ Cells (%)
F
Apoptotic CD4+ T Cell Count
Cells/gram of tissue
G
Necrotic CD4+ T Cells/Total CD45+ Cells
Necrotic CD4+ T Cells/ Total CD45+ Cells (%)
H
Necrotic CD4+ T Cell Count
Cells/gram of tissue
I
Apoptotic B220+CD11b+CD11c+ Cells/Total CD45+ Cells
Apoptotic B220+CD11b+CD11c+/ Total CD45+ Cells (%)
J
Apoptotic B220+CD11b+CD11c+ Cells Count
Cells/gram of tissue
K
Necrotic B220+CD11b+CD11c+ Cells/Total CD45+ Cells
Necrotic B220+CD11b+CD11c+/ Total CD45+ Cells (%)
L
Necrotic B220+CD11b+CD11c+ Cell Count
Cells/gram of tissue
Control
Day 3
Day 5

To determine whether these reductions in cell death were ILC2-specific, levels of apoptosis and necrosis were also quantified in $CD4^+$ T cells and B cell and myeloid (BCM; $B220^+CD11b^+CD11c^+$) immune cells (figure 3.9E-L). Akin to ILC2s, both the number of apoptotic and necrotic $CD4^+$ T cells were reduced by day 5 p.i. (figure 3.9E-H). Elsewhere, whilst the number of apoptotic BCM immune cells was also reduced at day 5 p.i. (figure 3.9I & J) a significant rise in the number of necrotic BCM immune cells was observed between day 3 and day 5 p.i. (figure 3.9K & L). Together, these results indicate that whilst $CD4^+$ T cells do not display enhanced levels of cell death during infection with *F. tularensis* LVS, certain cells in the BCM immune cell population undergo a necrotic form of cell death as infection progresses.

**Figure 3.9 - Levels of apoptotic and necrotic cell death are altered in multiple lung immune cell populations during infection with *F. tularensis* LVS**

Apoptotic (Annexin $V^+LD^-$) and necrotic (Annexin $V^+LD^+$) immune cell populations were identified in the lung of C57BL/6 mice at day 3 (D3) and day 5 (D5) p.i. with 1000 CFU *F. tularensis* LVS. Control mice were given PBS. **(A-D)** Apoptotic and necrotic ILC2, **(E-H)** $CD4^+$ T cell, and **(I-L)** $B220^+CD11b^+CD11c^+$ immune cell populations were quantified, and expressed as a frequency of total ILC2s (apoptotic/necrotic ILC2s), total $CD45^+$ cells (CD4+ T cells and $B220^+CD11b^+CD11c^+$ cells), and cell counts per gram of tissue (all cell populations; n=8). Statistical analysis was performed with either one-way ANOVA for parametric data, or Kruskal Wallis for non-parametric data, with Holm-Sidak's and Dunn's multiple comparisons tests performed for each method of analysis respectively; ** $p<0.01$; *** $p<0.001$; **** $p<0.0001$.

### 3.2.8 ILC2 numbers are also reduced in draining lymph nodes during infection with *F. tularensis* LVS

Finally, it was hypothesised that the reduction in ILC2s induced by *F. tularensis* LVS infection could be due to enhanced migration of these cells from the lung tissue into the mediastinal (lung-draining) lymph node (LN). To begin to test this possibility, ILCs in the mediastinal LN were identified as $Lin^-$ $CD127^+$ cells (figure 3.10A). Interestingly, instead of enhanced ILCs being present in the LN, the frequency of total ILCs was significantly reduced at day 3 p.i. when compared to control uninfected mice (figure 3.10B). Total ILC numbers were unchanged (figure 3.10C).

Next, specific ILC subsets were analysed in the mediastinal LN at different times p.i. ILC1 frequency and total number were unaltered in the mediastinal LN during infection with *F. tularensis* LVS (figure 3.10D & E). The frequency of ILC2s in the mediastinal LN was unaltered by infection, whereas the total number of ILC2s observed was in fact significantly reduced when compared to control uninfected mice (figure 3.10F & G). Thus, this indicates that ILC2s may not be migrating from the lung into the mediastinal LN during the later stages of infection.

As seen by others (Mackley *et al.*, 2015), the majority of ILCs in the mediastinal LN were RORγt$^+$ ILC3s (figure 3.10A & H). Indeed, approximately 60% of the steady-state ILC compartment in the mediastinal LN comprised RORγt$^+$ ILC3s (figure 3.10H), with this frequency of ILC3s enhanced at day 5 p.i. (figure 3.10H). Total ILC3 numbers were unchanged during infection (figure 3.10I), demonstrating that unlike the lung ILC compartment, the total number of the dominant ILC subset (RORγt$^+$ ILC3s) in the mediastinal LN is not significantly reduced during infection with *F. tularensis* LVS.

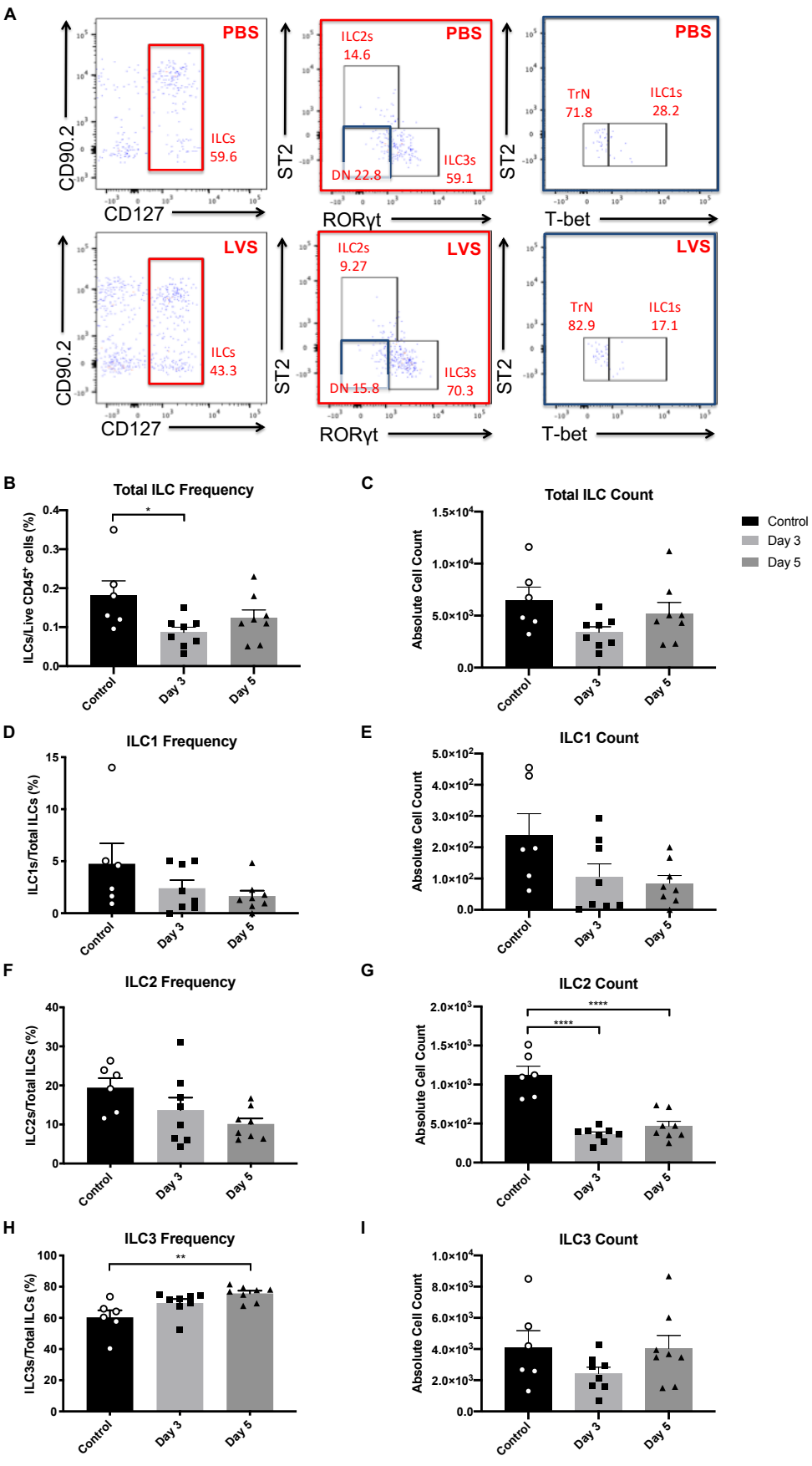
A
PBS
ILCs
59.6
CD90.2
CD127
ILC2s
14.6
ILC3s
59.1
DN 22.8
ST2
RORγt
TrN
71.8
ILC1s
28.2
T-bet
LVS
ILCs
43.3
ILC2s
9.27
ILC3s
70.3
DN 15.8
TrN
82.9
ILC1s
17.1
B
Total ILC Frequency
ILCs/Live CD45+ cells (%)
C
Total ILC Count
Absolute Cell Count
Control
Day 3
Day 5
D
ILC1 Frequency
ILC1s/Total ILCs (%)
E
ILC1 Count
F
ILC2 Frequency
ILC2s/Total ILCs (%)
G
ILC2 Count
H
ILC3 Frequency
ILC3s/Total ILCs (%)
I
ILC3 Count

## 3.3 Discussion

### 3.3.1 Understanding the changes in the lung ILC compartment during the later stages of infection with *F. tularensis* LVS

ILCs are capable of rapid response to immune challenges (Spits *et al.*, 2013; Artis and Spits, 2015). Here in this thesis chapter, it was shown that ILC2s ($ST2^+$/$GATA3^+$) represent the vast majority of the steady-state lung ILC compartment, which is in line with work by others (Monticelli *et al.*, 2011; Nussbaum *et al.*, 2013). Principally involved in immune responses against parasitic infections and allergic diseases (Artis and Spits, 2015), it would be reasonable to consider that ILC2s would not be as beneficial in the immune response against *F. tularensis* LVS, an intracellular bacterium, as perhaps the ILC1 or ILC3 subsets – given that these latter two subsets are associated with immune responses against intracellular and bacterial infections respectively (Artis and Spits, 2015). Despite this, lung ILC3 numbers were unchanged during infection with *F. tularensis* LVS, suggesting that this ILC subset may not be important for the control of *F. tularensis* infection.

**Figure 3.10 - ILCs of the mediastinal lymph node are altered during infection with *F. tularensis* LVS**

ILCs were identified in the mediastinal lymph node of C57BL/6 mice at day 3 and day 5 p.i. with 1000 CFU *F. tularensis* LVS. **(A)** Representative plots for identification of ILCs as Live $CD45^+Lin^-$ (i.e. CD3, CD5 CD11b, CD11c, B220, NK1.1) and $CD127^+$ cells in PBS (control) and LVS-infected mice. **(B-C)** Total ILCs, **(D-E)** ILC1s ($T\text{-}bet^+$), **(F-G)** ILC2s ($ST2^+$) and **(H-I)** ILC3s ($ROR\gamma t^+$) were quantified and expressed as a frequency of live $CD45^+$ cells (total ILCs), total ILCs (individual ILC subsets), and absolute cell counts (n=6 for control mice; n=8 for LVS-infected mice). Numbers in FACS plots represent the percentage of the previous gate (ILCs as a % of $Lin^-$ cells; ILC2s, ILC3s and DN gates as a % of total ILCs; TrN and ILC1s as a % of the DN ILC population). Statistical analysis was performed with either one-way ANOVA for parametric data, or Kruskal Wallis for non-parametric data, with Holm-Sidak's and Dunn's multiple comparisons tests performed for each method of analysis respectively; * $p<0.05$; ** $p<0.01$; **** $p<0.0001$.

Interestingly, ILC2s have proven to be of benefit in some intracellular infections, helping repair viral infection-induced tissue damage (Monticelli *et al.*, 2011), and displaying a degree of plasticity to convert to an ILC1-like phenotype (Silver *et al.*, 2016). Akin to the observations in this thesis chapter, ILC2 numbers have also been shown to be reduced in the context of influenza infection, with a concomitant rise in ILC1 numbers in response to this particular immunological challenge (Silver *et al.*, 2016). Here, T-bet$^{+}$ ILC1s arose from an ST2$^{+}$ ILC2 pool, with IL-12 and IL-18 critical for this ILC2-ILC1 conversion. It is therefore worthy of note that, following infection via the tracheal route, IL-12 is observed in the lungs of LVS-infected mice – with levels of this cytokine increasing as infection progresses (Lin *et al.*, 2009). Thus, the observed expansion of lung ILC1s during the later stages of infection with *F. tularensis* LVS could occur as a result of an ILC2-ILC1 conversion, at least in part due to enhanced levels of IL-12 present as infection progresses.

### 3.3.2 Investigating the phenotypic changes in ILC2s during the later stages of infection with *F. tularensis* LVS

As previously mentioned, it is possible that a potential ILC2-ILC1 conversion occurs during infection with *F. tularensis* LVS. In order for this to happen, changes in cell surface marker expression of ILC2s would potentially be observed. Thus, at least some insight into the phenomena of ILC2-ILC1 conversion during *Francisella* infection can be gained from the analysis of cell surface marker expression on each ILC subset.

In the lung, both natural and inflammatory ILC2s (nILC2 and iILC2 respectively) have been reported in response to different external stimuli (Mindt, Fritz and Duerr, 2018). Crucially however, nILC2s, which are responsive to IL-33, are considered the dominant ILC2 subset under steady-state conditions (Mindt, Fritz and Duerr, 2018). In contrast, iILC2s appear following stimulation with either IL-25, or parasitic infection (Huang *et al.*, 2015). These two subpopulations of ILC2s can also be differentiated based upon their expression of cell surface markers. Unlike nILC2s, iILC2s are an ST2$^{-}$ population of ILC2s that express the IL-25 receptor (IL-17RB), as well as higher levels of KLRG1 (Huang *et al.*, 2015). During infection with *F.*

*tularensis* LVS, whilst lung ILC2s showed decreased expression of ST2, this was not counteracted by an enhanced expression of KLRG1. In fact, lung ILC2s showed decreased expression of KLRG1 during *Francisella* infection, indicating a potential loss of ILC2 phenotype.

Lung ILC2s are also known to express CD25 (Bartemes *et al.*, 2012; Halim *et al.*, 2012a), with an early study identifying ILC2s as a $Lin^{-}CD127^{+}CD25^{+}$ population (Halim *et al.*, 2012a). However, this expression of CD25 (amongst other ILC2 markers) is lost upon viral infection, where ILC2s convert to an ILC1-like phenotype (Silver *et al.*, 2016). In line with this, the ILC1 population that arose during infection with *F. tularensis* LVS expressed lower levels of CD25 than ILC2s. Moreover, whilst ILC2s from the lungs of uninfected mice expressed high levels of CD25, expression levels decreased as infection progressed. Collectively, these data further support the idea that ILC2s lose their phenotype during infection with *F. tularensis* LVS. Despite this, it is currently unclear whether this loss of phenotype correlates with a transition into an ILC1-like phenotype.

As previously discussed, viral-induced converted ILC1s display significantly lower expression of CD25 than ILC2s. However, they also express lower levels of ICOS and ST2 (Silver *et al.*, 2016). In the context of *F. tularensis* LVS, this remained true for ST2 expression on ILC1s. Yet, in contrast to these viral-induced converted ILC1s, ICOS expression was significantly up-regulated on ILC1s during infection with *F. tularensis* LVS. This could therefore indicate multiple possibilities. Due to the inherent differences in the ILC1 population identified during infection with *F. tularensis* LVS and that previously identified during viral infection (Silver *et al.*, 2016), it could suggest that the ILC1s observed in *Francisella* model are not derived from the ILC2 pool. Alternatively, it may suggest that these ILC1s are phenotypically distinct from previously identified converted ILC1s (Silver *et al.*, 2016), and do originate from the lung ILC2 pool. This becomes increasingly plausible when considering the consistently high expression of ICOS on ILC2s, and the down-regulation of the other ILC2 cell surface markers CD25, KLRG1 and ST2 on ILC2s as infection progresses. Therefore, the similarities of the expression of these specific cell surface markers on ILC1s and ILC2s may indicate that ILC2s are plastic during infection with *F. tularensis* LVS. Nevertheless, in order to ascertain whether these ILC1s are in fact 'ex-

ILC2s', techniques that identify and trace ILC2s throughout the course of infection are required, such as an ST2-GFP fate mapper mouse model.

### 3.3.3 Attempting to uncover how lung ILC2s are reduced during LVS infection

Given that ILC1s can rapidly produce IFN-γ (Klose *et al.*, 2014; Abt *et al.*, 2015), and how this cytokine is essential for control of infection with *F. tularensis* LVS (Elkins *et al.*, 1996), it is clear that the emergence of a population of ILC1s during LVS infection could prove beneficial to the host immune response. However, the significance of a reduction in ILC2 numbers during infection is less clear, especially given their previously documented plasticity and roles in tissue repair in other intracellular infections (Monticelli *et al.*, 2011; Silver *et al.*, 2016). One possible explanation for the subset-specific reduction in ILC2s could be that this is a process engineered by *F. tularensis* LVS. Here, its rationale would be to reduce the total number of ILC2s that could adopt an ILC1-like phenotype, and thus limit their IFN-γ production. Alternatively, the reduction in ILC2s may be a host-mediated response to infection with *F. tularensis* LVS, reducing the type 2 response and thus favouring type 1-focused immunity – aspects of which are essential for control of infection with *F. tularensis* (Elkins *et al.*, 1996; Duckett *et al.*, 2005). As previously discussed, it has also been considered that the increased number of ILC1s may occur as a result of an ILC2-ILC1 conversion, thus resulting in a reduction in ILC2 numbers. Whilst future work is required to fully determine the validity of this phenomenon, the dramatic decrease in lung ILC2 numbers cannot be explained solely by an ILC2-ILC1 conversion. Thus, other reasons for this reduced number of ILC2s must be considered.

*F. tularensis* LVS invades multiple host cell types during its pathogenesis, with phagocytic cells ingesting bacteria through a process known as looping phagocytosis (Hall *et al.*, 2008). Non-phagocytic cells such as alveolar epithelial cells can also internalise the bacteria, although this appears to be through the use of the host cell cytoskeleton and phosphatidylinositol 3-kinase (PI3K) and tyrosine kinase activity (Craven *et al.*, 2008). Thus, given that invasion of host cells by *F. tularensis* LVS eventually leads to cell death (Lai, Golovliov and Sjostedt, 2001; Lai and Sjostedt, 2003; Mariathasan *et*

*al.*, 2005; Wickstrum *et al.*, 2009; Lindgren *et al.*, 2013; Jessop *et al.*, 2018), it was considered whether internalisation of bacteria and bacteria-induced cell lysis could be a mechanism by which ILC2 numbers were reduced. Here, it was important to quantify levels of infection in cells that are well known to be infected by the bacteria, macrophages and neutrophils (Hall *et al.*, 2008), to serve as a positive control for detection of intracellular bacteria. Indeed, whilst the number of infected neutrophils and macrophages increased as infection progressed, ILC2s remained uninfected throughout the course of infection. Thus, this indicates that the reduction in ILC2s during the later stages of infection is not due to infection of ILC2s with *F. tularensis* LVS.

ILC2s are known to be inhibited and undergo cell death upon exposure to IFN-γ, and type 1 interferons such as IFN-β (Molofsky *et al.*, 2015; Kudo *et al.*, 2016; Duerr *et al.*, 2016). Therefore, when considering the roles that these cytokines play in the immune response against *F. tularensis* (Elkins *et al.*, 1996; Duckett *et al.*, 2005; Cole *et al.*, 2008), it was considered whether the reduced number of ILC2s was due to an enhanced level of ILC2 cell death. It was therefore surprising that a significantly lower number of ILC2s were apoptotic in LVS-infected mice when compared to control (naïve) counterparts. Given the nature of infection with *F. tularensis* LVS and its ability to rapidly induce multi-organ inflammation (Parmely, Fischer and Pinson, 2009), it was also important to determine whether ILC2s were dying by necrosis - a more inflammatory type of cell death. Whilst the number of necrotic ILC2s was low in control mice, a further reduction in necrotic ILC2s was observed at day 5 p.i. Thus, neither apoptosis nor necrosis appear to be responsible for the reduction in ILC2s in the lung during the later stages of infection with *F. tularensis* LVS. It is unclear why ILC2s show reduced apoptosis during *Francisella* infection, especially given that multiple cytokines are present which have previously been shown to promote this form of cell death in ILC2s (Lopez *et al.*, 2004; Duerr *et al.*, 2016). It remains a possibility that ILC2s have already undergone apoptosis by the time of analysis, and have fragmented into apoptotic bodies. However, as these cell fragments share the same FSC/SSC properties as cellular debris, they were likely eliminated from analysis at that stage of gating. Thus, in order to ascertain whether fragmented ILC2s are amongst these apoptotic bodies, a deeper analysis of cell death would be required in future experiments. Here,

cellular debris could be differentiated from these apoptotic bodies through use of the nucleic acid-binding dye TO-PRO-3 (Jiang *et al.*, 2016).

Whilst ILCs are generally considered to be tissue-resident cells, there is now increasing evidence for migration of these cell types between tissues, and to draining lymph nodes in response to immunological challenges (Mackley *et al.*, 2015; Huang *et al.*, 2018; Dutton *et al.*, 2019; Ricardo-Gonzalez *et al.*, 2020). During infection with *F. tularensis* LVS, a significant proportion of extracellular bacteria are present in these draining LNs (Bar-Haim *et al.*, 2008), which would likely generate a response from ILC3s (amongst other cell types) (Satoh-Takayama *et al.*, 2008; Sonnenberg *et al.*, 2011; Klose *et al.*, 2013; Ardain *et al.*, 2019). It is therefore worthy of note that inflammatory ILC2s can acquire ILC3-like properties during certain immunological challenges, up-regulating expression of RORγt and producing IL-17 (Huang *et al.*, 2015). As this cytokine has previously been shown to be important in control of infection with *F. tularensis* LVS (Cowley *et al.*, 2010), it was considered that a reduced lung ILC2 number could be due to lung ILC2 migration to draining LNs, and subsequent acquisition of ILC3-like properties upon exposure to the extracellular phase of the bacteria. Indeed, this idea was supported by the reduced number of $ST2^+$ ILC2s observed in the draining LN during infection, given a characteristic of this inflammatory ILC2 phenotype is the reduced expression of ST2 (Huang *et al.*, 2015). Despite this, total $ROR\gamma t^+$ ILC3 numbers remained unchanged as infection progressed. Collectively, the lack of increases in either ILC subset therefore suggested that it was unlikely that ILC2s are migrating to the draining LN. Nevertheless, given that ILC3s persisted in the mediastinal LN during LVS infection, and that they were not significantly reduced like lung ILC2s, this could indicate that ILC3s at this site are involved in the immune response against the extracellular phase of *Francisella* infection. Further work is required to fully investigate whether ILC3s in the mediastinal LN play any role in control of infection with *F. tularensis* LVS.

Both lung ILC2s and draining LN ILC2s express ST2 (Chang *et al.*, 2011; Monticelli *et al.*, 2011; Martinez-Gonzalez *et al.*, 2016), and more importantly, no phenotypic differences in expression of surface markers or transcription factors are observed between resident ILC2s in either compartment (Chang *et al.*, 2011; Monticelli *et al.*, 2011; Martinez-Gonzalez *et al.*, 2016). Thus, a

potential caveat of the data concerning the migration of ILC2s to draining LNs is that these LN-resident ILC2s were not distinguishable in any way from lung-resident ILC2s. Therefore, whilst draining LN ILC2 numbers were reduced during infection with *F. tularensis* LVS, more advanced techniques would be required in order to fully ascertain whether the observed ILC2s in the draining LN are ILC2s that have trafficked from the lung. One such technique utilises the transgenic *Kaede* mouse model, in which cells express the Kaede protein – which is irreversibly converted from green to red fluorescence upon violet light exposure (Morton *et al.*, 2014). Indeed, this technique has previously been used to analyse the trafficking of labelled intestinal ILCs to mesenteric LNs (Mackley *et al.*, 2015; Kästele *et al.*, 2021). Thus, through a similar approach of shielding the mediastinal LNs, and careful exposure of the lungs to violet light, any potential trafficking of lung ILC2s could be identified and studied in more depth.

### 3.3.4 Understanding the reduction in cells of the lymphoid lineage during infection with *F. tularensis* LVS

As well as a reduction in ILCs, a significant reduction in NK cells and T cells was observed during infection, akin to previous observations by others (Schmitt *et al.*, 2013). Thus, this indicates a widespread reduction in cells of lymphoid origin during infection with *F. tularensis* LVS. As previously mentioned, ILC2s can undergo cell death upon exposure to IFN-γ, and type 1 interferons such as IFN-β (Molofsky *et al.*, 2015; Kudo *et al.*, 2016; Duerr *et al.*, 2016). Likewise, total T cell numbers have also been shown to be reduced by these cytokines (Kamphuis *et al.*, 2006; de Kleijn *et al.*, 2013). Therefore, the reduction in both T cells and ILCs may be regulated through the presence of both IFN-γ and type 1 interferons during infection with *F. tularensis* LVS (Elkins *et al.*, 1996; Duckett *et al.*, 2005; Cole *et al.*, 2008).

Whilst this is one possible explanation for the reduction in lymphocytes during infection with *F. tularensis* LVS, it is worthy of note that reduced T cell and NK cell numbers have been seen previously in several other models of infection, and are mainly attributed to an enhanced level of apoptosis as infection progressed (Hotchkiss *et al.*, 2005; Bradfute *et al.*, 2007; Boonnak *et al.*, 2014). Despite this, an enhanced level of apoptosis was not observed, nor necrosis of $CD4^+$ T cells during infection with *F. tularensis* LVS. Thus, as previously discussed with ILC2 cell death, further work is required to

determine whether T cells have fragmented into apoptotic bodies and were consequently eliminated from this analysis. As the levels of cell death in NK cells were not quantified, it is unclear whether this could be the cause of their reduction. Interestingly however, it has been suggested that *F. tularensis* can infect NK cells, but not replicate within them (Schmitt *et al.*, 2013) – suggesting that direct infection with *F. tularensis* could contribute to the reduced number of NK cells as infection progresses.

### 3.4 Conclusion

This thesis chapter has demonstrated that several phenotypic changes occur in the lung ILC compartment during infection with *F. tularensis* LVS. Specifically, whilst an ILC1 population emerges, the number of ILC2s is reduced, which is accompanied by an altered expression of several cell surface markers on each of these subsets. At present, it is currently unclear how these changes to the ILC compartment impact upon the host immune response to *F. tularensis* LVS. Thus, chapters 4 and 5 will seek to determine this, through manipulation of ILC numbers during infection with *F. tularensis* LVS.

# Chapter 4

## Determining the effects of expanding the ILC compartment during infection with *F. tularensis* LVS

## 4.1 Introduction

Chapter 3 of this thesis established that ILC2s are reduced during the later stages of intranasal infection with *F. tularensis* LVS. As previously discussed, ILC2s have been shown to play an important role in the control of infection in the lung. Specifically, ILC2s can participate in tissue repair responses against influenza virus (Monticelli *et al.*, 2011), and possess the ability to adopt an ILC1-like phenotype, thus contributing to a type 1-based immune response against pathogens such as *Haemophilus influenzae* and *Mycobacterium tuberculosis* (Silver *et al.*, 2016; Corral *et al.*, 2021). With this in mind, it was hypothesised that the observed reduction in ILC2s during infection with *F. tularensis* LVS may perturb their potentially beneficial roles, and therefore prove detrimental to the overall host response.

ILC2s are responsive to multiple stimuli including IL-25 and IL-33 (Artis and Spits, 2015). Despite this, adult lung ILC2s express high levels of IL-33R and low levels of IL-25R respectively, and are consequently more responsive to IL-33 than IL-25 (Steer *et al.*, 2020). Treatment with IL-33 can enhance ILC2 numbers, and is also capable of facilitating enhanced conversion of ILC2s to an ILC1-like IFN-γ-producing phenotype when combined with IL-12 and IL-18 (Silver *et al.*, 2016) – cytokines that are present in the LVS-infected lung environment (Duckett *et al.*, 2005; del Barrio *et al.*, 2015; Periasamy *et al.*, 2016). As such, IL-33 was the preferred candidate to induce proliferation and activation of ILC2s in the lung during infection with *F. tularensis* LVS. Here, it was hypothesised that an expansion of lung ILC2s would benefit the host immune response against the bacteria. Thus, this chapter focuses on how the expansion of ILC2 numbers impacts on the host immune response in the lung, and the overall control of infection with *F. tularensis* LVS.

## 4.2 Results

### 4.2.1 IL-33 treatment results in enhanced mortality and reduced control of infection with *F. tularensis* LVS

As ILC2s are reduced during the later stages of infection with *F. tularensis* LVS (figure 3.5), it was important to determine how their IL-33-induced expansion affected the progression of infection. To this end, mice were treated with IL-33 prior to infection with *F. tularensis* LVS, and subsequently monitored (figure 4.1A).

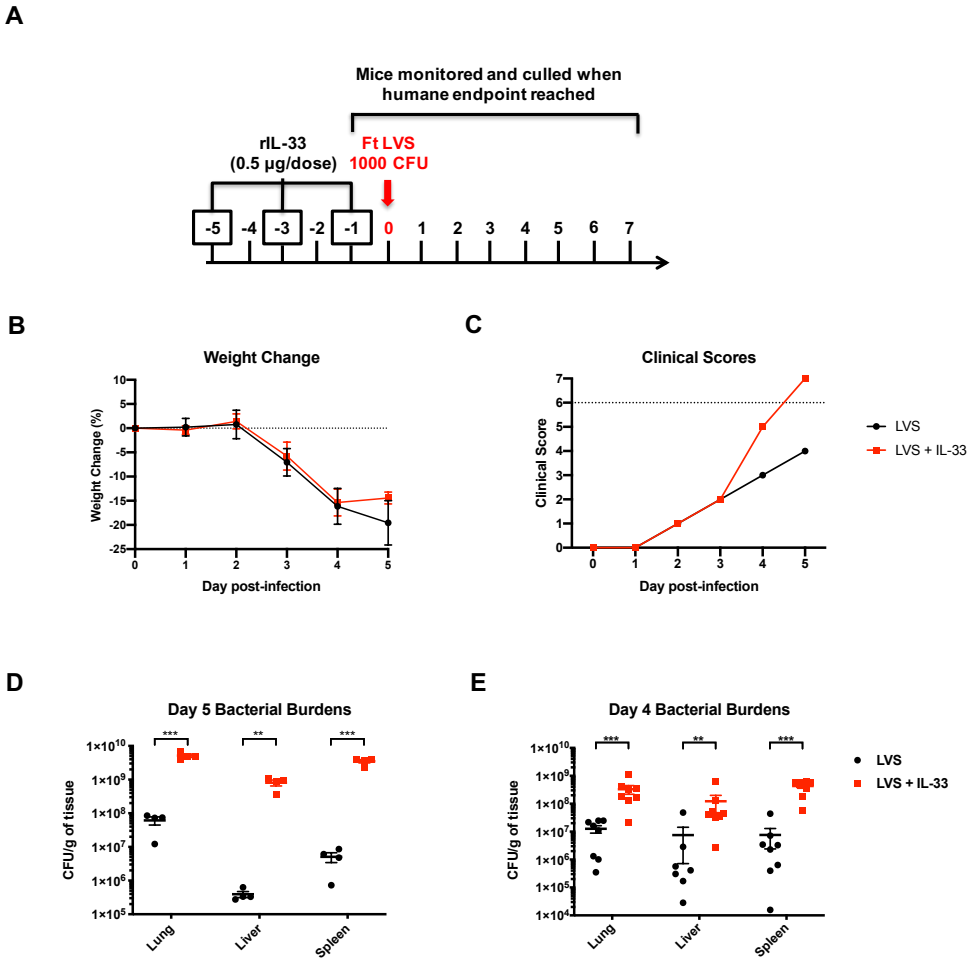


**Figure 4.1 - IL-33-treated C57BL/6 mice display enhanced bacterial burdens during infection with *F. tularensis* LVS**

**(A)** C57BL/6 mice were given 3 doses of IL-33 on alternate days leading up to infection with *F. tularensis* LVS. Mice were infected via the intranasal route with *F. tularensis* LVS (1000 CFU) and monitored daily and culled when the humane endpoint was reached. **(B)** Weight change was monitored daily in all mice, and plotted as a percentage loss of original body weight (0% = body weight at day 0). **(C)** Severity of infection was evaluated using a clinical scoring system (see methods). **(D)** Bacterial burdens (CFU/g of organ) were enumerated in the lung, liver and spleen of mice at day 5 and **(E)** day 4 p.i. (n=4-8). Statistical analysis was performed by unpaired t-test for parametric data or Mann-Whitney test for non-parametric data; ** $p<0.01$; *** $p<0.001$.

Despite no differences in the progression of weight loss when compared to untreated mice (figure 4.1B), all IL-33-treated mice exceeded the clinical score limit at day 5 p.i. (figure 4.1C), showing signs of illness such as hunched posture, piloerection and low mobility. Moreover, when bacterial burdens were enumerated, IL-33-treated mice displayed significantly enhanced bacterial burdens in the lung, liver and spleen when compared to untreated mice (figure 4.1D). As such, all mice that were used in subsequent IL-33-based experiments were culled one day earlier at day 4 p.i. to ensure the work met home office license restrictions. Nevertheless, significantly enhanced bacterial burdens were also observed in the lung, liver and spleen of IL-33-treated mice when compared to untreated mice at day 4 p.i. (figure 4.1E). Overall, this indicates that treatment with IL-33 prior to infection with *F. tularensis* LVS significantly exacerbates the progression of infection.

### 4.2.2 IL-33 treatment significantly enhances ILC2 numbers during *F. tularensis* LVS infection

At day 4 p.i., IL-33 administration resulted in a significant expansion of total ILCs – both as a frequency of live $CD45^+$ cells and total numbers - when compared to untreated mice (figure 4.2A-C). Importantly, as treatment with IL-33 produced a small, but significant portion of $CD90.2^-$ ILCs, ILCs were identified as live $Lin^-CD127^+$ cells in these studies (figure 4.2A). ILC2s were also significantly elevated both in frequency and total numbers following IL-33 treatment in both uninfected (control) and infected mice (4.2A and D-E). Interestingly however, the number of total ILCs and ILC2s were reduced in IL-33-treated LVS-infected mice when compared to IL-33-treated control mice (figure 4.2C and E), suggesting that infection with *F. tularensis* LVS still impacts on total ILC and ILC2 numbers despite their IL-33-mediated expansion. Nevertheless, these data still demonstrate that IL-33 treatment significantly expands ILC and ILC2s during infection with *F. tularensis* LVS.

As mentioned, previous reports have shown conversion of ILC2s to ILC1s (Bal *et al.*, 2016; Ohne *et al.*, 2016; Silver *et al.*, 2016; Corral *et al.*, 2021). Thus, the effect of IL-33-mediated ILC2 expansion on ILC1s was also determined. ILC1s were enhanced as a frequency of live $CD45^+$ cells (figure 4.2F) and total cell numbers (figure 4.2G) in IL-33-treated control mice when compared to untreated control mice. Interestingly, IL-33-treated infected

mice displayed significantly reduced ILC1s versus treated control mice (figure 4.2F-G). Thus, these results suggest that the expansion of ILC1s in IL-33-treated mice may arise due to an enhanced number of total ILCs, and that infection with *F. tularensis* LVS limits this expansion.

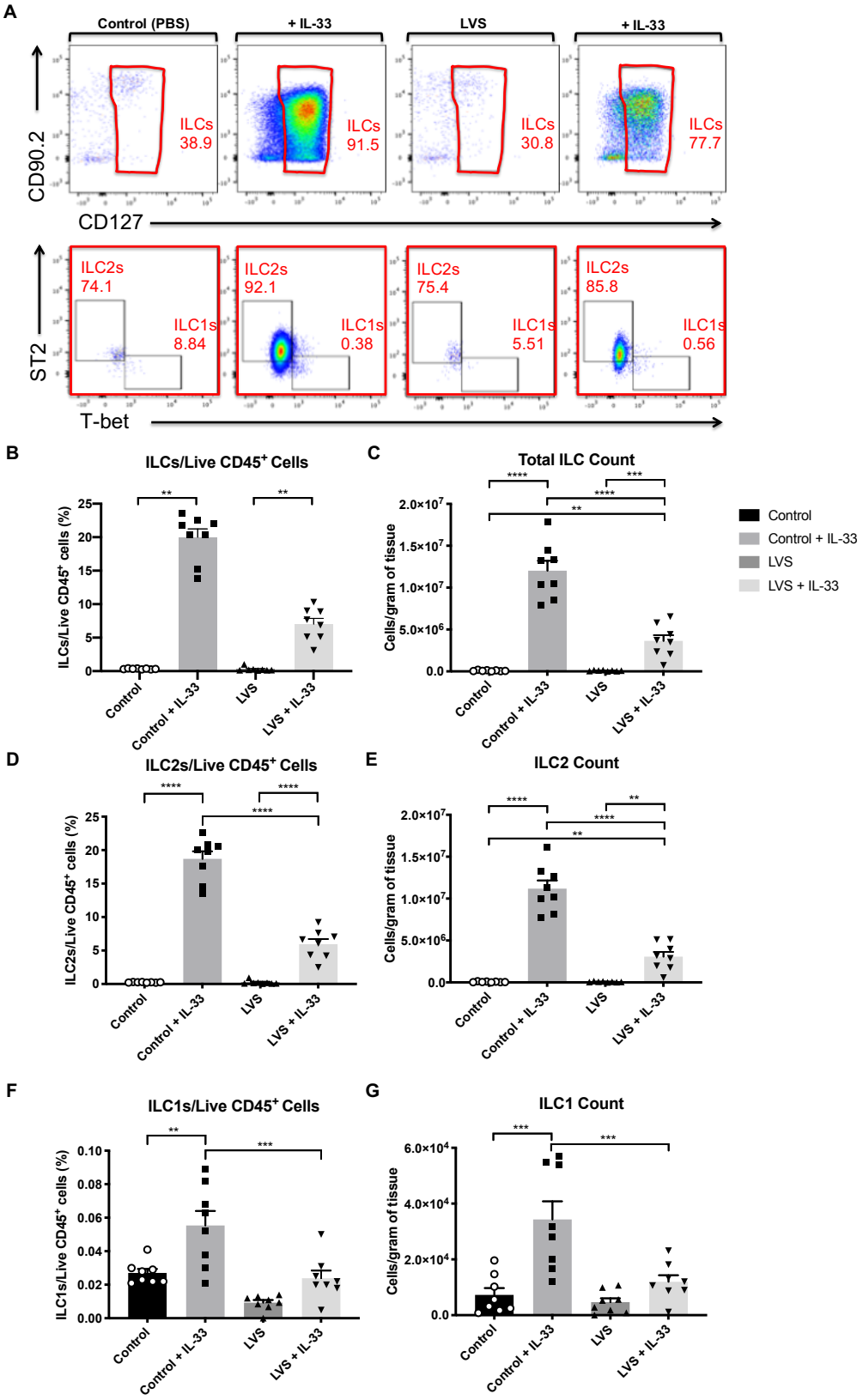

### 4.2.3 IL-33-treated LVS-infected mice exhibit an altered myeloid immune response

IL-33 also impacts on multiple other cell populations, including granulocytes and myeloid cells (Griesenauer and Paczesny, 2017). Moreover, as these cell types infiltrate the lung tissue and serve as reservoirs for *F. tularensis* LVS (Hall *et al.*, 2008; Casulli *et al.*, 2019), it was important to investigate the effects of IL-33 treatment on their numbers and relative levels of infection, and whether this could be contributing to the enhanced bacterial burdens observed in IL-33-treated mice.

Indeed, the frequency (figure 4.3A and C) and total number (figure 4.3D) of eosinophils ($Ly6G^{-}Siglec\text{-}F^{+}CD64^{-}$) were significantly enhanced in IL-33-treated LVS-infected mice when compared to untreated infected mice, indicating that IL-33 can induce the expansion of this myeloid population during infection with *F. tularensis* LVS. Of note, IL-33-treated control mice also exhibited eosinophilia (figure 4.3A and C-D), and no differences were observed between control and infected mice following IL-33 treatment (figure 4.3C and D). Elsewhere, whilst the frequency of macrophages ($Ly6G^{-}Siglec\text{-}F^{-}CD64^{+}$) and neutrophils ($Ly6G^{+}$), as well as total cell numbers were increased in all infected mice (figure 4.3B, E and G), IL-33 treatment did not further enhance this expansion (figure 4.3F and H). Together, these data suggest that IL-33 can impact on eosinophil, but not neutrophil and macrophage numbers during *F. tularensis* LVS infection.

**Figure 4.2 - IL-33 treatment significantly increases total ILC and ILC2 numbers during infection with *F. tularensis* LVS**

**(A)** Representative plots for identification of ILCs (live $CD45^{+}Lin^{-}CD127^{+}$ cells), **(B)** ILC1s (live $CD45^{+}Lin^{-}CD127^{+}T\text{-}bet^{+}$ cells) and ILC2s (live $CD45^{+}Lin^{-}CD127^{+}ST2^{+}$ cells) in the lungs of untreated or IL-33-treated mice at day 4 p.i. with *F. tularensis* LVS. **(C-H)** ILCs, ILC2s and ILC1s were quantified and expressed as a frequency of live $CD45^{+}$ cells, and cell counts per gram of tissue. (n=8). Numbers in FACS plots represent the percentage of the previous gate (ILCs as a % of $Lin^{-}$ cells; ILC2s and ILC1s as a % of total ILCs). Statistical analysis was performed using either one-way ANOVA for parametric data, or Kruskal Wallis for non-parametric data, with Holm-Sidak's and Dunn's multiple comparisons tests performed for each method of analysis respectively; * $p<0.05$; ** $p<0.01$; *** $p<0.001$; **** $p<0.0001$.

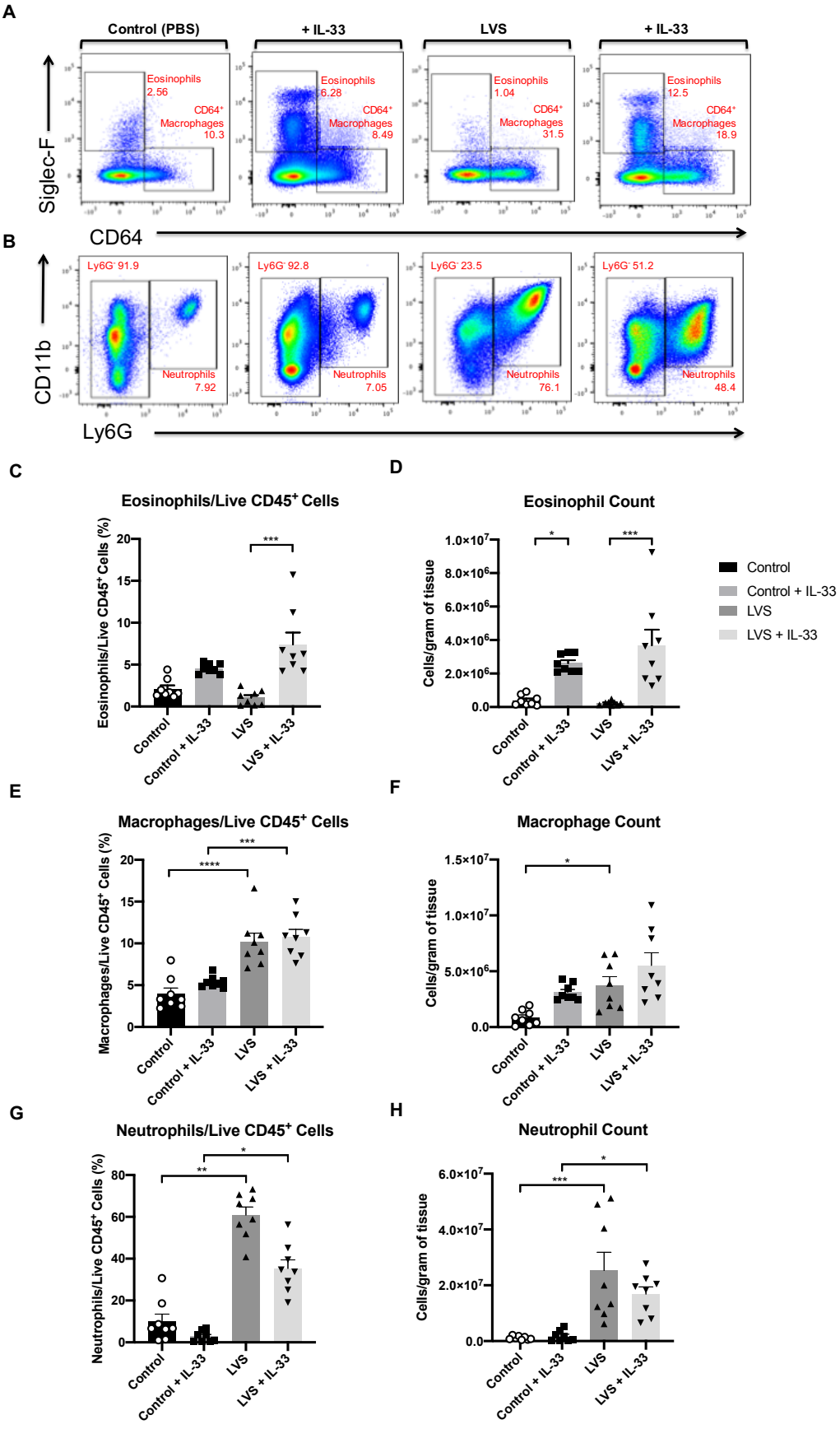
A
Control (PBS)
+ IL-33
LVS
+ IL-33
Eosinophils 2.56
CD64+ Macrophages 10.3
Eosinophils 6.28
CD64+ Macrophages 8.49
Eosinophils 1.04
CD64+ Macrophages 31.5
Eosinophils 12.5
CD64+ Macrophages 18.9
Siglec-F
CD64
B
Ly6G- 91.9
Neutrophils 7.92
Ly6G- 92.8
Neutrophils 7.05
Ly6G- 23.5
Neutrophils 76.1
Ly6G- 51.2
Neutrophils 48.4
CD11b
Ly6G
C
Eosinophils/Live CD45+ Cells
Eosinophils/Live CD45+ Cells (%)
D
Eosinophil Count
Cells/gram of tissue
Control
Control + IL-33
LVS
LVS + IL-33
E
Macrophages/Live CD45+ Cells
Macrophages/Live CD45+ Cells (%)
F
Macrophage Count
Cells/gram of tissue
G
Neutrophils/Live CD45+ Cells
Neutrophils/Live CD45+ Cells (%)
H
Neutrophil Count
Cells/gram of tissue

As eosinophils were significantly expanded in IL-33-treated LVS-infected mice, it was hypothesised that these cells could serve as an enhanced intracellular niche, and thus contribute to the exacerbated bacterial burdens in IL-33-treated mice. Indeed, whilst the frequency of infected eosinophils was unaltered (figure 4.4A-B), the total number of infected eosinophils was significantly increased following IL-33 treatment (figure 4.4C). Moreover, whilst macrophage and neutrophil numbers were unaltered by IL-33 treatment, it remained important to determine the relative level of infection in these cell types, given their roles as a replicative niche for *F. tularensis* LVS (Hall *et al.*, 2008; Casulli *et al.*, 2019). Thus, whilst the frequency of $LVS^+$ macrophages was unaltered in IL-33-treated infected mice (figure 4.4A and D), it was worthy of note that the total number of infected macrophages was significantly enhanced in IL-33-treated mice (figure 4.4E). In addition to this, the infected neutrophil pool was expanded when expressed as a frequency of total neutrophils (figure 4.4F). No differences were observed in the total number of infected neutrophils between groups (figure 4.4G). Thus, these results suggest that *F. tularensis* LVS exhibits an enhanced level of intracellular infection in multiple myeloid immune cells following IL-33 treatment, which may contribute to the enhanced bacterial burdens observed in these mice.

**Figure 4.3 - Effects of IL-33 treatment on the myeloid immune response during infection with *F. tularensis* LVS**

**(A-B)** Representative plots for identification of myeloid cell populations in the lungs of IL-33-treated mice at day 4 p.i. with *F. tularensis* LVS. **(C-D)** Eosinophil (live $CD45^+Ly6G^-Siglec\text{-}F^+CD64^-$), **(E-F)** $CD64^+$ macrophage (live $CD45^+Ly6G^-Siglec\text{-}F^-CD64^+$) and **(G-H)** neutrophil (live $CD45^+Ly6G^+$), and populations were identified and expressed as a frequency of live $CD45^+$ cells and cell counts per gram of tissue (n=8). Numbers in FACS plots represent the percentage of the previous gate (eosinophils and $CD64^+$ macrophages as a % of $Ly6G^-$ cells; neutrophils as a % of live $CD45^+$ cells). Statistical analysis was performed with either one-way ANOVA for parametric data, or Kruskal Wallis for non-parametric data, with Holm-Sidak's and Dunn's multiple comparisons tests performed for each method of analysis respectively; * $p<0.05$ ** $p<0.01$ *** $p<0.001$; **** $p<0.0001$.

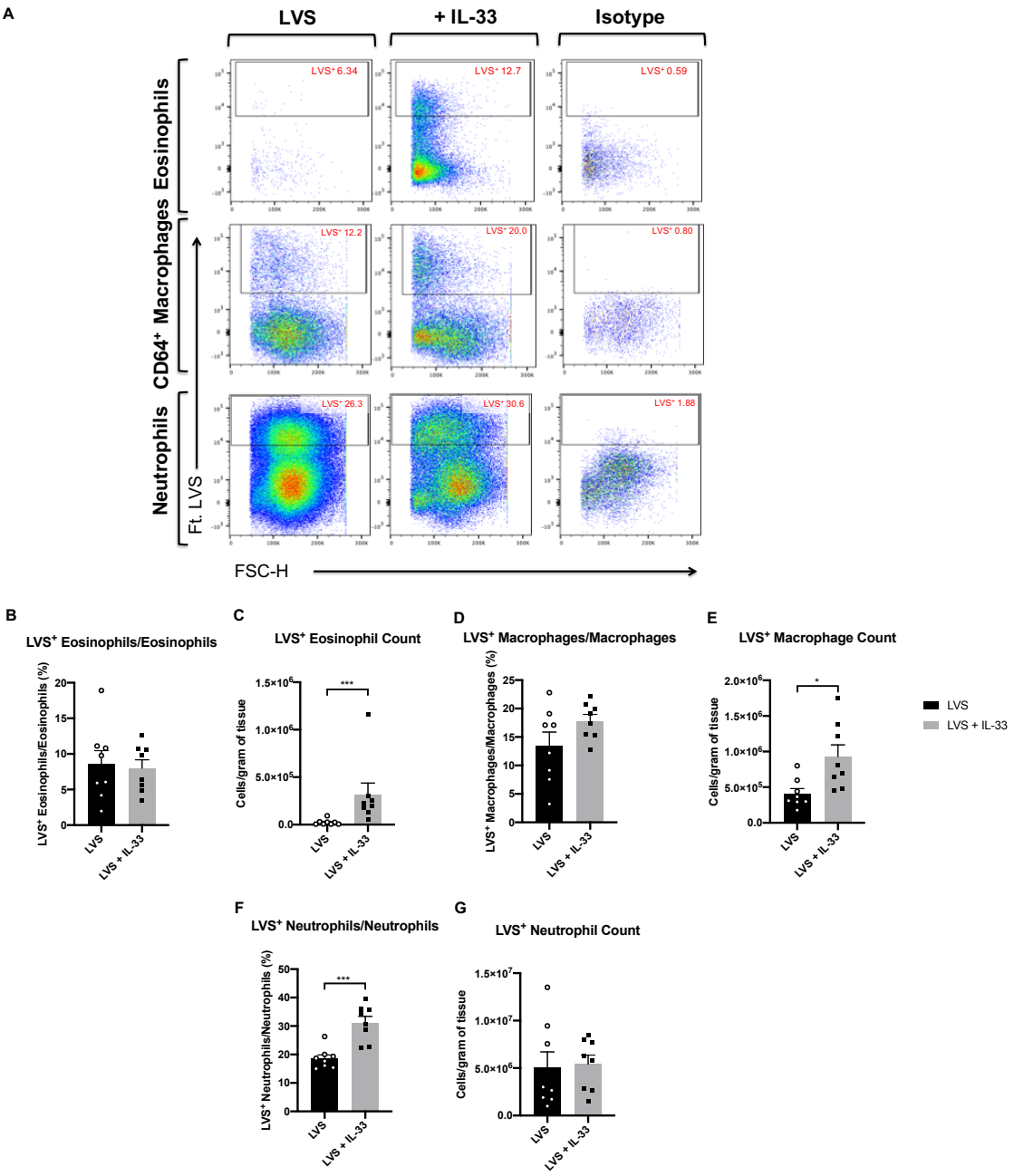


**Figure 4.4 - IL-33-treated mice display significantly enhanced levels of infection in multiple immune cells during infection with *F. tularensis* LVS**

**(A)** Representative plots for identification of infected myeloid populations in the lungs of IL-33-treated mice at day 4 p.i. with *F. tularensis* LVS. **(B-C)** LVS$^+$ eosinophil (live CD45$^+$Ly6G$^-$Siglec-F$^+$CD64$^-$) and **(D-E)** LVS$^+$ CD64$^+$ macrophage (live CD45$^+$Ly6G$^-$ Siglec-F$^-$CD64$^+$) and **(F-G)** LVS$^+$ neutrophil (live CD45$^+$Ly6G$^+$) populations were identified and expressed as a frequency of parent populations and cell counts per gram of tissue (n=8). Numbers in FACS plots represent the percentage of infected cells from individual immune cell populations. Statistical analysis was performed by unpaired t-test for parametric data or Mann-Whitney test for non-parametric data; * $p<0.05$; *** $p<0.001$.

### 4.2.4 NK cell numbers are unaltered following IL-33 treatment during infection with *F. tularensis* LVS

NK cells play a critical role during infection with *F. tularensis* LVS (Lopez *et al.*, 2004; Schmitt *et al.*, 2013). Moreover, as IL-33 can inhibit their responses in the context of type 1 immunity (Schuijs *et al.*, 2020), it was important to determine how administration of this cytokine impacted upon NK cells during infection with *F. tularensis* LVS, and whether this could also be contributing to the enhanced bacterial burdens in IL-33-treated mice. In the absence of infection, the frequency of NK cells was reduced in IL-33-treated mice versus untreated control mice (figure 4.5B). Interestingly however, the frequency (figure 4.5B) and total number (figure 4.5C) of NK cells was unaffected by IL-33 treatment during infection with *F. tularensis* LVS. Thus, these data suggest that IL-33 treatment does not impact upon NK cell numbers during infection with *F. tularensis* LVS.

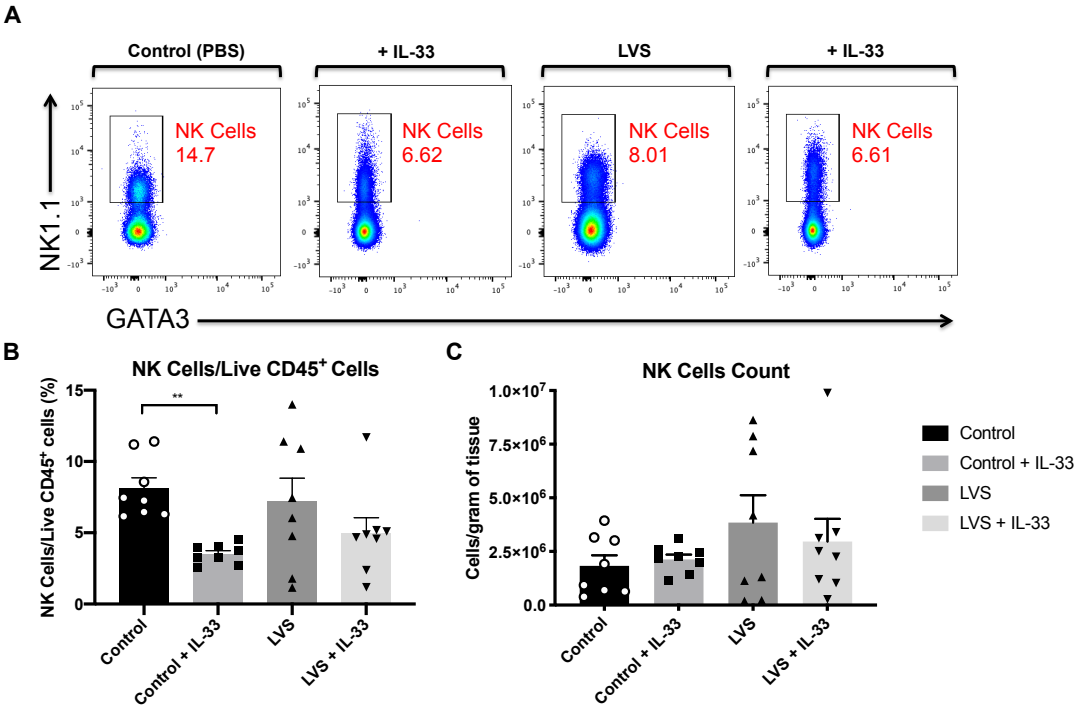


**Figure 4.5 - NK Cell numbers are unaffected in IL-33-treated LVS-infected mice**

**(A)** Representative plots for identification of NK Cells ($CD3^-CD5^-CD11b^+NK1.1^+$) in the lungs of untreated or IL-33-treated mice at day 4 p.i. with *F. tularensis* LVS. **(B-C)** Total NK Cells were quantified and expressed as a frequency of live $CD45^+$ cells and cell counts per gram of tissue (n=8). Numbers in FACS plots represent the percentage of NK cells of $CD3^-CD5^-CD11b^+$ cells. Statistical analysis was performed using Kruskal Wallis for non-parametric data, with Dunn's multiple comparisons tests performed; ** $p<0.01$.

### 4.2.5 IL-33 significantly alters adaptive immunity during infection with *F. tularensis* LVS

Elements of adaptive immunity are also known to be altered by IL-33. For example, the polarisation and differentiation of naïve $CD4^+$ T cells into T helper 2 (Th2) effector cells is enhanced by IL-33, as well as the expansion of $ST2^+Foxp3^+$ regulatory T cells (Tregs) (Molofsky, Savage and Locksley, 2015). As such, it was hypothesised that the expansion of these cell types could inhibit the induction of a more beneficial type 1 immune response, which is essential to the control of infection with *F. tularensis* LVS (Cowley and Elkins, 2011). Thus, it was next important to determine whether these cell types were also expanded following IL-33 treatment, and whether they could therefore be contributing to the enhanced bacterial burdens observed in IL-33-treated mice. Indeed, IL-33-treated infected mice displayed significantly enhanced numbers of $ST2^+Foxp3^-$ $CD4^+$ T cells (figure 4.6A-B). Moreover, an $ST2^+Foxp3^+$ Treg population was preferentially expanded over $ST2^-$ Tregs, both in terms of frequency (figure 4.6C and E) and cell numbers (figure 4.6D and F). Together, these results suggest that IL-33 treatment favours the induction of type 2 and regulatory T cell immunity during infection with *F. tularensis* LVS.

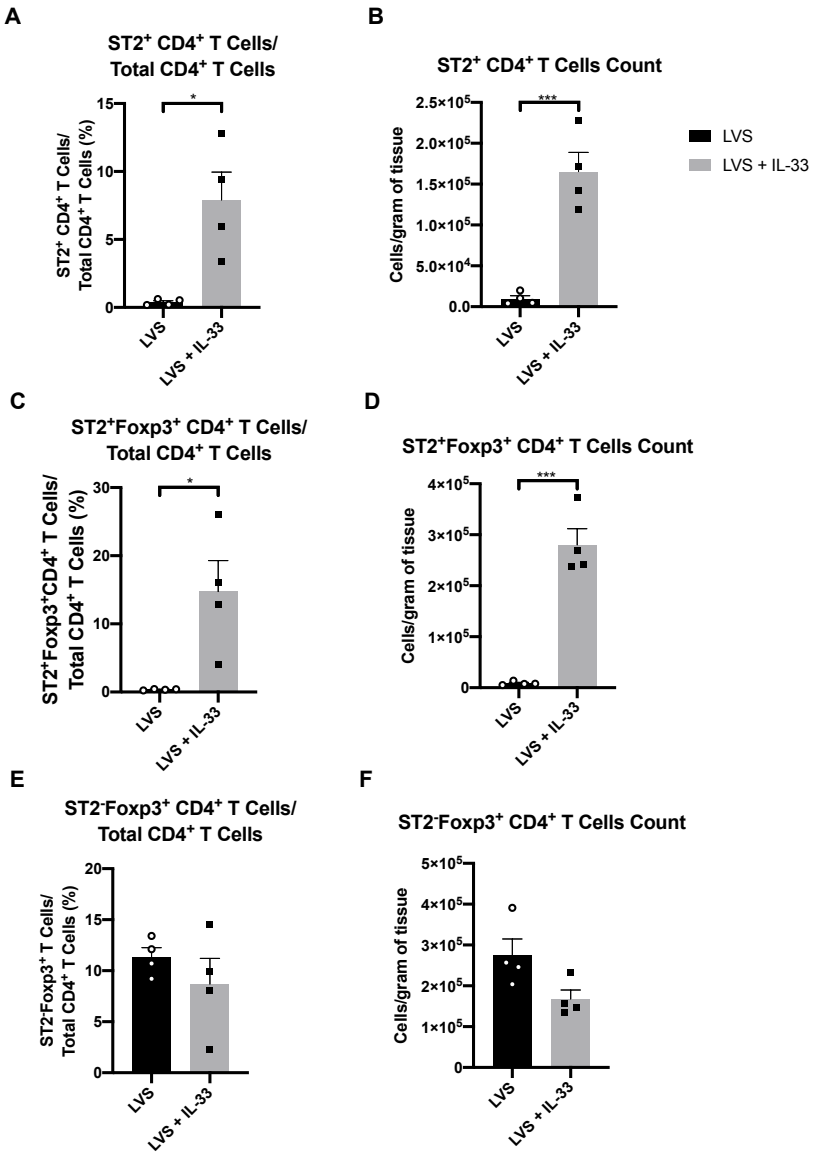


**Figure 4.6 - IL-33 treatment significantly alters the CD4$^+$ T cell compartment during infection with *F. tularensis* LVS**

CD4$^+$ T cell subsets (live CD45$^+$CD3$^+$CD5$^+$ cells) were identified in the lungs of untreated or IL-33-treated mice at day 4 p.i. with *F. tularensis* LVS. **(A-B)** ST2$^+$Foxp3$^-$ CD4$^+$ T cells, **(C-D)** ST2$^+$Foxp3$^+$ CD4$^+$ T cells and **(E-F)** ST2$^-$Foxp3$^+$ CD4$^+$ T cells were quantified and expressed as a frequency of total CD4$^+$ T cells, and cell counts per gram of tissue (n=4). Statistical analysis was performed by unpaired t-test for parametric data or Mann-Whitney test for non-parametric data; * $p<0.05$; *** $p<0.001$.

### 4.2.6 Adaptive immunity is dispensable in the control of infection with *F. tularensis* LVS

As IL-33-treated mice displayed significantly enhanced numbers of Th2 and ST2$^{+}$ Treg cells (figure 4.6), it was next important to investigate whether they are necessary for the enhanced bacterial burdens observed in these mice. To this end, bacterial burdens were enumerated in IL-33-treated Rag1$^{-/-}$ mice (which lack adaptive immune cells) to begin to interrogate this role.

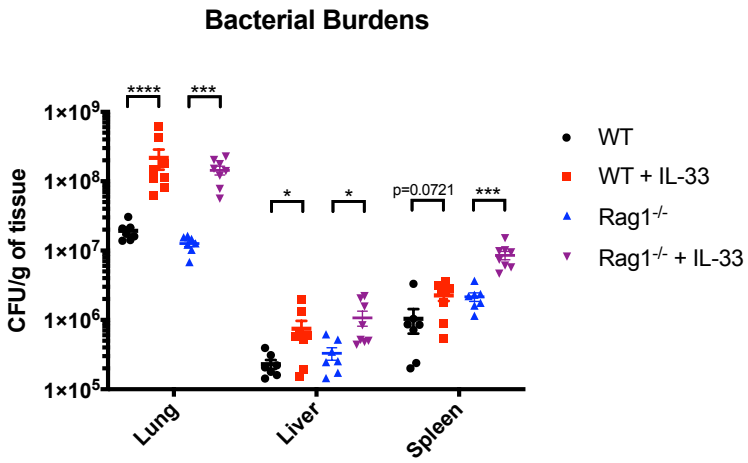


**Figure 4.7 - Infection kinetics in IL-33-treated LVS-infected C57BL/6 and Rag1$^{-/-}$ mice at day 4 p.i.**

C57BL/6 and Rag1$^{-/-}$ mice were pre-treated with IL-33 on alternate days as described previously, and infected via the intranasal route with *F. tularensis* LVS (1000 CFU). Bacterial burdens (CFU/g of organ) were enumerated in the lung, liver and spleen of mice at day 4 p.i. (n=7 for untreated mice; n=8 for treated mice). Statistical analysis was performed by unpaired t-test for parametric data or Mann-Whitney test for non-parametric data; * $p<0.05$; *** $p<0.001$ ;**** $p<0.001$.

As previously observed (figure 4.1), IL-33-treated WT mice displayed an enhanced bacterial burden in the lung, liver and spleen when compared to untreated mice (figure 4.7). Across all analysed organs, untreated Rag1$^{-/-}$ mice displayed bacterial burdens akin to that of untreated WT mice (figure 4.7), indicating innate immunity is sufficient for control of infection at day 4 p.i.. Interestingly, IL-33-treated Rag1$^{-/-}$ mice showed a similar level of infection in the lung to that of IL-33-treated WT mice (figure 4.7). Indeed, IL-33-treated Rag1$^{-/-}$ mice displayed a significantly enhanced bacterial burden in the lung when compared to untreated Rag1$^{-/-}$ mice (figure 4.7). Akin to IL-33-treated WT mice, liver and spleen burdens of IL-33-treated Rag1$^{-/-}$ mice were also significantly increased (figure 4.7). Together, these data indicate

that adaptive immunity does not play a major role in the enhanced bacterial burdens observed in IL-33-treated mice.

Next, it was important to assess whether innate immune cell types previously expanded by IL-33 treatment were also elevated in IL-33-treated Rag1$^{-/-}$ mice, to determine whether they may still contribute to the enhanced bacterial burdens in IL-33-treated mice. Consistent with previous observations (figure 4.2), total ILCs and ILC2s were also expanded in IL-33-treated Rag1$^{-/-}$ mice as a frequency (figure 4.8A and C) and total cell numbers (figure 4.8B and D), suggesting that the IL-33-induced expansion of ILC2s during LVS infection does not require adaptive immunity.

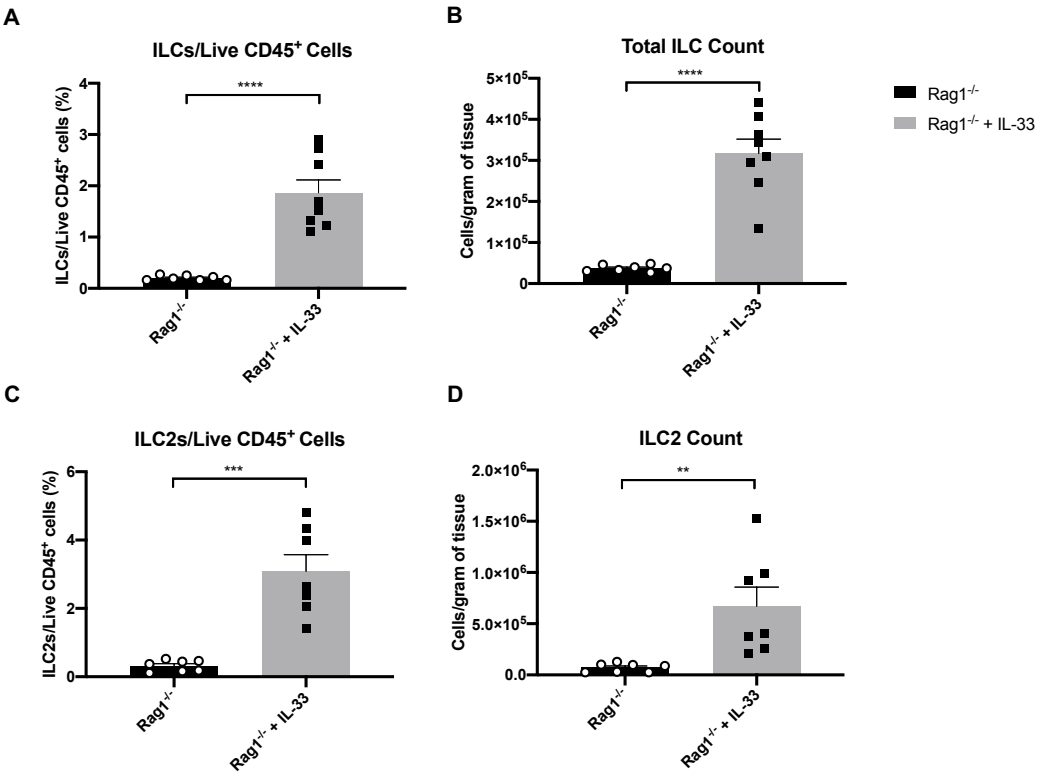


**Figure 4.8 - ILC and ILC2 numbers are significantly elevated in the absence of adaptive immunity during infection with *F. tularensis* LVS**

**(A)** ILCs (live CD45$^+$Lin$^-$CD127$^+$ cells) and **(B)** ILC2s (live CD45$^+$Lin$^-$CD127$^+$ST2$^+$ cells) were quantified in the lungs of untreated or IL-33-treated Rag1$^{-/-}$ mice at day 4 p.i. with *F. tularensis* LVS. Data were expressed as a frequency of live CD45$^+$ cells, and cell counts per gram of tissue (n=5-8). Statistical analysis was performed between untreated and treated groups for each genotype respectively, using an unpaired t test for parametric data, or Mann-Whitney for non-parametric data; ** p<0.01; *** p<0.001; **** p<0.0001.

Another innate immune cell population that was enhanced in IL-33-treated LVS-infected WT mice was eosinophils (figure 4.3). Akin to these observations, eosinophils were elevated when expressed as a frequency of live $CD45^+$ cells (figure 4.9A and C) and total cell numbers (figure 4.9D) in IL-33-treated $Rag1^{-/-}$ mice when compared to untreated $Rag1^{-/-}$ mice. Macrophages and neutrophils were unaffected by IL-33 treatment (figure 4.9A and E-H). Overall, this shows that eosinophils are elevated following IL-33 treatment, and this occurs irrespective of adaptive immunity.

As multiple myeloid populations displayed enhanced levels of infection in WT mice following IL-33 treatment (figure 4.4), it was also important to investigate whether this remained true in IL-33-treated $Rag1^{-/-}$ mice (figure 4.9), and could therefore be contributing to the enhanced bacterial burdens observed in this context. Indeed, both the frequency (figure 4.10A-B) and total number (figure 4.10C) of infected eosinophils was significantly elevated in IL-33-treated $Rag1^{-/-}$ mice when compared to untreated $Rag1^{-/-}$ mice. Interestingly however, the level of infection in macrophages (figure 4.10D-E) and neutrophils (figure 4.10F-G) was unaltered in IL-33-treated $Rag1^{-/-}$ mice when compared to untreated counterparts. Overall, these data therefore indicate that the enhanced level of infection in eosinophils could serve as a reservoir for bacteria in the lungs of IL-33-treated $Rag1^{-/-}$ mice.

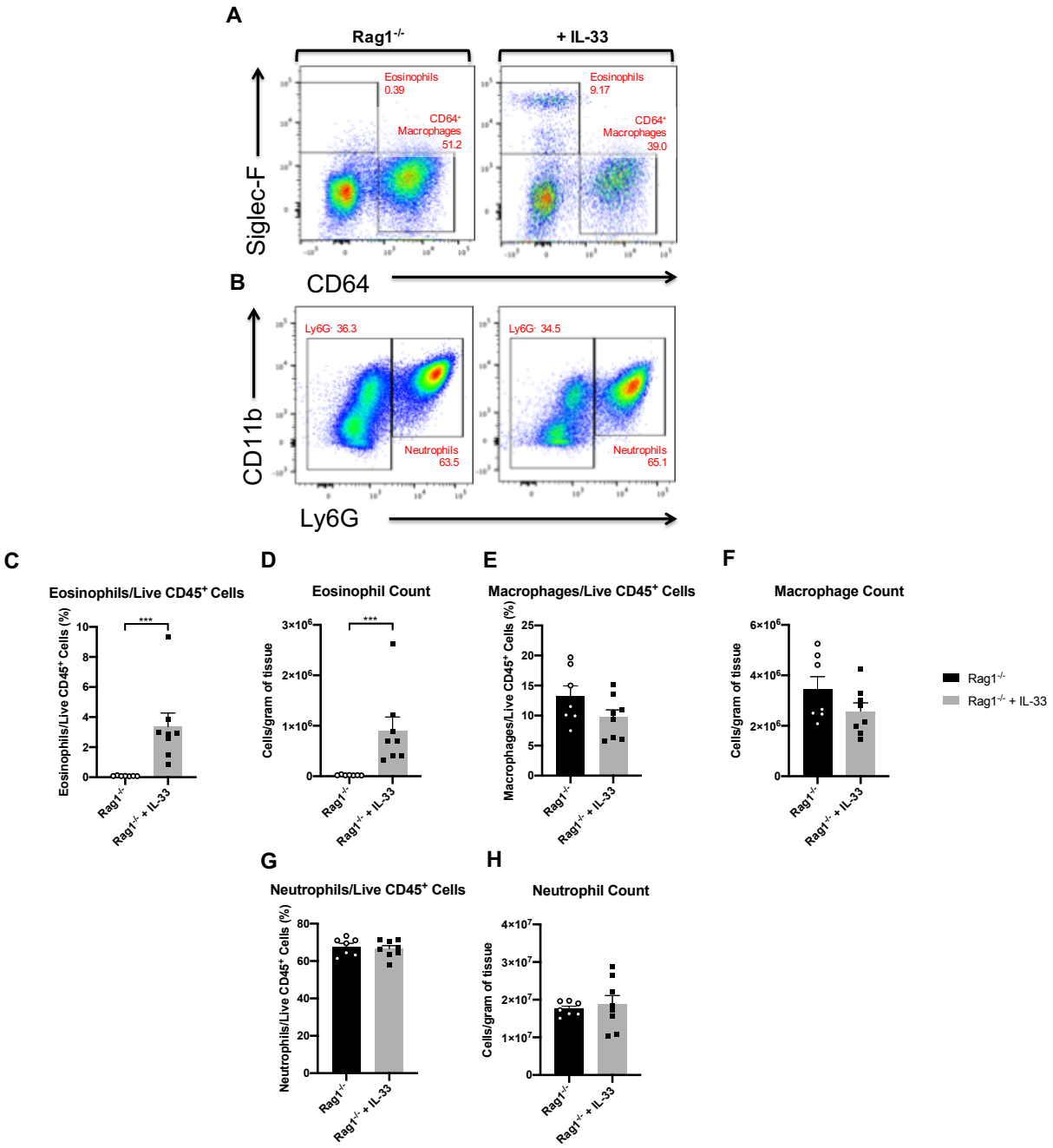


**Figure 4.9 - Effects of IL-33 treatment on the myeloid immune response in Rag1$^{-/-}$ mice during infection with *F. tularensis* LVS**

**(A-B)** Representative plots for identification of myeloid cell populations in the lungs of IL-33-treated Rag1$^{-/-}$ mice at day 4 p.i. with *F. tularensis* LVS. **(C-D)** Eosinophil (live CD45$^+$Ly6G$^-$Siglec-F$^+$CD64$^-$), **(E-F)** CD64$^+$ macrophage (live CD45$^+$Ly6G$^-$ Siglec-F$^-$CD64$^+$) and **(F-G)** neutrophil (live CD45$^+$Ly6G$^+$) populations were identified and expressed as a frequency of live CD45$^+$ cells and cell counts per gram of tissue (n=7 for untreated mice; n=8 for treated mice). Numbers in FACS plots represent the percentage of the previous gate (eosinophils and CD64$^+$ macrophages as a % of Ly6G$^-$ cells; neutrophils as a % of live CD45$^+$ cells). Statistical analysis was performed by unpaired t-test for parametric data or Mann-Whitney test for non-parametric data; ** p<0.01 *** p<0.001.

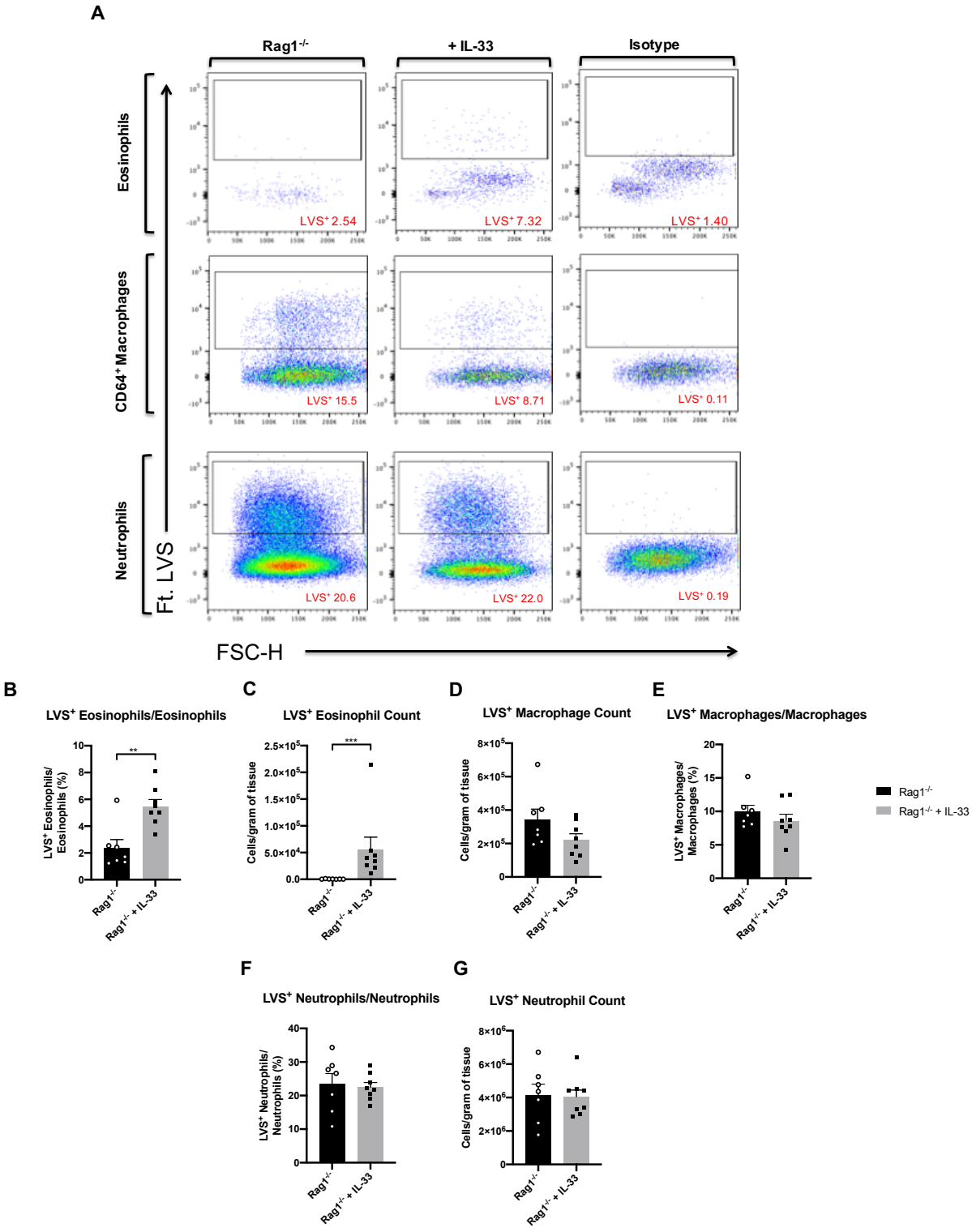


**Figure 4.10 - Lack of adaptive immunity alters the relative levels of infection in multiple myeloid immune cells at day 4 p.i.**

**(A)** Representative plots for identification of infected myeloid populations in the lungs of IL-33-treated Rag1$^{-/-}$ mice at day 4 p.i. with *F. tularensis* LVS. **(B-C)** LVS$^{+}$ eosinophil (live CD45$^{+}$Ly6G$^{-}$Siglec-F$^{+}$CD64$^{-}$), **(D-E)** LVS$^{+}$ CD64$^{+}$ macrophage (live CD45$^{+}$Ly6G$^{-}$Siglec-F$^{-}$CD64$^{+}$) and **(F-G)** LVS$^{+}$ neutrophil (live CD45$^{+}$Ly6G$^{+}$) populations were identified and expressed as a frequency of parent populations and cell counts per gram of tissue (n=7 for untreated mice; n=8 for treated mice). Numbers in FACS plots represent the percentage of infected cells from individual immune cell populations. Statistical analysis was performed by unpaired t-test for parametric data or Mann-Whitney test for non-parametric data; ** $p<0.01$; *** $p<0.001$.

### 4.2.7 Transfer of ILC2s to mice during *F. tularensis* LVS infection significantly exacerbates bacterial burdens

As innate immunity appears to be sufficient in driving enhanced bacterial burdens in IL-33-treated mice (figure 4.7), it was next important to investigate how innate sources could contribute to this phenomenon. Specifically, as ILC2s were increased following IL-33 treatment (figure 4.2 and 4.8), and these cells can drive eosinophilia (Halim *et al.*, 2012a; Nussbaum *et al.*, 2013), a more direct way of testing whether ILC2s were sufficient to induce enhanced bacterial burdens was devised. To this end, sort-purified lung ILC2s (live $CD45^+Lin^-CD127^+KLRG1^+$) from IL-33-treated donor mice were transferred into LVS-infected mice via the intranasal route at day 3 p.i., with bacterial burdens enumerated at peak infection (day 7 p.i.). In mice receiving ILC2 transfer, burdens were significantly elevated in the lung, liver and spleen of mice when compared to control mice (figure 4.11), indicating that transfer of ILC2s is detrimental to the control of infection.

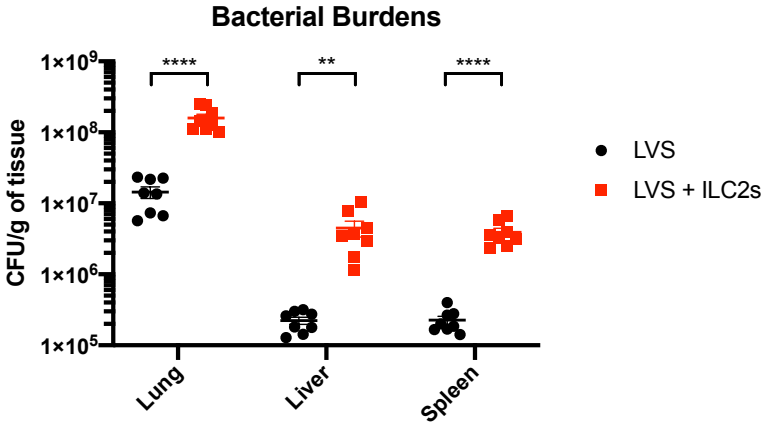


**Figure 4.11 - Intranasal transfer of ILC2s results in enhanced bacterial burdens in LVS-infected C57BL/6 mice at day 7 p.i.**

C57BL/6 mice were infected with 1000 CFU *F. tularensis* LVS, where one group of mice received $1x10^5$ FACS-sorted live $CD45^+Lin^-CD127^+KLRG1^+$ i.n. at day 3 p.i.. Bacterial burdens (CFU/g of organ) were enumerated in the lung, liver and spleen of C57BL/6 mice at day 7 p.i. (n=8 for all organs). Statistical analysis was performed with unpaired t-tests, ** $p<0.01$; **** $p<0.0001$.

### 4.2.8 ILC2 transfer does not increase type 2 adaptive cell numbers

One of the other major objectives with the ILC2 transfer was to eliminate other IL-33-mediated effects on the immune system. One such effect was the expansion of both Th2 ($ST2^+$) and $ST2^+$ Tregs (figure 4.6) in IL-33-treated LVS-infected mice. Thus, as ILC2s have been shown to interact with Th2 and Treg cells and potentiate their activation (Halim *et al.*, 2018), it was important to investigate how ILC2 transfer impacted upon T cell immunity during infection with *F. tularensis* LVS.

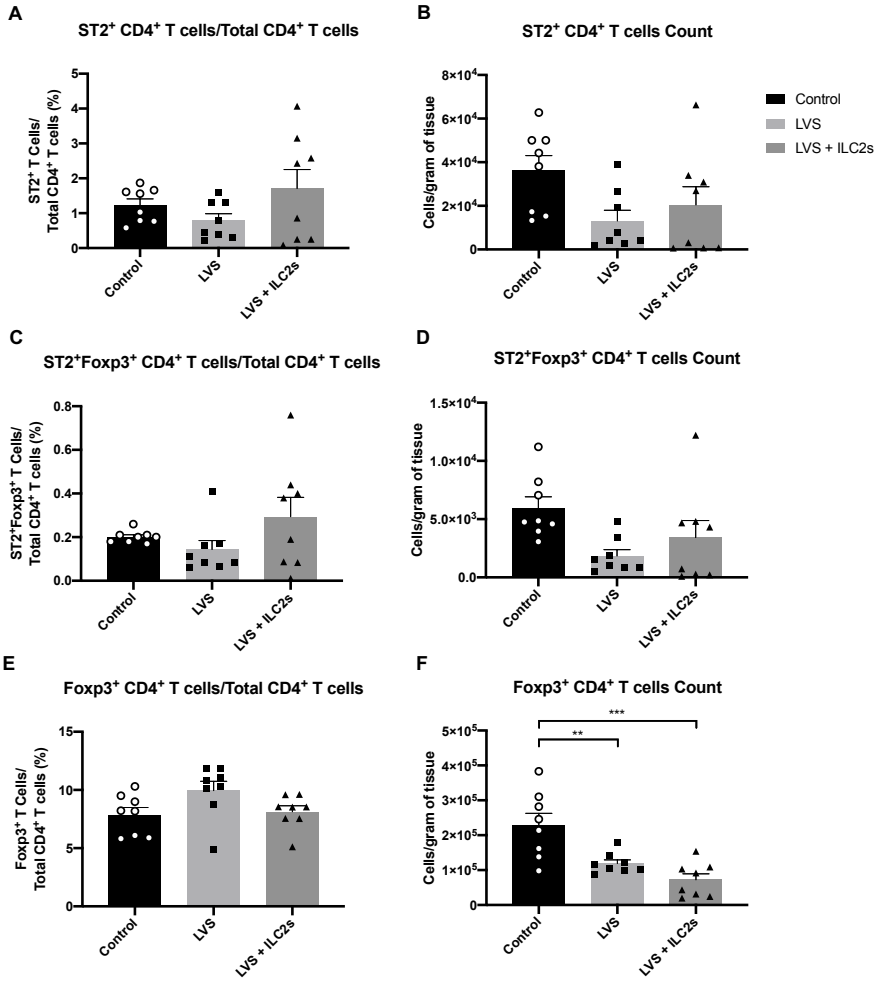


**Figure 4.12 - ILC2 transfer does not alter type 2 $CD4^+$ or regulatory T cell numbers during infection with *F. tularensis* LVS**

C57BL/6 mice were infected with 1000 CFU *F. tularensis* LVS, where one group of mice received $1x10^5$ FACS-sorted live $CD45^+Lin^-CD127^+KLRG1^+$ i.n. at day 3 p.i.. Control mice received PBS. Lung $CD4^+$ T cell populations were identified at day 7 p.i. **(A-B)** $ST2^+Foxp3^-$ $CD4^+$ T cells, **(C-D)** $ST2^+Foxp3^+$ $CD4^+$ T cells and **(E-F)** $ST2^-$ $Foxp3^+$ $CD4^+$ T cells were quantified and expressed as a frequency of total $CD4^+$ T cells, and cell counts per gram of tissue (n=8). Statistical analysis was performed using either one-way ANOVA for parametric data, or Kruskal Wallis for non-parametric data, with appropriate multiple comparisons tests performed for each method of analysis respectively; * $p<0.05$; *** $p<0.001$.

Both Th2 ($ST2^+$ $CD4^+$) cells and $ST2^+$ Tregs were unaffected by ILC2 transfer (figure 4.12A-D). Total $ST2^-$ Treg numbers were reduced during infection (figure 4.12F). Despite this, no differences were observed following ILC2 transfer (figure 4.12F). Taken together, these results indicate that transfer of ILC2s does not result in expansion of Th2 or Tregs during infection with *F. tularensis* LVS.

### 4.2.9 NK-derived IFN-γ is reduced post-ILC2 transfer

As ILC2 transfer did not impact on adaptive lymphocyte numbers, it was important to consider how their transfer could impact upon other aspects of the immune response. Indeed, an antagonistic relationship has previously been described between ILC2s and NK cells (Bi *et al.*, 2017; Schuijs *et al.*, 2020). Therefore, it was hypothesised that ILC2 transfer may attenuate NK cell function during infection with *F. tularensis* LVS. As such, this would mean disruption of a key element of the type 1 immune response against the bacteria (Lopez *et al.*, 2004; Schmitt *et al.*, 2013), potentially contributing to the enhanced bacterial burdens seen in ILC2 transfer mice (figure 4.13).

Akin to previous findings (figure 3.4), infection with *F. tularensis* LVS significantly reduced the frequency (figure 4.13A-B) and total number of NK cells (figure 4.13A and C). However, this was further exacerbated in mice receiving ILC2 transfer (figure 4.13A-C). Moreover, whilst their capacity to produce IFN-γ was not significantly altered by the ILC2 transfer (figure 4.13D), the total number of IFN-$\gamma^+$ NK cells was reduced in mice receiving ILC2s, to a level similar to that of uninfected mice not receiving ILC2s (figure 4.13E). Thus, these results suggest that transfer of ILC2s can impact upon NK cells in the host immune response against *F. tularensis* LVS, through an enhanced depletion of their total numbers and total IFN-γ output.

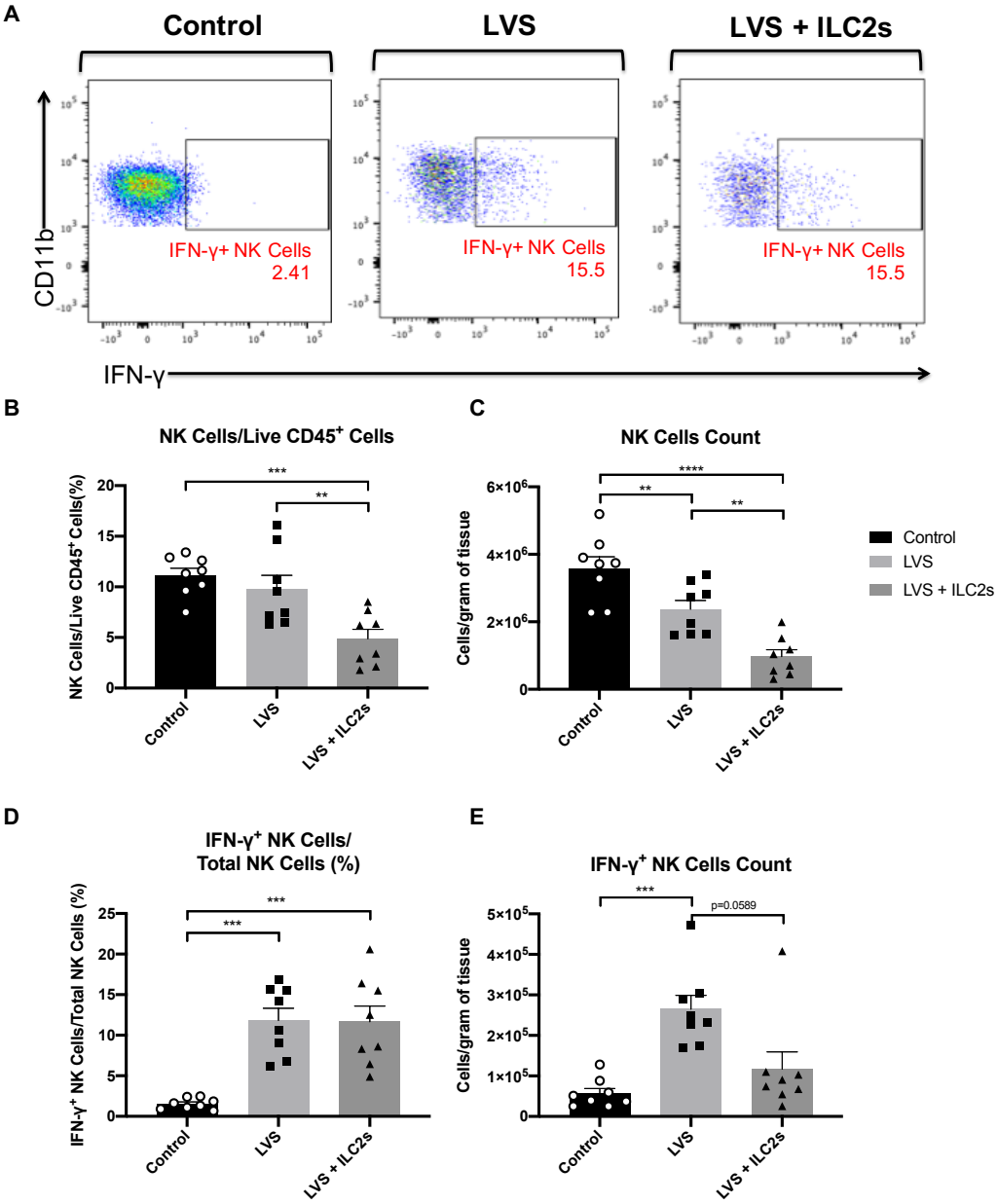


**Figure 4.13 - NK Cell numbers are significantly reduced following ILC2 transfer during infection with *F. tularensis* LVS**

C57BL/6 mice were infected with 1000 CFU *F. tularensis* LVS, where one group of mice received 1x10$^5$ FACS-sorted live CD45$^+$Lin$^-$CD127$^+$KLRG1$^+$ i.n. at day 3 p.i.. Control mice received PBS. Lung single cell suspensions were incubated for 4 hours at 37$^o$C with a cocktail of PMA, ionomycin, brefeldin A and monensin. **(A)** Representative plots for identification of IFN-γ$^+$ NK Cells (CD3$^-$CD5$^-$CD11b$^+$NK1.1$^+$) in the lung of PBS (control) and LVS-infected mice at day 7 p.i.. **(B-C)** Total NK Cells and **(D-E)** NK Cell-derived production of IFN-γ was quantified and expressed as a frequency of live CD45$^+$ cells, total NK Cells, and cell counts per gram of tissue (n=8 for all cell populations). Numbers in FACS plots represent the percentage of IFN-γ$^+$ NK cells from total NK cells. Statistical analysis was performed using either one-way ANOVA for parametric data, or Kruskal Wallis for non-parametric data, with appropriate multiple comparisons tests performed for each method of analysis respectively; ** p<0.01; *** p<0.001; **** p<0.0001.

### 4.2.10 Intranasal transfer of ILC2s is associated with alterations to the myeloid cell compartment at peak infection

Given that ILC2s are essential to the proliferation and maintenance of eosinophils (Nussbaum *et al.*, 2013), it was important to investigate the effect of ILC2 transfer on this cell population. Moreover, as neutrophils and macrophages play key roles in the immune response against *F. tularensis* LVS (Ellis *et al.*, 2002; Hall *et al.*, 2008), it was also important to consider whether the enhanced bacterial burdens in the lung could be due to significant changes in the number and infection of these cells (figure 4.14 and 4.15). Interestingly, the frequency (figure 4.14A) and number (figure 4.14B) of eosinophils were reduced in infected mice, to a similar level whether they received transferred ILC2s or not. Both the frequency (figure 4.14E) and total number (figure 4.14F) of $CD64^+$ macrophages were significantly enhanced in the lung during infection with *F. tularensis* LVS, with transfer of ILC2s not significantly altering these numbers (figure 4.14E-F). Neutrophils were also significantly increased following infection, and of note, further increased following ILC2 transfer (figure 4.14C-D). Together, whilst infection with *F. tularensis* LVS induces changes to cells of the myeloid compartment, these data indicate that neutrophils are the primary myeloid cell population impacted by the ILC2 transfer.

As multiple myeloid cell types serve as a replicative reservoir for *F. tularensis* LVS (Hall *et al.*, 2008), the relative infection of these myeloid cell types was determined after ILC2 transfer. Interestingly, the frequency of infected eosinophils was enhanced following ILC2 transfer (figure 4.15A-B). Despite this, the total number of infected eosinophils was unchanged (figure 4.15C). Moreover, whilst $LVS^+$ $CD64^+$ macrophages were unchanged following ILC2 transfer (figure 4.15A and D-E), the frequency (figure 4.15A and F) and total number (figure 4.15G) of infected neutrophils were enhanced in mice that received ILC2 transfer. Overall, these results suggest that intranasal transfer of ILC2s results in significantly enhanced infection of eosinophils and neutrophils, providing an intracellular replicative niche for *F. tularensis* LVS, which could contribute to the excessive bacterial burdens observed in mice receiving ILC2s.

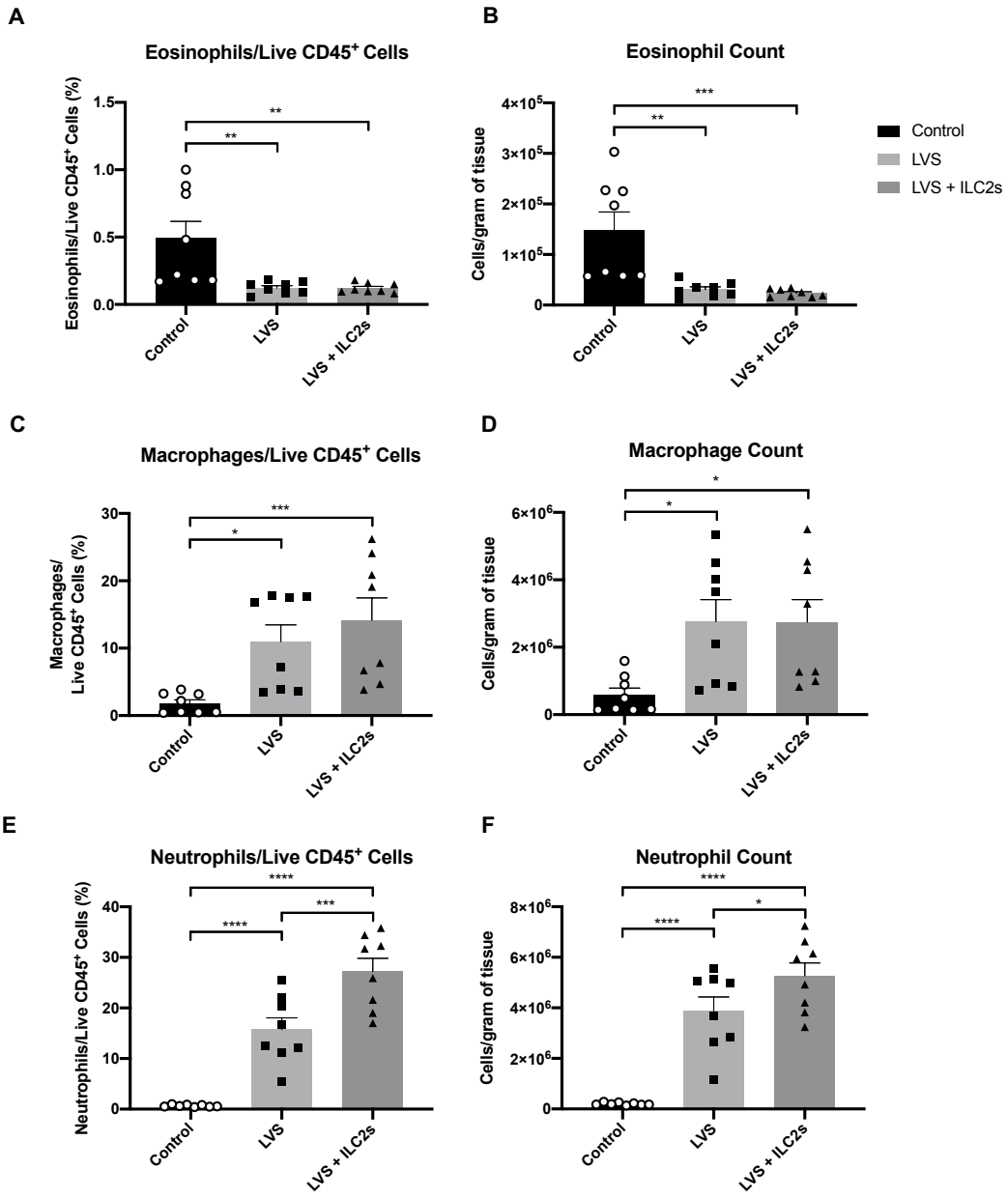


**Figure 4.14 - Characterisation of the myeloid immune compartment in the lung of LVS-infected C57BL/6 mice following ILC2 transfer**

C57BL/6 mice were infected with 1000 CFU *F. tularensis* LVS, where one group of mice received 1x10$^5$ FACS-sorted live CD45$^+$Lin$^-$CD127$^+$KLRG1$^+$ i.n. at day 3 p.i.. Control mice received PBS. Flow cytometry analysis of the myeloid immune compartment in the lung of C57BL/6 mice at day 7 p.i. **(A-B)** Eosinophils (CD45$^+$Ly6G$^-$Siglec-F$^+$CD64$^-$), **(C-D)** CD64$^+$ macrophages (CD45$^+$Ly6G$^-$Siglec-F$^-$ CD64$^+$) and **(E-F)** neutrophils (CD45$^+$Ly6G$^+$) were quantified, and expressed as a frequency of live CD45$^+$ cells, and cell counts per gram of tissue (n=8 for all cell populations). Statistical analysis was performed with either one-way ANOVA for parametric data, or Kruskal Wallis for non-parametric data, with appropriate multiple comparisons tests performed for each method of analysis; * p<0.05; ** p<0.01; *** p<0.001; **** p<0.0001.

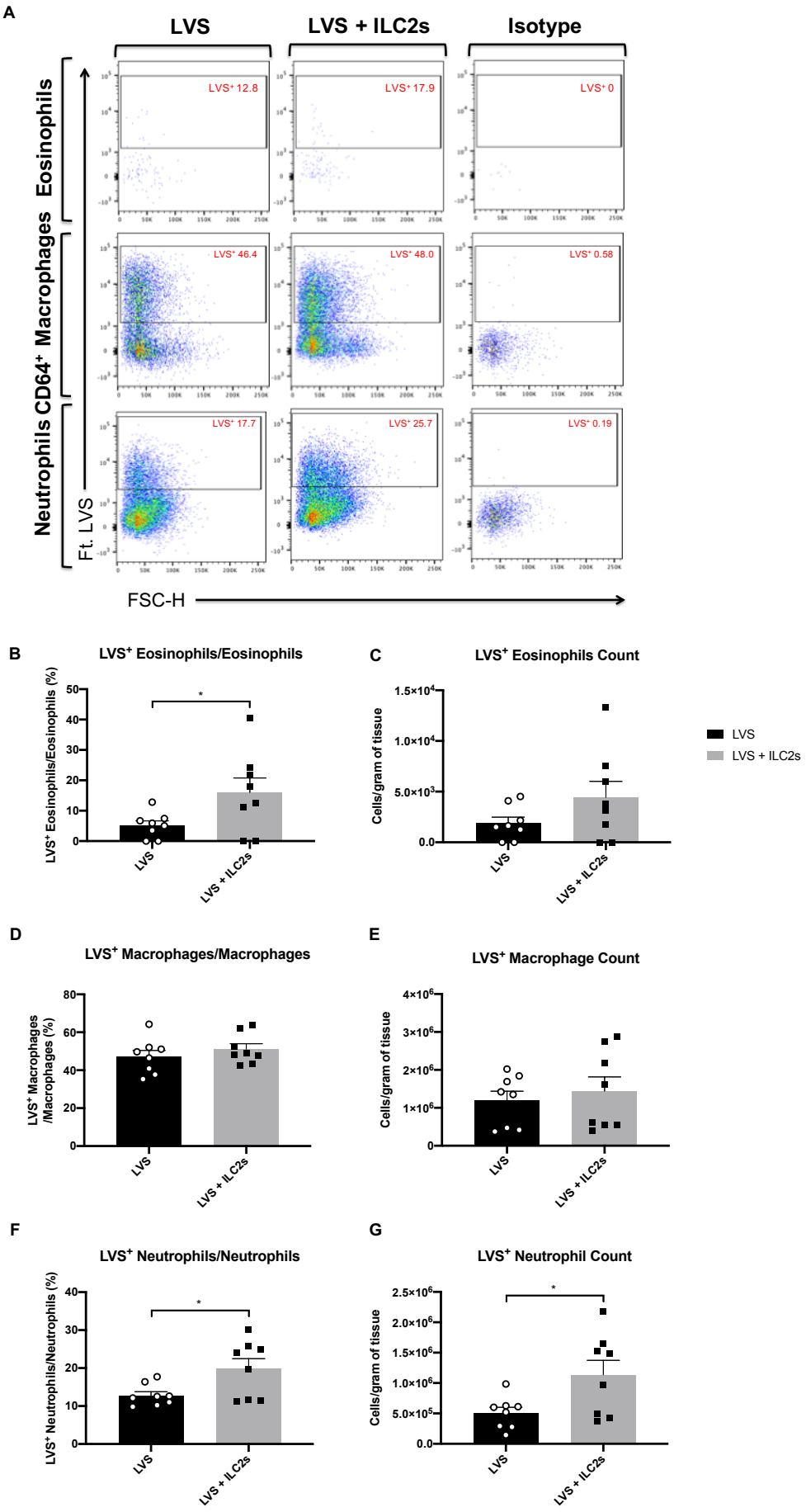
A
LVS
LVS + ILC2s
Isotype
Neutrophils CD64+ Macrophages Eosinophils
Ft. LVS
FSC-H
LVS+ 12.8
LVS+ 17.9
LVS+ 0
LVS+ 46.4
LVS+ 48.0
LVS+ 0.58
LVS+ 17.7
LVS+ 25.7
LVS+ 0.19
B
LVS+ Eosinophils/Eosinophils
LVS+ Eosinophils/Eosinophils (%)
C
LVS+ Eosinophils Count
Cells/gram of tissue
LVS
LVS + ILC2s
D
LVS+ Macrophages/Macrophages
LVS+ Macrophages /Macrophages (%)
E
LVS+ Macrophage Count
Cells/gram of tissue
F
LVS+ Neutrophils/Neutrophils
LVS+ Neutrophils/Neutrophils (%)
G
LVS+ Neutrophil Count
Cells/gram of tissue

## 4.3 Discussion

### 4.3.1 Determining how IL-33-induced expansion and activation of ILC2s impacts upon infection with *F. tularensis* LVS

The cytokine IL-33 has previously been shown to induce significant expansion and activation of ILC2s (Artis and Spits, 2015). This thesis chapter has demonstrated that both IL-33-induced expansion of ILC2s, and direct transfer of these cells to the lung of mice are detrimental to the control of infection against *F. tularensis* LVS, resulting in enhanced bacterial burdens in the lung, liver and spleen.

Other studies have also examined the role of IL-33 and the associated expansion of ILC2s in intracellular and bacterial infections. For example, the presence of high levels of IL-33 in the lungs of influenza-infected mice (Le Goffic *et al.*, 2011) allows for the activation of ILC2s, which contribute to the repair of the airway epithelium via production of amphiregulin (AREG) (Monticelli *et al.*, 2011). Moreover, IL-33-activated ILC2s are important in the maintenance of epithelial integrity during infection with the bacterium *Clostridium difficile* (Frisbee *et al.*, 2019). Interestingly, these contributions appear to be independent of viral titres and bacterial burdens, as depletion of ILC2s in these contexts does not lead to significant exacerbation of either readout (Monticelli *et al.*, 2011; Frisbee *et al.*, 2019). Thus, whilst IL-33-activated ILC2s appear to be beneficial in these models, it remains to be determined whether an expansion of ILC2s could also contribute to the repair of the airway epithelium in the context of *F. tularensis* LVS. Moreover, it is also important to dissect the relative contribution of ILC2-derived AREG in this reparatory role, given that the expanded $ST2^+$ Treg subset observed in this chapter could also contribute to tissue repair (Arpaia *et al.*, 2015).

**Figure 4.15 - Characterisation of infected myeloid cell populations in the LVS-infected lung of C57BL/6 mice following ILC2 transfer**

C57BL/6 mice were infected with 1000 CFU *F. tularensis* LVS, where one group of mice received $1x10^5$ FACS-sorted live $CD45^+Lin^-CD127^+KLRG1^+$ i.n. at day 3 p.i.. Flow cytometry analysis of infected immune cell populations in the lung of C57BL/6 mice at day 7 p.i. **(A)** Representative plots for identification of $LVS^+$ eosinophils ($CD45^+Ly6G^-Siglec\text{-}F^+CD64^-$), $LVS^+$ $CD64^+$ macrophages ($CD45^+Ly6G^-Siglec\text{-}F^-CD64^+$) and $LVS^+$ neutrophils ($CD45^+Ly6G^+$). **(B-G)** $LVS^+$ myeloid immune cells were quantified, and expressed as a frequency of individual cell populations, and cell counts per gram of tissue (n=8 for all cell populations). Numbers in FACS plots represent the percentage of infected cells from individual immune cell populations. Statistical analysis was performed with unpaired t-test; * $p<0.05$.

Production of AREG by this $ST2^+$ Treg subset plays a vital role in the control of tissue inflammation during viral infection, with AREG-deficient Tregs exhibiting significantly more tissue damage (Arpaia *et al.*, 2015). Moreover, Treg-derived AREG does not influence T effector cell function in this context, indicating a more protective and less inhibitory role for these regulatory cells in limiting an excessively inflammatory phenotype (Arpaia *et al.*, 2015). Despite this, it is currently unclear whether this is also the case in the IL-33-treated LVS-infected mice studied in this thesis chapter. Furthermore, whilst the enhanced bacterial burdens in IL-33-treated $Rag1^{-/-}$ mice may suggest that innate immunity is sufficient to perturb the control of infection, it does not indicate that tissue repair mechanisms are impeded in the absence of adaptive immunity. As such, a way in which this anti-inflammatory role for ILC2s and Tregs could be interrogated further is through use of IL-33-treated WT, $Rag1^{-/-}$ and $ICOS\text{-}T^{-/-}$ knockout mice, the last of which lack ILC2s (Oliphant *et al.*, 2014). In short, lung H&E sections would be obtained in conjunction with tissue levels of AREG, to investigate the relative contribution of innate and adaptive sources of AREG in the maintenance of epithelial integrity in IL-33-treated mice.

### 4.3.2 IL-33-activated ILC2 effector functions during infection with *F. tularensis* LVS

Given that IL-33 is a potent activator of ILC2s (Artis and Spits, 2015), it is important to consider the impact of this cytokine in inducing their effector functions, and how this could lead to an altered immune response against *F. tularensis* LVS. Two of the major cytokines produced by ILC2s upon their activation are IL-5 and IL-13, which act on many downstream targets, including eosinophils and macrophages (Artis and Spits, 2015). Indeed, ILC2-derived IL-5 is critical to the maintenance and function of eosinophil numbers (Nussbaum *et al.*, 2013), and can result in significant eosinophilia which contributes to airway inflammation following challenge with the protease allergen papain (Halim *et al.*, 2012a). Interestingly, this can also occur in the absence of adaptive immunity, indicating a critical role for activated ILC2s in driving eosinophilia (Halim *et al.*, 2012a). In line with this, enhanced numbers of eosinophils were observed in both WT and $Rag1^{-/-}$ LVS-infected mice following IL-33 treatment, which could suggest that ILC2s are acting in a similar way during LVS infection.

An effective way to test the ILC2-eosinophil relationship could be through use of an anti-IL-5 antibody in IL-33-treated mice. Importantly, as cytokine levels were not determined in this thesis chapter, confirmation of ILC2-derived IL-5 would first be required. Nevertheless, the benefits of this approach have been demonstrated recently in the context of anti-tumour immunity, where blockade of IL-5 significantly reduced eosinophil recruitment to the lung, alongside a concurrent decrease in the number of lung metastases (Schuijs *et al.*, 2020). This becomes especially important in the context of LVS infection, when it is considered that eosinophils also exhibit enhanced levels of infection following IL-33 treatment, and may therefore act as a reservoir to propagate enhanced bacterial burdens in the lung.

Traditionally, *F. tularensis* is taken up by a process known as looping phagocytosis (Ozanic *et al.*, 2015). Despite this, little is known about the mechanism by which *F. tularensis* can enter eosinophils. Interestingly, eosinophils can phagocytose other pathogens, such as *Histoplasma capsulatum*, which triggers an enhanced non-protective type 2 immune response (Verma *et al.*, 2017). Moreover, eosinophils can take up *Staphylococcus aureus* in a complement receptor 1 (CR1)-dependent manner, which can be inhibited through blockade of this receptor (Hatano *et al.*, 2009). Thus, as it has been shown that neutrophils can ingest *F. tularensis* using CR1 (Schwartz *et al.*, 2012), it could be possible that eosinophils also phagocytose *F. tularensis* in a similar manner. Irrespective of the mechanism by which this occurs, the observation that eosinophils are the only myeloid cell identified in this thesis chapter to exhibit consistently elevated levels of infection in IL-33-treated WT and Rag1$^{-/-}$ mice suggests that this cell type could contribute to the enhanced bacterial burdens in IL-33-treated mice by providing a site for extensive bacterial replication.

In the context of respiratory infections, ILC2-derived IL-13 can drive airway hyper-reactivity (Chang *et al.*, 2011; Stier *et al.*, 2016; Wu *et al.*, 2019). Moreover, this can also result in the polarisation of macrophages to an 'anti-inflammatory' phenotype, characterised by enhanced expression of Arginase 1, Fizz1 and Ym1, which proves detrimental in the clearance of *Streptococcus pneumoniae* (Saluzzo *et al.*, 2017). Indeed, IL-13$^{-/-}$ mice show a more rapid clearance of the bacteria, indicating the detrimental role of this

ILC2-associated cytokine in the control of another bacterial infection. Interestingly, IL-13 can also induce an 'anti-inflammatory' state in macrophages in the context of infection with *F. tularensis* LVS, which results in enhanced intracellular replication and survival of bacteria (Shirey *et al.*, 2008). However, it is currently unclear whether this is the case in the context of IL-33-treated LVS-infected mice, as the activation state of macrophages was not considered in this model. Moreover, the data concerning the level of infection in macrophages in IL-33-treated mice is conflicting between WT and Rag1$^{-/-}$ mice, and it is therefore difficult to conclude the effects of IL-33 in this particular cell type. Future work should at least consider investigating the phenotype of these macrophages in more depth, by analysis of polarisation markers such as Arginase 1 (M2) and iNOS (M1) by RT-PCR, in order to begin to fully dissect the role that macrophages may play in the enhanced bacterial burdens in IL-33-treated mice – even if this is not due to direct cellular infection.

### 4.3.3 The relationship between NK cells and ILC2s during LVS infection

ILC2s have previously been shown to exhibit an antagonistic role on lung NK cells in anti-tumour immunity (Schuijs *et al.*, 2020). The mechanism by which this occurs has been previously described, occurring via an ILC2-eosinophil cross-talk, with blockade of this by either anti-IL-5 or IL-33R-Fc restoring NK cell function and numbers (Schuijs *et al.*, 2020). Thus, it was somewhat surprising that NK cell numbers were unaffected by the IL-33-mediated expansion of ILC2s and eosinophils. Moreover, whilst NK cells were reduced as a frequency live CD45$^{+}$ cells in IL-33-treated uninfected mice, this is likely to be due to preferential expansion of other lymphocyte populations known to be activated by IL-33 such as ILC2s, Th2 and regulatory T cells (Molofsky, Savage and Locksley, 2015). Interestingly, intranasal transfer of ILC2s did appear to significantly impact on NK cell numbers and function, as shown by a reduction in total IFN-γ$^{+}$ NK cells. Furthermore, this appears to be mediated by an eosinophil-independent mechanism, as a decrease in eosinophils was observed in the lung of LVS-infected mice receiving ILC2 transfer. Of course, as ILC2s were transferred via the intranasal route and would have come into direct contact with the airways, an enhanced number of eosinophils could still be present here, and potentially identified in the bronchoalveolar lavage

fluid (BALF). Nevertheless, the data presented in this thesis chapter suggests that distinct mechanisms may exist in the control of NK cell numbers, depending on the manner in which ILC2 numbers are expanded.

In the wider context of understanding the role of ILC2s in the host immune response against *F. tularensis* LVS, it is important to further explore the relationship between ILC2s and NK cells, and whether this is bi-directional. Previous work has identified that whilst IL-33-activated ILC2s antagonise NK cell function (Schuijs *et al.*, 2020), activated NK cells can inhibit the production of ILC2-derived IL-5 and IL-13, and alleviate bleomycin-induced lung inflammation when transferred in to NK-depleted mice (Bi *et al.*, 2017). Moreover, as NK cells serve as a major source of IFN-γ during infection with *F. tularensis* LVS (Lopez *et al.*, 2004; Schmitt *et al.*, 2013), and this cytokine can inhibit ILC2 function (Molofsky *et al.*, 2015; Duerr *et al.*, 2016), interrogating the NK-ILC2 relationship further in the context of IL-33-treated mice may highlight potential therapeutic avenues that could antagonise ILC2 numbers earlier in infection, and result in a more type 1-polarised immune response. Thus, future work should seek to address how IL-33 treatment impacts on the activation status of NK cells and their function, and whether blockade of IL-33 can alleviate this.

### 4.3.4 ILC2-ILC1 plasticity

As aforementioned, viral infection results in elevated levels of tissue IL-33 (Le Goffic *et al.*, 2011). Moreover, direct ILC2-ILC1 conversion has been observed in this context, which is mediated by the cytokines IL-12 and IL-18 (Silver *et al.*, 2016). Here, ILC2s upregulate expression of IL-12Rβ2 and IL-18Rα and begin to produce IFN-γ, which enhances anti-viral immunity (Silver *et al.*, 2016). Thus, another objective of the IL-33-mediated expansion of ILC2s during infection with *F. tularensis* LVS was to determine whether a combination of this cytokine and IL-12 in the LVS-infected lung environment (Lin *et al.*, 2009) could promote a similarly plastic behaviour in the expanded ILC2 population, and thus benefit the host immune response against the bacteria. Despite this, no differences were observed in ILC1 numbers in IL-33-treated LVS-infected mice versus untreated infected mice. As such, this may suggest that ILC2 plasticity may not be applicable in the context of IL-33 treatment, as the strength of this cytokine signal may heavily bias the lung

immune environment to type 2 immunity, and override any potential type 1 signals and interconversion between ILC2 and ILC1s. In future, it would therefore be more useful to administer a combination of IL-12 and IL-33, to attempt to polarise an expanded ILC2 population to an ILC1-like phenotype.

The cytokine IFN-γ plays a critical role during infection with *F. tularensis* LVS (Leiby *et al.*, 1992; Elkins *et al.*, 1996), and as previously mentioned, can inhibit ILC2 function and proliferation (Molofsky *et al.*, 2015; Kudo *et al.*, 2016; Duerr *et al.*, 2016). Indeed, mice with elevated levels of constitutive IFN-γ display diminished ILC2 responses during infection with the nematode *Nippostrongylus brasiliensis* (Molofsky *et al.*, 2015). This IFN-γ-mediated effect is also observed during co-infection with *N. brasiliensis* and *Listeria monocytogenes*, a bacterium that provokes a strong IFN-γ-mediated response (Molofsky *et al.*, 2015). Thus, the reduced IL-33-mediated expansion of ILC2s during LVS infection could be due to the persistence of hallmarks of a type 1 immune response in the LVS-infected lung environment. For example, it has previously been demonstrated that a combination of IL-12, IL-18 and IL-33 administered to mice induces a significantly diminished expansion of lung ILC2s when compared to IL-33 treatment alone (Silver *et al.*, 2016). Thus, as it is already known that IL-12 is present in the lung of LVS-infected mice by day 3 p.i. (Lin *et al.*, 2009), this could contribute to the observed reduction in ILC2s in IL-33-treated LVS-infected mice.

### 4.3.5 Investigating the effects of IL-33 on T cell responses during infection with *F. tularensis* LVS

Whilst ILC2s were significantly expanded during infection with *F. tularensis* LVS, it is important to note that IL-33 can expand other cells of the lymphoid lineage, notably Th2 and Tregs (Molofsky, Savage and Locksley, 2015). It has been discussed earlier that the specifically expanded $ST2^+$ Treg subset seen in this chapter can produce AREG (Arpaia *et al.*, 2015), but they are also capable of production of the type 2 cytokines IL-5 and IL-13 (Alvarez, Fritz and Piccirillo, 2019). Indeed, either IL-33 or challenge with an allergen cocktail (*Alternaria alternata*, *Aspergillus fumigatus*, house dust mite and ovalbumin) is sufficient to induce a Th2-like phenotype in this Treg subset, characterised by enhanced IL-5 and IL-13 production when compared to

PBS controls (Chen *et al.*, 2017). Importantly, the IL-33-mediated release of these cytokines is critical in driving allergic airway inflammation, with their production ameliorated in IL-33$^{-/-}$ mice (Louten *et al.*, 2011). However, it remains to be seen whether the production of IL-5 and IL-13 by adaptive immune cells is capable of driving airway hyperreactivity and inflammation in IL-33-treated LVS-infected mice, especially given that the progression of infection is still significantly exacerbated in the absence of adaptive immunity (Kondo *et al.*, 2008).

Although IL-33 can act upon both Th2 and Treg cells directly, the activation of ILC2s and their subsequent interaction with these adaptive immune cells also drives their extensive proliferation and activation (Molofsky, Savage and Locksley, 2015). Indeed, the expansion and efficient function of Th2 and Treg cells is dependent on ILC2s in the immune response against the parasite *Nippostrongylus brasiliensis* (Oliphant *et al.*, 2014; Halim *et al.*, 2018). Thus, it was considered that a similar ILC2-T cell cross-talk occurs in IL-33-treated LVS-infected mice. Importantly however, whilst this relationship was not examined here, the data presented in this thesis chapter would instead suggest that adaptive immunity (and this cross-talk) is dispensable in causing an exacerbated level of infection in the lung, with IL-33-treated Rag1$^{-/-}$ mice displaying significantly elevated bacterial burdens in line with those observed in IL-33-treated WT mice. With that in mind, it was considered that the sources of the enhanced bacterial burdens in IL-33-treated LVS-infected mice are derived from the innate immune system.

### 4.3.6 Understanding the relationship between ILC2s and neutrophils during infection with *F. tularensis* LVS

In the first part of this chapter, it became evident that whilst IL-33 treatment successfully expanded the ILC compartment, it also enhanced the numbers of multiple other immune cell populations. Thus, an intranasal transfer of ILC2s was seen as a more focused method to expand ILC2s during infection with *F. tularensis* LVS. Indeed, ILC2 transfer did not elicit the same effects on the immune system as observed in IL-33-treated mice, with a lack of expansion of Th2, ST2$^{+}$ Treg cells and eosinophils post-transfer. Nevertheless, it was interesting to observe that ILC2 transfer also

exacerbated bacterial burdens akin to those seen in IL-33-treated mice, indicating that ILC2s may be detrimental to the control of infection.

As mentioned throughout this thesis, neutrophil recruitment is important to the survival of *F. tularensis* LVS, given their ability to provide the bacterium with a replicative niche (Hall *et al.*, 2008; Casulli *et al.*, 2019). Taken in combination with the fact that IL-33 can promote neutrophil influx, and improve bacterial clearance and control of sepsis (Alves-Filho *et al.*, 2010), it was important to investigate the impact of IL-33 treatment and ILC2 transfer on neutrophils. In the context of type 2 lung inflammation, an ILC2-neutrophil cross-talk has been demonstrated, where ILC2s activated by either IL-33 or papain adopt an inflammatory phenotype (iILC2), promoting neutrophil migration through the production of IL-17 (Cai *et al.*, 2019). Interestingly however, IL-33 treatment had no effect upon neutrophil recruitment to the lung during infection with *F. tularensis* LVS. This may in fact be due to the vast majority of ILC2s expressing higher levels of CD90, and IL-17 being produced by ILC2s with lower expression of this marker (Huang *et al.*, 2015). As such, the major cytokine signals produced from ILC2s in IL-33-treated LVS-infected mice are more likely to be IL-5 and IL-13. Nevertheless, it remains of interest to determine the cytokine production of ILC2s in this context, and whether any disparity in their effector function is observed based on expression of CD90. Moreover, as IL-25 is a more potent inducer of this iILC2 population (Huang *et al.*, 2015), it is also important to consider whether pre-treatment of mice with this cytokine in lieu of IL-33 would in fact enhance neutrophil migration, and how this would impact on bacterial burdens during infection with *F. tularensis* LVS.

Interestingly, unlike IL-33-treated LVS-infected mice, an enhanced number of lung neutrophils was observed following ILC2 transfer, potentially suggesting that ILC2 effector functions are distinct in these two mechanisms. It is currently unclear how this occurs in ILC2 transfer mice, but could be considered due to differences in the cytokine milieu between models. For example, the expansion of ILC2s by treatment with IL-33 will likely result in robust production of type 2 cytokines, which will polarise the lung immune environment towards type 2 immunity prior to infection with *F. tularensis* LVS. Conversely, the intranasal transfer of ILC2s into the LVS-infected environment at day 3 p.i. will mean that these ILC2s are exposed to type 1

stimuli such as IL-12 (Lin *et al.*, 2009; Cowley and Elkins, 2011), which can induce the production of IL-17 in ILC2s (Huang *et al.*, 2015). As such, tissue signals may dictate the effector function of ILC2s in both of these contexts, resulting in different outcomes for the host immune response.

Finally, it was considered whether the enhanced migration of neutrophils could instead be in response to the enhanced number of ILC2s, as neutrophils have previously been shown to attenuate ILC2 activity (Patel *et al.*, 2019). However, it is currently unclear whether a similarly protective role exists for neutrophils in the context of the data presented in this thesis chapter, especially given that infection levels of neutrophils were exacerbated in IL-33-treated WT and ILC2 transfer mice. Thus, this indicated that these cells may instead serve as an enhanced replicative niche, contributing to the enhanced bacterial burdens observed in these models.

## 4.4 Conclusion

Overall, this chapter has demonstrated that IL-33 impacts on multiple immune cells in the context of infection with *F. tularensis* LVS, and this treatment results in significantly enhanced bacterial burdens in the lung, liver and spleen of mice. Indeed, ILC2s, eosinophils, $ST2^+$ $CD4^+$ T cells and $ST2^+$ Tregs are all expanded in IL-33-treated mice. However, the consistently elevated bacterial burdens in IL-33-treated $Rag1^{-/-}$ mice, and following intranasal transfer of sort-purified ILC2s, indicated that ILC2s are detrimental to the control of infection. This may be due to multiple potential mechanisms, such as promoting enhanced recruitment of myeloid cells, which leads to an enhanced number of infected cells; or by inhibition of NK cell function, which would disrupt the induction of a type 1 immune response. Thus, it is therefore important to investigate how the absence of ILC2s would impact on the progression of infection, and how their numbers can be manipulated earlier in infection – topics that will be addressed in the next results chapter.

# Chapter 5

## Determining the impact of the ablation of innate lymphocytes on the progress of infection with *F. tularensis* LVS

## 5.1 Introduction

In chapter 3 of this thesis, a subset-specific reduction in ILC2s was observed from day 5 p.i. with *F. tularensis*. Chapter 4 then investigated whether rescuing this reduction could influence infectious outcome. Indeed, it was demonstrated that either IL-33-mediated activation, or transfer of sort-purified ILC2s by the intranasal route appears to be detrimental to the host immune response against *F. tularensis* LVS, with exacerbated bacterial burdens in both contexts. Nevertheless, it remained unclear why ILC2s are reduced during infection with *F. tularensis* LVS.

It was hypothesised that the reduced number of ILC2s could be caused by a shift of the host immune response to a more type 1-biased immune response, thus suppressing a cell type that is associated with type 2-driven pathologies (Artis and Spits, 2015). As such, this chapter now considers whether ILCs are necessary for the host immune response against *F. tularensis* LVS, by interrogating their relative contribution alongside adaptive immunity, and other elements of innate immunity, through the use of knockout mouse models. Specifically, this chapter uses $Rag1^{-/-}$ mice (which lack adaptive immunity), $il2rg^{-/-}$ mice (which lack the interleukin 2 receptor gamma chain (il2rg), causing immune defects including a loss of ILCs) and $Rag1^{-/-}il2rg^{-/-}$ mice (which lack both adaptive immunity and ILCs). Moreover, it addresses the specific role of ILC2s in the control of infection using ICOS-T mice (which can have their ILC2s selectively depleted through treatment with diphtheria toxin (DTx)) (Oliphant *et al.*, 2014). Finally, this chapter begins to assess the mechanisms by which ILC2s are reduced in the lung during infection with *F. tularensis* LVS, with a focus on the potential of cytokines in regulating ILC2 numbers, and the cellular sources of these cytokines.

## 5.2 Results

### 5.2.1 Lack of adaptive immunity does not alter bacterial burdens during infection with *F. tularensis* LVS

Whilst ILCs are lineage negative ($Lin^-$) cells, they share their effector functions with adaptive lymphocytes (Bando and Colonna, 2016). Moreover, as most models that deplete ILCs will also impact on elements of adaptive immunity, it is difficult to interrogate the role of ILCs during infections without first considering the contributions of adaptive immunity. In order to begin to separate these roles, the $Rag1^{-/-}$ mouse model (which lacks adaptive immunity) was used, to first address the relative importance of adaptive immunity in the control of infection with *F. tularensis* LVS. $Rag1^{-/-}$ mice displayed no difference in weight loss (figure 5.1A) or clinical scores (figure 5.1B) when compared to WT mice during infection with *F. tularensis* LVS. In addition, $Rag1^{-/-}$ mice displayed no differences in bacterial burdens in the lung, liver and spleen versus WT mice (figure 5.1C-D). Thus, this indicates that adaptive immunity is not essential for the control of primary infection with *F. tularensis* LVS.

### 5.2.2 Common gamma chain (il2rg) deficiency results in enhanced bacterial burdens during infection with *F. tularensis* LVS

As innate immunity appears to be sufficient for the control of infection with *F. tularensis* LVS (figure 5.1C-D), the common gamma chain KO ($il2rg^{-/-}$) mouse model was next used to investigate whether ILCs are important in this context (figure 5.1). These mice lack ILCs, but also display significantly reduced numbers of NK cells, and adaptive immune cells (Zhao *et al.*, 2019). Nevertheless, given the aforementioned dispensability of adaptive immunity in the control of infection, this model therefore served to begin to dissect the relative contribution of innate lymphocytes in the control of infection with *F. tularensis* LVS. Despite no differences in weight loss between WT, $Rag1^{-/-}$ and $il2rg^{-/-}$ mice (figure 5.1A), only $il2rg^{-/-}$ mice exceeded the clinical score threshold at day 7 p.i. (figure 5.1B). Moreover, bacterial burdens were significantly enhanced in the liver of $il2rg^{-/-}$ mice when compared to both WT and $Rag1^{-/-}$ mice at day 7 p.i. (figure 5.1C). Spleen burdens were also significantly elevated in $il2rg^{-/-}$ mice when compared to WT mice (figure 5.1C). As such, all mice strains used in subsequent studies were culled at

day 6 p.i. due to licence restrictions. At this earlier time point, il2rg$^{-/-}$ mice showed significantly enhanced bacterial burdens in the lung, liver and spleen when compared to WT and Rag1$^{-/-}$ mice (figure 5.1D). Overall, these results suggest that ILCs could contribute to the control of infection with *F. tularensis* LVS.

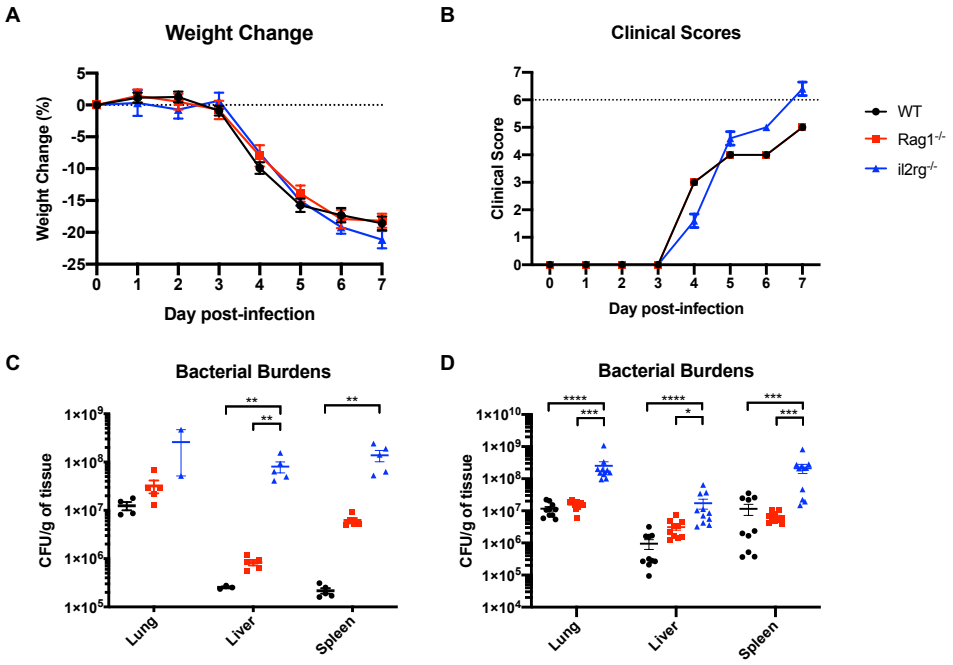


**Figure 5.1 - il2rg$^{-/-}$ mice display exacerbated bacterial burdens and enhanced mortality, whilst adaptive immunity is dispensable during infection with *F. tularensis* LVS**

C57BL/6, Rag1$^{-/-}$ and il2rg$^{-/-}$ mice were infected via the intranasal route with *F. tularensis* LVS (1000 CFU) and monitored up to day 7 p.i. **(A)** Weight change was monitored daily in all mice, and plotted as a percentage loss of original body weight (0% = body weight at day 0). **(B)** Severity of infection was evaluated using a clinical scoring system (see methods). **(C)** Bacterial burdens (CFU/g of organ) were enumerated in the lung, liver and spleen of mice at day 7 p.i. (n=2-5) and **(D)** day 6 p.i. (n=10 for C57BL/6 and Rag1$^{-/-}$ mice; n=11 for il2rg$^{-/-}$ mice). Statistical analysis was performed using either one-way ANOVA for parametric data, or Kruskal Wallis for non-parametric data, with Holm-Sidak's and Dunn's multiple comparisons tests performed for each method of analysis respectively; * p<0.05; ** p<0.01; *** p<0.001; **** p<0.0001.

### 5.2.3 The proportions of myeloid cells are altered in Rag1$^{-/-}$ and il2rg$^{-/-}$ mice

As mentioned throughout this thesis, myeloid cells play an integral role in infection with *F. tularensis* LVS, with their dysregulation and enhanced numbers providing an intracellular reservoir for bacterial replication (Hall *et al.*, 2008; Casulli *et al.*, 2019). Thus, as multiple lymphocyte-derived cytokines also contribute to the induction of effective bacterial killing in myeloid cells (Ellis and Beaman, 2004; Elkins *et al.*, 2009), it was important to investigate how the numbers and relative levels of infection of myeloid cells were impacted on in the il2rg$^{-/-}$ KO model, and whether this could contribute to the enhanced bacterial burdens observed in these mice during infection with *F. tularensis* LVS. In addition to this, whilst the proportion of myeloid cells has been somewhat characterised in the spleen of il2rg$^{-/-}$ mice (Cao *et al.*, 1995), little is known about the lung myeloid immune compartment in this KO model. Thus, it was important to determine its composition under steady-state conditions, and whether it differs in il2rg$^{-/-}$ mice when compared to WT and Rag1$^{-/-}$ mice, and could therefore predispose mice to the observed exacerbations in bacterial burdens.

The frequency of neutrophils was significantly elevated in both Rag1$^{-/-}$ and il2rg$^{-/-}$ mice when compared to WT mice at steady state (figure 5.2A and B). Upon infection, the frequency of neutrophils was further elevated in il2rg$^{-/-}$ mice when compared to both infected WT and Rag1$^{-/-}$ mice (figure 5.2A and B). Moreover, whilst infected Rag1$^{-/-}$ mice displayed no increase in the frequency of neutrophils when compared to Rag1$^{-/-}$ controls (figure 5.2B), both infected WT and il2rg$^{-/-}$ mice exhibited a significantly enhanced frequency of neutrophils when compared to their respective controls (figure 5.2B). Importantly however, no differences were observed in total neutrophil numbers between strains during infection (figure 5.2C). Thus, this suggests that the changes in the frequency of neutrophils in Rag1$^{-/-}$ and il2rg$^{-/-}$ mice could be due to ablation of lymphocyte populations in these models.

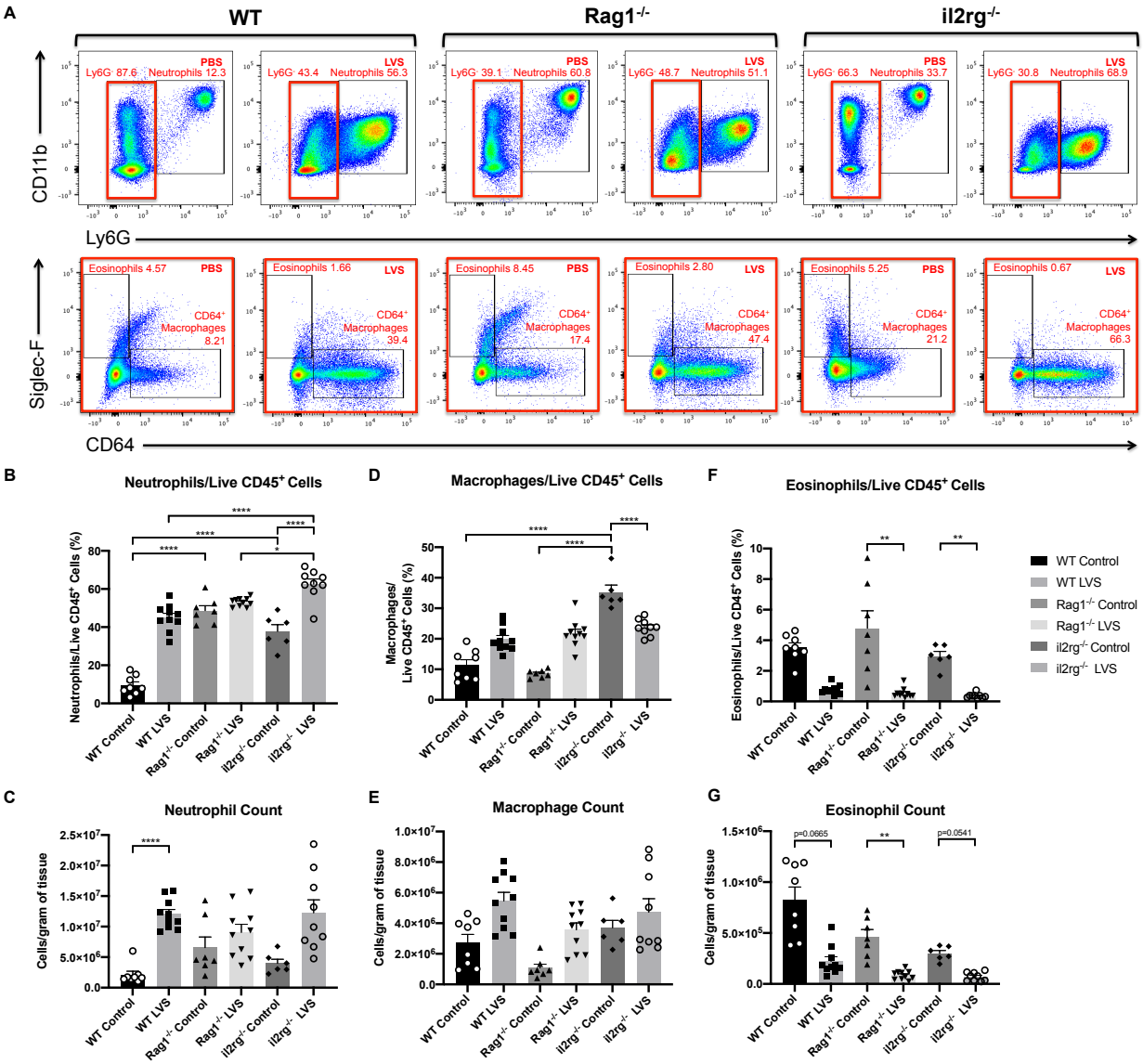


**Figure 5.2 - Effects of ablation of adaptive and innate lymphocytes on the myeloid immune response during infection with *F. tularensis* LVS**

**(A)** Representative plots for identification of myeloid cell populations in the lung of C57BL/6, Rag1$^{-/-}$ and il2rg$^{-/-}$ mice at day 6 p.i. with *F. tularensis* LVS. Control mice were given PBS. **(B-C)** neutrophil (live CD45$^{+}$Ly6G$^{+}$), **(D-E)** CD64$^{+}$ macrophage (live CD45$^{+}$Ly6G$^{-}$Siglec-F$^{-}$CD64$^{+}$) and **(F-G)** eosinophil (live CD45$^{+}$Ly6G$^{-}$Siglec-F$^{+}$CD64$^{-}$) populations were identified and expressed as a frequency of live CD45$^{+}$ cells and cell counts per gram of tissue (n=6-10). Numbers in FACS plots represent the percentage of the previous gate (eosinophils and CD64$^{+}$ macrophages as a % of Ly6G$^{-}$ cells; neutrophils as a % of live CD45$^{+}$ cells). Statistical analysis was performed with either one-way ANOVA for parametric data, or Kruskal Wallis for non-parametric data, with Holm-Sidak's and Dunn's multiple comparisons tests performed for each method of analysis respectively; * p<0.05; ** p<0.01; **** p<0.0001.

At steady state, the frequency of macrophages was significantly elevated in il2rg$^{-/-}$ mice when compared to both WT and Rag1$^{-/-}$ mice (figure 5.2A and

D). Upon infection, the frequency of macrophages in il2rg$^{-/-}$ mice was no different to that of WT and Rag1$^{-/-}$ mice (Figure 5.2A and D). No changes were observed in the total number (figure 5.2E) of macrophages between all three strains during infection with *F. tularensis* LVS. Thus, this indicates that the absence of ILCs and adaptive immunity has minimal impact on macrophages during infection. Finally, whilst no differences were observed in the frequency of eosinophils between WT, Rag1$^{-/-}$ and il2rg$^{-/-}$ mice at steady state, infection resulted in a significant decrease in both frequency (figure 5.2A and F) and number (figure 5.2G) of eosinophils relative to the respective steady state counterparts of each strain, suggesting an infection-induced decrease in eosinophils irrespective of genetic background.

Next, it was important to investigate whether the levels of infection of myeloid cells were impacted upon in il2rg$^{-/-}$ mice, to determine whether this could contribute to the enhanced bacterial burdens in il2rg$^{-/-}$ mice when compared to WT and Rag1$^{-/-}$ mice. Both the level of infection and number of infected neutrophils was unchanged between WT and il2rg$^{-/-}$ mice (figure 5.3A-C), suggesting that neutrophils may not represent an enhanced reservoir for bacteria in il2rg$^{-/-}$ mice. Of note, whilst a significant increase in the number of infected neutrophils was observed in il2rg$^{-/-}$ mice when compared to Rag1$^{-/-}$ mice, infected neutrophil numbers were unchanged in il2rg$^{-/-}$ mice versus WT counterparts (figure 5.3C).

Macrophages of il2rg$^{-/-}$ mice displayed a significantly increased level of infection when compared to both WT and Rag1$^{-/-}$ mice (figure 5.3A and D), with the total number of infected cells also elevated when compared to those of Rag1$^{-/-}$ mice (figure 5.3E). Akin to neutrophils however, the number of infected macrophages was unchanged in il2rg$^{-/-}$ mice versus WT mice (figure 5.3E). Finally, eosinophils also displayed a significantly enhanced level of infection in il2rg$^{-/-}$ mice when compared to WT and Rag1$^{-/-}$ mice (figure 5.3A and F). Total numbers of infected eosinophils were unaffected in il2rg$^{-/-}$ mice when compared to WT and Rag1$^{-/-}$ mice (figure 5.3G). Thus, these results suggest that macrophages and eosinophils could provide an enhanced intracellular niche in il2rg$^{-/-}$ mice.

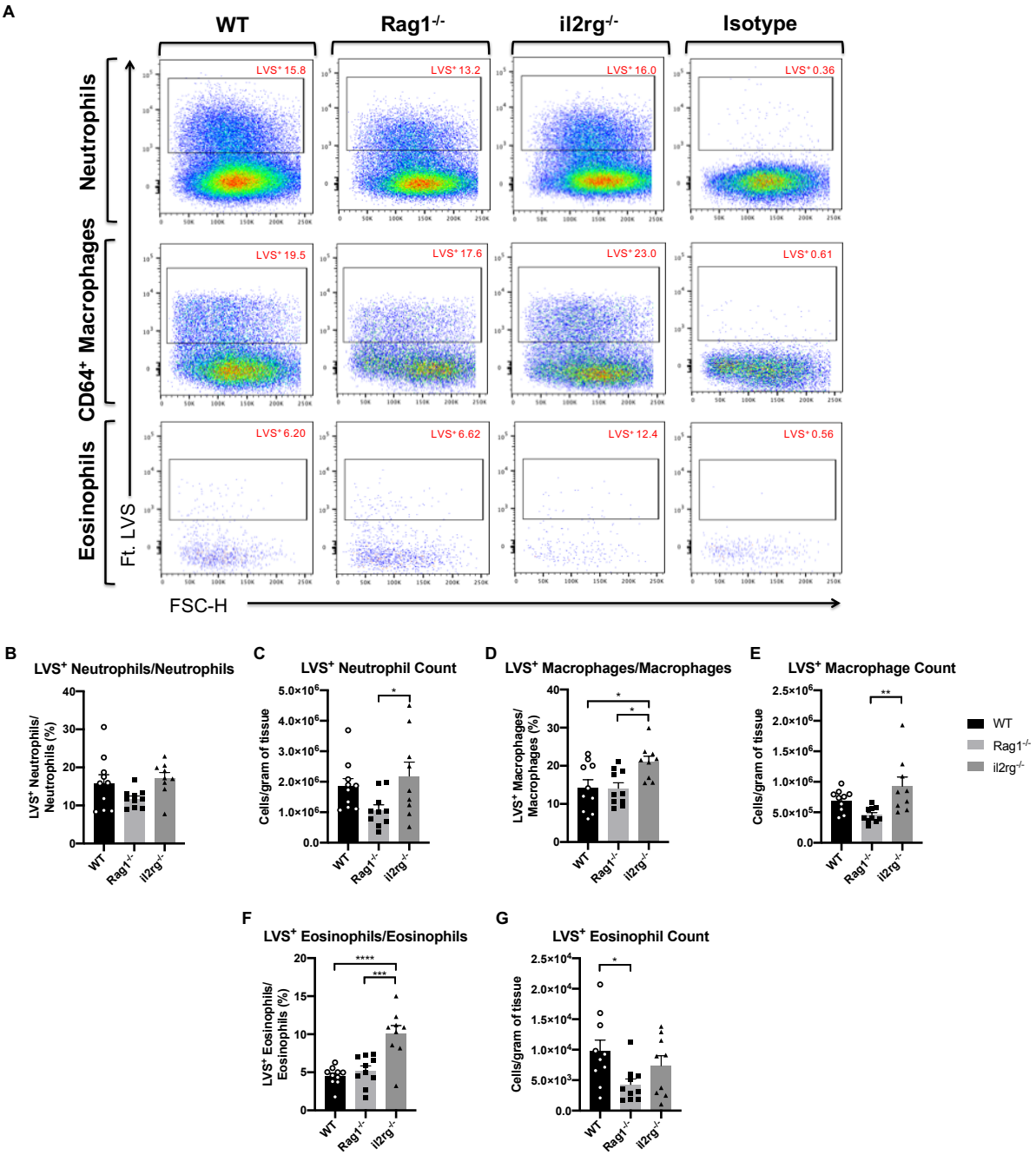


**Figure 5.3 - Effects of ablation of adaptive and innate lymphocytes on the infectious niche during infection with *F. tularensis* LVS**

**(A)** Representative plots for identification of myeloid cell populations in the lung of C57BL/6, Rag1$^{-/-}$ and il2rg$^{-/-}$ mice at day 6 p.i. with *F. tularensis* LVS. Control mice were given PBS. **(B-C)** LVS$^{+}$ neutrophil (live CD45$^{+}$Ly6G$^{+}$) and **(D-E)** LVS$^{+}$ CD64$^{+}$ macrophage (live CD45$^{+}$Ly6G$^{-}$Siglec-F$^{-}$CD64$^{+}$) and **(F-G)** eosinophil (live CD45$^{+}$Ly6G$^{-}$Siglec-F$^{+}$CD64$^{-}$) populations were identified and expressed as a frequency of parent populations and cell counts per gram of tissue (n=9-10). Numbers in FACS plots represent the percentage of infected cells from identified immune cell populations. Statistical analysis was performed with either one-way ANOVA for parametric data, or Kruskal Wallis for non-parametric data, with Holm-Sidak's and Dunn's multiple comparisons tests performed for each method of analysis respectively; * p<0.05; ** p<0.01; *** p<0.001; **** p<0.0001.

### 5.2.4 Loss of ILCs and NK cells in Rag1$^{-/-}$il2rg$^{-/-}$ mice is associated with enhanced bacterial burdens during LVS infection

When combined, the bacterial burden data from Rag1$^{-/-}$ and il2rg$^{-/-}$ mice (figure 5.1) demonstrate the importance of innate lymphocytes in the control of infection with *F. tularensis* LVS, as well as the dispensability of adaptive immunity. However, il2rg$^{-/-}$ mice also possess a residual number of T cells, which display a more pro-inflammatory phenotype (DiSanto *et al.*, 1995; Cao *et al.*, 1995; Nakajima *et al.*, 1997). Thus, it remained important to fully dissect the relative roles of innate and adaptive lymphocytes in the control of infection with *F. tularensis* LVS. To this end, the double KO Rag1$^{-/-}$il2rg$^{-/-}$ mouse model was used (figure 5.4). Unlike the previously described Rag1$^{-/-}$ and il2rg$^{-/-}$ models, Rag1$^{-/-}$il2rg$^{-/-}$ mice fully lack adaptive immunity as well as ILCs and NK cells. Thus, these mice serve as a useful tool to determine the importance of both ILCs and NK cells in the control of infection with *F. tularensis* LVS, without the potential contribution of pro-inflammatory T cells. Akin to il2rg$^{-/-}$ mice, Rag1$^{-/-}$il2rg$^{-/-}$ mice also displayed significantly enhanced bacterial burdens in the lung, liver and spleen at day 6 p.i. when compared to WT and Rag1$^{-/-}$ mice (figure 5.1D and 5.4A), further indicating that innate lymphocytes are important for the control of infection with *F. tularensis* LVS.

Next, it was important to investigate how the myeloid immune response was impacted in Rag1$^{-/-}$il2rg$^{-/-}$ mice. Whilst, the frequency of neutrophils was significantly enhanced in Rag1$^{-/-}$il2rg$^{-/-}$ mice when compared to WT mice (figure 5.4B), no differences were observed in total numbers (figure 5.4C). Moreover, no differences were observed in the frequency or total number of macrophages (figure 5.4D-E) or eosinophils (figure 5.4F-G). Thus, these results suggest that the proportion and numbers of myeloid immune cells are relatively unaltered in Rag1$^{-/-}$il2rg$^{-/-}$ mice during infection with *F. tularensis* LVS.

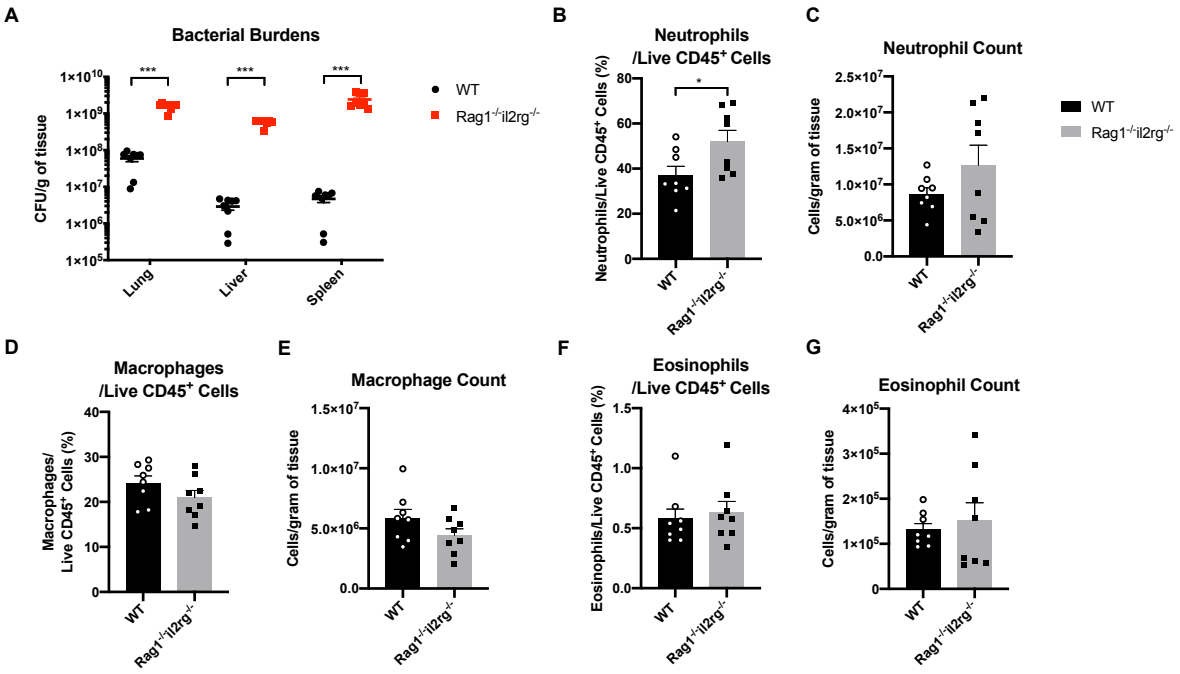


**Figure 5.4 – Rag1$^{-/-}$il2rg$^{-/-}$ mice display enhanced bacterial burdens and altered infectious niche in the lung during infection with *F. tularensis* LVS**

C57BL/6 and Rag1$^{-/-}$il2rg$^{-/-}$ mice were infected with 1000 CFU F. *tularensis* LVS and **(A)** bacterial burdens (CFU/g of organ) enumerated in the lung, liver and spleen of mice at day 6 p.i. Flow cytometry analysis of myeloid immune cell populations in the lung at day 6 p.i. identified **(B-C)** neutrophils (live CD45$^+$Ly6G$^+$) **(D-E)** CD64$^+$ macrophages (live CD45$^+$Ly6G$^-$Siglec-F$^-$CD64$^+$) and **(F-G)** eosinophils (live CD45$^+$Ly6G$^-$Siglec-F$^+$CD64$^-$). Populations were expressed as a frequency of live CD45$^+$ cells and cell counts per gram of tissue. (n=8). Statistical analysis performed with unpaired t-test for parametric data or Mann-Whitney test for non-parametric data; * p<0.05; ** p<0.01; **** p<0.0001.

Interestingly, the frequency (figure 5.5A) and number (figure 5.5B) of infected neutrophils was significantly enhanced in Rag1$^{-/-}$il2rg$^{-/-}$ mice. The frequency of LVS$^+$ macrophages was also increased in Rag1$^{-/-}$il2rg$^{-/-}$ mice (figure 5.5C). Despite this, no differences were seen in the total number of infected macrophages (figure 5.5D). The frequency (figure 5.5E) and total number of infected eosinophils were significantly enhanced in Rag1$^{-/-}$il2rg$^{-/-}$ mice (figure 5.5F). Overall, these results suggest that the absence of innate lymphocytes in Rag1$^{-/-}$il2rg$^{-/-}$ mice results in significant changes to the level of infection in cells of the myeloid compartment, and that these may contribute to the enhanced bacterial burdens observed in these mice during infection with *F. tularensis* LVS.

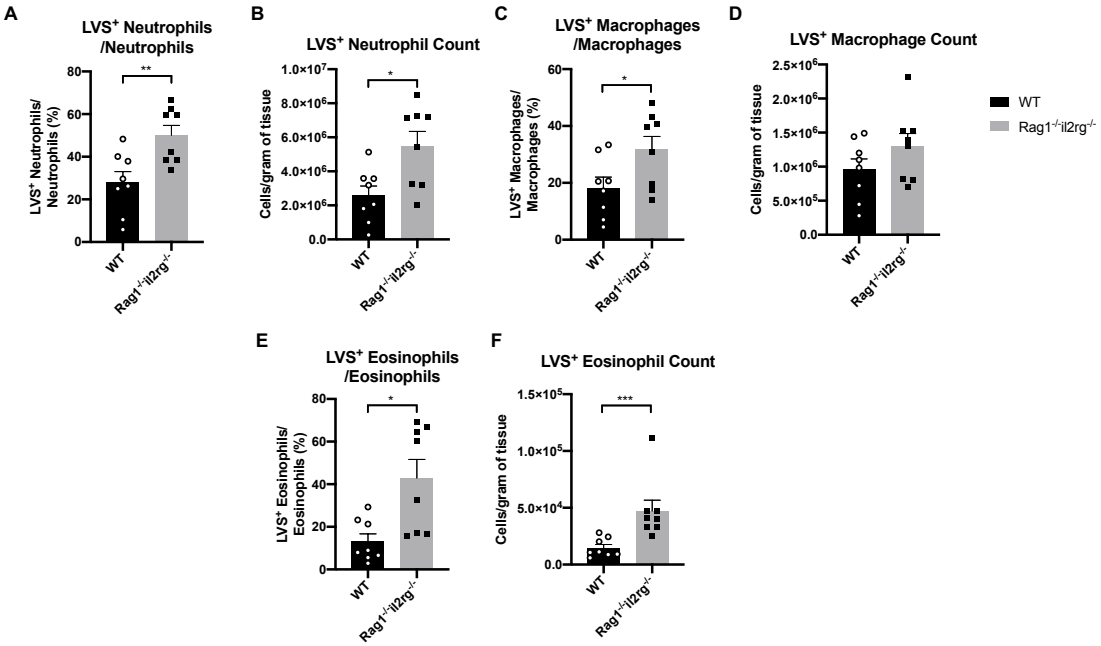


**Figure 5.5 - Rag1$^{-/-}$il2rg$^{-/-}$ mice display enhanced infectious niche in the lung during infection with *F. tularensis* LVS**

C57BL/6 and Rag1$^{-/-}$il2rg$^{-/-}$ mice were infected with 1000 CFU F. *tularensis* LVS and levels of infection were measured for myeloid cell populations in the lung at day 6 p.i. **(A-B)** Infected neutrophil (live CD45$^{+}$Ly6G$^{+}$), **(C-D)** CD64$^{+}$ macrophage (live CD45$^{+}$Ly6G$^{-}$Siglec-F$^{-}$CD64$^{+}$) and **(E-F)** eosinophil (live CD45$^{+}$Ly6G$^{-}$Siglec-F$^{+}$CD64$^{-}$) populations were identified and expressed as a frequency of individual cell types and cell counts per gram of tissue (n=8). Statistical analysis performed with unpaired t-test for parametric data or Mann-Whitney test for non-parametric data; * $p<0.05$; ** $p<0.01$; *** $p<0.001$.

### 5.2.5 ILC1s and NK cells represent innate sources of IFN-γ during infection with *F. tularensis* LVS

The enhanced bacterial burdens in both il2rg$^{-/-}$ and Rag1$^{-/-}$il2rg$^{-/-}$ mice indicate that an absence of ILCs may be detrimental to the control of infection of *F. tularensis* LVS. However, as chapter 4 of this thesis has already demonstrated, an expansion of ILC2s can play a detrimental role in the control of infection with *F. tularensis* LVS. Yet, the observed expansion of an ILC1 population during the later stages of *F. tularensis* LVS infection (figure 3.5) could represent a source of IFN-γ – a cytokine that is critical to the control of this infection (Leiby *et al.*, 1992; Lopez *et al.*, 2004; Schmitt *et al.*, 2013). Moreover, as NK cells are another innate lymphocyte population that

are ablated in the double KO Rag1$^{-/-}$il2rg$^{-/-}$ mouse model (Song *et al.*, 2010), and these cells are already known as a major source of IFN-γ during infection with *F. tularensis* LVS (Leiby *et al.*, 1992; Lopez *et al.*, 2004; Schmitt *et al.*, 2013), it was important to consider whether the enhanced bacterial burdens in the double KO Rag1$^{-/-}$il2rg$^{-/-}$ mouse model were instead due to the ablation of IFN-γ-producing innate lymphocyte populations. Thus, in order to further assess the relative contribution of these innate populations to the immune response against *F. tularensis* LVS, it was next important to determine their cytokine output as infection progressed.

Initially, levels of ILC-derived IFN-γ were quantified at days 3 and 5 p.i. (figure 5.6). ILC1s showed an enhanced capacity to produce IFN-γ (figure 5.6A-B), with the total number of IFN-γ$^{+}$ ILC1s also significantly elevated as infection progressed (figure 5.6C). Despite their ability to upregulate expression of IFN-γ during certain infections (Silver *et al.*, 2016), ILC2s displayed no changes in IFN-γ production (figure 5.6A, D and E). Thus, these data suggest that whilst ILC1s represent a source of IFN-γ, ILC2s are not capable of IFN-γ production during infection with *F. tularensis* LVS.

As ILC2s are known to primarily produce type 2 cytokines such as IL-5 and IL-13 (Artis and Spits, 2015), it was next important to consider whether they were doing so during infection with *F. tularensis* LVS, and potentially perturbing a type 1 immune response through expansion of type 2 immune cells. Indeed, the frequency of IL-5$^{+}$ ILC2s was significantly enhanced at day 3 p.i., (figure 5.7A and B). Despite this, the total number of IL-5-producing ILC2s was unchanged during infection (figure 5.7E). IL-13 production was also unaffected by infection with *F. tularensis* LVS (figure 5.7C and D), with IL-5$^{+}$IL-13$^{+}$ ILC2s also unchanged (figure 5.7F and G). Overall, these results indicate that the production of these ILC2-derived type 2 cytokines is generally limited throughout LVS infection.

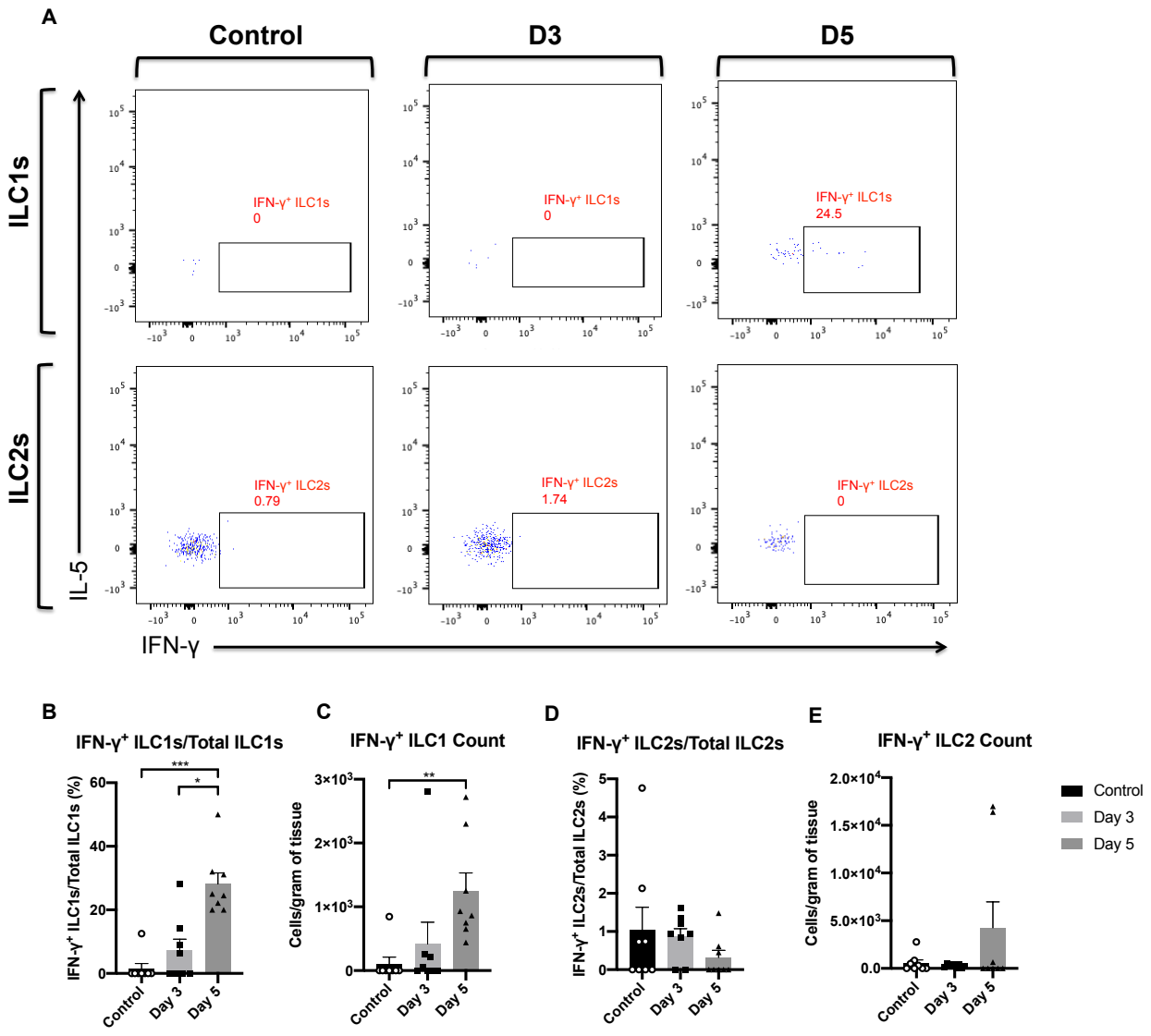


**Figure 5.6 - ILC1s display enhanced IFN-γ production during infection with *F. tularensis* LVS**

C57BL/6 mice were infected with 1000 CFU *F. tularensis* LVS and ILCs identified in the lung at different time points p.i. Control mice were given PBS. Single cell suspensions were incubated for 4 hours at 37°C with a cocktail of PMA, ionomycin, brefeldin A and monensin. **(A)** Representative plots for identification of ILC subsets and their production of IFN-γ in PBS (control) and LVS-infected mice at days 3 (D3) and 5 (D5) p.i.. **(B-C)** IFN-γ production in ILC1s (T-bet$^+$) and **(F-G)** ILC2s (ST2$^+$) was quantified and expressed as a frequency of individual ILC subsets, and cell counts per gram of tissue (n=7 for control, n=8 for day 3 and 5 p.i.). Numbers in FACS plots represent the percentage of IFN-γ$^+$ cells from ILC1 and ILC2 subsets respectively. Statistical analysis was performed using either one-way ANOVA for parametric data, or Kruskal Wallis for non-parametric data, with Holm-Sidak's and Dunn's multiple comparisons tests performed for each method of analysis respectively; * $p<0.05$; ** $p<0.01$; *** $p<0.001$.

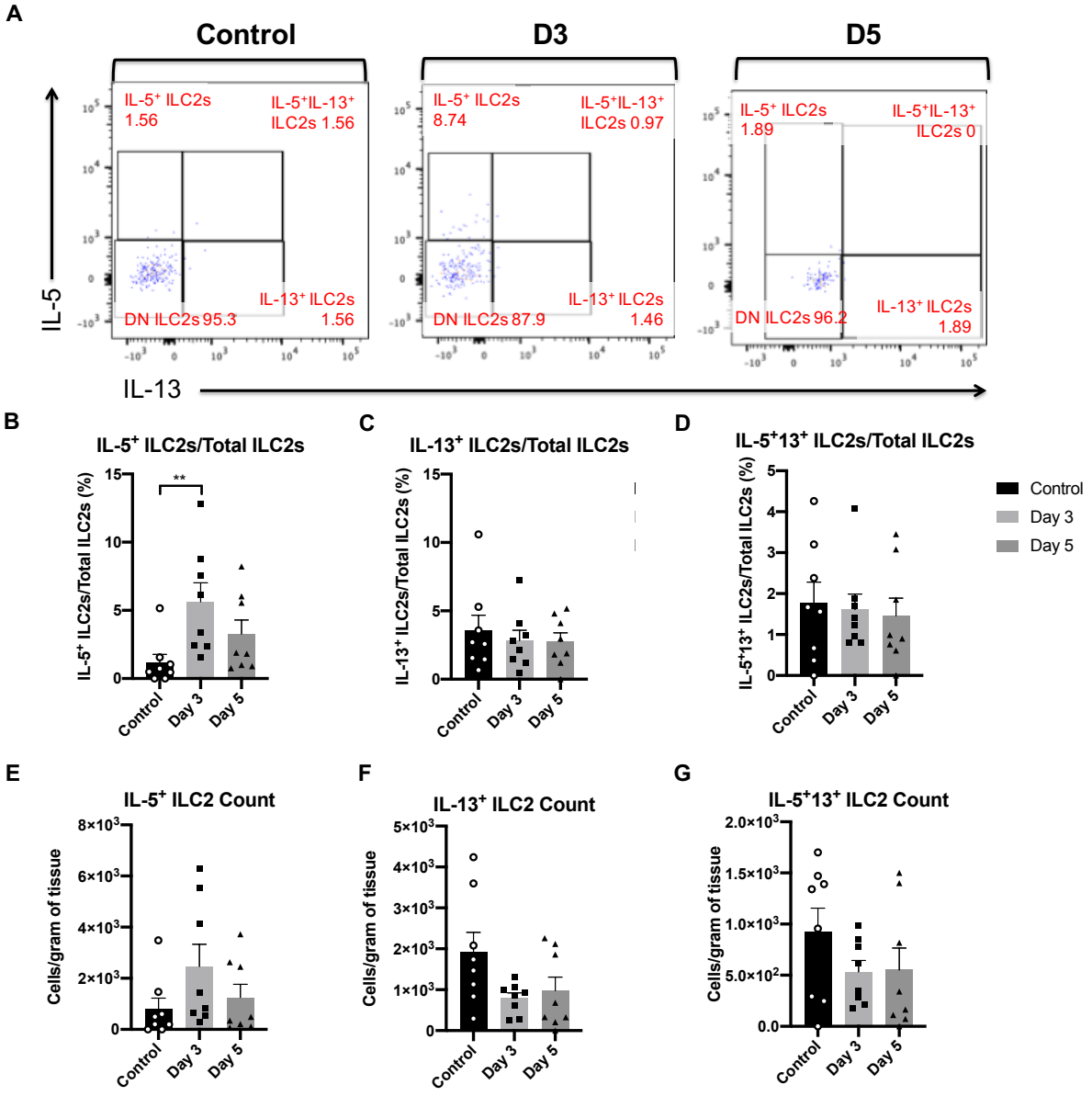


**Figure 5.7 - ILC2s display enhanced IL-5 production early during infection with *F. tularensis* LVS**

C57BL/6 mice were infected with 1000 CFU *F. tularensis* LVS and ILCs identified in the lung at different time points p.i. Control mice were given PBS. Single cell suspensions were incubated for 4 hours at 37ºC with a cocktail of PMA, ionomycin, brefeldin A and monensin. **(A)** Representative plots for ILC2 production of IL-5 and IL-13 in PBS (control) and LVS-infected mice at days 3 (D3) and 5 (D5) p.i.. **(B-G)** IL-5 and IL-13 production by ILC2s was quantified and expressed as a frequency of ILC2s, and cell counts per gram of tissue (n=7 for control, n=8 for day 3 and 5 p.i.). Numbers in FACS plots represent the percentage of ILC2s producing IL-5, IL-13, or both. The DN ILC2 population represents ILC2s that did not produce any of these cytokines. Statistical analysis was performed using either one-way ANOVA for parametric data, or Kruskal Wallis for non-parametric data, with Holm-Sidak's and Dunn's multiple comparisons tests performed for each method of analysis respectively; ** $p<0.01$.

Finally, the relative contribution of NK cell-derived IFN-γ was assessed (figure 5.8). Here, both the capacity of NK cells to produce IFN-γ (figure 5.8A-B) and the total number of IFN-γ$^+$ NK cells were significantly elevated by day 5 p.i. (figure 5.8C). Thus, these data demonstrate that NK cells are a potent source of IFN-γ in the lung during infection with *F. tularensis* LVS.

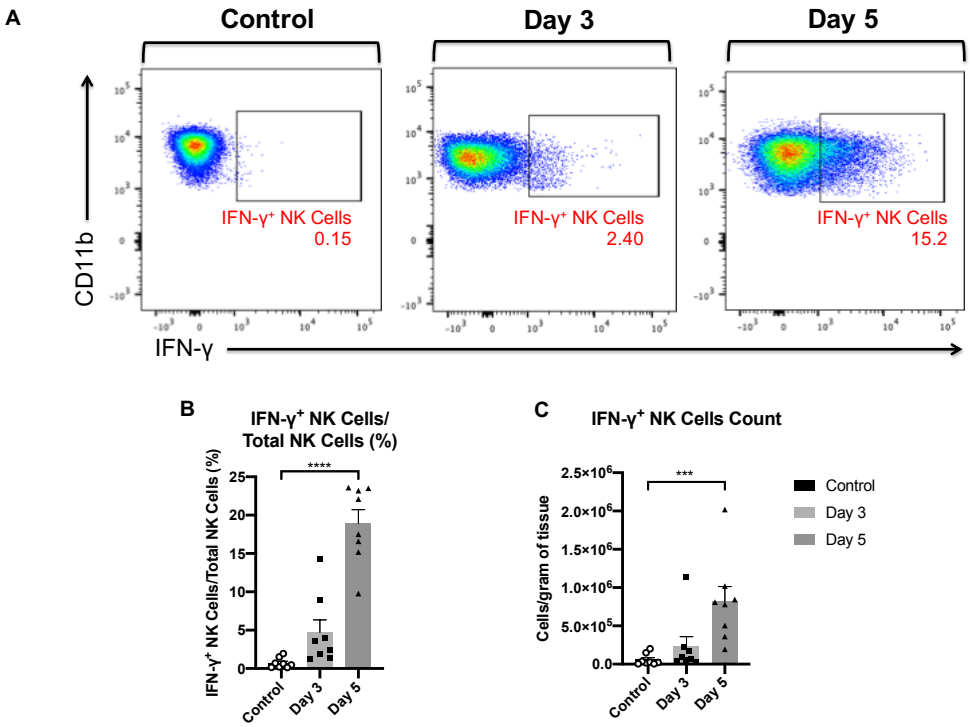


**Figure 5.8 - NK Cells display enhanced IFN-γ production during infection with *F. tularensis* LVS**

C57BL/6 mice were infected with 1000 CFU *F. tularensis* LVS and NK cells identified in the lung at different time points p.i. Control mice were given PBS. Single cell suspensions were incubated for 4 hours at 37°C with a cocktail of PMA, ionomycin, brefeldin A and monensin. **(A)** Representative plots for identification of IFN-γ production in NK Cells (CD11b$^+$NK1.1$^+$T-bet$^+$) in PBS (control) and LVS-infected mice at days 3 (D3) and 5 (D5) p.i.. **(B-C)** NK Cell production of IFN-γ was quantified and expressed as a frequency of total NK Cells, and cell counts per gram of tissue (n=7 for control, n=8 for day 3 and 5 p.i.). Numbers in FACS plots represent the percentage of IFN-γ$^+$ NK cells from total NK cells. Statistical analysis was performed using either one-way ANOVA for parametric data, or Kruskal Wallis for non-parametric data, with Holm-Sidak's and Dunn's multiple comparisons tests performed for each method of analysis respectively; ** p<0.01; *** p<0.001.

### 5.2.6 IFN-γ in the infected lung environment appears important in driving infection-induced reduction in ILC2 numbers

IFN-γ has previously been shown to inhibit ILC2 function and induce cell death (Molofsky *et al.*, 2015; Duerr *et al.*, 2016). Moreover, as data in this thesis chapter (figures 5.6 and 5.8) and in previous studies (Lopez *et al.*,

2004; De Pascalis, Taylor and Elkins, 2008) have identified multiple sources of this cytokine during infection with *F. tularensis* LVS, it was next considered whether IFN-γ was important in the control of ILC2 numbers in this context. Thus, in order to further investigate this relationship, an *ex vivo* ILC2 culture system was established. Here, ILC2s were cultured with either naïve or LVS-infected cell-free lung supernatant, with the impact of IFN-γ in this context determined by functional blockade of this cytokine (figure 5.9).

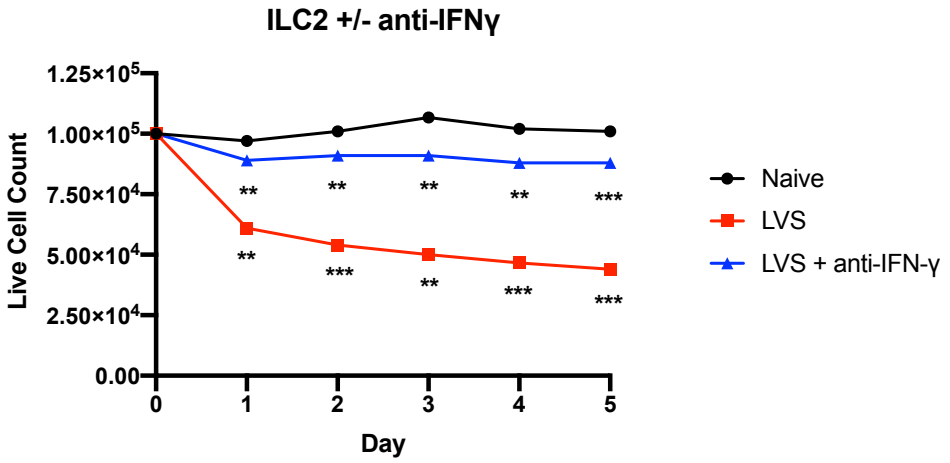


**Figure 5.9 - *In vitro* culture of sort-purified lung ILC2s with cell-free lung supernatants**

$1x10^5$ FACS-sorted live $CD45^+Lin^-CD90.2^{mid-hi}CD127^+KLRG1^+$ lung ILC2s were allowed to rest for 7 days in media with IL-7 (25 ng/ml), before culturing with either naïve or *F. tularensis* LVS-infected cell-free lung supernatant. ILC2s cultured with *F. tularensis* LVS-infected supernatant were cultured in the presence, or absence of an anti-IFN-γ antibody (10 μg/ml). Data are representative of two independent experiments with cells pooled from 4 mice in each. Statistical analysis was performed using repeated-measures one-way ANOVA, with Holm-Sidak's multiple comparisons tests. Significance is shown as LVS-infected versus naïve (below red line), and LVS-infected + anti-IFN-γ versus LVS-infected (below blue line); ** $p<0.01$; *** $p<0.001$.

The number of live ILC2s was significantly decreased in LVS-infected supernatant cultures, suggesting that a soluble mediator is important in driving the infection-induced reduction in ILC2 numbers (figure 5.9). Upon blockade of IFN-γ in these infected lung supernatant cultures, the total number of live ILC2s was significantly enhanced (figure 5.9). Thus, these results suggest that the presence of IFN-γ in *F. tularensis* LVS supernatants could contribute to the reduction in ILC2s in this *in vitro* model.

### 5.2.7 Anti-NK1.1-mediated depletion of NK cells does not rescue ILC2 numbers

Whilst it has been previously mentioned that there are multiple sources of IFN-γ during infection with *F. tularensis* LVS (Lopez *et al.*, 2004; De Pascalis, Taylor and Elkins, 2008), NK cells represent the major source (Lopez *et al.*, 2004; Schmitt *et al.*, 2013). Thus, given that IFN-γ from the LVS-infected lung can reduce ILC2 numbers *in vitro*, it was next investigated whether NK cells are required to reduce ILC2 numbers *in vivo*. In order to test this, NK cells were depleted using an anti-NK1.1 antibody, to determine whether ILC2 numbers are reduced in their absence.

Initially, depletion was confirmed via flow cytometric analysis (figure 5.10A), with anti-NK1.1 antibody-treated mice displaying a significant reduction in total NK cells and IFN-γ-producing NK cells both in frequency (figure 5.10B and C) and total cell numbers (figure 5.10D and E). Next, the NK cell absence on ILC2 numbers was assessed. Whilst the frequency of ILC2s was significantly reduced during infection in IgG-treated mice, NK cell depletion had no effect upon the frequency of ILC2s (figure 5.10F) or total ILC2 numbers (figure 5.10G). Interestingly, whilst NK cell depletion had no effect on bacterial burdens in the lung or spleen, liver burdens were significantly elevated in NK1.1-treated mice (figure 5.10H). Overall, this indicates that NK cell depletion does not impact on ILC2 numbers, or control of infection in the lung of WT mice.

Another cell type that can produce IFN-γ during infection with *F. tularensis* LVS is the T cell (Roberts, Powell and Frelinger, 2018). Thus, it was next important to assess whether T cell-derived IFN-γ could be compensating for the absence of NK-derived IFN-γ and thus potentiating the ILC2 crash. Indeed, a $CD3^{+}CD5^{+}IFN\text{-}\gamma^{+}$ cell population was identified (figure 5.11A), which showed enhanced IFN-γ production in the absence of NK cells (figure 5.11B-C). As a result, this suggests that the presence of an alternative source of IFN-γ may be sufficient to reduce ILC2 numbers during infection with *F. tularensis* LVS in the absence of NK cells.

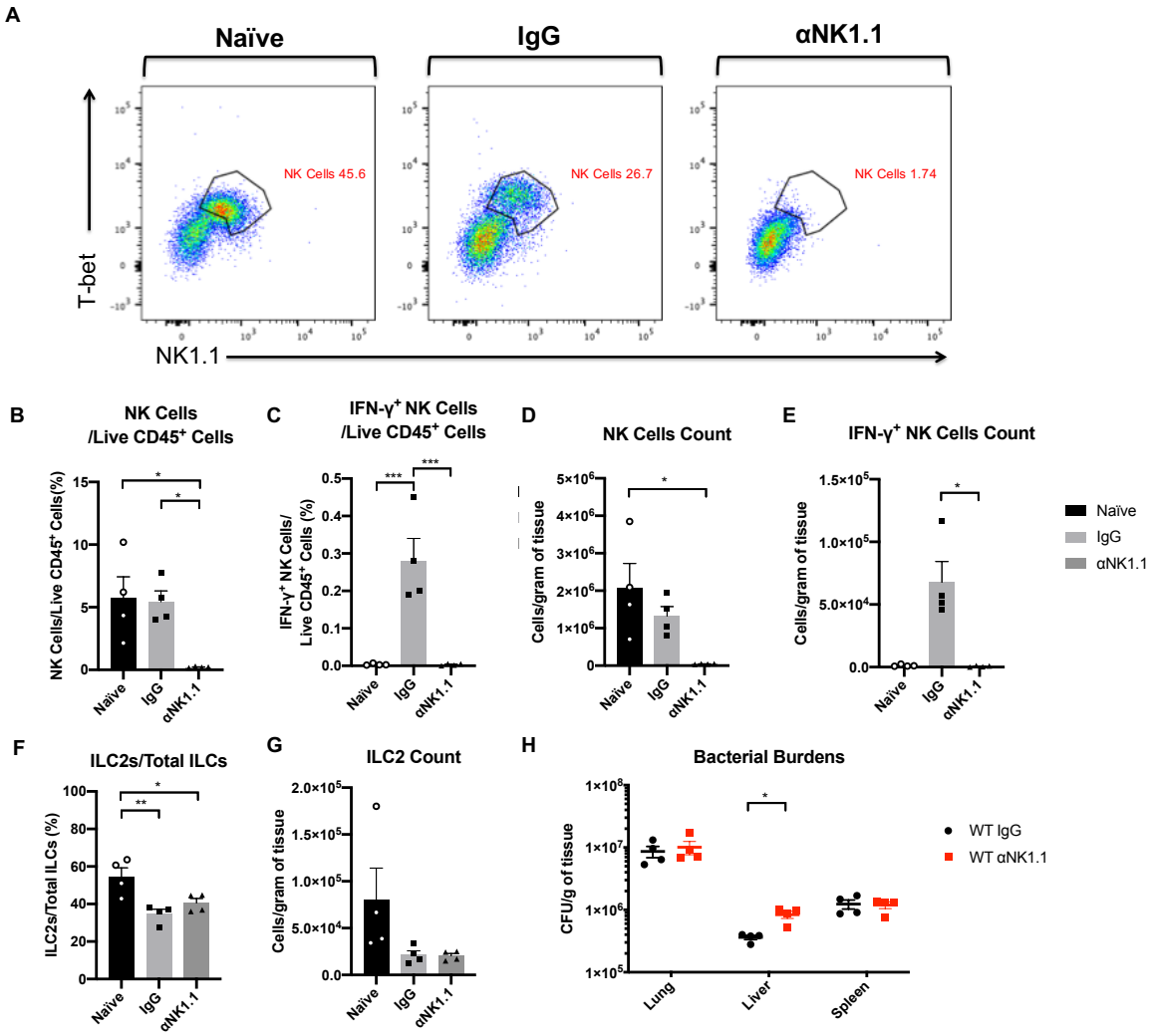


**Figure 5.10 - Anti-NK1.1-mediated NK cell depletion does not alter ILC2 numbers in C57BL/6 mice during infection with *F. tularensis* LVS**

C57BL/6 mice were infected with 1000 CFU *F. tularensis* LVS, and treated with 3 doses of anti-NK1.1 or IgG control (200 µg/mouse) every 2 days starting 1 day before infection with *F. tularensis* LVS. Flow cytometry analysis performed in the lung at day 7 p.i. following incubation of single cell suspensions for 4 hours at 37ºC with a cocktail of PMA, ionomycin, brefeldin A and monensin. **(A)** Representative plots for identification of NK cells (live $CD45^+CD3^-CD5^-CD11b^+NK1.1^+T\text{-}bet^+$). **(B-C)** Total NK, **(D-E)** IFN-$\gamma^+$ NK cells and **(F-G)** ILC2s (live $CD45^+Lin^-CD90^+ST2^+$) were quantified and expressed as a frequency of live $CD45^+$ cells, or total ILCs and cell counts per gram of tissue. **(H)** Bacterial burdens (CFU/g of organ) enumerated in the lung, liver and spleen of mice at day 7 p.i. (n=4 for all cell populations). Numbers in FACS plots represent NK cells as a % of live $CD45^+CD3^-CD5^-CD11b^+$ cells. Statistical analysis was performed using either unpaired t-test or one-way ANOVA for parametric data, or Mann-Whitney test or Kruskal Wallis for non-parametric data, with appropriate multiple comparisons tests performed for each method of analysis respectively; * $p<0.05$; ** $p<0.01$; *** $p<0.001$.

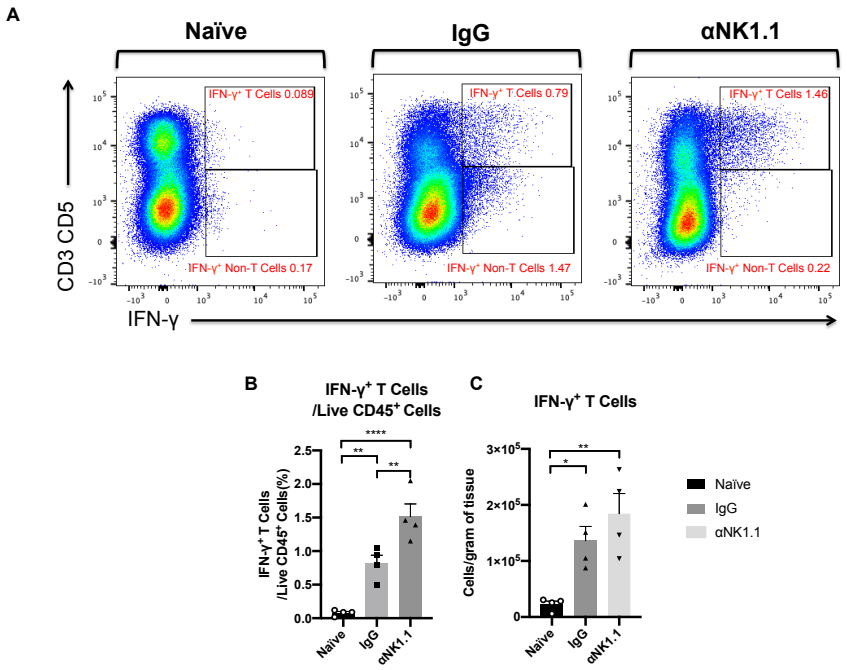


**Figure 5.11 - T cell-derived IFN-γ compensates for the loss of NK-derived IFN-γ in C57BL/6 mice during infection with *F. tularensis* LVS**

C57BL/6 mice were infected with 1000 CFU *F. tularensis* LVS, and treated as previously indicated, with flow cytometry analysis performed at day 7 p.i. Single cell suspensions were incubated for 4 hours at 37°C with a cocktail of PMA, ionomycin, brefeldin A and monensin. **(A)** Representative plots for identification of IFN-γ-producing cells (previously identified as live CD45$^+$ cells) in the lung of mice. **(B-C)** Total IFN-γ$^+$ T Cells (live CD45$^+$CD3$^+$CD5$^+$) were quantified and expressed as a frequency of live CD45$^+$ cells, and cell counts per gram of tissue (n=4 for all cell populations). Statistical analysis was performed using either one-way ANOVA for parametric data, or Kruskal Wallis for non-parametric data, with appropriate multiple comparisons tests performed for each method of analysis respectively; * p<0.05; ** p<0.01; **** p<0.0001.

### 5.2.8 Anti-NK1.1-mediated depletion of NK cells does not rescue ILC2 numbers in Rag1$^{-/-}$ mice

In order to exclude the potential role of T-cell-derived IFN-γ impacting upon ILC2s during LVS infection in the absence of NK cells, Rag1$^{-/-}$ mice (which lack adaptive immunity) were used in a subsequent experiment. Here, the compensatory T cell-derived IFN-γ response seen in WT mice would be eliminated, and the effect of the absence of NK cells on ILC2 numbers fully assessed. Akin to WT mice, anti-NK1.1-mediated depletion of NK cells in Rag1$^{-/-}$ mice resulted in a significantly reduced number of NK cells when compared to both IgG-treated LVS-infected mice and naïve controls (figure 5.12A-C) – as well as a significant reduction in the number of IFN-γ-producing NK cells (figure 5.12D and E).

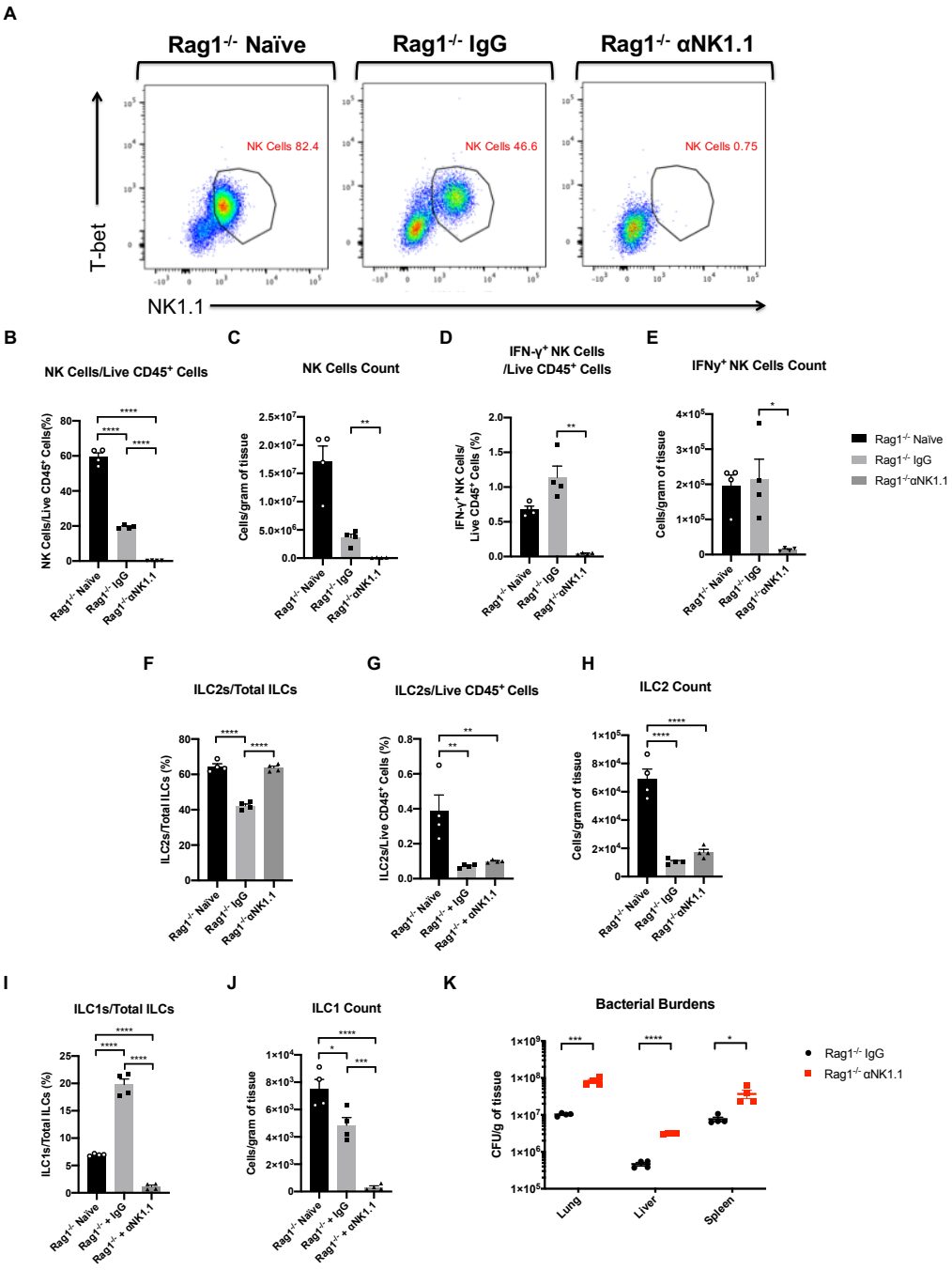


**Figure 5.12 - Anti-NK1.1-mediated depletion of NK cells in Rag1$^{-/-}$ mice does not rescue ILC2 numbers during infection with *F. tularensis* LVS**

Rag1$^{-/-}$ mice were infected with 1000 CFU *F. tularensis* LVS, with mice treated as previously indicated in figure 5.10. Naïve controls were uninfected and untreated. Flow cytometry analysis was performed in the lung at day 5 p.i. following incubation of single cell suspensions for 4 hours at 37°C with a cocktail of PMA, ionomycin, brefeldin A and monensin. **(A)** Representative plots for identification of NK cells (live CD45$^+$CD3$^-$CD5$^-$CD11b$^+$NK1.1$^+$T-bet$^+$) in the lung of mice. **(B-C)** Total NK Cells, **(D-E)** NK Cell-derived production of IFN-γ, **(F-H)** ILC2s (live CD45$^+$Lin$^-$CD90$^+$CD127$^+$ST2$^+$) and **(I-J)** ILC1s (live CD45$^+$Lin$^-$CD90$^+$CD127$^+$T-bet$^+$) were quantified and expressed as a frequency of live CD45$^+$ cells or total ILCs, and cell counts per gram of tissue. **(K)** Bacterial burdens (CFU/g of organ) were enumerated in the lung, liver and spleen of mice at day 5 p.i. for all mice (n=4 for all cell populations). Numbers in FACS plots represent NK cells as a % of live CD45$^+$CD3$^-$CD5$^-$CD11b$^+$ cells. Statistical analysis was performed using either one-way ANOVA for parametric data, or Kruskal Wallis for non-parametric data, with appropriate multiple comparisons tests performed for each method of analysis respectively; * p<0.05; ** p<0.01; *** p<0.001; **** p<0.0001.

Interestingly, when expressed as a frequency of total ILCs, ILC2s were increased in anti-NK1.1-treated LVS-infected Rag1$^{-/-}$ mice when compared to IgG-treated LVS-infected Rag1$^{-/-}$ mice at day 5 p.i. (figure 5.12F). Despite this, both ILC2s as a frequency of live CD45$^{+}$ cells and total ILC2 numbers were similarly decreased in both infected Rag1$^{-/-}$ mice groups when compared to naïve Rag1$^{-/-}$ controls (figure 5.12G-H). As aforementioned, ILC1s also express NK1.1 (Jiao *et al.*, 2016). Thus, both the frequency (figure 5.12I) and total number (figure 5.12J) of ILC1s were also significantly reduced in anti-NK1.1-treated Rag1$^{-/-}$ mice. Overall, these results indicate that NK- and T-cell-derived IFN-γ may not impact on ILC2s during infection with *F. tularensis* LVS. Moreover, they suggest that the enhanced ILC2s when expressed as a frequency of total ILCs in anti-NK1.1-treated mice may only be due to the depletion of ILC1s in these mice.

Nevertheless, as depletion of NK cells and ILC1 is indicative of a reduction in IFN-γ levels in the lung which cannot be compensated for by T cells in Rag1$^{-/-}$ mice, it was also important to assess how this depletion impacted upon the control of infection in the absence of adaptive immunity. Unlike WT mice, NK-depleted Rag1$^{-/-}$ mice exhibited an exacerbated phenotype, with anti-NK1.1-treated Rag1$^{-/-}$ mice displaying significantly elevated bacterial burdens in the lung, liver and spleen when compared to IgG-treated Rag1$^{-/-}$ mice (figure 5.12K). Indeed, as this was associated with enhanced morbidity, mice were required to be culled at day 5 p.i. due to licence restrictions. Overall, these data demonstrate the importance of NK-derived IFN-γ in the control of infection with *F. tularensis* LVS, with this exacerbated phenotype in anti-NK1.1-treated Rag1$^{-/-}$ mice also highlighting a potential caveat in interpreting whether ILC2 numbers are reduced by NK- and T cell-derived IFN-γ.

### 5.2.9 Blockade of IFN-γ in NK-ILC2 co-cultures does not reduce ILC2 numbers *in vitro*

As the lung tissue environment is complex, multiple inflammatory signals aside from IFN-γ could contribute to the reduction in ILC2s during infection with *F. tularensis* LVS (Cowley and Elkins, 2011; Molofsky *et al.*, 2015; Duerr *et al.*, 2016). Nevertheless, as the previous *in vitro* data presented in this chapter indicated a role for IFN-γ in reducing ILC2 numbers, it remained

important to investigate whether NK cells could reduce ILC2 numbers in an *in vitro* setting. As a result, an *in vitro* co-culture system was developed where sort-purified ILC2s were cultured alone, or alongside sort-purified lung NK cells from either naïve or LVS-infected mice, in the presence or absence of anti-IFN-γ antibody. Cells were cultured in a 1:1 ratio for 72 hours, with ILC2 cell death assessed at 24, 48 and 72 hour time points. Whilst no differences were seen in the frequency of total live ILC2s cultured alone or with NK cells from naïve mice at any time point (figure 5.13A-D), live ILC2s were significantly reduced when co-cultured with NK cells from LVS-infected mice (figure 5.13A-D). Interestingly however, blockade of IFN-γ did not reverse this reduction (figure 5.13A-D). Thus, although NK cells from infected mice reduced ILC2 cell counts *in vitro*, blocking IFN-γ was not sufficient to reverse this effect.

Irrespective of the inhibition of IFN-γ, the frequency of apoptotic ILC2s was increased at 24 hours when cultured with NK cells from LVS-infected mice versus ILC2s cultured alone (figure 5.13E). Whilst no differences were observed in apoptotic ILC2s at 48 hours (figure 5.13F), apoptotic ILC2s were increased at 72 hours when cultured with NK cells from either PBS control mice, or those cultured with NK cells from LVS-infected mice with anti-IFN-γ antibody present in the media (figure 5.13G). Thus, this suggests that ILC2s cultured with NK cells may exhibit higher levels of apoptotic cell death *in vitro*. Interestingly, the frequency of necrotic ILC2s was only significantly enhanced at 48 hours, and only when ILC2s were cultured with NK cells from LVS-infected mice (figure 5.13H-J). The frequency of dead ILC2s was unaltered throughout the time course (figure 5.13K-M). Overall, these data indicate that multiple mechanisms of cell death are induced in ILC2s cultured with NK cells, irrespective of the inhibition of IFN-γ.

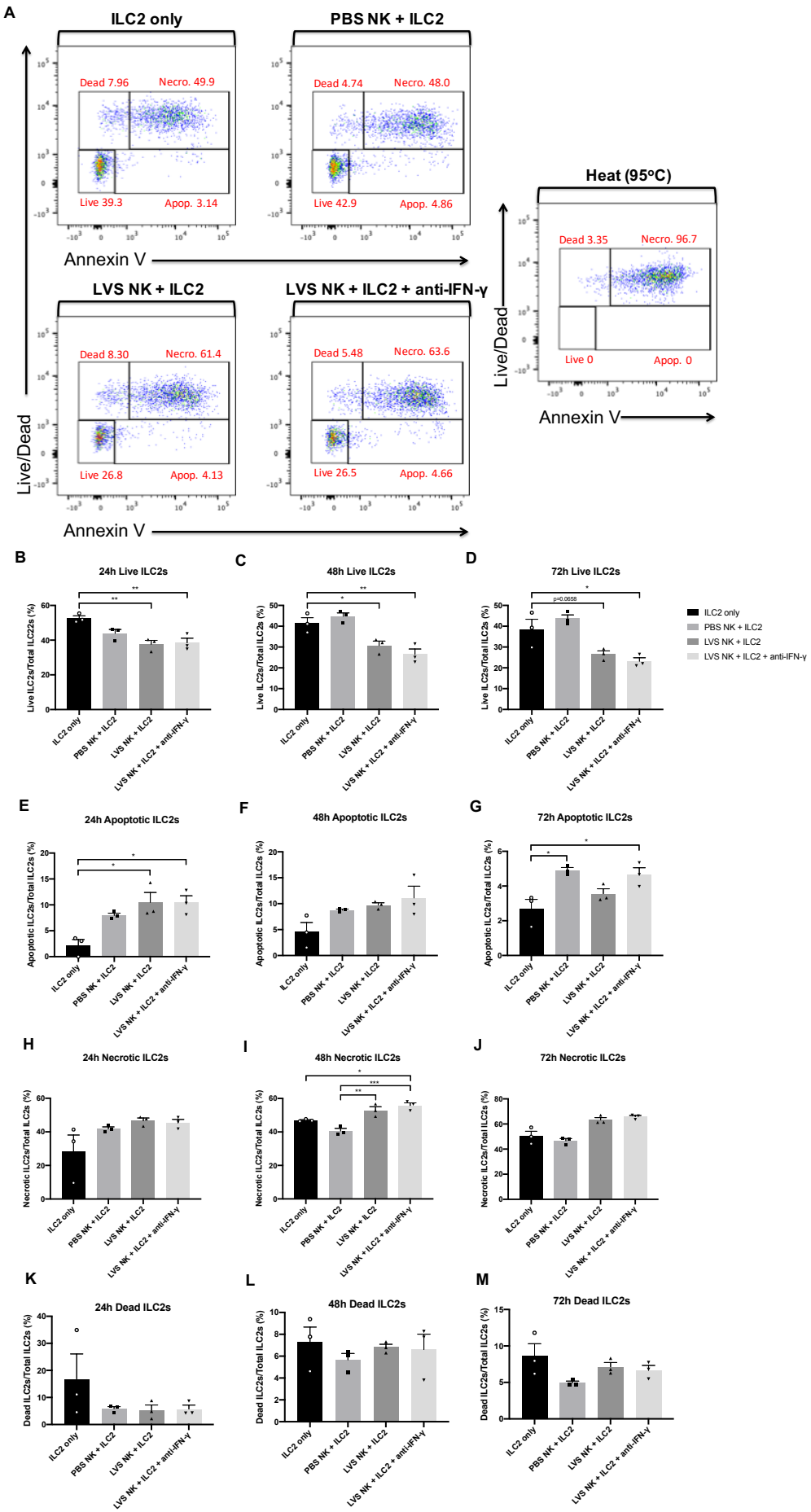
A
ILC2 only
Dead 7.96
Necro. 49.9
Live 39.3
Apop. 3.14
PBS NK + ILC2
Dead 4.74
Necro. 48.0
Live 42.9
Apop. 4.86
Annexin V
LVS NK + ILC2
Dead 8.30
Necro. 61.4
Live 26.8
Apop. 4.13
LVS NK + ILC2 + anti-IFN-γ
Dead 5.48
Necro. 63.6
Live 26.5
Apop. 4.66
Live/Dead
Annexin V
Heat (95°C)
Dead 3.35
Necro. 96.7
Live 0
Apop. 0
Live/Dead
Annexin V
B
24h Live ILC2s
Live ILC2s/Total ILC2s (%)
C
48h Live ILC2s
Live ILC2s/Total ILC2s (%)
D
72h Live ILC2s
Live ILC2s/Total ILC2s (%)
ILC2 only
PBS NK + ILC2
LVS NK + ILC2
LVS NK + ILC2 + anti-IFN-γ
E
24h Apoptotic ILC2s
Apoptotic ILC2s/Total ILC2s (%)
F
48h Apoptotic ILC2s
Apoptotic ILC2s/Total ILC2s (%)
G
72h Apoptotic ILC2s
Apoptotic ILC2s/Total ILC2s (%)
H
24h Necrotic ILC2s
Necrotic ILC2s/Total ILC2s (%)
I
48h Necrotic ILC2s
Necrotic ILC2s/Total ILC2s (%)
J
72h Necrotic ILC2s
Necrotic ILC2s/Total ILC2s (%)
K
24h Dead ILC2s
Dead ILC2s/Total ILC2s (%)
L
48h Dead ILC2s
Dead ILC2s/Total ILC2s (%)
M
72h Dead ILC2s
Dead ILC2s/Total ILC2s (%)

### 5.2.10 Treatment with diphtheria toxin results in significantly enhanced bacterial burdens during infection with *F. tularensis* LVS, with this effect attenuated upon depletion of ILC2s

Finally, as chapter 4 of this thesis demonstrated that ILC2s play a detrimental role in the control of infection, it was important to investigate the effect of their specific ablation on the progress of infection. To this end, the ICOS-diphtheria toxin receptor (ICOS-T) mouse model was used (5.14A). As ILC2s express ICOS, this model allows for their specific depletion in mice treated with diphtheria toxin (DTx) (Oliphant *et al.*, 2014). Furthermore, as ICOS is also expressed on $CD4^+$ T cells, the insertion of a floxed DTx receptor (DTR) gene into the *Icos* locus allows for the CD4-cre-mediated excision of this gene i.e. the DTR gene is removed from $CD4^+$ T cells, and as a result does not result in their depletion upon DTx treatment.

Indeed, this was confirmed by flow cytometric analysis, with a significant reduction in the frequency (figure 5.14B) and total number (figure 5.14C) of ILC2s in DTx-treated ICOS-T mice when compared to both WT DTx-treated and WT untreated mice at day 3 p.i.. Unexpectedly, ILC2s were also significantly reduced in DTx-treated littermate controls (herein referred to as WT in this study) mice when compared to untreated infected WT mice, although not to the same extent as in ICOS-T mice (figure 5.14B-C). In total, DTx-treated ICOS-T mice showed an 87% reduction in ILC2 numbers when compared to WT untreated mice, and an 80% reduction when compared to DTx-treated WT mice (figure 5.14C).

**Figure 5.13 - Assessment of ILC2 apoptosis during *in vitro* co-culture of sort-purified lung ILC2s and NK cells**

FACS-sorted lung ILC2s (live $CD45^+Lin^-CD127^+KLRG1^+$) were allowed to rest for 7 days in media with IL-7, before culturing with FACS-sorted NK cells (live $CD45^+CD3^-CD5^-CD11b^+NK1.1^+$) from naïve or LVS-infected lungs (day 5 p.i.) in a 1:1 ratio, and ILC2 cell death was subsequently assessed using the Annexin V apoptosis assay. Where indicated, cells were also cultured in the presence of an anti-IFN-γ antibody (10 µg/ml). **(A)** Representative plots from 48 hours post-culture for ILC2 (live $CD45^+CD11b^-CD127^+ST2^+$) cell death when cultured alone, with NK cells (live $CD45^+CD11b^+$) from naïve (PBS) lung, or NK cells from LVS-infected lung. Apop. = apoptotic; Necro. = Necrotic. **(B-D)** Live ILC2s were quantified and expressed as a frequency of total ILC2s at 24, 48, and 72 hour time points. Numbers in FACS plots represent the proportion of live, apop., necro. and dead ILC2s as a % of total ILC2s. Statistical analysis was performed using either one-way ANOVA for parametric data, or Kruskal Wallis for non-parametric data, with appropriate multiple comparisons tests performed for each method of analysis respectively; * $p<0.05$; ** $p<0.01$.

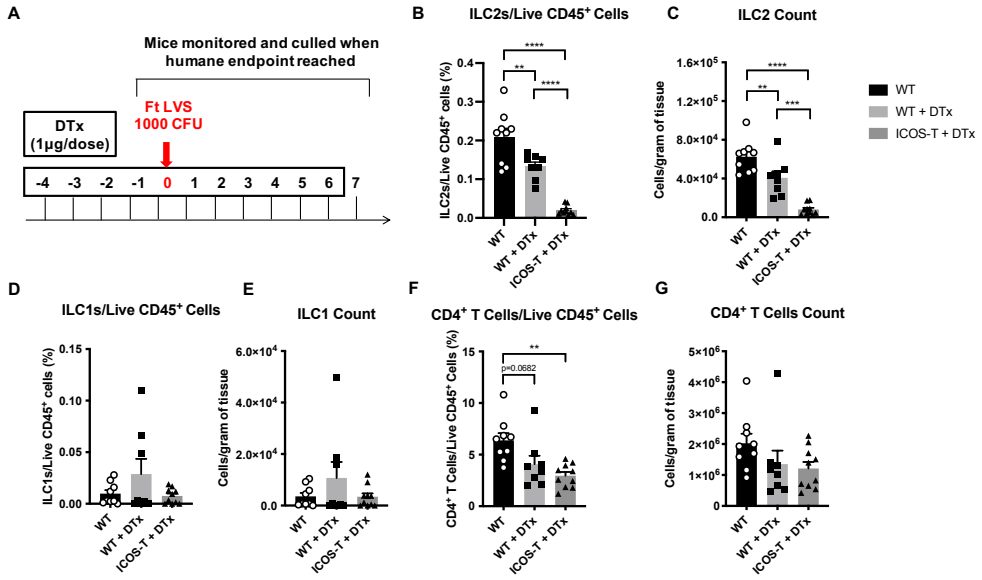


**Figure 5.14 - Diphtheria toxin (DTx)-mediated depletion of ILC2 cells in ICOS-T mice during infection with *F. tularensis* LVS**

WT and ICOS-T mice were treated with Diphtheria toxin (DTx) daily at 1 µg/dose where indicated, and subsequently infected with 1000 CFU *F. tularensis* LVS, with flow cytometry analysis of lung cells performed at day 3 p.i. **(A)** Mice were treated as indicated. **(B-C)** ILC2s (live $CD45^+Lin^-CD90^+CD127^+ST2^+$), **(D-E)** ILC1s (live $CD45^+Lin^-CD90^+CD127^+T\text{-}bet^+$) and **(F-G)** $CD4^+$ T cells (live $CD45^+CD3^+CD5^+$) were quantified and expressed as a frequency of live $CD45^+$ cells and cell counts per gram of tissue (n=8-10). Statistical analysis was performed using either one-way ANOVA for parametric data, or Kruskal Wallis for non-parametric data, with appropriate multiple comparisons tests performed for each method of analysis respectively; ** $p<0.01$; *** $p<0.001$; **** $p<0.0001$.

Moreover, frequency and total numbers of ILC1s were unaffected by DTx treatment (figure 5.14D-E), and although a significant reduction in frequency of $CD4^+$ T cells was observed in DTx-treated WT and ICOS-T mice when compared to untreated WT mice (figure 5.14F), no differences were observed between DTx-treated WT mice and DTx-treated ICOS-T mice in $CD4^+$ T cell frequency (figure 5.14F) and no difference in $CD4^+$ T cell numbers observed between any groups (figure 5.14G). Overall, these results suggest that whilst some DTx-mediated effects were apparent, ILC2s can be selectively depleted using the ICOS-T mouse model during infection with *F. tularensis* LVS.

Next, to investigate the impact of ILC2 depletion on the progression of infection, mice were monitored and bacterial burdens enumerated. Unexpectedly, treatment with DTx in both WT mice infected with *F. tularensis* LVS resulted in significantly enhanced weight loss (figure 5.15A) and

mortality (figure 5.15B), with mice required to be culled at day 3 p.i. due to licence restrictions.

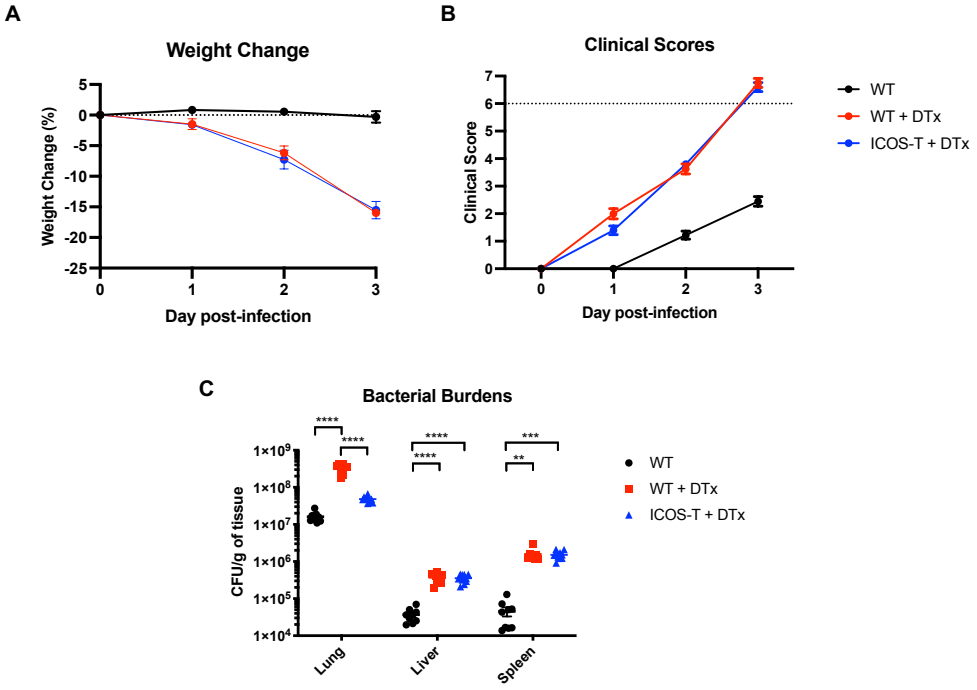


**Figure 5.15 - DTx enhances bacterial burdens in WT mice during infection with *F. tularensis* LVS**

Progression of infection in WT and ICOS-T mice during infection with *F. tularensis* LVS. Where indicated, mice were treated with Diphtheria toxin (DTx) daily at 1 µg/dose. **(A)** Weight change was monitored daily in all mice, and plotted as a percentage loss of original body weight (0% = body weight at day 0). **(B)** Severity of infection was evaluated using a clinical scoring system (see methods). **(C)** Bacterial burdens (CFU/g of organ) were enumerated in the lung, liver and spleen of mice at day 3 p.i. (n=8-10). Statistical analysis was performed using either one-way ANOVA for parametric data, or Kruskal Wallis for non-parametric data, with appropriate multiple comparisons tests performed for each method of analysis respectively; ** $p<0.01$; *** $p<0.001$; **** $p<0.0001$.

Interestingly, whilst, bacterial burdens were significantly enhanced in the liver and spleen of both infected WT and ICOS-T mice treated with DTx, only DTx-treated WT mice displayed a significant exacerbation of infection in the lung (figure 5.15C). Indeed, lung burdens in DTx-treated ICOS-T mice were significantly reduced down to a similar level to that of untreated WT mice (figure 5.15C). Together, these results indicate that whilst treatment with DTx is detrimental to the control of infection with *F. tularensis* LVS, selective depletion of ILC2s appears to benefit the host immune response in this context.

### 5.2.11 The myeloid immune response is significantly altered following DTx treatment

In order to understand how DTx treatment and the ablation of ILC2s impacts upon the host immune response and control of infection with *F. tularensis* LVS, it was next important to assess the myeloid immune compartment in this model. Both the frequency (figure 5.16A) and total number of neutrophils (figure 5.16B) were significantly enhanced in DTx-treated WT and ICOS-T mice following infection with *F. tularensis* LVS when compared to infected WT mice not treated with DTx. Whilst the frequency of $CD64^+$ macrophages was significantly reduced in ICOS-T mice (figure 5.16C), total cell numbers showed no differences between groups (figure 5.16D). Interestingly, eosinophils were significantly reduced in both WT and ICOS-T mice following DTx treatment both as a frequency of live $CD45^+$ cells (figure 5.16E) and total numbers (figure 5.16F). Overall, these results indicate that DTx treatment, regardless of whether ILC2s are depleted or not, induces significant changes to the myeloid immune compartment in the lung during infection with *F. tularensis* LVS.

To determine whether the enhanced bacterial burdens observed following DTx treatment were due to enhanced levels of intracellular infection, levels of infection were quantified in myeloid cell types. Both DTx-treated WT and ICOS-T mice displayed enhanced levels of infection in neutrophils (figure 5.17A-B), macrophages (figure 5.17C-D) and eosinophils (figure 5.17E-F). Thus, these results suggest that the enhanced bacterial burdens observed in DTx-treated mice during infection with *F. tularensis* LVS may arise as a result of enhanced intracellular infection in multiple types of myeloid cell.

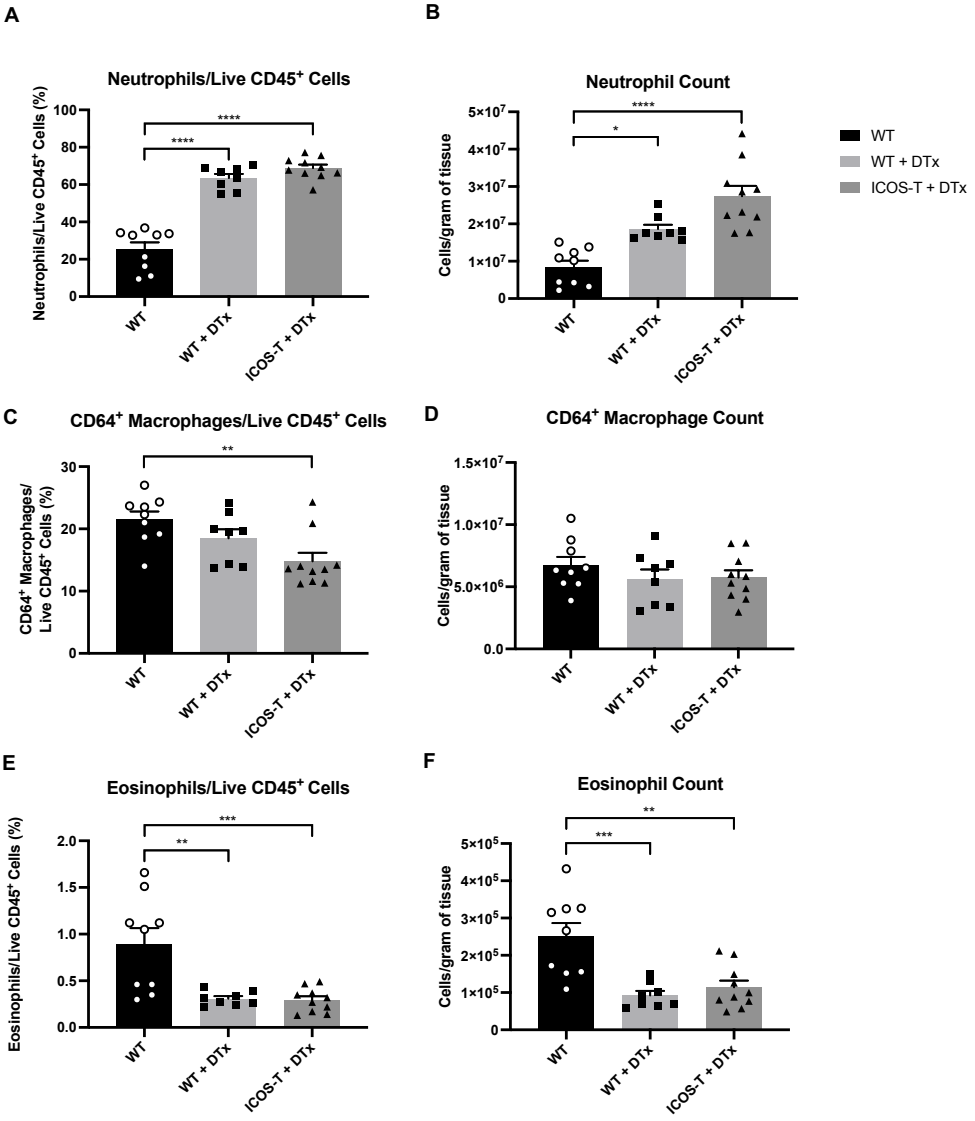


**Figure 5.16 - Effect of DTx administration on the myeloid compartment during infection with *F. tularensis* LVS**

Myeloid cell populations were identified by flow cytometry analysis in the lung of WT and ICOS-T mice at day 3 p.i. **(A-B)** neutrophil (live $CD45^+Ly6G^+$), **(C-D)** $CD64^+$ macrophage (live $CD45^+Ly6G^-Siglec\text{-}F^-CD64^+$) and **(E-F)** eosinophil (live $CD45^+Ly6G^-Siglec\text{-}F^+CD64^-$) populations were identified and expressed as a frequency of live $CD45^+$ cells and cell counts per gram of tissue (n=8-10). Statistical analysis was performed with either one-way ANOVA for parametric data, or Kruskal Wallis for non-parametric data, with Holm-Sidak's and Dunn's multiple comparisons tests performed for each method of analysis respectively; * $p<0.05$; ** $p<0.01$; *** $p<0.001$; **** $p<0.0001$.

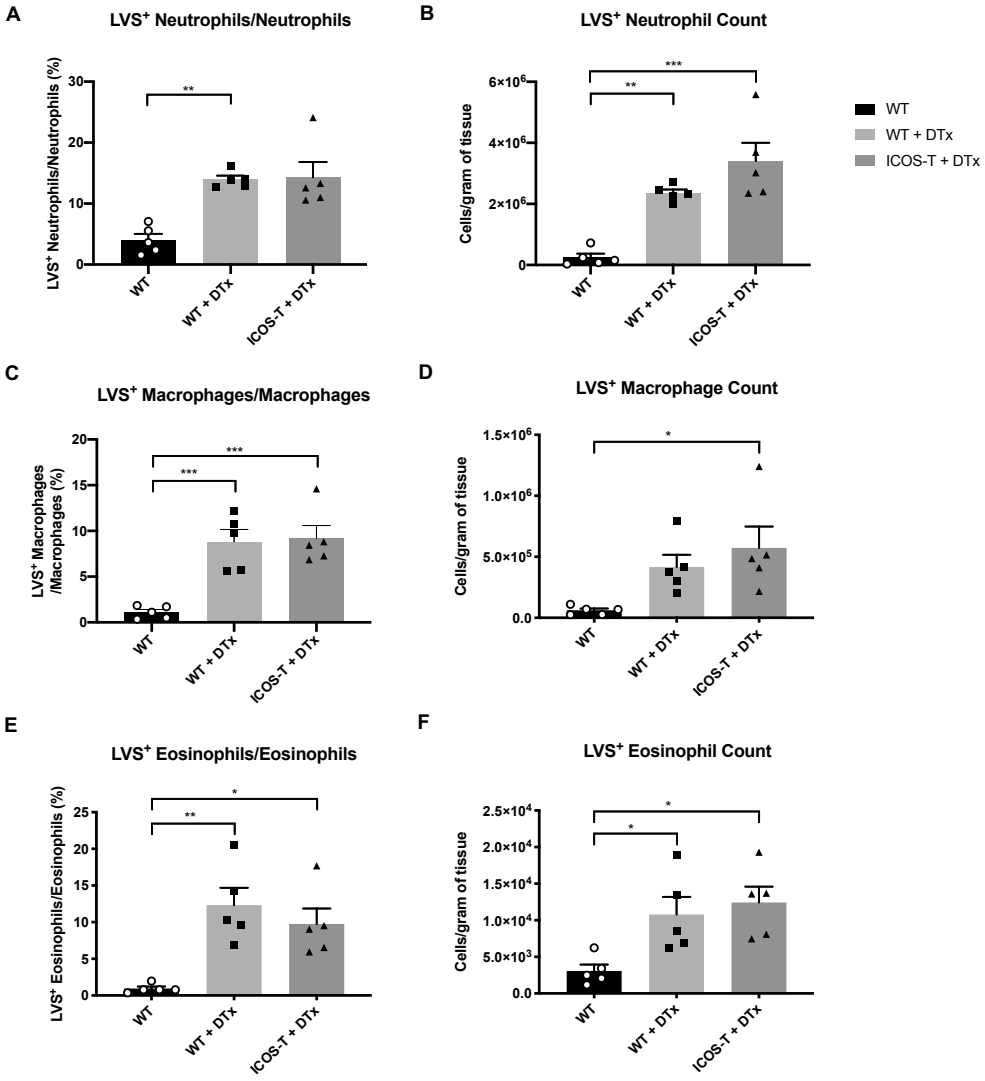


**Figure 5.17 - DTx enhances levels of infection in multiple myeloid cell populations during infection with *F. tularensis* LVS**

$LVS^+$ myeloid cell populations were identified in the lung by flow cytometry analysis in WT and ICOS-T mice at day 3 p.i. **(A-B)** $LVS^+$ neutrophil (live $CD45^+Ly6G^+$) and **(C-D)** $LVS^+$ $CD64^+$ macrophage (live $CD45^+Ly6G^-Siglec\text{-}F^-CD64^+$) and **(E-F)** $LVS^+$ eosinophil (live $CD45^+Ly6G^-Siglec\text{-}F^+CD64^-$) populations were identified and expressed as a frequency parent populations and cell counts per gram of tissue (n=5). Statistical analysis was performed using either one-way ANOVA for parametric data, or Kruskal Wallis for non-parametric data, with appropriate multiple comparisons tests performed for each method of analysis respectively; * $p<0.05$; ** $p<0.01$; *** $p<0.001$.

## 5.3 Discussion

### 5.3.1 Determining the relative contributions of innate and adaptive lymphocytes during infection with *F. tularensis* LVS

Given the similarities between T cells and ILCs in their effector programs, the Rag1$^{-/-}$, il2rg$^{-/-}$ and Rag1$^{-/-}$il2rg$^{-/-}$ mouse models can be used to dissect the relative importance of innate and adaptive lymphocytes during infection (Bando and Colonna, 2016). Indeed, adaptive immunity is essential for the clearance of multiple other respiratory pathogens such as *Brucella melitensis, Streptococcus pneumoniae* and influenza A, with Rag1$^{-/-}$ mice displaying impaired clearance of these infections (Izadjoo *et al.*, 2000; Blair *et al.*, 2005; Wu *et al.*, 2010). Yet, Rag1$^{-/-}$ mice were no less susceptible to infection with *F. tularensis* LVS, with bacterial burdens akin to those observed in WT mice, suggesting that adaptive immunity is dispensable for the control of primary *Francisella* infection.

Given the inherent lethality of *F. tularensis* LVS, and the fact that mice succumb to the infection within 7 days (Conlan *et al.*, 2002), it is more likely that innate lymphocytes play a greater role in the host immune response against *F. tularensis* LVS than their adaptive counterparts. Indeed, ILCs have previously been shown to be essential in the control of other intracellular and bacterial infections (Vivier *et al.*, 2018). For example, Rag1$^{-/-}$il2rg$^{-/-}$ mice (which lack ILCs and NK cells, as well as adaptive immunity) display reduced protection against *C. difficile* infection – with this protection restored upon adoptive transfer of ILCs (Abt *et al.*, 2015). Moreover, ILC3-derived IL-22 is essential for the control of *Citrobacter rodentium* infection, with ablation of these cells in Rag2$^{-/-}$il2rg$^{-/-}$ mice resulting in significantly reduced levels of IL-22 and reduced survival when compared to Rag2$^{-/-}$ mice (Satoh-Takayama *et al.*, 2008). Indeed, faecal bacterial CFU counts are unchanged in mice lacking adaptive immunity, and are only elevated in those that lack the capacity to produce IL-22 in all RORγt-expressing cells – a phenomenon that can be rescued upon transfer of ILC3s into these mice (Guo *et al.*, 2014). In line with this, results in this thesis also demonstrate the importance of innate lymphocytes in the control of infection with *F. tularensis* LVS, with exacerbated bacterial burdens and enhanced mortality in both il2rg$^{-/-}$ and Rag1$^{-/-}$il2rg$^{-/-}$ mice during infection. Nevertheless, it is currently unclear

whether a loss of ILCs, NK cells, or both causes the exacerbated phenotype observed in il2rg$^{-/-}$ and Rag1$^{-/-}$il2rg$^{-/-}$ mice during infection with *F. tularensis* LVS, and requires further investigation - with ways in which this can be achieved being considered throughout this chapter's discussion.

It is well known that NK cells represent a major source of IFN-γ during infection with *F. tularensis* LVS (Lopez *et al.*, 2004; Schmitt *et al.*, 2013). Now, this thesis chapter has begun to uncover the importance of this effector function. Specifically, as the work in Rag1$^{-/-}$ mice demonstrated that adaptive immunity appears dispensable for the control of infection, the enhanced mortality and exacerbated bacterial burdens in Rag1$^{-/-}$ NK1.1-deficient mice highlights the potential importance of NK-derived IFN-γ in the control of infection with *F. tularensis* LVS. However, it is important to recognize that ILC1s also express NK1.1 (Jiao *et al.*, 2016), and were also depleted alongside NK cells in the experiments involving anti-NK1.1 treatment of mice in this thesis chapter. Indeed, as the expanded ILC1 population during the later stages of infection demonstrate significant increases in their IFN-γ output, it is currently unclear how much each of these cell types contributes to the control of infection with *F. tularensis* LVS. It may be possible to consider their relative importance in the liver, where ILC1s and NK cells represent the dominant innate lymphocyte populations (Sojka *et al.*, 2014). Interestingly, ILC1s may represent a more critical source of innate IFN-γ in the liver of mice during infection with *F. tularensis* LVS. Specifically, whilst depletion of NK cells using an anti-asialo-GM1 antibody results in a significant reduction in tissue IFN-γ levels, bacterial burdens are unaffected (Bokhari *et al.*, 2008). Conversely, research in this thesis chapter demonstrated a significant organ-specific increase in bacterial burdens in the liver of WT anti-NK1.1-treated mice. Thus, as ILC1s would not be depleted by an anti-asialo-GM1 antibody, the disparity in these methods of NK cell depletion may also indirectly highlight the importance of ILC1-derived IFN-γ in the control of *F. tularensis* LVS infection in the liver. It is therefore essential to interrogate the precise roles of ILC1s and NK cells in the future, with a suggested model being the *NK-Eomes*$^{-/-}$ (*Nkp46*$^{Cre}$ *x Eomes*$^{fl/fl}$) mouse, which allows for specific ablation of NK cells, but not ILC1s or CD8$^{+}$ T cells (Weizman *et al.*, 2017). Thus, differences observed between these mice and NK1.1-depleted mice could help to unearth the relative role of NK cells and ILC1s during infection with *F. tularensis* LVS.

### 5.3.2 Considering the impact of innate lymphocytes on myeloid cells during LVS infection

An important area of investigation in this thesis chapter was to determine how the absence of innate and adaptive lymphocytes impacted upon myeloid cell numbers, given that cells such as neutrophils and macrophages serve as important reservoirs for bacterial replication (Hall *et al.*, 2008), and their dysregulation, or enhanced recruitment can result in significantly enhanced bacterial burdens (Casulli *et al.*, 2019). Previously, it has been shown that the spleens of il2rg$^{-/-}$ mice possess a significantly enhanced frequency of macrophages, monocytes and granulocytes (Cao *et al.*, 1995). Despite this, the relative proportions of these cells in the lung tissue are not well studied. Unsurprisingly, data in this thesis chapter also presented a consistently elevated proportion of neutrophils in the lungs of il2rg$^{-/-}$, but also Rag1$^{-/-}$ and Rag1$^{-/-}$il2rg$^{-/-}$ mice. However, this data is perhaps somewhat misleading, considering the elevated proportions of this cell type are likely as a result of ablation of adaptive immunity and ILCs and NK cells in il2rg$^{-/-}$ and Rag1$^{-/-}$ il2rg$^{-/-}$ mice.

Nevertheless, whilst the general composition of the myeloid immune compartment appears to be relatively unaltered, it is still important to consider why some of these cell types exhibit significantly enhanced levels of infection in il2rg$^{-/-}$ and Rag1$^{-/-}$il2rg$^{-/-}$ mice, and whether ablation of innate lymphocytes may contribute to the ability of these myeloid cells to internalise and kill bacteria. Interestingly, NK-derived effector molecules are vital for the control of intracellular replication of *Francisella* in macrophages (Elkins *et al.*, 2009). Specifically, CpG (bacterial) DNA-activated NK cells co-cultured with LVS-infected macrophages exhibit significantly lower levels of bacterial growth than those cultured with either control methylated DNA, or alone (Elkins *et al.*, 2009). Here, control of bacterial growth could be reversed through blockade of IFN-γ, TNF-α, IL-12 or iNOS (Elkins *et al.*, 2009), indicating that these components of NK effector function are critical to controlling intracellular growth of *Francisella* in myeloid cells. Thus, the absence of NK cells in il2rg$^{-/-}$ and Rag1$^{-/-}$il2rg$^{-/-}$ mice may provide an explanation as to why macrophages exhibit enhanced levels of infection in in this context, and consequently contribute to the exacerbated bacterial

burdens observed in these mice. Conversely, the underlying mechanism for this extensive replication in neutrophils remains unclear, although this may also be due to the absence of NK cells, given that IFN-γ can prime neutrophils for more efficient killing (Ellis and Beaman, 2004). The importance of NK-derived IFN-γ in the control of bacterial growth in these myeloid cells could of course be considered through use of an *in vitro* co-culture system similar to that described in Elkins et al. (2009), with either LVS-infected neutrophils or macrophages from these immunodeficient mice co-cultured with activated NK cells from WT mice. However, it is critical that this approach considers the impact of other NK effectors alongside IFN-γ, such as TNF-α and IL-12, as each of these are critical for the control of intramacrophage growth of bacteria at least (Elkins *et al.*, 2009). Overall, this would not only help to uncover what makes these myeloid cells so susceptible to infection with *F. tularensis* LVS, but also further understand the importance of NK-derived IFN-γ to each of these myeloid cell types.

In the context of infection with *F. tularensis* LVS, ILC2s appear to contribute very little in the way of cytokine responses, suggesting that signals that result in the activation of ILC2s are either absent, or present at very low levels, in the lung tissue throughout infection. Of course, the transient increase in IL-5 production observed at day 3 p.i. may indicate a brief period of activation of ILC2s during the initial stages of infection, which may have been missed by the time points considered in this thesis chapter. However, as tissue levels of IL-5 remain low throughout infection (Griffin *et al.*, 2013), it is more likely that this element of ILC2 effector function becomes less important as infection progresses. Interestingly, when taken alongside the overall reduction in ILC2 numbers as infection progresses, this could also help to explain why lung eosinophil numbers are reduced in WT mice, given that ILC2-derived IL-5 maintains the homeostatic function of eosinophils (Nussbaum *et al.*, 2013). Indeed, ILC2s may be key to the function of eosinophils in infection with *F. tularensis* LVS, given a similar reduction in their frequency and numbers is observed in infected il2rg$^{-/-}$ and Rag1$^{-/-}$il2rg$^{-/-}$ mice, where ILC2s are ablated (Bando and Colonna, 2016). Nevertheless, it was interesting to observe that eosinophils display significantly enhanced levels of infection in these immunodeficient mice when compared to WT mice – although this could simply reflect an exacerbated level of bacterial replication as a whole, arising from an overall lack of pro-inflammatory

cytokines in the tissue due to the ablation of innate and adaptive lymphocytes. Indeed, the enhanced levels of infection present in neutrophils and macrophages of il2rg$^{-/-}$ and Rag1$^{-/-}$il2rg$^{-/-}$ mice would support this. Thus, administration of such cytokines as IFN-γ to these immunodeficient mice may help to interrogate whether the enhanced level of infection in these myeloid cells is in fact due to a reduced proinflammatory immune response against the bacteria.

### 5.3.3 Identifying a soluble mediator to successfully modulate ILC2 numbers during infection with *F. tularensis* LVS

Data presented in this thesis chapter demonstrates that IFN-γ from the LVS-infected lung can reduce ILC2 numbers in an *ex vivo* setting. As NK cells represent a major source of IFN-γ during infection with *F. tularensis* LVS (Lopez *et al.*, 2004; Schmitt *et al.*, 2013), it was therefore considered that some degree of cross-talk occurs between ILC2s and NK cells in this context. Others have demonstrated an antagonistic relationship between ILC2s and NK cells, with NK-derived IFN-γ inhibiting ILC2 proliferation and cytokine production (Bi *et al.*, 2017). Interestingly however, whilst the *in vitro* NK-ILC2 co-culture system developed in this chapter indicates that NK cells are capable of reducing ILC2 numbers *in vitro*, this reduction appears to be IFN-γ-independent, as blockade of IFN-γ in this system does not impact on the number of live ILC2s present in culture. This is further complicated by the persistent reduction in ILC2s during infection, even after anti-NK1.1-mediated depletion of NK cells. It remains to be elucidated whether alternative mechanisms are in place to reduce ILC2 numbers in the absence of NK-derived IFN-γ, although this could potentially be addressed in the ILC2-NK *in vitro* culture system presented in this chapter, adopting a similar approach to that discussed in Elkins et al. (2009), with inhibition of multiple other NK effector molecules such as TNF-α and IL-12. Between the latter two cytokines, it appears more likely that IL-12 may negatively impact on ILC2 survival – as TNF-α has been shown to be protective in ILC2 function and survival by signalling through TNF-receptor 2 (Hurrell *et al.*, 2019), whilst IL-12 is critical for the conversion of ILC2s to ILC1s (Silver *et al.*, 2016). However as previously alluded to, this may then become more complex *in vivo*, when other type 1 mediators are present in the LVS-infected lung environment and potential compensatory mechanisms arise – an example of

which may be seen in the enhanced levels of T cell-derived IFN-γ when NK-derived IFN-γ is removed in WT anti-NK1.1-treated mice.

Importantly, type 1 interferons and IL-27 can also inhibit ILC2 function and survival (Molofsky *et al.*, 2015; Duerr *et al.*, 2016). Interestingly however, type 1 interferons play a larger role in control of infection with *F. tularensis novicida*, another type B strain of the bacterium (McLendon, Apicella and Allen, 2006; Krocova, Macela and Kubelkova, 2017). Whilst this is true, infection with *F. tularensis* LVS can still induce the production of the type 1 interferon IFN-β in macrophages *in vitro* (Cole *et al.*, 2007). Thus, this may still be a potential contributor to the reduction in ILC2 numbers observed during infection with *F. tularensis* LVS. This could be tested *in vitro* through antibody-mediated inhibition of IFN-β in a co-culture system of ILC2s and LVS-infected macrophages, but also *in vivo* in type 1 interferon receptor KO (IFN-IR$^{-/-}$) mice. However, the use of these KO mice must be carefully considered, as it has previously been demonstrated that the absence of type 1 interferon receptor signalling in influenza A-challenged mice causes type 2 immunopathology, which is associated with enhanced ILC2s, eosinophilia and increased susceptibility to infection (Duerr *et al.*, 2016). Thus, whilst this may serve to identify a soluble mediator in the control of ILC2 numbers during LVS infection, it may also result in enhanced bacterial burdens and enhanced mortality in these mice – perhaps akin to that observed in chapter 4 of this thesis in IL-33-treated mice.

### 5.3.4 Dissecting the importance of ILC2s during infection with *F. tularensis* LVS

Data presented in chapter 4 of this thesis demonstrated a detrimental role for elevated ILC2 responses in the control of infection. Thus, use of the ICOS-T mouse model was seen as an effective way to assess whether depletion of ILC2s would benefit the host immune response against *F. tularensis* LVS. Indeed, this model has been described elsewhere (Oliphant *et al.*, 2014), with ablation of ILC2s during infection with *N. brasiliensis* highlighting their importance in the induction of an effective type 2 immune response (Oliphant *et al.*, 2014). Whilst the regimen detailed in Oliphant et al. (2014) began on the day of infection, it was critical to ensure ILC2s were depleted prior to challenge in the context of infection with *F. tularensis* LVS,

to fully assess the impact of their absence throughout the course of infection. As such, the dosing regimen presented in this thesis chapter was significantly altered when compared to previously published work (Oliphant *et al.*, 2014), with treatment starting 4 days prior to infection.

Over the years, treatment with diphtheria toxin (DTx) has been well established to produce side effects in mice such as weight loss and proteinuria (Meyer Zu Hörste *et al.*, 2010; Goldwich *et al.*, 2012). Moreover, mice display enhanced susceptibility to other intracellular infections such as influenza A and lymphocytic choriomeningitis virus (LCMV) during DTx administration (Schmitz *et al.*, 2013; Mayer *et al.*, 2014). Thus, whilst the weight loss observed during the early stages of infection with *F. tularensis* LVS may represent a side effect of treatment with DTx, the rapid deterioration in the condition of DTx-treated mice during infection with *F. tularensis* LVS may in fact indicate a significantly more lethal infection in this model.

ILC2s represent the dominant ILC subset in the lung at steady-state, and during the early stages of infection with *F. tularensis* LVS. Elsewhere, the relative proportions of murine ILC subsets are much more diverse in the liver and spleen. For example, NK cells and ILC1s represent the dominant innate lymphocyte populations in the liver (Sojka *et al.*, 2014), with their importance in the control of infection discussed earlier. Thus, it is perhaps unsurprising that the impact of ILC2 depletion on the control of infection was more apparent in the lung of ICOS-T DTx-treated mice when compared to WT DTx-treated mice. Thus, these results highlight a potentially negative role for ILC2s in the control of infection with *F. tularensis* LVS. Nevertheless, the interpretation of these findings must be considered carefully, as the inherent lethality of DTx in this context indicates that this model requires optimization. This should at least include adjusting the quantity of DTx administered per dose, frequency of dosing, length of treatment, and the start and end dates of treatment. Through optimization of these parameters in the context of infection with *F. tularensis* LVS, the role of ILC2s may be able to be interrogated further using this model.

Should optimization of the ICOS-T mouse model not prove successful, other approaches should also be considered in investigating the role of ILC2s in LVS infection. For example, adoptive transfer of sort-purified, rested ILC2s

into Rag1$^{-/-}$il2rg$^{-/-}$ mice, which has been exemplified by others in papain-induced airway inflammation and during infection with *C. difficile* (Halim *et al.*, 2012a; Abt *et al.*, 2015). Alternatively, another method of studying the role of ILC2s during LVS infection could be the *Rag2*$^{-/-}$*Il7ra*$^{Cre/+}$*Rora*$^{loxP/loxP}$ mouse model (Schuijs *et al.*, 2020). Here, mice display total ablation of adaptive immunity, alongside deficiency in ILC2s – as all IL-7Rα$^{+}$ cells that express RORα are deleted, and this transcription factor is essential for the development of ILC2s (Wong *et al.*, 2012; Halim *et al.*, 2012b). Thus, as data in this thesis chapter has demonstrated that innate immunity is sufficient for the control of infection with *F. tularensis* LVS, this could present an attractive alternative to the ICOS-T mouse model in determining the role of ILC2s during LVS infection. It is important to note however, that this model has a potential caveat, given that RORα is also expressed by ILC3s (Lo *et al.*, 2016; Lo *et al.*, 2019). Nevertheless, ILC3s represent a very small proportion of lung ILCs, and are not enhanced as LVS infection progresses, meaning that whilst this should be acknowledged, it may not be of concern in dissecting the role of ILC2s in the lung during infection with *F. tularensis* LVS using this model.

## 5.4 Conclusion

This chapter has begun to highlight the relative importance of innate lymphocyte populations in the control of infection with *F. tularensis* LVS, as well as the dispensability of adaptive immunity. Indeed, the enhanced mortality and elevated bacterial burdens in il2rg$^{-/-}$, Rag1$^{-/-}$il2rg$^{-/-}$, and anti-NK1.1-treated Rag1$^{-/-}$ mice demonstrates that NK cells and ILC1s likely play important roles in the control of infection with *F. tularensis* LVS. Moreover, whilst lung bacterial burdens are significantly lower in ILC2-depleted mice when compared to DTx-treated mice, this approach must be optimised, or alternative approaches considered in lieu of this, in order to further explore the significance of the absence of ILC2s in the host immune response against *F. tularensis* LVS. Overall, these findings suggest that early interventions that reduce ILC2 numbers, and bolster NK and ILC1 effector functions, could prove to be of benefit for the host immune response against *F. tularensis* LVS. If successful, these could widen the therapeutic window for antibiotic treatments, and potentially limit the severity of infection.

# Chapter 6

# General Discussion

## 6.1 General Discussion

This thesis aimed to address the role of ILCs during pulmonary infection with *F. tularensis* (figure 6.1). Initially, data in chapter 3 of this thesis identified multiple changes to the ILC compartment during infection with *F. tularensis* LVS. For example, a reduction in the total number of ILCs was observed as infection progressed, which was associated with a subset-specific reduction in ILC2s, and a concurrent increase in ILC1s. At first, it was hypothesised that this could be of potential benefit to the immune response, given the role of ILC2s in the control of intracellular infections (Monticelli *et al.*, 2011). However, chapter 4 of this thesis revealed that expansion of ILC2 numbers by IL-33, or by direct transfer of ILC2s, proved to be detrimental to the control of infection, with enhanced bacterial burdens in the lung, liver and spleen in these studies. Thus, it was next considered that the reduction in ILC2s seen during infection could occur as a result of an enhanced type 1 immune response, and therefore be beneficial to the host's control of infection.

Chapter 5 of this thesis began to explore the relative contribution of lymphocyte populations in the host immune response against *F. tularensis* LVS. Initially, it was revealed that whilst adaptive immunity is dispensable, the absence of innate lymphocytes was detrimental to the control of infection. Here, it was demonstrated that the absence of NK cells and ILC1s proved detrimental to the control of infection. Specifically, the exacerbated bacterial burdens observed in anti-NK1.1-treated $Rag1^{-/-}$ mice revealed the importance of innate lymphocyte sources of IFN-γ in the host immune response against *F. tularensis* LVS. Elsewhere, as ILC2-depleted ICOS-T mice displayed reduced bacterial burdens when compared to WT DTx-treated controls, this further demonstrated a detrimental role for ILC2s in the control of infection with *F. tularensis* LVS. This chapter will now consider the implications of the findings presented in this thesis in a wider context, and address areas of interest for future work in order to further understand how the ILC compartment can be successfully manipulated to the benefit of the host during infection with *F. tularensis* LVS.

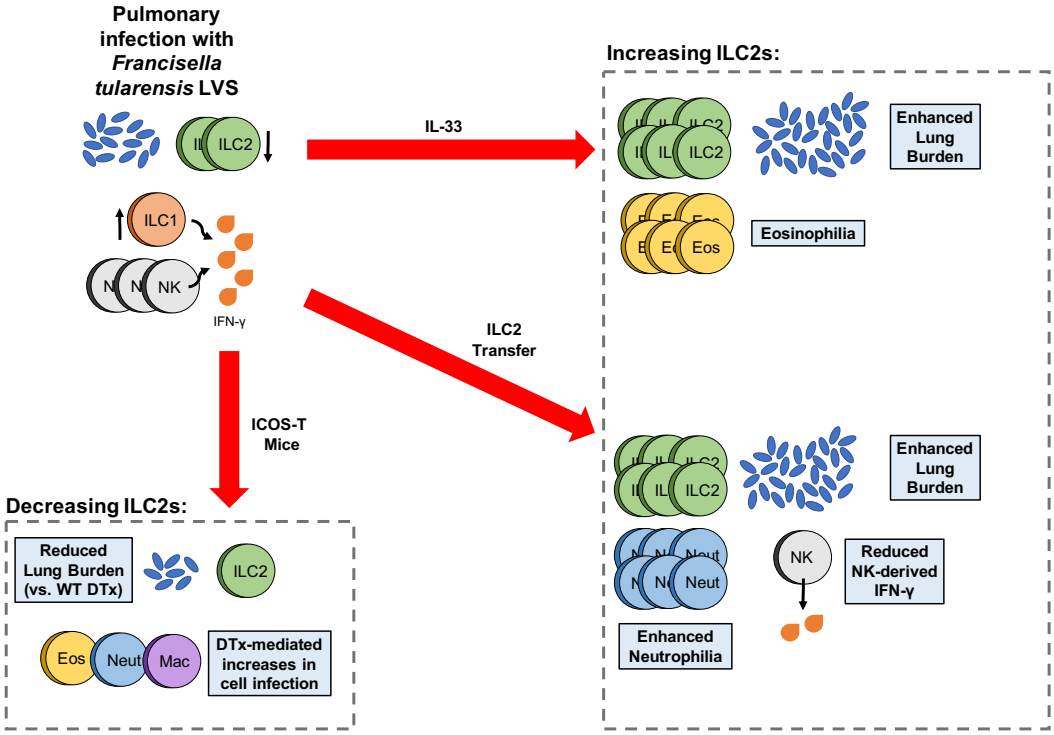


**Figure 6.1 – ILC2s are detrimental to the host immune response during infection with *F. tularensis* LVS**

Pulmonary infection with *F. tularensis* LVS results in a reduction in ILC2 numbers, with a concurrent increase in ILC1s. Alongside NK cells, this expanded ILC1 population provides an important source of IFN-γ during infection. Increasing ILC2 numbers either by IL-33 treatment, or direct intranasal transfer of ILC2s, results in significantly enhanced lung bacterial burdens, likely arising from enhanced recruitment and infection of myeloid cells, and reduced NK-derived IFN-γ. Conversely, specific ablation of ILC2s in ICOS-T mice does reduce lung burdens when compared to WT diphtheria toxin (DTx)-treated mice, though some DTx-mediated side effects are also observed in this model.

## 6.2 Generating an appropriate immune response against *F. tularensis*

Type 1 cytokines are critical to the control of intracellular infections (Spellberg and Edwards, 2001). Indeed, several of these are essential for control of infection with *F. tularensis* (Cowley and Elkins, 2011). As such, this would suggest that the presence of innate cells that are capable of producing these cytokines during early infection might be of benefit to the host. ILC1s represent one potential source of these cytokines, capable of rapid production of IFN-γ and TNF-α (Artis and Spits, 2015). Despite this, the dominant ILC subset in the murine lung at steady state is the ILC2 (Mindt, Fritz and Duerr, 2018), which are predominantly involved in the immune response against type 2 insults (Artis and Spits, 2015). Thus, the lack of early

expansion of ILC1s, and the fact that ILC2s remain the dominant subset during the early stages of infection with *F. tularensis* LVS indicates a potentially inappropriate immune response from the ILC compartment. Moreover, it is important to note that the relative composition of ILC subsets in the lung differs between mice and humans. Specifically, whilst ILC2s represent nearly all ILCs in the murine lung (Mindt, Fritz and Duerr, 2018), the healthy human lung is predominantly composed of ILC3s (Bal *et al.*, 2016; Yudanin *et al.*, 2019). Thus, these differences must be considered, as well as how the results presented in this thesis are interpreted in the context of human infection.

As elements of a type 1 immune response are required to mount a successful immune response against *F. tularensis* (Cowley and Elkins, 2011), it would be interesting to see how augmenting ILC1 numbers during early infection, through cytokines such as IL-12 and IL-18, would impact on the control of infection. Investigating the potential benefits of ILC1s in this context becomes even more intriguing when considering the importance of ILC1s in the control of liver-based infections, where ILC1s represent the dominant ILC subset (Jiao *et al.*, 2016). For example, infection with mouse cytomegalovirus (MCMV) yields enhanced viral burdens and mortality in ILC1-deficient mice, with this rescued upon adoptive transfer of IFN-γ-producing ILC1s (Weizman *et al.*, 2017). Thus, this demonstrates how the presence of an abundant ILC1 population during early infection can positively impact on the control of infection. Conversely, data in this thesis highlighted that an ILC1 population only begins to manifest during the later stages of infection with *F. tularensis* LVS (day 5 p.i. onwards) – a time point which may be too late to benefit to the host immune response against the bacterium. Evidence for this is that the $LD_{50}$ (the dose of bacteria required to cause death in 50% mice) is reduced upon neutralisation of IFN-γ at day 0 and 2 p.i., but not at day 4 p.i. (Leiby *et al.*, 1992). Thus, this highlights the potential importance of the earlier expansion of an IFN-γ-producing ILC1 population. Importantly however, as NK cells were also shown to provide a large source of IFN-γ at day 5 p.i., and significantly exacerbated bacterial burdens were observed in anti-NK1.1-treated $Rag1^{-/-}$ mice (which lack NK cells and ILC1s), a role for this innate lymphocyte population in this excessive cytokine response cannot be excluded. Overall, future work should therefore seek to manipulate both of these innate lymphocyte populations earlier during infection by treatment

with recombinant cytokines, and attempt to dissect the functional importance of each population – perhaps through comparison of ILC1-deficient and NK-deficient mice.

If a type 1 immune response is mounted early enough in infection with *F. tularensis* LVS, then this could perhaps lead to bacterial clearance. At this point, it would be important to consider the role of type 2 immune cells such as ILC2s and their roles in tissue repair responses. ILC2-derived amphiregulin (AREG) has already been shown to be critical to this process after viral infection (Monticelli *et al.*, 2011). Thus, it would be important to identify whether enhancing levels of ILC2s during the resolution phase of infection would result in a similar reparatory role in the context of LVS infection. This could be further investigated perhaps in future studies where the infectious dose of bacteria is lowered to sub-lethal levels – as bacteria are cleared after 1-3 weeks in this context (Elkins, Cowley and Bosio, 2003).

### 6.3 Missing the therapeutic window during infection with *F. tularensis*

It is often difficult to diagnose infection with *F. tularensis*, due to non-specific clinical symptoms (Maurin, 2020). This difficulty in diagnosis becomes even more problematic when considering the timing of treatment of *F. tularensis* infection is of critical importance to the control and clearance of infection (Klimpel *et al.*, 2008). This is exemplified with an antibiotic model used during intranasal infection with *F. tularensis*. Specifically, treatment with the fluoroquinolone levofloxacin at 72 hours p.i. confers 100% protection from infection, whilst administration at 120 hours p.i. results in a no protection (Klimpel *et al.*, 2008). Thus, these results highlight the importance of enhancing the understanding of the early immune response against this pathogen, in order to widen the therapeutic window for effective treatment of infection.

Reduced effectiveness of antibiotic treatments when delivered at a later time point p.i. could suggest an enhanced severity of infection, and an inability to control bacterial growth. However, infectious outcome may instead be related to an exacerbated response by the host immune system in attempting to control and clear the pathogen. Thus, the use of immunomodulatory

agents could also benefit the host immune response against *F. tularensis* if the initial therapeutic window has closed, which has been suggested to have occurred when a patient presents with symptoms of an infection (D'Elia *et al.*, 2013). As such, if treatment is not given prior to the development of symptoms, the use of an immunomodulator at a later time point may help to regulate an otherwise exacerbated pro-inflammatory response.

The effectiveness of immunomodulation during pulmonary infection has been observed recently, with treatment of hospitalised SARS-CoV-2 patients with the glucocorticoid and immunosuppressant dexamethasone (Horby *et al.*, 2021). Here, the incidence of death was lower in hospitalised patients receiving respiratory support that were treated with dexamethasone (Horby *et al.*, 2021). Thus, as dexamethasone is capable of inhibiting IFN-γ (Giles *et al.*, 2018), its use in this context may have been key in limiting tissue damage caused by an excessive host immune response (Quirch, Lee and Rehman, 2020). These observations highlight the potential use of immunomodulators as a potential therapeutic option to other pulmonary infections associated with a 'cytokine storm', such as *F. tularensis*. Thus, it would be interesting to assess whether addition of immunomodulatory agents at a late stage of infection with *F. tularensis* could regulate the host immune response against the bacteria, and allow for a more controlled immune response if the initial therapeutic window is missed. Indeed, immunomodulatory therapies are already in circulation that act upon ILC-derived cytokines (Cobb and Verneris, 2021). For example, treatment with an IL-12/23 p40 monoclonal antibody (mAb) can reduce the levels of an inflammatory ILC1 population in Crohn's disease, which is associated with mucosal healing (Li *et al.*, 2016). Thus, the expansion of ILC1s observed in the latter stages of infection with *F. tularensis* could be modulated by use of such an approach, or even if the ILC1 population was initially expanded, in order to limit excessive inflammation.

### 6.4 Future directions

This thesis utilised a lethal dose of bacteria when administered via the intranasal route (Fortier *et al.*, 1991), and focused more so on how ILC2s were detrimental during this period. However, the complete mechanism by which this occurs remains to be elucidated. It can at least be considered that

this may occur via ILC2s and eosinophils in the context of IL-33-treated mice. Indeed, this appears increasingly likely when considering that both of these cell populations are expanded following IL-33 treatment, and this is associated with enhanced levels of eosinophil infection. Moreover, ILC2-derived IL-5 is essential for the maintenance and tissue recruitment of eosinophils (Nussbaum *et al.*, 2013). Thus, it is critical that this ILC2-eosinophil relationship be tested further. Specifically, this could occur through use of an anti-IL-5 neutralising antibody in IL-33-treated mice, in order to block the recruitment of eosinophils to the lung. Here, a reduction in bacterial burdens could indicate that ILC2-derived IL-5 is important in the enhanced bacterial burdens observed in IL-33-treated mice. It would also be important to ascertain whether aspects of type 1 immunity, such as NK cell-derived IFN-γ production, are also impacted upon by blockade of this eosinophil recruitment – especially as ILC2-induced eosinophilia has already been shown to inhibit NK cell function in the context of anti-tumour immunity (Schuijs *et al.*, 2020).

The relationship between ILC2s and eosinophils can be further considered in the context of untreated LVS-infected mice, with data in chapters 3 and 5 of this thesis highlighting that both ILC2 and eosinophil numbers are reduced during the later stages of infection. Indeed, data in chapter 3 demonstrated that ILC2s show reduced levels of KLRG1 (a marker of ILC2 activation) in the later stages of infection with *F. tularensis* LVS, potentially reflecting a reduction in cytokine production at this stage. It appears that the mechanism by which ILC2s are reduced occurs at least in part through production of IFN-γ in the lung tissue, as highlighted with the *in vitro* data presented in chapter 5 of this thesis. Indeed, this has been demonstrated previously by others, with IFN-γ inhibiting ILC2 activation, cytokine production and enhancing levels of ILC2 cell death (Molofsky *et al.*, 2015; Duerr *et al.*, 2016). However, it is currently unclear whether IFN-γ represents the only cytokine that can reduce ILC2 numbers and inhibit their function in the context of LVS infection. Indeed, whilst the loss of ILC2s at day 5 p.i. is associated with enhanced IFN-γ-producing NK cells and ILC1s, the fact that the reduction in ILC2 numbers is not rescued following depletion of NK cell and ILC1s suggests that other ILC2 inhibitors such as IL-27 and type 1 interferons (Duerr *et al.*, 2016) may also impact on ILC2 numbers during LVS infection. This could be confirmed through similar *in vitro* cultures of sort-purified ILC2s with

neutralising antibodies against these cytokines, or a combination of them, and subsequently tested *in vivo* through treatment of mice with the same antibodies to observe the effects of their inhibition on ILC2 numbers.

As previously mentioned, ILC2s can inhibit NK cell function during anti-tumour immune responses (Schuijs *et al.*, 2020). Thus, it was therefore interesting to observe that ILC2s also appear to negatively impact on NK cell function in the context of infection with *F. tularensis* LVS, with reduced NK-derived IFN-γ following ILC2 transfer. Given the protective effects of IFN-γ during infection with the bacteria (Leiby *et al.*, 1992; Lopez *et al.*, 2004), it may therefore be considered that this reduced IFN-γ output could contribute to the enhanced bacterial burdens in ILC2 transfer mice. In order to test this further, the impact of ablation of ILC2s on NK cell function must be determined using ICOS-T mice. Specifically, as data in this thesis has already identified that these mice display reduced lung bacterial burdens, determining how this model impacts on NK cell function could therefore help to further interrogate an ILC2-NK relationship, and highlight the importance of reducing ILC2 numbers earlier in infection. Of note, this work would likely require the use of an anti-NK1.1-treated group, to determine the functional importance of this relationship between ILC2s and NK cells, and whether the loss of NK cell-derived IFN-γ would reverse the decrease in lung bacterial burdens seen in ICOS-T mice.

Infection with *F. tularensis* LVS causes a reduction in ILC2s and a concurrent increase in ILC1s. However, this thesis did not determine the exact mechanisms driving these changes. It may be possible that this ILC1 population arises from local proliferation of the small number of bona fide ILC1s in the lung – especially given the relatively small increase in ILC1s when compared to the larger decrease in ILC2s during infection. However, in the context of other intracellular infections, ILC1-like IFN-γ-producing populations have been shown to be derived from ILC2s in the lung, and are identified as an $ST2^{+}IL\text{-}18R\alpha^{+}$ ILC population (Silver *et al.*, 2016). More recently, ILC1s have also been proposed to arise from an immature population of $IL\text{-}18R\alpha^{+}ST2^{-}$ ILC2s (Zeis *et al.*, 2020). Indeed, this has been demonstrated in the context of infection with another intracellular bacterium *Mycobacterium tuberculosis* (Corral *et al.*, 2021). Thus, it is important to determine the exact origin of these ILC1s in the context of infection with *F.*

*tularensis* LVS, with studies that interrogate this ILC2-ILC1 relationship likely requiring the use of fate mapping tools such as ST2 reporter mice - which track ST2-expressing cells over their lifetime. Overall, this could help determine how ILC1 and ILC2 numbers can be manipulated, in order to benefit the host immune response.

The cytokines IL-12 and IL-18 have been highlighted throughout this thesis as critical players in pulmonary infections, where they can facilitate the conversion of ILC2s to ILC1-like cells (Silver *et al.*, 2016; Corral *et al.*, 2021). Moreover, they are also of vital importance to the control of infection with *F. tularensis* LVS (Duckett *et al.*, 2005; del Barrio *et al.*, 2015; Periasamy *et al.*, 2016). Thus, uncovering whether ILC2s are impacted upon by these cytokines during infection with *F. tularensis* LVS may help to further determine the origins of ILC1s during infection, whilst uncovering how ILC2 numbers can be successfully manipulated to the host's advantage. Initially, this could be achieved by flow cytometry analysis for expression of IL-12Rβ2 and IL-18Rα on ILC2s. Should expression be confirmed, subsequent studies may then seek to assess how inhibition of either of these cytokines impacts on ILC2 numbers during infection, and whether early administration of these cytokines could facilitate the conversion of ILC2s to an ILC1-like IFN-γ-producing population.

## 6.5 Thesis conclusion

In conclusion, this thesis has begun to address the role of ILCs during infection with *F. tularensis* LVS (figure 6.2). It demonstrates that ILC2s are reduced as infection progresses, and this is likely to be of benefit to the host immune response. Specifically, as both IL-33-mediated expansion of ILC2s and direct intranasal transfer of ILC2s result in significantly exacerbated bacterial burdens, it highlights their detrimental role in the control of infection, and a potential need to reduce ILC2 numbers earlier during infection. Indeed, the decreased bacterial burden in the lungs of ILC2-deficient mice confirms this, providing an example of the potential benefits of an earlier loss of ILC2s. Moreover, whilst IFN-γ can serve as one potential mediator for reducing ILC2 numbers, further study is required to uncover the overall mechanism by which ILC2s can be manipulated during infection with *F. tularensis* LVS. Overall, it can therefore be considered that targeted approaches that allow

for ILC2 depletion during early infection with *F. tularensis* may prove to be of great benefit to the host immune response against the bacterium.

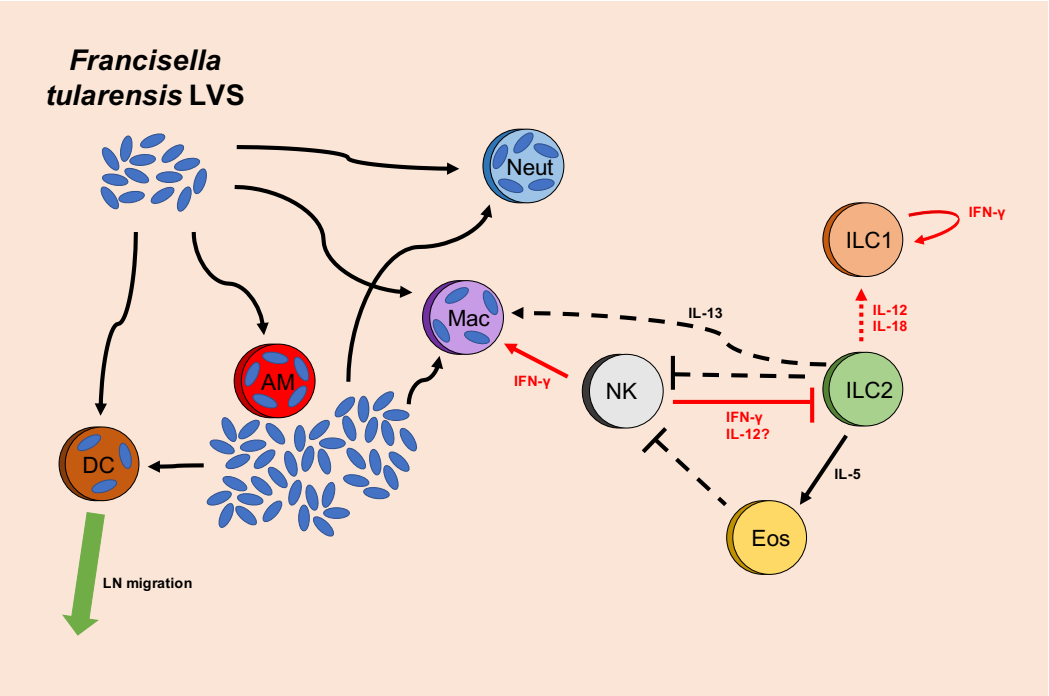


**Figure 6.2 – Immune cell interactions in the lung during infection with *F. tularensis* LVS**

*F. tularensis* LVS infects multiple cell types in the lung following intranasal inoculation. Alveolar macrophages (AMs) are the principal cell type infected during the initial stages of infection, where the bacteria replicates and exits the cell to infect other cell types. Infected dendritic cells (DCs) migrate to draining lymph nodes (LNs), which facilitates dissemination of the bacteria to peripheral organs such as the liver and spleen. At day 3 post-infection (p.i.), the extensive recruitment of neutrophils means that this cell type becomes the major replicative niche for *F. tularensis*. During this early stage of infection, ILC2s represent the dominant ILC subset. These cells are postulated to inhibit NK cell function, either through direct cellular interactions, or through an ILC2-derived IL-5 eosinophil-mediated mechanism. ILC2-dervied IL-13 may also induce alternative activation of macrophages to enhance their susceptibility to infection (solid and dashed black arrows). As infection progresses (red arrows), levels of bacteria rise significantly and NK cells produce soluble mediators such as IFN-γ and IL-12 to inhibit ILC2 survival. NK-derived IFN-γ can also increase the efficiency of bacterial killing in macrophages. A small proportion of ILC2s may convert to an ILC1-like phenotype in response to IL-12 and IL-18 in the infected lung environment (red dotted arrow). These ILC1-like cells are capable of IFN-γ production, which may act in an autocrine feedback loop to propagate their survival.

# Chapter 7 References


Abplanalp, A. L., Morris, I. R., Parida, B. K., Teale, J. M. and Berton, M. T. (2009) 'TLR-dependent control of Francisella tularensis infection and host inflammatory responses', *PLoS One,* 4(11).

Abt, M. C., Lewis, B. B., Caballero, S., Xiong, H., Carter, R. A., Susac, B., Ling, L., Leiner, I. and Pamer, E. G. (2015) 'Innate Immune Defenses Mediated by Two ILC Subsets Are Critical for Protection against Acute Clostridium difficile Infection', *Cell Host Microbe,* 18(1).

Alvarez, F., Fritz, J. H. and Piccirillo, C. A. (2019) 'Pleiotropic Effects of IL-33 on CD4(+) T Cell Differentiation and Effector Functions', *Front Immunol,* 10.

Alves-Filho, J. C., Sonego, F., Souto, F. O., Freitas, A., Verri, W. A., Jr., Auxiliadora-Martins, M., Basile-Filho, A., McKenzie, A. N., Xu, D., Cunha, F. Q. and Liew, F. Y. (2010) 'Interleukin-33 attenuates sepsis by enhancing neutrophil influx to the site of infection', *Nat Med,* 16(6).

Anthony, L. D., Burke, R. D. and Nano, F. E. (1991) 'Growth of Francisella spp. in rodent macrophages', *Infect Immun,* 59(9).

Anthony, L. S. and Kongshavn, P. A. (1988) 'H-2 restriction in acquired cell-mediated immunity to infection with Francisella tularensis LVS', *Infect Immun,* 56(2).

Ardain, A., Domingo-Gonzalez, R., Das, S., Kazer, S. W., Howard, N. C., Singh, A., Ahmed, M., Nhamoyebonde, S., Rangel-Moreno, J., Ogongo, P., Lu, L., Ramsuran, D., de la Luz Garcia-Hernandez, M., T, K. U., Darby, M., Park, E., Karim, F., Melocchi, L., Madansein, R., Dullabh, K. J., Dunlap, M., Marin-Agudelo, N., Ebihara, T., Ndung'u, T., Kaushal, D., Pym, A. S., Kolls, J. K., Steyn, A., Zuniga, J., Horsnell, W., Yokoyama, W. M., Shalek, A. K., Kloverpris, H. N., Colonna, M., Leslie, A. and Khader, S. A. (2019) 'Group 3 innate lymphoid cells mediate early protective immunity against tuberculosis', *Nature,* 570(7762).

Arpaia, N., Green, J. A., Moltedo, B., Arvey, A., Hemmers, S., Yuan, S., Treuting, P. M. and Rudensky, A. Y. (2015) 'A Distinct Function of Regulatory T Cells in Tissue Protection', *Cell,* 162(5).

Artis, D. and Spits, H. (2015) 'The biology of innate lymphoid cells', *Nature,* 517(7534).

Aujla, S. J., Chan, Y. R., Zheng, M., Fei, M., Askew, D. J., Pociask, D. A., Reinhart, T. A., McAllister, F., Edeal, J., Gaus, K., Husain, S., Kreindler, J. L., Dubin, P. J., Pilewski, J. M., Myerburg, M. M., Mason, C. A., Iwakura, Y. and Kolls, J. K. (2008) 'IL-22 mediates mucosal host defense against Gram-negative bacterial pneumonia', *Nat Med,* 14(3).

Bal, S. M., Bernink, J. H., Nagasawa, M., Groot, J., Shikhagaie, M. M., Golebski, K., van Drunen, C. M., Lutter, R., Jonkers, R. E., Hombrink, P., Bruchard, M., Villaudy, J., Munneke, J. M., Fokkens, W., Erjefalt, J. S., Spits, H. and Ros, X. R. (2016) 'IL-1beta, IL-4 and IL-12 control the fate of group 2 innate lymphoid cells in human airway inflammation in the lungs', *Nat Immunol,* 17(6).

Bando, J. K. and Colonna, M. (2016) 'Innate lymphoid cell function in the context of adaptive immunity', *Nat Immunol,* 17(7).

Bar-Haim, E., Gat, O., Markel, G., Cohen, H., Shafferman, A. and Velan, B. (2008) 'Interrelationship between dendritic cell trafficking and Francisella tularensis dissemination following airway infection', *PLoS Pathog,* 4(11).

Baron, S. D., Singh, R. and Metzger, D. W. (2007) 'Inactivated Francisella tularensis live vaccine strain protects against respiratory tularemia by

intranasal vaccination in an immunoglobulin A-dependent fashion', *Infect Immun,* 75(5).
Bartemes, K. R., Iijima, K., Kobayashi, T., Kephart, G. M., McKenzie, A. N. and Kita, H. (2012) 'IL-33-responsive lineage- CD25+ CD44(hi) lymphoid cells mediate innate type 2 immunity and allergic inflammation in the lungs', *Journal of immunology (Baltimore, Md. : 1950),* 188(3).
Behnsen, J., Jellbauer, S., Wong, C. P., Edwards, R. A., George, M. D., Ouyang, W. and Raffatellu, M. (2014) 'The cytokine IL-22 promotes pathogen colonization by suppressing related commensal bacteria', *Immunity,* 40(2).
Ben Nasr, A., Haithcoat, J., Masterson, J. E., Gunn, J. S., Eaves-Pyles, T. and Klimpel, G. R. (2006) 'Critical role for serum opsonins and complement receptors CR3 (CD11b/CD18) and CR4 (CD11c/CD18) in phagocytosis of Francisella tularensis by human dendritic cells (DC): uptake of Francisella leads to activation of immature DC and intracellular survival of the bacteria', *J Leukoc Biol,* 80(4).
Ben Nasr, A. and Klimpel, G. R. (2008) 'Subversion of complement activation at the bacterial surface promotes serum resistance and opsonophagocytosis of Francisella tularensis', *J Leukoc Biol,* 84(1).
Berdal, B. P., Mehl, R., Meidell, N. K., Lorentzen-Styr, A. M. and Scheel, O. (1996) 'Field investigations of tularemia in Norway', *FEMS Immunol Med Microbiol,* 13(3).
Bernink, J. H., Peters, C. P., Munneke, M., te Velde, A. A., Meijer, S. L., Weijer, K., Hreggvidsdottir, H. S., Heinsbroek, S. E., Legrand, N., Buskens, C. J., Bemelman, W. A., Mjosberg, J. M. and Spits, H. (2013) 'Human type 1 innate lymphoid cells accumulate in inflamed mucosal tissues', *Nat Immunol,* 14(3).
Bi, J., Cui, L., Yu, G., Yang, X., Chen, Y. and Wan, X. (2017) 'NK Cells Alleviate Lung Inflammation by Negatively Regulating Group 2 Innate Lymphoid Cells', *J Immunol,* 198(8).
Bingle, L. E., Bailey, C. M. and Pallen, M. J. (2008) 'Type VI secretion: a beginner's guide', *Curr Opin Microbiol,* 11(1).
Blair, C., Naclerio, R. M., Yu, X., Thompson, K. and Sperling, A. (2005) 'Role of type 1 T helper cells in the resolution of acute Streptococcus pneumoniae sinusitis: a mouse model', *The Journal of infectious diseases,* 192(7).
Bokhari, S. M., Kim, K. J., Pinson, D. M., Slusser, J., Yeh, H. W. and Parmely, M. J. (2008) 'NK cells and gamma interferon coordinate the formation and function of hepatic granulomas in mice infected with the Francisella tularensis live vaccine strain', *Infect Immun,* 76(4).
Bonemann, G., Pietrosiuk, A. and Mogk, A. (2010) 'Tubules and donuts: a type VI secretion story', *Mol Microbiol,* 76(4).
Boonnak, K., Vogel, L., Feldmann, F., Feldmann, H., Legge, K. L. and Subbarao, K. (2014) 'Lymphopenia associated with highly virulent H5N1 virus infection due to plasmacytoid dendritic cell mediated apoptosis of T cells', *J Immunol,* 192(12).
Bosio, C. M. (2011) 'The Subversion of the Immune System by Francisella Tularensis', *Front Microbiol,* 2.
Bosio, C. M., Bielefeldt-Ohmann, H. and Belisle, J. T. (2007) 'Active suppression of the pulmonary immune response by Francisella tularensis Schu4', *J Immunol,* 178(7).
Bosio, C. M. and Dow, S. W. (2005) 'Francisella tularensis induces aberrant activation of pulmonary dendritic cells', *J Immunol,* 175(10).
Bouchery, T., Kyle, R., Camberis, M., Shepherd, A., Filbey, K., Smith, A., Harvie, M., Painter, G., Johnston, K., Ferguson, P., Jain, R., Roediger, B., Delahunt, B., Weninger, W., Forbes-Blom, E. and Le Gros, G. (2015) 'ILC2s

and T cells cooperate to ensure maintenance of M2 macrophages for lung immunity against hookworms', *Nat Commun,* 6.
Boyce, J. M. (1975) 'Recent trends in the epidemiology of tularemia in the United States', *J Infect Dis,* 131(2).
Bradburne, C. E., Verhoeven, A. B., Manyam, G. C., Chaudhry, S. A., Chang, E. L., Thach, D. C., Bailey, C. L. and van Hoek, M. L. (2013) 'Temporal Transcriptional Response during Infection of Type II Alveolar Epithelial Cells with Francisella tularensis Live Vaccine Strain (LVS) Supports a General Host Suppression and Bacterial Uptake by Macropinocytosis*', *J Biol Chem: Vol. 15*.
Bradfute, S. B., Braun, D. R., Shamblin, J. D., Geisbert, J. B., Paragas, J., Garrison, A., Hensley, L. E. and Geisbert, T. W. (2007) 'Lymphocyte death in a mouse model of Ebola virus infection', *The Journal of infectious diseases,* 196 Suppl 2.
Brinkmann, V. (2018) 'Neutrophil Extracellular Traps in the Second Decade', *J Innate Immun,* 10(5-6).
Bröms, J. E., Meyer, L. and Sjöstedt, A. (2017) 'A mutagenesis-based approach identifies amino acids in the N-terminal part of Francisella tularensis IglE that critically control Type VI system-mediated secretion', *Virulence: Vol. 6*.
Broms, J. E., Meyer, L., Sun, K., Lavander, M. and Sjostedt, A. (2012) 'Unique substrates secreted by the type VI secretion system of Francisella tularensis during intramacrophage infection', *PLoS One,* 7(11).
Butchar, J. P., Cremer, T. J., Clay, C. D., Gavrilin, M. A., Wewers, M. D., Marsh, C. B., Schlesinger, L. S. and Tridandapani, S. (2008) 'Microarray analysis of human monocytes infected with Francisella tularensis identifies new targets of host response subversion', *PLoS One,* 3(8).
Cai, T., Qiu, J., Ji, Y., Li, W., Ding, Z., Suo, C., Chang, J., Wang, J., He, R., Qian, Y., Guo, X., Zhou, L., Sheng, H. and Shen, L. (2019) 'IL-17-producing ST2(+) group 2 innate lymphoid cells play a pathogenic role in lung inflammation', *J Allergy Clin Immunol,* 143(1).
Cao, X., Shores, E. W., Hu-Li, J., Anver, M. R., Kelsall, B. L., Russell, S. M., Drago, J., Noguchi, M., Grinberg, A., Bloom, E. T. and et al. (1995) 'Defective lymphoid development in mice lacking expression of the common cytokine receptor gamma chain', *Immunity,* 2(3).
Carlsson, H. E., Lindberg, A. A., Lindberg, G., Hederstedt, B., Karlsson, K. A. and Agell, B. O. (1979) 'Enzyme-linked immunosorbent assay for immunological diagnosis of human tularemia', *J Clin Microbiol,* 10(5).
Casulli, J., Fife, M. E., Houston, S. A., Rossi, S., Dow, J., Williamson, E. D., Clark, G. C., Hussell, T., D'Elia, R. V. and Travis, M. A. (2019) 'CD200R deletion promotes a neutrophil niche for Francisella tularensis and increases infectious burden and mortality', *Nat Commun,* 10.
Cella, M., Fuchs, A., Vermi, W., Facchetti, F., Otero, K., Lennerz, J. K., Doherty, J. M., Mills, J. C. and Colonna, M. (2009) 'A human natural killer cell subset provides an innate source of IL-22 for mucosal immunity', *Nature,* 457(7230).
Celli, J. and Zahrt, T. C. (2013) 'Mechanisms of Francisella tularensis intracellular pathogenesis', *Cold Spring Harb Perspect Med,* 3(4).
Chang, Y. J., Kim, H. Y., Albacker, L. A., Baumgarth, N., McKenzie, A. N., Smith, D. E., Dekruyff, R. H. and Umetsu, D. T. (2011) 'Innate lymphoid cells mediate influenza-induced airway hyper-reactivity independently of adaptive immunity', *Nature immunology,* 12(7).
Chen, C. C., Kobayashi, T., Iijima, K., Hsu, F. C. and Kita, H. (2017) 'IL-33 dysregulates regulatory T cells and impairs established immunologic tolerance in the lungs', *J Allergy Clin Immunol,* 140(5).

Chen, W., Kuolee, R., Austin, J. W., Shen, H., Che, Y. and Conlan, J. W. (2005a) 'Low dose aerosol infection of mice with virulent type A Francisella tularensis induces severe thymus atrophy and CD4+ CD8+ thymocyte depletion', *Microb Pathog,* 39(5-6).
Chen, W., KuoLee, R., Shen, H., Busa, M. and Conlan, J. W. (2004a) 'Toll-like receptor 4 (TLR4) does not confer a resistance advantage on mice against low-dose aerosol infection with virulent type A Francisella tularensis', *Microb Pathog,* 37(4).
Chen, W., Kuolee, R., Shen, H., Busa, M. and Conlan, J. W. (2005b) 'Toll-like receptor 4 (TLR4) plays a relatively minor role in murine defense against primary intradermal infection with Francisella tularensis LVS', *Immunol Lett,* 97(1).
Chen, W., KuoLee, R., Shen, H. and Conlan, J. W. (2004b) 'Susceptibility of immunodeficient mice to aerosol and systemic infection with virulent strains of Francisella tularensis', *Microb Pathog,* 36(6).
Chong, A., Wehrly, T. D., Nair, V., Fischer, E. R., Barker, J. R., Klose, K. E. and Celli, J. (2008) 'The early phagosomal stage of Francisella tularensis determines optimal phagosomal escape and Francisella pathogenicity island protein expression', *Infect Immun,* 76(12).
Clarridge, J. E., 3rd, Raich, T. J., Sjösted, A., Sandström, G., Darouiche, R. O., Shawar, R. M., Georghiou, P. R., Osting, C. and Vo, L. (1996) 'Characterization of two unusual clinically significant Francisella strains', *J Clin Microbiol,* 34(8).
Clemens, D. L. and Horwitz, M. A. (2007) 'Uptake and intracellular fate of Francisella tularensis in human macrophages', *Ann N Y Acad Sci,* 1105.
Clemens, D. L., Lee, B. Y. and Horwitz, M. A. (2004) 'Virulent and Avirulent Strains of Francisella tularensis Prevent Acidification and Maturation of Their Phagosomes and Escape into the Cytoplasm in Human Macrophages', *Infect Immun: Vol. 6*.
Clemens, D. L., Lee, B. Y. and Horwitz, M. A. (2009) 'Francisella tularensis phagosomal escape does not require acidification of the phagosome', *Infect Immun,* 77(5).
Cobb, L. M. and Verneris, M. R. (2021) 'Therapeutic manipulation of innate lymphoid cells', *JCI Insight,* 6(6).
Cole, L. E., Santiago, A., Barry, E., Kang, T. J., Shirey, K. A., Roberts, Z. J., Elkins, K. L., Cross, A. S. and Vogel, S. N. (2008) 'Macrophage proinflammatory response to Francisella tularensis live vaccine strain requires coordination of multiple signaling pathways', *J Immunol,* 180(10).
Cole, L. E., Shirey, K. A., Barry, E., Santiago, A., Rallabhandi, P., Elkins, K. L., Puche, A. C., Michalek, S. M. and Vogel, S. N. (2007) 'Toll-like receptor 2-mediated signaling requirements for Francisella tularensis live vaccine strain infection of murine macrophages', *Infect Immun,* 75(8).
Collazo, C. M., Sher, A., Meierovics, A. I. and Elkins, K. L. (2006) 'Myeloid differentiation factor-88 (MyD88) is essential for control of primary in vivo Francisella tularensis LVS infection, but not for control of intra-macrophage bacterial replication', *Microbes Infect,* 8(3).
Conlan, J. W., KuoLee, R., Shen, H. and Webb, A. (2002) 'Different Host Defences Are Required to Protect Mice From Primary Systemic vs Pulmonary Infection With the Facultative Intracellular Bacterial Pathogen, Francisella Tularensis LVS', *Microbial pathogenesis,* 32(3).
Corral, D., Charton, A., M.Z., K., Blanquart, E., Levillain, F., Lefrançais, E., Girard, J. P., Eberl, G., Poquet, Y., Guéry, J. C., Arguello, R. J., Hepworth, M. R., Neyrolles, O. and Hudrisier, D. (2021) 'Metabolic control of type 2 innate lymphoid cells plasticity toward protective type 1-like cells

during *Mycobacterium tuberculosis* infection', *bioRxiv,* doi: 10.1101/2021.01.19.427257.
Cowley, S. C. and Elkins, K. L. (2011) 'Immunity to Francisella', *Front Microbiol,* 2.
Cowley, S. C., Meierovics, A. I., Frelinger, J. A., Iwakura, Y. and Elkins, K. L. (2010) 'Lung CD4-CD8- double-negative T cells are prominent producers of IL-17A and IFN-gamma during primary respiratory murine infection with Francisella tularensis live vaccine strain', *J Immunol,* 184(10).
Craig, A., Mai, J., Cai, S. and Jeyaseelan, S. (2009) 'Neutrophil Recruitment to the Lungs during Bacterial Pneumonia ▿ ', *Infect Immun,* 77(2).
Crane, D. D., Scott, D. P. and Bosio, C. M. (2012) 'Generation of a Convalescent Model of Virulent Francisella tularensis Infection for Assessment of Host Requirements for Survival of Tularemia', *PLoS One,* 7(3).
Craven, R. R., Hall, J. D., Fuller, J. R., Taft-Benz, S. and Kawula, T. H. (2008) 'Francisella tularensis Invasion of Lung Epithelial Cells ▿ ', *Infect Immun,* 76(7).
Cross, J. T., Jr., Schutze, G. E. and Jacobs, R. F. (1995) 'Treatment of tularemia with gentamicin in pediatric patients', *Pediatr Infect Dis J,* 14(2).
D'Elia, R., Jenner, D. C., Laws, T. R., Stokes, M. G., Jackson, M. C., Essex-Lopresti, A. E. and Atkins, H. S. (2011) 'Inhibition of Francisella tularensis LVS infection of macrophages results in a reduced inflammatory response: evaluation of a therapeutic strategy for intracellular bacteria', *FEMS Immunol Med Microbiol,* 62(3).
D'Elia, R. V., Harrison, K., Oyston, P. C., Lukaszewski, R. A. and Clark, G. C. (2013) 'Targeting the "cytokine storm" for therapeutic benefit', *Clin Vaccine Immunol,* 20(3).
de Kleijn, S., Langereis, J. D., Leentjens, J., Kox, M., Netea, M. G., Koenderman, L., Ferwerda, G., Pickkers, P. and Hermans, P. W. (2013) 'IFN-γ-stimulated neutrophils suppress lymphocyte proliferation through expression of PD-L1', *PloS one,* 8(8).
De Pascalis, R., Taylor, B. C. and Elkins, K. L. (2008) 'Diverse myeloid and lymphoid cell subpopulations produce gamma interferon during early innate immune responses to Francisella tularensis live vaccine strain', *Infect Immun,* 76(9).
del Barrio, L., Sahoo, M., Lantier, L., Reynolds, J. M., Ceballos-Olvera, I. and Re, F. (2015) 'Production of anti-LPS IgM by B1a B cells depends on IL-1β and is protective against lung infection with Francisella tularensis LVS', *PLoS Pathog,* 11(3).
Dennis, D. T., Inglesby, T. V., Henderson, D. A., Bartlett, J. G., Ascher, M. S., Eitzen, E., Fine, A. D., Friedlander, A. M., Hauer, J., Layton, M., Lillibridge, S. R., McDade, J. E., Osterholm, M. T., O'Toole, T., Parker, G., Perl, T. M., Russell, P. K. and Tonat, K. (2001) 'Tularemia as a biological weapon: medical and public health management', *Jama,* 285(21).
Diefenbach, A. (2013) 'Innate lymphoid cells in the defense against infections', *Eur J Microbiol Immunol (Bp): Vol. 3*.
DiSanto, J. P., Muller, W., Guy-Grand, D., Fischer, A. and Rajewsky, K. (1995) 'Lymphoid development in mice with a targeted deletion of the interleukin 2 receptor gamma chain', *Proc Natl Acad Sci U S A,* 92(2).
Duckett, N. S., Olmos, S., Durrant, D. M. and Metzger, D. W. (2005) 'Intranasal interleukin-12 treatment for protection against respiratory infection with the Francisella tularensis live vaccine strain', *Infect Immun,* 73(4).

Duerr, C. U. and Fritz, J. H. (2016) 'Regulation of group 2 innate lymphoid cells', *Cytokine,* 87.
Duerr, C. U., McCarthy, C. D., Mindt, B. C., Rubio, M., Meli, A. P., Pothlichet, J., Eva, M. M., Gauchat, J. F., Qureshi, S. T., Mazer, B. D., Mossman, K. L., Malo, D., Gamero, A. M., Vidal, S. M., King, I. L., Sarfati, M. and Fritz, J. H. (2016) 'Type I interferon restricts type 2 immunopathology through the regulation of group 2 innate lymphoid cells', *Nat Immunol,* 17(1).
Dutton, E. E., Camelo, A., Sleeman, M., Herbst, R., Carlesso, G., Belz, G. T. and Withers, D. R. (2017) 'Characterisation of innate lymphoid cell populations at different sites in mice with defective T cell immunity', *Wellcome Open Res,* 2.
Dutton, E. E., Gajdasik, D. W., Willis, C., Fiancette, R., Bishop, E. L., Camelo, A., Sleeman, M. A., Coccia, M., Didierlaurent, A. M., Tomura, M., Pilataxi, F., Morehouse, C. A., Carlesso, G. and Withers, D. R. (2019) 'Peripheral lymph nodes contain migratory and resident innate lymphoid cell populations', *Sci Immunol,* 4(35).
Elkins, K. L., Colombini, S. M., Krieg, A. M. and De Pascalis, R. (2009) 'NK cells activated in vivo by bacterial DNA control the intracellular growth of Francisella tularensis LVS', *Microbes Infect,* 11(1).
Elkins, K. L., Cowley, S. C. and Bosio, C. M. (2003) 'Innate and adaptive immune responses to an intracellular bacterium, Francisella tularensis live vaccine strain', *Microbes Infect,* 5(2).
Elkins, K. L., Rhinehart-Jones, T. R., Culkin, S. J., Yee, D. and Winegar, R. K. (1996) 'Minimal requirements for murine resistance to infection with Francisella tularensis LVS', *Infect Immun,* 64(8).
Ellis, J., Oyston, P. C., Green, M. and Titball, R. W. (2002) 'Tularemia', *Clinical microbiology reviews,* 15(4).
Ellis, T. N. and Beaman, B. L. (2004) 'Interferon-gamma activation of polymorphonuclear neutrophil function', *Immunology,* 112(1).
Enderlin, G., Morales, L., Jacobs, R. F. and Cross, J. T. (1994) 'Streptomycin and alternative agents for the treatment of tularemia: review of the literature', *Clin Infect Dis,* 19(1).
Evans, M. E., Gregory, D. W., Schaffner, W. and McGee, Z. A. (1985) 'Tularemia: a 30-year experience with 88 cases', *Medicine (Baltimore),* 64(4).
Fachinger, P., Tini, G. M., Grobholz, R., Gambazzi, F., Fankhauser, H. and Irani, S. (2015) 'Pulmonary tularaemia: all that looks like cancer is not necessarily cancer - case report of four consecutive cases', *BMC Pulm Med,* 15.
Feldman, K. A., Stiles-Enos, D., Julian, K., Matyas, B. T., Telford, S. R., 3rd, Chu, M. C., Petersen, L. R. and Hayes, E. B. (2003) 'Tularemia on Martha's Vineyard: seroprevalence and occupational risk', *Emerg Infect Dis,* 9(3).
Forsman, M., Sandström, G. and Sjöstedt, A. (1994) 'Analysis of 16S ribosomal DNA sequences of Francisella strains and utilization for determination of the phylogeny of the genus and for identification of strains by PCR', *Int J Syst Bacteriol,* 44(1).
Fortier, A. H., Slayter, M. V., Ziemba, R., Meltzer, M. S. and Nacy, C. A. (1991) 'Live vaccine strain of Francisella tularensis: infection and immunity in mice', *Infection and immunity,* 59(9).
Frisbee, A. L., Saleh, M. M., Young, M. K., Leslie, J. L., Simpson, M. E., Abhyankar, M. M., Cowardin, C. A., Ma, J. Z., Pramoonjago, P., Turner, S. D., Liou, A. P., Buonomo, E. L. and Petri, W. A., Jr. (2019) 'IL-33 drives group 2 innate lymphoid cell-mediated protection during Clostridium difficile infection', *Nat Commun,* 10(1).
Fuchs, A., Vermi, W., Lee, J. S., Lonardi, S., Gilfillan, S., Newberry, R. D., Cella, M. and Colonna, M. (2013) 'Intraepithelial type 1 innate lymphoid cells

are a unique subset of IL-12- and IL-15-responsive IFN-gamma-producing cells', *Immunity,* 38(4).
Geier, H. and Celli, J. (2011) 'Phagocytic Receptors Dictate Phagosomal Escape and Intracellular Proliferation of Francisella tularensis ▿ ', *Infect Immun: Vol. 6*.
Gentry, M., Taormina, J., Pyles, R. B., Yeager, L., Kirtley, M., Popov, V. L., Klimpel, G. and Eaves-Pyles, T. (2007) 'Role of Primary Human Alveolar Epithelial Cells in Host Defense against Francisella tularensis Infection ▿ ', *Infect Immun,* 75(8).
Geremia, A., Arancibia-Cárcamo, C. V., Fleming, M. P., Rust, N., Singh, B., Mortensen, N. J., Travis, S. P. and Powrie, F. (2011) 'IL-23-responsive innate lymphoid cells are increased in inflammatory bowel disease', *J Exp Med,* 208(6).
Giles, A. J., Hutchinson, M. N. D., Sonnemann, H. M., Jung, J., Fecci, P. E., Ratnam, N. M., Zhang, W., Song, H., Bailey, R., Davis, D., Reid, C. M., Park, D. M. and Gilbert, M. R. (2018) 'Dexamethasone-induced immunosuppression: mechanisms and implications for immunotherapy', *J Immunother Cancer,* 6(1).
Gill, V. and Cunha, B. A. (1997) 'Tularemia pneumonia', *Semin Respir Infect,* 12(1).
Gladiator, A., Wangler, N., Trautwein-Weidner, K. and LeibundGut-Landmann, S. (2013) 'Cutting edge: IL-17-secreting innate lymphoid cells are essential for host defense against fungal infection', *J Immunol,* 190(2).
Goldwich, A., Steinkasserer, A., Gessner, A. and Amann, K. (2012) 'Impairment of podocyte function by diphtheria toxin--a new reversible proteinuria model in mice', *Lab Invest,* 92(12).
Golovliov, I., Baranov, V., Krocova, Z., Kovarova, H. and Sjostedt, A. (2003) 'An attenuated strain of the facultative intracellular bacterium Francisella tularensis can escape the phagosome of monocytic cells', *Infect Immun,* 71(10).
Golovliov, I., Sandström, G., Ericsson, M., Sjöstedt, A. and Tärnvik, A. (1995) 'Cytokine expression in the liver during the early phase of murine tularemia', *Infect Immun,* 63(2).
Goto, Y., Obata, T., Kunisawa, J., Sato, S., Ivanov, II, Lamichhane, A., Takeyama, N., Kamioka, M., Sakamoto, M., Matsuki, T., Setoyama, H., Imaoka, A., Uematsu, S., Akira, S., Domino, S. E., Kulig, P., Becher, B., Renauld, J. C., Sasakawa, C., Umesaki, Y., Benno, Y. and Kiyono, H. (2014) 'Innate lymphoid cells regulate intestinal epithelial cell glycosylation', *Science,* 345(6202).
Griesenauer, B. and Paczesny, S. (2017) 'The ST2/IL-33 Axis in Immune Cells during Inflammatory Diseases', *Front Immunol,* 8.
Griffin, A. J., Crane, D. D., Wehrly, T. D., Scott, D. P. and Bosio, C. M. (2013) 'Alternative activation of macrophages and induction of arginase are not components of pathogenesis mediated by Francisella species', *PLoS One,* 8(12).
Grunow, R., Splettstoesser, W., McDonald, S., Otterbein, C., O'Brien, T., Morgan, C., Aldrich, J., Hofer, E., Finke, E. J. and Meyer, H. (2000) 'Detection of Francisella tularensis in biological specimens using a capture enzyme-linked immunosorbent assay, an immunochromatographic handheld assay, and a PCR', *Clin Diagn Lab Immunol,* 7(1).
Guo, X., Qiu, J., Tu, T., Yang, X., Deng, L., Anders, R. A., Zhou, L. and Fu, Y. X. (2014) 'Induction of innate lymphoid cell-derived interleukin-22 by the transcription factor STAT3 mediates protection against intestinal infection', *Immunity,* 40(1).

Hacker, H., Redecke, V., Blagoev, B., Kratchmarova, I., Hsu, L. C., Wang, G. G., Kamps, M. P., Raz, E., Wagner, H., Hacker, G., Mann, M. and Karin, M. (2006) 'Specificity in Toll-like receptor signalling through distinct effector functions of TRAF3 and TRAF6', *Nature,* 439(7073).
Halim, T. Y., Krauss, R. H., Sun, A. C. and Takei, F. (2012a) 'Lung natural helper cells are a critical source of Th2 cell-type cytokines in protease allergen-induced airway inflammation', *Immunity,* 36(3).
Halim, T. Y., MacLaren, A., Romanish, M. T., Gold, M. J., McNagny, K. M. and Takei, F. (2012b) 'Retinoic-acid-receptor-related orphan nuclear receptor alpha is required for natural helper cell development and allergic inflammation', *Immunity,* 37(3).
Halim, T. Y., Steer, C. A., Mathä, L., Gold, M. J., Martinez-Gonzalez, I., McNagny, K. M., McKenzie, A. N. and Takei, F. (2014) 'Group 2 innate lymphoid cells are critical for the initiation of adaptive T helper 2 cell-mediated allergic lung inflammation', *Immunity,* 40(3).
Halim, T. Y. F., Rana, B. M. J., Walker, J. A., Kerscher, B., Knolle, M. D., Jolin, H. E., Serrao, E. M., Haim-Vilmovsky, L., Teichmann, S. A., Rodewald, H. R., Botto, M., Vyse, T. J., Fallon, P. G., Li, Z., Withers, D. R. and McKenzie, A. N. J. (2018) 'Tissue-Restricted Adaptive Type 2 Immunity Is Orchestrated by Expression of the Costimulatory Molecule OX40L on Group 2 Innate Lymphoid Cells', *Immunity*.
Hall, J. D., Craven, R. R., Fuller, J. R., Pickles, R. J. and Kawula, T. H. (2007) 'Francisella tularensis replicates within alveolar type II epithelial cells in vitro and in vivo following inhalation', *Infect Immun,* 75(2).
Hall, J. D., Kurtz, S. L., Rigel, N. W., Gunn, B. M., Taft-Benz, S., Morrison, J. P., Fong, A. M., Patel, D. D., Braunstein, M. and Kawula, T. H. (2009) 'The impact of chemokine receptor CX3CR1 deficiency during respiratory infections with Mycobacterium tuberculosis or Francisella tularensis', *Clin Exp Immunol,* 156(2).
Hall, J. D., Woolard, M. D., Gunn, B. M., Craven, R. R., Taft-Benz, S., Frelinger, J. A. and Kawula, T. H. (2008) 'Infected-Host-Cell Repertoire and Cellular Response in the Lung following Inhalation of Francisella tularensis Schu S4, LVS, or U112 ▿ ', *Infect Immun: Vol. 12*.
Hatano, Y., Taniuchi, S., Masuda, M., Tsuji, S., Ito, T., Hasui, M., Kobayashi, Y. and Kaneko, K. (2009) 'Phagocytosis of heat-killed Staphylococcus aureus by eosinophils: comparison with neutrophils', *Apmis,* 117(2).
Hernandez, P. P., Mahlakoiv, T., Yang, I., Schwierzeck, V., Nguyen, N., Guendel, F., Gronke, K., Ryffel, B., Hoelscher, C., Dumoutier, L., Renauld, J. C., Suerbaum, S., Staeheli, P. and Diefenbach, A. (2015) 'Interferon-lambda and interleukin 22 act synergistically for the induction of interferon-stimulated genes and control of rotavirus infection', *Nat Immunol,* 16(7).
Hestvik, G., Warns-Petit, E., Smith, L. A., Fox, N. J., Uhlhorn, H., Artois, M., Hannant, D., Hutchings, M. R., Mattsson, R., Yon, L. and Gavier-Widen, D. (2015) 'The status of tularemia in Europe in a one-health context: a review', *Epidemiol Infect,* 143(10).
Hill, T. M., Gilchuk, P., Cicek, B. B., Osina, M. A., Boyd, K. L., Durrant, D. M., Metzger, D. W., Khanna, K. M. and Joyce, S. (2015) 'Border Patrol Gone Awry: Lung NKT Cell Activation by Francisella tularensis Exacerbates Tularemia-Like Disease', *PLoS Pathog,* 11(6).
Hilligan, K. L. and Ronchese, F. (2020) 'Antigen presentation by dendritic cells and their instruction of CD4+ T helper cell responses', *Cell Mol Immunol,* 17(6).
Horby, P., Lim, W. S., Emberson, J. R., Mafham, M., Bell, J. L., Linsell, L., Staplin, N., Brightling, C., Ustianowski, A., Elmahi, E., Prudon, B., Green, C., Felton, T., Chadwick, D., Rege, K., Fegan, C., Chappell, L. C., Faust, S. N.,

Jaki, T., Jeffery, K., Montgomery, A., Rowan, K., Juszczak, E., Baillie, J. K., Haynes, R. and Landray, M. J. (2021) 'Dexamethasone in Hospitalized Patients with Covid-19', *N Engl J Med,* 384(8).
Hotchkiss, R. S., Osmon, S. B., Chang, K. C., Wagner, T. H., Coopersmith, C. M. and Karl, I. E. (2005) 'Accelerated lymphocyte death in sepsis occurs by both the death receptor and mitochondrial pathways', *Journal of immunology (Baltimore, Md. : 1950),* 174(8).
Huang, Y., Guo, L., Qiu, J., Chen, X., Hu-Li, J., Siebenlist, U., Williamson, P. R., Urban, J. F. and Paul, W. E. (2015) 'IL-25-responsive, lineage-negative KLRG1hi cells are multipotential "inflammatory" type 2 innate lymphoid cells', *Nat Immunol,* 16(2).
Huang, Y., Mao, K., Chen, X., Sun, M. A., Kawabe, T., Li, W., Usher, N., Zhu, J., Urban, J. F., Jr., Paul, W. E. and Germain, R. N. (2018) 'S1P-dependent interorgan trafficking of group 2 innate lymphoid cells supports host defense', *Science,* 359(6371).
Hubalek, Z., Sixl, W. and Halouzka, J. (1998) 'Francisella tularensis in Dermacentor reticulatus ticks from the Czech Republic and Austria', *Wien Klin Wochenschr,* 110(24).
Hurrell, B. P., Galle-Treger, L., Jahani, P. S., Howard, E., Helou, D. G., Banie, H., Soroosh, P. and Akbari, O. (2019) 'TNFR2 Signaling Enhances ILC2 Survival, Function, and Induction of Airway Hyperreactivity', *Cell Rep,* 29(13).
Izadjoo, M. J., Polotsky, Y., Mense, M. G., Bhattacharjee, A. K., Paranavitana, C. M., Hadfield, T. L. and Hoover, D. L. (2000) 'Impaired control of Brucella melitensis infection in Rag1-deficient mice', *Infection and immunity,* 68(9).
Jacobs, R. F. and Narain, J. P. (1983) 'Tularemia in children', *Pediatr Infect Dis,* 2(6).
Jessop, F., Schwarz, B., Heitmann, E., Buntyn, R., Wehrly, T. and Bosio, C. M. (2018) 'Temporal Manipulation of Mitochondrial Function by Virulent Francisella tularensis To Limit Inflammation and Control Cell Death', *Infect Immun,* 86(8).
Jiang, L., Tixeira, R., Caruso, S., Atkin-Smith, G. K., Baxter, A. A., Paone, S., Hulett, M. D. and Poon, I. K. (2016) 'Monitoring the Progression of Cell Death and the Disassembly of Dying Cells by Flow Cytometry', *Nature protocols,* 11(4).
Jiao, Y., Huntington, N. D., Belz, G. T. and Seillet, C. (2016) 'Type 1 Innate Lymphoid Cell Biology: Lessons Learnt from Natural Killer Cells', *Front Immunol,* 7.
Johansson, A., Urich, S. K., Chu, M. C., Sjostedt, A. and Tarnvik, A. (2002) 'In vitro susceptibility to quinolones of Francisella tularensis subspecies tularensis', *Scand J Infect Dis,* 34(5).
Kamphuis, E., Junt, T., Waibler, Z., Forster, R. and Kalinke, U. (2006) 'Type I interferons directly regulate lymphocyte recirculation and cause transient blood lymphopenia', *Blood,* 108(10).
Kästele, V., Mayer, J., Lee, E. S., Papazian, N., Cole, J. J., Cerovic, V., Belz, G., Tomura, M., Eberl, G., Goodyear, C., Maciewicz, R. A., Wall, D., Cupedo, T., Withers, D. R. and Milling, S. (2021) 'Intestinal-derived ILCs migrating in lymph increase IFNγ production in response to Salmonella Typhimurium infection', *Mucosal Immunol,* 14(3).
Keim, P., Johansson, A. and Wagner, D. M. (2007) 'Molecular epidemiology, evolution, and ecology of Francisella', *Ann N Y Acad Sci,* 1105.
Ketavarapu, J. M., Rodriguez, A. R., Yu, J. J., Cong, Y., Murthy, A. K., Forsthuber, T. G., Guentzel, M. N., Klose, K. E., Berton, M. T. and Arulanandam, B. P. (2008) 'Mast cells inhibit intramacrophage Francisella

tularensis replication via contact and secreted products including IL-4', *Proc Natl Acad Sci U S A,* 105(27).
Killig, M., Glatzer, T. and Romagnani, C. (2014) 'Recognition strategies of group 3 innate lymphoid cells', *Front Immunol,* 5.
Klimpel, G. R., Eaves-Pyles, T., Moen, S. T., Taormina, J., Peterson, J. W., Chopra, A. K., Niesel, D. W., Carness, P., Haithcoat, J. L., Kirtley, M. and Nasr, A. B. (2008) 'Levofloxacin rescues mice from lethal intra-nasal infections with virulent Francisella tularensis and induces immunity and production of protective antibody', *Vaccine,* 26(52).
Klose, C. S., Kiss, E. A., Schwierzeck, V., Ebert, K., Hoyler, T., d'Hargues, Y., Goppert, N., Croxford, A. L., Waisman, A., Tanriver, Y. and Diefenbach, A. (2013) 'A T-bet gradient controls the fate and function of CCR6-RORgammat+ innate lymphoid cells', *Nature,* 494(7436).
Klose, C. S. N., Flach, M., Mohle, L., Rogell, L., Hoyler, T., Ebert, K., Fabiunke, C., Pfeifer, D., Sexl, V., Fonseca-Pereira, D., Domingues, R. G., Veiga-Fernandes, H., Arnold, S. J., Busslinger, M., Dunay, I. R., Tanriver, Y. and Diefenbach, A. (2014) 'Differentiation of type 1 ILCs from a common progenitor to all helper-like innate lymphoid cell lineages', *Cell,* 157(2).
Kondo, Y., Yoshimoto, T., Yasuda, K., Futatsugi-Yumikura, S., Morimoto, M., Hayashi, N., Hoshino, T., Fujimoto, J. and Nakanishi, K. (2008) 'Administration of IL-33 induces airway hyperresponsiveness and goblet cell hyperplasia in the lungs in the absence of adaptive immune system', *Int Immunol,* 20(6).
Koskela, P. and Salminen, A. (1985) 'Humoral immunity against Francisella tularensis after natural infection', *J Clin Microbiol,* 22(6).
Krocova, Z., Härtlova, A., Souckova, D., Zivna, L., Kroca, M., Rudolf, E., Macela, A. and Stulik, J. (2008) 'Interaction of B Cells With Intracellular Pathogen Francisella Tularensis', *Microbial pathogenesis,* 45(2).
Krocova, Z., Macela, A. and Kubelkova, K. (2017) 'Innate Immune Recognition: Implications for the Interaction of Francisella tularensis with the Host Immune System', *Front Cell Infect Microbiol,* 7.
Kudo, F., Ikutani, M., Seki, Y., Otsubo, T., Kawamura, Y. I., Dohi, T., Oshima, K., Hattori, M., Nakae, S., Takatsu, K. and Takaki, S. (2016) 'Interferon-gamma constrains cytokine production of group 2 innate lymphoid cells', *Immunology,* 147(1).
Kumar, H., Kawai, T. and Akira, S. (2011) 'Pathogen recognition by the innate immune system', *Int Rev Immunol,* 30(1).
Kurtz, S. L., Chou, A. Y., Kubelkova, K., Cua, D. J. and Elkins, K. L. (2014) 'IL-23 p19 knockout mice exhibit minimal defects in responses to primary and secondary infection with Francisella tularensis LVS', *PLoS One,* 9(10).
Kurtz, S. L., Foreman, O., Bosio, C. M., Anver, M. R. and Elkins, K. L. (2013) 'Interleukin-6 is essential for primary resistance to Francisella tularensis live vaccine strain infection', *Infect Immun,* 81(2).
Kveštak, D., Juranić Lisnić, V., Lisnić, B., Tomac, J., Golemac, M., Brizić, I., Indenbirken, D., Cokarić Brdovčak, M., Bernardini, G., Krstanović, F., Rožmanić, C., Grundhoff, A., Krmpotić, A., Britt, W. J. and Jonjić, S. (2021) 'NK/ILC1 cells mediate neuroinflammation and brain pathology following congenital CMV infection', *J Exp Med,* 218(5).
Labayru, C., Palop, A., López-Urrutia, L., Avellaneda, C., Mazón, M. A., Alberte, A. and Pascual, P. P. (1999) '[Francisella tularensis: update on microbiological diagnosis after an epidemic outbreak]', *Enferm Infecc Microbiol Clin,* 17(9).
Lai, X. H., Golovliov, I. and Sjostedt, A. (2001) 'Francisella tularensis induces cytopathogenicity and apoptosis in murine macrophages via a mechanism that requires intracellular bacterial multiplication', *Infect Immun,* 69(7).

Lai, X. H. and Sjostedt, A. (2003) 'Delineation of the molecular mechanisms of Francisella tularensis-induced apoptosis in murine macrophages', *Infect Immun,* 71(8).
Larson, M. A., Nalbantoglu, U., Sayood, K., Zentz, E. B., Cer, R. Z., Iwen, P. C., Francesconi, S. C., Bishop-Lilly, K. A., Mokashi, V. P., Sjöstedt, A. and Hinrichs, S. H. (2016) 'Reclassification of Wolbachia persica as Francisella persica comb. nov. and emended description of the family Francisellaceae', *Int J Syst Evol Microbiol,* 66(3).
Le Goffic, R., Arshad, M. I., Rauch, M., L'Helgoualc'h, A., Delmas, B., Piquet-Pellorce, C. and Samson, M. (2011) 'Infection with influenza virus induces IL-33 in murine lungs', *Am J Respir Cell Mol Biol,* 45(6).
Leiby, D. A., Fortier, A. H., Crawford, R. M., Schreiber, R. D. and Nacy, C. A. (1992) 'In vivo modulation of the murine immune response to Francisella tularensis LVS by administration of anticytokine antibodies', *Infect Immun,* 60(1).
Li, J., Doty, A. L., Iqbal, A. and Glover, S. C. (2016) 'The differential frequency of Lineage(-)CRTH2(-)CD45(+)NKp44(-)CD117(-)CD127(+)ILC subset in the inflamed terminal ileum of patients with Crohn's disease', *Cell Immunol,* 304-305.
Liang, S. C., Tan, X. Y., Luxenberg, D. P., Karim, R., Dunussi-Joannopoulos, K., Collins, M. and Fouser, L. A. (2006) 'Interleukin (IL)-22 and IL-17 are coexpressed by Th17 cells and cooperatively enhance expression of antimicrobial peptides', *J Exp Med,* 203(10).
Lin, Y., Ritchea, S., Logar, A., Slight, S., Messmer, M., Rangel-Moreno, J., Guglani, L., Alcorn, J. F., Strawbridge, H., Park, S. M., Onishi, R., Nyugen, N., Walter, M. J., Pociask, D., Randall, T. D., Gaffen, S. L., Iwakura, Y., Kolls, J. K. and Khader, S. A. (2009) 'Interleukin-17 is required for T helper 1 cell immunity and host resistance to the intracellular pathogen Francisella tularensis', *Immunity,* 31(5).
Lindemann, S. R., McLendon, M. K., Apicella, M. A. and Jones, B. D. (2007) 'An In Vitro Model System Used To Study Adherence and Invasion of Francisella tularensis Live Vaccine Strain in Nonphagocytic Cells ▿ ', *Infect Immun,* 75(6).
Lindgren, M., Eneslatt, K., Broms, J. E. and Sjostedt, A. (2013) 'Importance of PdpC, IglC, IglI, and IglG for modulation of a host cell death pathway induced by Francisella tularensis', *Infect Immun,* 81(6).
Liu, T., Wu, J., Zhao, J., Wang, J., Zhang, Y., Liu, L., Cao, L., Liu, Y. and Dong, L. (2015) 'Type 2 innate lymphoid cells: A novel biomarker of eosinophilic airway inflammation in patients with mild to moderate asthma', *Respir Med,* 109(11).
Lo, B. C., Canals Hernaez, D., Scott, R. W., Hughes, M. R., Shin, S. B., Underhill, T. M., Takei, F. and McNagny, K. M. (2019) 'The Transcription Factor RORα Preserves ILC3 Lineage Identity and Function during Chronic Intestinal Infection', *J Immunol,* 203(12).
Lo, B. C., Gold, M. J., Hughes, M. R., Antignano, F., Valdez, Y., Zaph, C., Harder, K. W. and McNagny, K. M. (2016) 'The orphan nuclear receptor ROR alpha and group 3 innate lymphoid cells drive fibrosis in a mouse model of Crohn's disease', *Sci Immunol,* 1(3).
Lopez, M. C., Duckett, N. S., Baron, S. D. and Metzger, D. W. (2004) 'Early activation of NK cells after lung infection with the intracellular bacterium, Francisella tularensis LVS', *Cell Immunol,* 232(1-2).
López-Yglesias, A. H., Burger, E., Camanzo, E., Martin, A. T., Araujo, A. M., Kwok, S. F. and Yarovinsky, F. (2021) 'T-bet-dependent ILC1- and NK cell-derived IFN-γ mediates cDC1-dependent host resistance against Toxoplasma gondii', *PLoS Pathog,* 17(1).

Louten, J., Rankin, A. L., Li, Y., Murphy, E. E., Beaumont, M., Moon, C., Bourne, P., McClanahan, T. K., Pflanz, S. and de Waal Malefyt, R. (2011) 'Endogenous IL-33 enhances Th2 cytokine production and T-cell responses during allergic airway inflammation', *Int Immunol,* 23(5).
Luci, C., Reynders, A., Ivanov, II, Cognet, C., Chiche, L., Chasson, L., Hardwigsen, J., Anguiano, E., Banchereau, J., Chaussabel, D., Dalod, M., Littman, D. R., Vivier, E. and Tomasello, E. (2009) 'Influence of the transcription factor RORgammat on the development of NKp46+ cell populations in gut and skin', *Nat Immunol,* 10(1).
Lund, S., Walford, H. H. and Doherty, T. A. (2013) 'Type 2 Innate Lymphoid Cells in Allergic Disease', *Curr Immunol Rev: Vol. 4*.
Maazi, H., Patel, N., Sankaranarayanan, I., Suzuki, Y., Rigas, D., Soroosh, P., Freeman, G. J., Sharpe, A. H. and Akbari, O. (2015) 'ICOS:ICOS-Ligand interaction is required for type 2 innate lymphoid cell function, homeostasis and induction of airway hyperreactivity', *Immunity,* 42(3).
Mackley, E. C., Houston, S., Marriott, C. L., Halford, E. E., Lucas, B., Cerovic, V., Filbey, K. J., Maizels, R. M., Hepworth, M. R., Sonnenberg, G. F., Milling, S. and Withers, D. R. (2015) 'CCR7-dependent trafficking of RORgamma(+) ILCs creates a unique microenvironment within mucosal draining lymph nodes', *Nat Commun,* 6.
Maggio, S., Takeda, K., Stark, F., Meierovics, A. I., Yabe, I. and Cowley, S. C. (2015) 'Control of Francisella tularensis Intracellular Growth by Pulmonary Epithelial Cells', *PLoS One,* 10(9).
Malik, M., Bakshi, C. S., Sahay, B., Shah, A., Lotz, S. A. and Sellati, T. J. (2006) 'Toll-Like Receptor 2 Is Required for Control of Pulmonary Infection with Francisella tularensis', *Infect Immun: Vol. 6*.
Mares, C. A., Ojeda, S. S., Morris, E. G., Li, Q. and Teale, J. M. (2008) 'Initial Delay in the Immune Response to Francisella tularensis Is Followed by Hypercytokinemia Characteristic of Severe Sepsis and Correlating with Upregulation and Release of Damage-Associated Molecular Patterns ▿ ', *Infect Immun,* 76(7).
Mariathasan, S., Weiss, D. S., Dixit, V. M. and Monack, D. M. (2005) 'Innate immunity against Francisella tularensis is dependent on the ASC/caspase-1 axis', *J Exp Med: Vol. 8*.
Markel, G., Bar-Haim, E., Zahavy, E., Cohen, H., Cohen, O., Shafferman, A. and Velan, B. (2010) 'The involvement of IL-17A in the murine response to sub-lethal inhalational infection with Francisella tularensis', *PLoS One,* 5(6).
Martinez-Gonzalez, I., Mathä, L., Steer, C. A., Ghaedi, M., Poon, G. F. and Takei, F. (2016) 'Allergen-Experienced Group 2 Innate Lymphoid Cells Acquire Memory-like Properties and Enhance Allergic Lung Inflammation', *Immunity,* 45(1).
Maurin, M. (2015) 'Francisella tularensis as a potential agent of bioterrorism?', *Expert Rev Anti Infect Ther,* 13(2).
Maurin, M. (2020) 'Francisella tularensis, Tularemia and Serological Diagnosis', *Front Cell Infect Microbiol,* 10.
Mayer, C. T., Lahl, K., Milanez-Almeida, P., Watts, D., Dittmer, U., Fyhrquist, N., Huehn, J., Kopf, M., Kretschmer, K., Rouse, B. and Sparwasser, T. (2014) 'Advantages of Foxp3+ regulatory T cell depletion using DEREG mice', *Immun Inflamm Dis,* 2(3).
McCaffrey, R. L. and Allen, L. A. H. (2006) 'Pivotal Advance: Francisella tularensis LVS evades killing by human neutrophils via inhibition of the respiratory burst and phagosome escape', *J Leukoc Biol,* 80(6).
McCaffrey, R. L., Schwartz, J. T., Lindemann, S. R., Moreland, J. G., Buchan, B. W., Jones, B. D. and Allen, L. A. H. (2010) 'Multiple mechanisms of

NADPH oxidase inhibition by type A and type B Francisella tularensis', *J Leukoc Biol,* 88(4).
McHedlidze, T., Kindermann, M., Neves, A. T., Voehringer, D., Neurath, M. F. and Wirtz, S. (2016) 'IL-27 suppresses type 2 immune responses in vivo via direct effects on group 2 innate lymphoid cells', *Mucosal Immunol,* 9(6).
McKinstry, K. K., Strutt, T. M., Buck, A., Curtis, J. D., Dibble, J. P., Huston, G., Tighe, M., Hamada, H., Sell, S., Dutton, R. W. and Swain, S. L. (2009) 'IL-10 deficiency unleashes an influenza-specific Th17 response and enhances survival against high-dose challenge', *J Immunol,* 182(12).
McLendon, M. K., Apicella, M. A. and Allen, L. A. (2006) 'Francisella tularensis: taxonomy, genetics, and Immunopathogenesis of a potential agent of biowarfare', *Annu Rev Microbiol,* 60.
Meininger, I., Carrasco, A., Rao, A., Soini, T., Kokkinou, E. and Mjösberg, J. (2020) 'Tissue-Specific Features of Innate Lymphoid Cells', *Trends Immunol*.
Melillo, A. A., Foreman, O. and Elkins, K. L. (2013) 'IL-12Rbeta2 is critical for survival of primary Francisella tularensis LVS infection', *J Leukoc Biol,* 93(5).
Melo-Gonzalez, F. and Hepworth, M. R. (2017) 'Functional and phenotypic heterogeneity of group 3 innate lymphoid cells', *Immunology,* 150(3).
Metzger, D. W., Salmon, S. L. and Kirimanjeswara, G. (2013) 'Differing effects of interleukin-10 on cutaneous and pulmonary Francisella tularensis live vaccine strain infection', *Infect Immun,* 81(6).
Meyer Zu Hörste, G., Zozulya, A. L., El-Haddad, H., Lehmann, H. C., Hartung, H. P., Wiendl, H. and Kieseier, B. C. (2010) 'Active immunization induces toxicity of diphtheria toxin in diphtheria resistant mice--implications for neuroinflammatory models', *J Immunol Methods,* 354(1-2).
Miller, M. M. and Reinhardt, R. L. (2020) 'The Heterogeneity, Origins, and Impact of Migratory iILC2 Cells in Anti-helminth Immunity', *Front Immunol,* 11.
Mindt, B. C., Fritz, J. H. and Duerr, C. U. (2018) 'Group 2 Innate Lymphoid Cells in Pulmonary Immunity and Tissue Homeostasis', *Front Immunol,* 9.
Mjosberg, J. and Spits, H. (2016) 'Human innate lymphoid cells', *J Allergy Clin Immunol,* 138(5).
Mjosberg, J. M., Trifari, S., Crellin, N. K., Peters, C. P., van Drunen, C. M., Piet, B., Fokkens, W. J., Cupedo, T. and Spits, H. (2011) 'Human IL-25- and IL-33-responsive type 2 innate lymphoid cells are defined by expression of CRTH2 and CD161', *Nat Immunol,* 12(11).
Mohapatra, A., Van Dyken, S. J., Schneider, C., Nussbaum, J. C., Liang, H. E. and Locksley, R. M. (2016) 'Group 2 innate lymphoid cells utilize the IRF4-IL-9 module to coordinate epithelial cell maintenance of lung homeostasis', *Mucosal Immunol,* 9(1).
Molofsky, A. B., Savage, A. K. and Locksley, R. M. (2015) 'Interleukin-33 in Tissue Homeostasis, Injury, and Inflammation', *Immunity,* 42(6).
Molofsky, A. B., Van Gool, F., Liang, H. E., Van Dyken, S. J., Nussbaum, J. C., Lee, J., Bluestone, J. A. and Locksley, R. M. (2015) 'Interleukin-33 and Interferon-gamma Counter-Regulate Group 2 Innate Lymphoid Cell Activation during Immune Perturbation', *Immunity,* 43(1).
Mombaerts, P., Iacomini, J., Johnson, R. S., Herrup, K., Tonegawa, S. and Papaioannou, V. E. (1992) 'RAG-1-deficient mice have no mature B and T lymphocytes', *Cell,* 68(5).
Monticelli, L. A., Sonnenberg, G. F., Abt, M. C., Alenghat, T., Ziegler, C. G., Doering, T. A., Angelosanto, J. M., Laidlaw, B. J., Yang, C. Y., Sathaliyawala, T., Kubota, M., Turner, D., Diamond, J. M., Goldrath, A. W., Farber, D. L., Collman, R. G., Wherry, E. J. and Artis, D. (2011) 'Innate lymphoid cells promote lung tissue homeostasis following acute influenza virus infection', *Nat Immunol,* 12(11).

Morner, T. (1992) 'The ecology of tularaemia', *Rev Sci Tech,* 11(4).
Moro, K., Kabata, H., Tanabe, M., Koga, S., Takeno, N., Mochizuki, M., Fukunaga, K., Asano, K., Betsuyaku, T. and Koyasu, S. (2016) 'Interferon and IL-27 antagonize the function of group 2 innate lymphoid cells and type 2 innate immune responses', *Nat Immunol,* 17(1).
Morris, D. G., Huang, X., Kaminski, N., Wang, Y., Shapiro, S. D., Dolganov, G., Glick, A. and Sheppard, D. (2003) 'Loss of integrin alpha(v)beta6-mediated TGF-beta activation causes Mmp12-dependent emphysema', *Nature,* 422(6928).
Morton, A. M., Sefik, E., Upadhyay, R., Weissleder, R., Benoist, C. and Mathis, D. (2014) 'Endoscopic photoconversion reveals unexpectedly broad leukocyte trafficking to and from the gut', *Proceedings of the National Academy of Sciences of the United States of America,* 111(18).
Mougous, J. D., Cuff, M. E., Raunser, S., Shen, A., Zhou, M., Gifford, C. A., Goodman, A. L., Joachimiak, G., Ordoñez, C. L., Lory, S., Walz, T., Joachimiak, A. and Mekalanos, J. J. (2006) 'A Virulence Locus of Pseudomonas aeruginosa Encodes a Protein Secretion Apparatus', *Science,* 312(5779).
Munger, J. S., Huang, X., Kawakatsu, H., Griffiths, M. J., Dalton, S. L., Wu, J., Pittet, J. F., Kaminski, N., Garat, C., Matthay, M. A., Rifkin, D. B. and Sheppard, D. (1999) 'The integrin alpha v beta 6 binds and activates latent TGF beta 1: a mechanism for regulating pulmonary inflammation and fibrosis', *Cell,* 96(3).
Muraoka, W. T., Korchagina, A. A., Xia, Q., Shein, S. A., Jing, X., Lai, Z., Weldon, K. S., Wang, L. J., Chen, Y., Kummer, L. W., Mohrs, M., Vivier, E., Koroleva, E. P. and Tumanov, A. V. (2021) 'Campylobacter infection promotes IFNγ-dependent intestinal pathology via ILC3 to ILC1 conversion', *Mucosal Immunol,* 14(3).
Nakajima, H., Shores, E. W., Noguchi, M. and Leonard, W. J. (1997) 'The Common Cytokine Receptor γ Chain Plays an Essential Role in Regulating Lymphoid Homeostasis', *J Exp Med,* 185(2).
Nano, F. E. and Schmerk, C. (2007) 'The Francisella pathogenicity island', *Ann N Y Acad Sci,* 1105.
Neill, D. R., Wong, S. H., Bellosi, A., Flynn, R. J., Daly, M., Langford, T. K., Bucks, C., Kane, C. M., Fallon, P. G., Pannell, R., Jolin, H. E. and McKenzie, A. N. (2010) 'Nuocytes represent a new innate effector leukocyte that mediates type-2 immunity', *Nature,* 464(7293).
Nguyen, G. T., Green, E. R. and Mecsas, J. (2017) 'Neutrophils to the ROScue: Mechanisms of NADPH Oxidase Activation and Bacterial Resistance', *Front Cell Infect Microbiol,* 7.
Nishikado, H., Mukai, K., Kawano, Y., Minegishi, Y. and Karasuyama, H. (2011) 'NK cell-depleting anti-asialo GM1 antibody exhibits a lethal off-target effect on basophils in vivo', *J Immunol,* 186(10).
Nussbaum, J. C., Van Dyken, S. J., von Moltke, J., Cheng, L. E., Mohapatra, A., Molofsky, A. B., Thornton, E. E., Krummel, M. F., Chawla, A., Liang, H. E. and Locksley, R. M. (2013) 'Type 2 innate lymphoid cells control eosinophil homeostasis', *Nature,* 502(7470).
Odegaard, K., Boersma, B. and Keegan, J. (2017) 'Atypical Presentations of Tularemia', *S D Med,* 70(5).
Ohara, Y., Sato, T., Fujita, H., Ueno, T. and Homma, M. (1991) 'Clinical manifestations of tularemia in Japan--analysis of 1,355 cases observed between 1924 and 1987', *Infection,* 19(1).
Ohne, Y., Silver, J. S., Thompson-Snipes, L., Collet, M. A., Blanck, J. P., Cantarel, B. L., Copenhaver, A. M., Humbles, A. A. and Liu, Y. J. (2016) 'IL-

1 is a critical regulator of group 2 innate lymphoid cell function and plasticity', *Nat Immunol,* 17(6).
Öhrman, C., Sahl, J. W., Sjödin, A., Uneklint, I., Ballard, R., Karlsson, L., McDonough, R. F., Sundell, D., Soria, K., Bäckman, S., Chase, K., Brindefalk, B., Sozhamannan, S., Vallesi, A., Hägglund, E., Ramirez-Paredes, J. G., Thelaus, J., Colquhoun, D., Myrtennäs, K., Birdsell, D., Johansson, A., Wagner, D. M. and Forsman, M. (2021) 'Reorganized Genomic Taxonomy of Francisellaceae Enables Design of Robust Environmental PCR Assays for Detection of Francisella tularensis', *Microorganisms,* 9(1).
Ojeda, S. S., Wang, Z. J., Mares, C. A., Chang, T. A., Li, Q., Morris, E. G., Jerabek, P. A. and Teale, J. M. (2008) 'Rapid dissemination of Francisella tularensis and the effect of route of infection', *BMC Microbiol,* 8.
Oliphant, C., Hwang, Y., Walker, J., Salimi, M., Wong, S., Brewer, J., Englezakis, A., Barlow, J., Hams, E., Scanlon, S., Ogg, G., Fallon, P. and McKenzie, A. (2014) 'MHCII-Mediated Dialog between Group 2 Innate Lymphoid Cells and CD4+ T Cells Potentiates Type 2 Immunity and Promotes Parasitic Helminth Expulsion', *Immunity: Vol. 2*.
Oliveira-Nascimento, L., Massari, P. and Wetzler, L. M. (2012) 'The Role of TLR2 in Infection and Immunity', *Front Immunol,* 3.
Ouyang, W. and O'Garra, A. (2019) 'IL-10 Family Cytokines IL-10 and IL-22: from Basic Science to Clinical Translation', *Immunity,* 50(4).
Ozanic, M., Marecic, V., Abu Kwaik, Y. and Santic, M. (2015) 'The Divergent Intracellular Lifestyle of Francisella tularensis in Evolutionarily Distinct Host Cells', *PLoS Pathog: Vol. 12*.
Panda, S. K. and Colonna, M. (2019) 'Innate Lymphoid Cells in Mucosal Immunity', *Front Immunol,* 10.
Parmely, M. J., Fischer, J. L. and Pinson, D. M. (2009) 'Programmed Cell Death and the Pathogenesis of Tissue Injury Induced by Type A Francisella tularensis', *FEMS Microbiol Lett,* 301(1).
Patel, D. F., Peiró, T., Bruno, N., Vuononvirta, J., Akthar, S., Puttur, F., Pyle, C. J., Suveizdytė, K., Walker, S. A., Singanayagam, A., Carlin, L. M., Gregory, L. G., Lloyd, C. M. and Snelgrove, R. J. (2019) 'Neutrophils restrain allergic airway inflammation by limiting ILC2 function and monocyte-dendritic cell antigen presentation', *Science immunology,* 4(41).
Periasamy, S., Le, H. T., Duffy, E. B., Chin, H. and Harton, J. A. (2016) 'Inflammasome-Independent NLRP3 Restriction of a Protective Early Neutrophil Response to Pulmonary Tularemia', *PLoS Pathog,* 12(12).
Periasamy, S., Singh, A., Sahay, B., Rahman, T., Feustel, P. J., Pham, G. H., Gosselin, E. J. and Sellati, T. J. (2011) 'Development of tolerogenic dendritic cells and regulatory T cells favors exponential bacterial growth and survival during early respiratory tularemia', *J Leukoc Biol,* 90(3).
Phillips, N. J., Schilling, B., McLendon, M. K., Apicella, M. A. and Gibson, B. W. (2004) 'Novel modification of lipid A of Francisella tularensis', *Infect Immun,* 72(9).
Pierini, L. M. (2006) 'Uptake of serum-opsonized Francisella tularensis by macrophages can be mediated by class A scavenger receptors', *Cell Microbiol,* 8(8).
Pietras, E. M., Miller, L. S., Johnson, C. T., O'Connell, R. M., Dempsey, P. W. and Cheng, G. (2011) 'A MyD88-dependent IFNγR-CCR2 signaling circuit is required for mobilization of monocytes and host defense against systemic bacterial challenge', *Cell Res,* 21(7).
Plzakova, L., Krocova, Z., Kubelkova, K. and Macela, A. (2015) 'Entry of Francisella tularensis into Murine B Cells: The Role of B Cell Receptors and Complement Receptors', *PLoS One,* 10(7).

Polsinelli, T., Meltzer, M. S. and Fortier, A. H. (1994) 'Nitric oxide-independent killing of Francisella tularensis by IFN-gamma-stimulated murine alveolar macrophages', *J Immunol,* 153(3).
Pulavendran, S., Prasanthi, M., Ramachandran, A., Grant, R., Snider, T. A., Chow, V. T. K., Malayer, J. R. and Teluguakula, N. (2020) 'Production of Neutrophil Extracellular Traps Contributes to the Pathogenesis of Francisella tularemia', *Front Immunol,* 11.
Putzova, D., Panda, S., Hartlova, A., Stulik, J. and Gekara, N. O. (2017) 'Subversion of innate immune responses by Francisella involves the disruption of TRAF3 and TRAF6 signalling complexes', *Cell Microbiol,* 19(11).
Quirch, M., Lee, J. and Rehman, S. (2020) 'Hazards of the Cytokine Storm and Cytokine-Targeted Therapy in Patients With COVID-19: Review', *J Med Internet Res,* 22(8).
Rankin, L. C., Girard-Madoux, M. J., Seillet, C., Mielke, L. A., Kerdiles, Y., Fenis, A., Wieduwild, E., Putoczki, T., Mondot, S., Lantz, O., Demon, D., Papenfuss, A. T., Smyth, G. K., Lamkanfi, M., Carotta, S., Renauld, J. C., Shi, W., Carpentier, S., Soos, T., Arendt, C., Ugolini, S., Huntington, N. D., Belz, G. T. and Vivier, E. (2016) 'Complementarity and redundancy of IL-22-producing innate lymphoid cells', *Nat Immunol,* 17(2).
Ricardo-Gonzalez, R. R., Schneider, C., Liao, C., Lee, J., Liang, H. E. and Locksley, R. M. (2020) 'Tissue-specific Pathways Extrude Activated ILC2s to Disseminate Type 2 Immunity', *The Journal of experimental medicine,* 217(4).
Roberts, L. M., Powell, D. A. and Frelinger, J. A. (2018) 'Adaptive Immunity to Francisella tularensis and Considerations for Vaccine Development', *Front Cell Infect Microbiol,* 8.
Roberts, L. M., Tuladhar, S., Steele, S. P., Riebe, K. J., Chen, C. J., Cumming, R. I., Seay, S., Frothingham, R., Sempowski, G. D., Kawula, T. H. and Frelinger, J. A. (2014) 'Identification of early interactions between Francisella and the host', *Infect Immun,* 82(6).
Roediger, B. and Weninger, W. (2015) 'Group 2 innate lymphoid cells in the regulation of immune responses', *Adv Immunol,* 125.
Rohmer, L., Fong, C., Abmayr, S., Wasnick, M., Larson Freeman, T. J., Radey, M., Guina, T., Svensson, K., Hayden, H. S., Jacobs, M., Gallagher, L. A., Manoil, C., Ernst, R. K., Drees, B., Buckley, D., Haugen, E., Bovee, D., Zhou, Y., Chang, J., Levy, R., Lim, R., Gillett, W., Guenthener, D., Kang, A., Shaffer, S. A., Taylor, G., Chen, J., Gallis, B., D'Argenio, D. A., Forsman, M., Olson, M. V., Goodlett, D. R., Kaul, R., Miller, S. I. and Brittnacher, M. J. (2007) 'Comparison of Francisella tularensis genomes reveals evolutionary events associated with the emergence of human pathogenic strains', *Genome Biol,* 8(6).
Rotz, L. D. and Hughes, J. M. (2004) 'Advances in detecting and responding to threats from bioterrorism and emerging infectious disease', *Nat Med,* 10(12 Suppl).
Saluzzo, S., Gorki, A. D., Rana, B. M. J., Martins, R., Scanlon, S., Starkl, P., Lakovits, K., Hladik, A., Korosec, A., Sharif, O., Warszawska, J. M., Jolin, H., Mesteri, I., McKenzie, A. N. J. and Knapp, S. (2017) 'First-Breath-Induced Type 2 Pathways Shape the Lung Immune Environment', *Cell Rep,* 18(8).
Sanos, S. L., Bui, V. L., Mortha, A., Oberle, K., Heners, C., Johner, C. and Diefenbach, A. (2009) 'RORgammat and commensal microflora are required for the differentiation of mucosal interleukin 22-producing NKp46+ cells', *Nat Immunol,* 10(1).
Santic, M., Asare, R., Skrobonja, I., Jones, S. and Abu Kwaik, Y. (2008) 'Acquisition of the vacuolar ATPase proton pump and phagosome

acidification are essential for escape of Francisella tularensis into the macrophage cytosol', *Infect Immun,* 76(6).
Santic, M., Molmeret, M., Klose, K. E., Jones, S. and Kwaik, Y. A. (2005) 'The Francisella tularensis pathogenicity island protein IglC and its regulator MglA are essential for modulating phagosome biogenesis and subsequent bacterial escape into the cytoplasm', *Cell Microbiol,* 7(7).
Satoh-Takayama, N., Vosshenrich, C. A., Lesjean-Pottier, S., Sawa, S., Lochner, M., Rattis, F., Mention, J. J., Thiam, K., Cerf-Bensussan, N., Mandelboim, O., Eberl, G. and Di Santo, J. P. (2008) 'Microbial flora drives interleukin 22 production in intestinal NKp46+ cells that provide innate mucosal immune defense', *Immunity,* 29(6).
Schmitt, D. M., O'Dee, D. M., Brown, M. J., Horzempa, J., Russo, B. C., Morel, P. A. and Nau, G. J. (2013) 'Role of NK cells in host defense against pulmonary type A Francisella tularensis infection', *Microbes Infect,* 15(3).
Schmitz, I., Schneider, C., Fröhlich, A., Frebel, H., Christ, D., Leonard, W. J., Sparwasser, T., Oxenius, A., Freigang, S. and Kopf, M. (2013) 'IL-21 restricts virus-driven Treg cell expansion in chronic LCMV infection', *PLoS Pathog,* 9(5).
Schuijs, M. J., Png, S., Richard, A. C., Tsyben, A., Hamm, G., Stockis, J., Garcia, C., Pinaud, S., Nicholls, A., Ros, X. R., Su, J., Eldridge, M. D., Riedel, A., Serrao, E. M., Rodewald, H. R., Mack, M., Shields, J. D., Cohen, E. S., McKenzie, A. N. J., Goodwin, R. J. A., Brindle, K. M., Marioni, J. C. and Halim, T. Y. F. (2020) 'ILC2-driven innate immune checkpoint mechanism antagonizes NK cell antimetastatic function in the lung', *Nat Immunol,* 21(9).
Schulert, G. S. and Allen, L. A. (2006) 'Differential infection of mononuclear phagocytes by Francisella tularensis: role of the macrophage mannose receptor', *J Leukoc Biol,* 80(3).
Schwartz, C., Khan, A. R., Floudas, A., Saunders, S. P., Hams, E., Rodewald, H. R., McKenzie, A. N. J. and Fallon, P. G. (2017) 'ILC2s regulate adaptive Th2 cell functions via PD-L1 checkpoint control', *J Exp Med,* 214(9).
Schwartz, J. T., Barker, J. H., Long, M. E., Kaufman, J., McCracken, J. and Allen, L. A. H. (2012) 'Natural IgM mediates complement-dependent uptake of Francisella tularensis by human neutrophils via CR1 and CR3 in nonimmune serum', *J Immunol,* 189(6).
Serbina, N. V., Shi, C. and Pamer, E. G. (2012) 'Monocyte-Mediated Immune Defense Against Murine Listeria monocytogenes Infection', *Adv Immunol,* 113.
Sharma, J., Mares, C. A., Li, Q., Morris, E. G. and Teale, J. M. (2011) 'Features of sepsis caused by pulmonary infection with Francisella tularensis Type A strain', *Microb Pathog,* 51(1-2).
Shirey, K. A., Cole, L. E., Keegan, A. D. and Vogel, S. N. (2008) 'Francisella tularensis LVS induces Macrophage Alternative Activation As a Survival Mechanism1', *J Immunol,* 181(6).
Silver, J. S., Kearley, J., Copenhaver, A. M., Sanden, C., Mori, M., Yu, L., Pritchard, G. H., Berlin, A. A., Hunter, C. A., Bowler, R., Erjefalt, J. S., Kolbeck, R. and Humbles, A. A. (2016) 'Inflammatory triggers associated with exacerbations of COPD orchestrate plasticity of group 2 innate lymphoid cells in the lungs', *Nat Immunol,* 17(6).
Simoni, Y. and Newell, E. W. (2018) 'Dissecting human ILC heterogeneity: more than just three subsets', *Immunology,* 153(3).
Sjostedt, A. (2007) 'Tularemia: history, epidemiology, pathogen physiology, and clinical manifestations', *Ann N Y Acad Sci,* 1105.
Sjöstedt, A., Conlan, J. and North, R. (1994) 'Neutrophils Are Critical for Host Defense Against Primary Infection With the Facultative Intracellular

Bacterium Francisella Tularensis in Mice and Participate in Defense Against Reinfection', *Infection and immunity,* 62(7).
Sjostedt, A., North, R. J. and Conlan, J. W. (1996) 'The requirement of tumour necrosis factor-alpha and interferon-gamma for the expression of protective immunity to secondary murine tularaemia depends on the size of the challenge inoculum', *Microbiology,* 142 ( Pt 6).
Slight, S. R., Lin, Y., Messmer, M. and Khader, S. A. (2011) 'Francisella tularensis LVS-induced Interleukin-12 p40 cytokine production mediates dendritic cell migration through IL-12 Receptor β1', *Cytokine,* 55(3).
Smith, S. G., Chen, R., Kjarsgaard, M., Huang, C., Oliveria, J. P., O'Byrne, P. M., Gauvreau, G. M., Boulet, L. P., Lemiere, C., Martin, J., Nair, P. and Sehmi, R. (2016) 'Increased numbers of activated group 2 innate lymphoid cells in the airways of patients with severe asthma and persistent airway eosinophilia', *J Allergy Clin Immunol,* 137(1).
Snelgrove, R. J., Godlee, A. and Hussell, T. (2011) 'Airway immune homeostasis and implications for influenza-induced inflammation', *Trends Immunol,* 32(7).
Sojka, D. K., Plougastel-Douglas, B., Yang, L., Pak-Wittel, M. A., Artyomov, M. N., Ivanova, Y., Zhong, C., Chase, J. M., Rothman, P. B., Yu, J., Riley, J. K., Zhu, J., Tian, Z. and Yokoyama, W. M. (2014) 'Tissue-resident natural killer (NK) cells are cell lineages distinct from thymic and conventional splenic NK cells', *eLife,* 3.
Song, C., Lee, J. S., Gilfillan, S., Robinette, M. L., Newberry, R. D., Stappenbeck, T. S., Mack, M., Cella, M. and Colonna, M. (2015) 'Unique and redundant functions of NKp46+ ILC3s in models of intestinal inflammation', *J Exp Med,* 212(11).
Song, J., Willinger, T., Rongvaux, A., Eynon, E. E., Stevens, S., Manz, M. G., Flavell, R. A. and Galán, J. E. (2010) 'A mouse model for the human pathogen Salmonella typhi', *Cell Host Microbe,* 8(4).
Sonnenberg, G. F., Monticelli, L. A., Elloso, M. M., Fouser, L. A. and Artis, D. (2011) 'CD4(+) lymphoid tissue-inducer cells promote innate immunity in the gut', *Immunity,* 34(1).
Spellberg, B. and Edwards, J. E., Jr. (2001) 'Type 1/Type 2 immunity in infectious diseases', *Clin Infect Dis,* 32(1).
Spencer, S. P., Wilhelm, C., Yang, Q., Hall, J. A., Bouladoux, N., Boyd, A., Nutman, T. B., Urban, J. F., Jr., Wang, J., Ramalingam, T. R., Bhandoola, A., Wynn, T. A. and Belkaid, Y. (2014) 'Adaptation of innate lymphoid cells to a micronutrient deficiency promotes type 2 barrier immunity', *Science,* 343(6169).
Spits, H., Artis, D., Colonna, M., Diefenbach, A., Di Santo, J. P., Eberl, G., Koyasu, S., Locksley, R. M., McKenzie, A. N., Mebius, R. E., Powrie, F. and Vivier, E. (2013) 'Innate lymphoid cells--a proposal for uniform nomenclature', *Nat Rev Immunol,* 13(2).
Spits, H. and Cupedo, T. (2012) 'Innate lymphoid cells: emerging insights in development, lineage relationships, and function', *Annu Rev Immunol,* 30.
Spooner, C. J., Lesch, J., Yan, D., Khan, A. A., Abbas, A., Ramirez-Carrozzi, V., Zhou, M., Soriano, R., Eastham-Anderson, J., Diehl, L., Lee, W. P., Modrusan, Z., Pappu, R., Xu, M., DeVoss, J. and Singh, H. (2013) 'Specification of type 2 innate lymphocytes by the transcriptional determinant Gfi1', *Nat Immunol,* 14(12).
Steele, S., Radlinski, L., Taft-Benz, S., Brunton, J. and Kawula, T. H. (2016) 'Trogocytosis-associated cell to cell spread of intracellular bacterial pathogens', *Elife,* 5.

Steele, S. P., Chamberlain, Z., Park, J. and Kawula, T. H. (2019) 'Francisella tularensis enters a double membraned compartment following cell-cell transfer', *Elife,* 8.
Steer, C. A., Mathä, L., Shim, H. and Takei, F. (2020) 'Lung Group 2 Innate Lymphoid Cells Are Trained by Endogenous IL-33 in the Neonatal Period', *JCI insight*.
Steiner, D. J., Furuya, Y., Jordan, M. B. and Metzger, D. W. (2017) 'Protective Role for Macrophages in Respiratory Francisella tularensis Infection', *Infect Immun,* 85(6).
Stenmark, S., Sunnemark, D., Bucht, A. and Sjostedt, A. (1999) 'Rapid local expression of interleukin-12, tumor necrosis factor alpha, and gamma interferon after cutaneous Francisella tularensis infection in tularemia-immune mice', *Infect Immun,* 67(4).
Stewart, S. J. (1996) 'Tularemia: association with hunting and farming', *FEMS Immunol Med Microbiol,* 13(3).
Stier, M. T., Bloodworth, M. H., Toki, S., Newcomb, D. C., Goleniewska, K., Boyd, K. L., Quitalig, M., Hotard, A. L., Moore, M. L., Hartert, T. V., Zhou, B., McKenzie, A. N. and Peebles, R. S. (2016) 'Respiratory syncytial virus infection activates IL-13-producing group 2 innate lymphoid cells through thymic stromal lymphopoietin', *The Journal of allergy and clinical immunology,* 138(3).
Taylor, P. R., Martinez-Pomares, L., Stacey, M., Lin, H. H., Brown, G. D. and Gordon, S. (2005) 'Macrophage receptors and immune recognition', *Annu Rev Immunol,* 23.
Teunissen, M. B. M., Munneke, J. M., Bernink, J. H., Spuls, P. I., Res, P. C. M., Te Velde, A., Cheuk, S., Brouwer, M. W. D., Menting, S. P., Eidsmo, L., Spits, H., Hazenberg, M. D. and Mjösberg, J. (2014) 'Composition of innate lymphoid cell subsets in the human skin: enrichment of NCR(+) ILC3 in lesional skin and blood of psoriasis patients', *J Invest Dermatol,* 134(9).
Trent, M. S., Stead, C. M., Tran, A. X. and Hankins, J. V. (2006) 'Diversity of endotoxin and its impact on pathogenesis', *J Endotoxin Res,* 12(4).
Trinchieri, G. (2003) 'Interleukin-12 and the regulation of innate resistance and adaptive immunity', *Nat Rev Immunol,* 3(2).
Turner, J. E., Morrison, P. J., Wilhelm, C., Wilson, M., Ahlfors, H., Renauld, J. C., Panzer, U., Helmby, H. and Stockinger, B. (2013) 'IL-9-mediated survival of type 2 innate lymphoid cells promotes damage control in helminth-induced lung inflammation', *J Exp Med,* 210(13).
Van Maele, L., Carnoy, C., Cayet, D., Ivanov, S., Porte, R., Deruy, E., Chabalgoity, J. A., Renauld, J. C., Eberl, G., Benecke, A. G., Trottein, F., Faveeuw, C. and Sirard, J. C. (2014) 'Activation of Type 3 innate lymphoid cells and interleukin 22 secretion in the lungs during Streptococcus pneumoniae infection', *J Infect Dis,* 210(3).
Verma, A. H., Bueter, C. L., Rothenberg, M. E. and Deepe, G. S. (2017) 'Eosinophils subvert host resistance to an intracellular pathogen by instigating non-protective IL-4 in CCR2(-/-) mice', *Mucosal Immunol,* 10(1).
Vivier, E., Artis, D., Colonna, M., Diefenbach, A., Di Santo, J. P., Eberl, G., Koyasu, S., Locksley, R. M., McKenzie, A. N. J., Mebius, R. E., Powrie, F. and Spits, H. (2018) 'Innate Lymphoid Cells: 10 Years On', *Cell,* 174(5).
von Moltke, J., Ji, M., Liang, H. E. and Locksley, R. M. (2016) 'Tuft-cell-derived IL-25 regulates an intestinal ILC2-epithelial response circuit', *Nature,* 529(7585).
Walker, J. A., Oliphant, C. J., Englezakis, A., Yu, Y., Clare, S., Rodewald, H. R., Belz, G., Liu, P., Fallon, P. G. and McKenzie, A. N. (2015) 'Bcl11b is essential for group 2 innate lymphoid cell development', *J Exp Med,* 212(6).

Wehrly, T. D., Chong, A., Virtaneva, K., Sturdevant, D. E., Child, R., Edwards, J. A., Brouwer, D., Nair, V., Fischer, E. R., Wicke, L., Curda, A. J., Kupko, J. J., 3rd, Martens, C., Crane, D. D., Bosio, C. M., Porcella, S. F. and Celli, J. (2009) 'Intracellular biology and virulence determinants of Francisella tularensis revealed by transcriptional profiling inside macrophages', *Cell Microbiol,* 11(7).
Weizman, O. E., Adams, N. M., Schuster, I. S., Krishna, C., Pritykin, Y., Lau, C., Degli-Esposti, M. A., Leslie, C. S., Sun, J. C. and O'Sullivan, T. E. (2017) 'ILC1 Confer Early Host Protection at Initial Sites of Viral Infection', *Cell,* 171(4).
Wickstrum, J. R., Bokhari, S. M., Fischer, J. L., Pinson, D. M., Yeh, H. W., Horvat, R. T. and Parmely, M. J. (2009) 'Francisella tularensis induces extensive caspase-3 activation and apoptotic cell death in the tissues of infected mice', *Infect Immun,* 77(11).
Williams, K. P., Gillespie, J. J., Sobral, B. W., Nordberg, E. K., Snyder, E. E., Shallom, J. M. and Dickerman, A. W. (2010) 'Phylogeny of gammaproteobacteria', *J Bacteriol,* 192(9).
Wong, S. H., Walker, J. A., Jolin, H. E., Drynan, L. F., Hams, E., Camelo, A., Barlow, J. L., Neill, D. R., Panova, V., Koch, U., Radtke, F., Hardman, C. S., Hwang, Y. Y., Fallon, P. G. and McKenzie, A. N. (2012) 'Transcription factor RORalpha is critical for nuocyte development', *Nat Immunol,* 13(3).
Woolard, M. D., Hensley, L. L., Kawula, T. H. and Frelinger, J. A. (2008) 'Respiratory Francisella tularensis live vaccine strain infection induces Th17 cells and prostaglandin E2, which inhibits generation of gamma interferon-positive T cells', *Infect Immun,* 76(6).
Wright, G. J., Cherwinski, H., Foster-Cuevas, M., Brooke, G., Puklavec, M. J., Bigler, M., Song, Y., Jenmalm, M., Gorman, D., McClanahan, T., Liu, M. R., Brown, M. H., Sedgwick, J. D., Phillips, J. H. and Barclay, A. N. (2003) 'Characterization of the CD200 Receptor Family in Mice and Humans and Their Interactions With CD200', *Journal of immunology (Baltimore, Md. : 1950),* 171(6).
Wu, H., Haist, V., Baumgärtner, W. and Schughart, K. (2010) 'Sustained viral load and late death in Rag2-/- mice after influenza A virus infection', *Virology journal,* 7.
Wu, Y. H., Lai, A. C., Chi, P. Y., Thio, C. L., Chen, W. Y., Tsai, C. H., Lee, Y. L., Lukacs, N. W. and Chang, Y. J. (2019) 'Pulmonary IL-33 orchestrates innate immune cells to mediate RSV-evoked airway hyperreactivity and eosinophilia', *Allergy*.
Xiong, H., Keith, J. W., Samilo, D. W., Carter, R. A., Leiner, I. M. and Pamer, E. G. (2016) 'Innate lymphocyte/Ly6Chi monocyte crosstalk promotes Klebsiella pneumoniae clearance', *Cell,* 165(3).
Yasuda, K., Muto, T., Kawagoe, T., Matsumoto, M., Sasaki, Y., Matsushita, K., Taki, Y., Futatsugi-Yumikura, S., Tsutsui, H., Ishii, K. J., Yoshimoto, T., Akira, S. and Nakanishi, K. (2012) 'Contribution of IL-33-activated type II innate lymphoid cells to pulmonary eosinophilia in intestinal nematode-infected mice', *Proc Natl Acad Sci U S A,* 109(9).
Yu, Y., Wang, C., Clare, S., Wang, J., Lee, S. C., Brandt, C., Burke, S., Lu, L., He, D., Jenkins, N. A., Copeland, N. G., Dougan, G. and Liu, P. (2015) 'The transcription factor Bcl11b is specifically expressed in group 2 innate lymphoid cells and is essential for their development', *J Exp Med,* 212(6).
Yudanin, N. A., Schmitz, F., Flamar, A. L., Thome, J. J. C., Tait Wojno, E., Moeller, J. B., Schirmer, M., Latorre, I. J., Xavier, R. J., Farber, D. L., Monticelli, L. A. and Artis, D. (2019) 'Spatial and Temporal Mapping of Human Innate Lymphoid Cells Reveals Elements of Tissue Specificity', *Immunity,* 50(2).

Zeis, P., Lian, M., Fan, X., Herman, J. S., Hernandez, D. C., Gentek, R., Elias, S., Symowski, C., Knöpper, K., Peltokangas, N., Friedrich, C., Doucet-Ladeveze, R., Kabat, A. M., Locksley, R. M., Voehringer, D., Bajenoff, M., Rudensky, A. Y., Romagnani, C., Grün, D. and Gasteiger, G. (2020) 'In Situ Maturation and Tissue Adaptation of Type 2 Innate Lymphoid Cell Progenitors', *Immunity,* 53(4).
Zhao, Y., Liu, P., Xin, Z., Shi, C., Bai, Y., Sun, X., Wang, X., Liu, L., Zhao, X., Chen, Z. and Zhang, H. (2019) 'Biological Characteristics of Severe Combined Immunodeficient Mice Produced by CRISPR/Cas9-Mediated Rag2 and IL2rg Mutation', *Front Genet,* 10.
Zhou, W., Toki, S., Zhang, J., Goleniewksa, K., Newcomb, D. C., Cephus, J. Y., Dulek, D. E., Bloodworth, M. H., Stier, M. T., Polosuhkin, V., Gangula, R. D., Mallal, S. A., Broide, D. H. and Peebles, R. S., Jr. (2016) 'Prostaglandin I2 Signaling and Inhibition of Group 2 Innate Lymphoid Cell Responses', *Am J Respir Crit Care Med,* 193(1).